# EXHIBIT 1

Docket No. 107
Filed: 2/2/24

# Lysosomes as a therapeutic target

*Srinivasa Reddy Bonam*[1,2], *Fengjuan Wang*[1,2] *and Sylviane Muller*[1,2,3,4]*

Abstract | Lysosomes are membrane-bound organelles with roles in processes involved in degrading and recycling cellular waste, cellular signalling and energy metabolism. Defects in genes encoding lysosomal proteins cause lysosomal storage disorders, in which enzyme replacement therapy has proved successful. Growing evidence also implicates roles for lysosomal dysfunction in more common diseases including inflammatory and autoimmune disorders, neurodegenerative diseases, cancer and metabolic disorders. With a focus on lysosomal dysfunction in autoimmune disorders and neurodegenerative diseases — including lupus, rheumatoid arthritis, multiple sclerosis, Alzheimer disease and Parkinson disease — this Review critically analyses progress and opportunities for therapeutically targeting lysosomal proteins and processes, particularly with small molecules and peptide drugs.

Endocytosis
A vesicle-mediated process by which cells engulf membrane and extracellular materials. Several endocytic pathways — phagocytosis, pinocytosis and receptor-mediated endocytosis — utilize different mechanisms to internalize material. Clathrin-mediated endocytosis is the major endocytic pathway in mammalian cells.

[1]*CNRS–University of Strasbourg, Biotechnology and Cell Signalling, Illkirch, France.*

[2]*Laboratory of Excellence Medalis, Team Neuroimmunology and Peptide Therapy, Institut de Science et d'Ingénierie Supramoléculaire (ISIS), Strasbourg, France.*

[3]*University of Strasbourg Institute for Advanced Study, Strasbourg, France.*

[4]*Fédération Hospitalo-Universitaire OMICARE, Fédération de Médecine Translationnelle de Strasbourg, Strasbourg University, Strasbourg, France.*

**e-mail: sylviane.muller@unistra.fr*

https://doi.org/10.1038/s41573-019-0036-1

Discovered in the 1950s by Christian de Duve, lysosomes are membrane-bound vesicles containing numerous hydrolytic enzymes that can break down biological polymers such as proteins, lipids, nucleic acids and polysaccharides[1,2]. Lysosomes have long been known to have a key role in the degradation and recycling of extracellular material via endocytosis and phagocytosis, and intracellular material via autophagy (reviewed elsewhere[2–5]) (FIG. 1). The products of lysosomal degradation through these processes can be trafficked to the Golgi apparatus for reuse or for release from the cell through lysosomal exocytosis, which is important in immune system processes. In addition, it has become clear more recently that lysosomes have an important role in other cellular processes including nutrient sensing and the control of energy metabolism[3,5–7] (FIG. 1).

Alterations in lysosomal functions, either in the fusion processes involved in the general pathways mentioned above or related to the function of lysosomal enzymes and non-enzymatic proteins, can result in broad detrimental effects, including failure to clear potentially toxic cellular waste, inflammation, apoptosis and dysregulation of cellular signalling[8]. Such defects have been implicated in many diseases, ranging from rare lysosomal storage disorders (LSDs), which are caused by the dysfunction of particular lysosomal proteins, to more common autoimmune and neurodegenerative disorders[5,9,10]. Despite some limitations, impressive results have been achieved in treating several LSDs through enzyme replacement therapy (ERT). In addition, substantial efforts have been focused on therapeutically targeting the autophagy processes upstream of lysosomes[11–14]. However, there has so far been less attention on investigating the potential to directly target lysosomes with small molecules and peptide drugs.

Nevertheless, with recent advances in understanding of lysosomal function and dysfunction in diseases, promising novel opportunities for therapeutic intervention through targeting lysosomes specifically are beginning to emerge. This Review will provide a brief overview of lysosomal biogenesis, structure and function, and describe the role of lysosomal dysfunction in LSDs as well as other, more common diseases. Specifically, the article will focus on organ-specific and non-organ-specific autoimmune diseases, including lupus, rheumatoid arthritis (RA) and multiple sclerosis (MS), as these have not been extensively reviewed elsewhere, but will also briefly highlight neurodegenerative disorders such as Alzheimer disease (AD) and Parkinson disease (PD), to further illustrate the breadth and nature of the emerging therapeutic opportunities. The current 'toolbox' of pharmacological agents that modulate lysosomal functions and emerging novel targets and strategies in this set of indications will be highlighted. It should be noted that therapeutic approaches to treat inflammatory and autoimmune diseases aim to inhibit the deleterious excessive lysosomal activity, whereas lysosomal activation would be the goal in the treatment of neurodegenerative diseases. Although beyond the scope of this review, such approaches may have applications in other diseases in which lysosomes may play a role, including cancer, metabolic diseases and ageing (reviewed elsewhere[15,16]).

## Lysosomal biogenesis, structure and function

The formation of mature lysosomes is a complex process, which involves the fusion of late endosomes that contain material taken up at the cell surface with transport vesicles that bud from the *trans*-Golgi network[5,8,17]. These vesicles contain nearly 60 different hydrolytic enzymes (grouped into nucleases, proteases, phosphatases, lipases,



DEFS00023214

Case 1:23-cv-00328-JLH-SRF Document 125 Filed 02/20/24 Page 3 of 73 PageID #: 4310

**Phagocytosis**
An endocytic process by which certain cells called phagocytes (for example, macrophages) internalize large particles (>0.5 μm) such as bacteria, other microorganisms, foreign particles or aged red blood cells, for example, to form a phagosome.

**Autophagy**
A vital, finely-regulated and evolutionarily-conserved intracellular pathway that continuously degrades, recycles and clears unnecessary or dysfunctional cellular components. Autophagy is crucial for cell adaptation to the environment and to maintain cell homeostasis, especially under stress conditions.

**Golgi apparatus**
Cytosolic apparatus, meant for the regulation of proteins (modification, storing and transportation) and some forms of lipids to the other cytosolic compartments via the *trans*-Golgi network or outside the cell.

**Lysosomal exocytosis**
A process of the secretory pathway in which lysosomes are fused with the plasma membrane and empty their contents outside the cell. This process plays an important role in plasma membrane repair, bone resorption, immune response and elimination of pathogenic stores (mainly in lysosomal storage disorders).

**Lysosomal storage disorders**
(LSDs). A group of heterogeneous disorders caused by defects in the lysosomal enzymes leading to the accumulation of unmodified or unprocessed components in the lysosomes, which ultimately influence other vital pathways in the cells. LSDs implicate various vital systems of the human body including the skeleton, brain, skin, heart and central nervous system, which are connected with different metabolic pathways.

**Rheumatoid arthritis**
(RA). An autoimmune disease involving inflammation and degeneration of the joints that affects an estimated 1% of the population, making it the most common inflammatory arthritis.

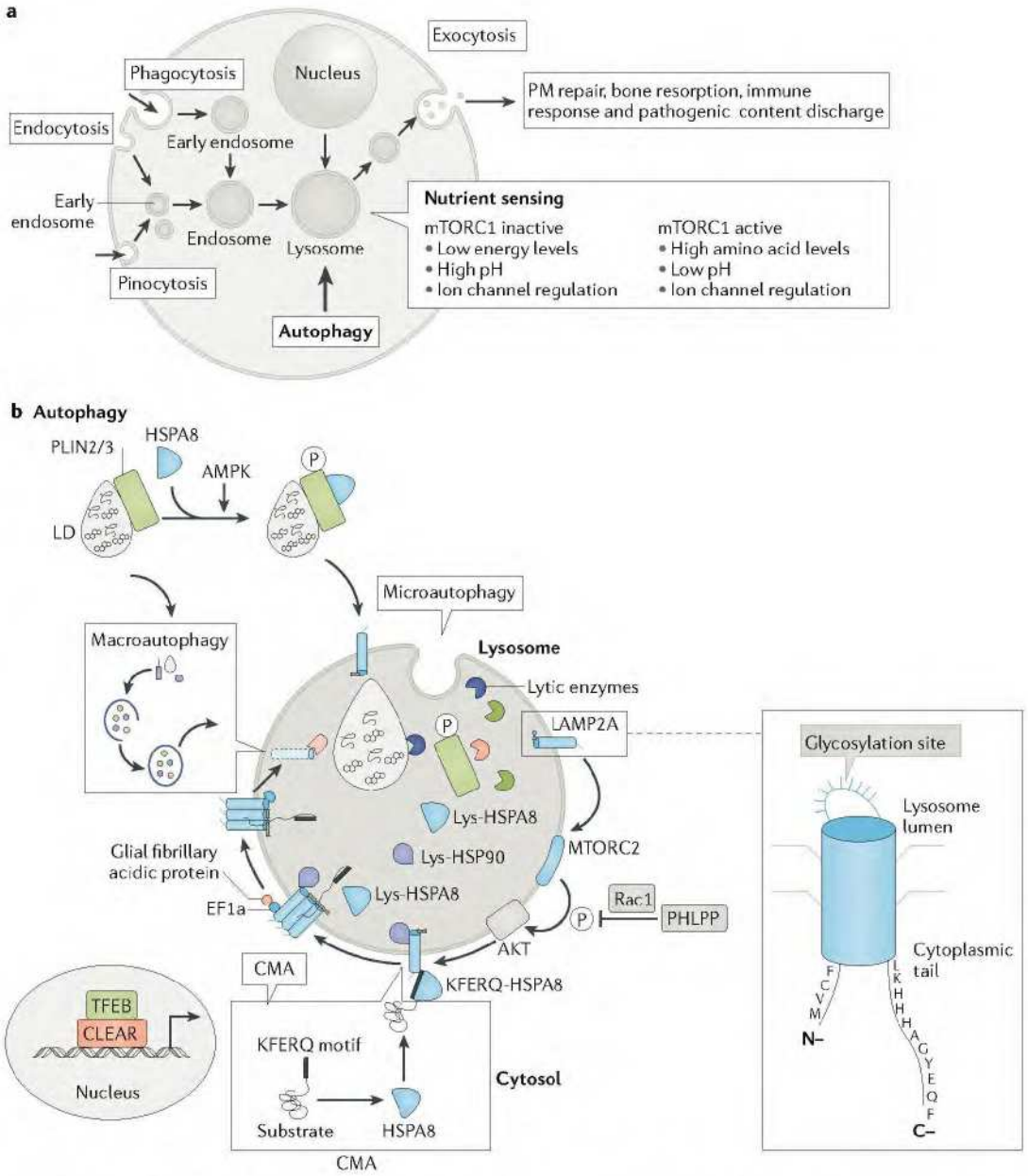


Fig. 1 | **The central position of lysosomes at the crossroads of major autophagic pathways. a** | Functional lysosomes are involved in the degradation (endocytic and autophagic) and regulation of exogenous and endogenous cellular material, including recycling processes. Extracellular material endocytosed by the endosomes and intracellular cargo internalized by the autophagosomes fuse with lysosomes for degradation, which produces energy (ATP production) and source molecules for the macromolecules. Mechanistic target of rapamycin complex 1 (mTORC1) plays a key role in lysosomal nutrient sensing signals (lysosome-to-nucleus axis) to regulate energy metabolism. Factors such as energy levels, type of pH, ion channel regulation and others decide the fate of the catabolic process. During lysosomal exocytosis, the lysosomal content favours plasma membrane (PM) repair, bone resorption, immune response and elimination of pathogenic stores. **b** | The lysosome is the ultimate cell compartment that digests unwanted protein materials generated by macroautophagy, microautophagy (pathways during which the cytoplasmic material is trapped in the lysosome by a process of membrane invagination) and chaperone-mediated autophagy (CMA). In general, lipid droplets (LDs) are degraded by lipophagy, a subtype of macroautophagy, which is activated by cytosolic lipases. CMA has also been demonstrated to participate in the degradation of LDs in which perilipin (PLIN2/3) proteins are phosphorylated (P) by AMP-activated protein kinase (AMPK) with the help of the HSPA8 chaperone. Mechanistic target of rapamycin complex 2 (mTORC2) and AKT (also known as protein kinase B) are negative regulators of CMA, where they exert their effect on the translocation complex of CMA. In situations of starvation, negative regulators are controlled by pleckstrin homology domain and leucine-rich repeat protein phosphatase (PHLPP). Lysosomal stability effects the transcription factor EB (TFEB) translation to the nucleus in which TFEB binds to the coordinated lysosomal expression and regulation (CLEAR) motifs to regulate the transcription of genes. EF1a, elongation factor 1a; Lys, lysosome; Rac1, Ras-related C3 botulinum toxin substrate 1.



DEFS00023215

sulfatases and others), which are synthesized in the endoplasmic reticulum and delivered to the transport vesicles via diverse systems, such as mannose-6-phosphate tags that are recognized by mannose-6-phosphate receptors (MPRs) at the membrane[8,18] or glucocerebrosidase (GCase) that is transported to lysosomes by lysosomal integral membrane protein-2, an ubiquitously expressed type III transmembrane glycoprotein mainly located in endosomes and lysosomes[19].

Mature lysosomes have an acidic internal pH, at which the lysosomal hydrolases are active, and a lining known as a glycocalyx that protects the internal lysosomal perimeter from the acidic environment of the lumen[5,8,20]. This acidic environment is maintained through the activity of a vacuolar-type proton adenosine triphosphatase (v-ATPase), which harnesses energy from hydrolysing ATP to drive the translocation of protons through a $V_0$ membrane domain (reviewed elsewhere[5,21]). Other key lysosomal proteins include structural proteins such as lysosome-associated membrane protein 1 (LAMP1); proteins involved in trafficking and fusion, such as soluble *N*-ethylmaleimide-sensitive factor attachment protein receptors (SNAREs) and RAB GTPases; transporters such as LAMP2A, which has a key role in chaperone-mediated autophagy (CMA); and ion channels such as the chloride channel ClC7 and the cation channel mucolipin 1, a member of the transient receptor potential (TRP) family that is also known as TRPML1 (REFS[22,23]). Most of the proteins are delivered through the clathrin adaptor protein 3-alkaline phosphatase (ALP) pathway, but some proteins are translocated through the lysosome-associated-protein transmembrane-5, a protein that is preferentially expressed in immune cells[3,24].

Although the concept still remains controversial, two lysosome species — conventional or secretory — are often distinguished based on their physical, biochemical and functional properties. Catabolism is the main function of conventional lysosomes, and several other lysosome-related organelles (LROs), such as melanosomes, the late endosomal major histocompatibility complex class II (MHCII) compartment (MIIC), lytic granules from neutrophils, eosinophils, basophils, mast cells, $CD8^+$ T cells and platelets, complement these functions[8,25–29]. Many of the LROs act as professional secretory organelles. LROs share with lysosomes the majority of typical characteristics (acidic environment, lysosomal transmembrane proteins, fusion property to phagosomes and others), in addition to particular properties resulting from their specific cargoes (for example, melanosomes contain melanosome-specific transmembrane glycoprotein, and natural killer cells and $CD8^+$ T cells contain perforins and granzymes). The detailed mechanisms of biogenesis and secretion of LROs remain unclear, although it is known that genetic defects in LROs are involved in rare autosomal recessive disorders characterized by reduced pigmentation, such as Chediak–Higashi disease and Hermansky–Pudlak syndrome[30]. Secretory lysosomes contain many more proteins in addition to those contained in conventional lysosomes, and they participate in multiple cell functions such as plasma membrane repair, tissue and bone regeneration, apoptotic cell death, cholesterol homeostasis, pathogen defence and cell signalling[8].

Lysosomal biogenesis and function are regulated by the basic helix–loop–helix leucine zipper transcription factor EB (TFEB) and the coordinated lysosomal expression and regulation (CLEAR) network[4,31,32] (FIG. 2). For example, autophagy, a crucial process in immunity and autoimmunity[33], is transcriptionally regulated by TFEB[31]. Interestingly, lysosomal exocytosis, which is important in many immune functions, also depends on TFEB activation[31,32]. Moreover, it has been demonstrated that TFEB orchestrates lysosomal $Ca^{2+}$ signalling[34]. The fact that multiple lysosomal processes are dependent on TFEB activation strengthens its role as a master regulator in lysosomal functions. Like other transcription factors, TFEB undergoes phosphorylation and dephosphorylation via different cytosolic and lysosomal pathways (FIG. 2), processes regulated by mechanistic target of rapamycin complex 1 (mTORC1), a master controller of cell growth[35,36].

Lysosomes are at the crossroads of various degradative pathways, including endocytosis (phagocytosis) and autophagy (FIG. 1). Three main forms of autophagy have been described: macroautophagy (the most extensively characterized form), microautophagy and CMA. At the initiation of macroautophagy, a double-membrane sequestering compartment termed the phagophore, which contains cytoplasmic material, is formed and matures into a vesicle called the autophagosome. The cargo is degraded into vacuoles issued from the fusion of autophagic vesicles and lysosomes (called autolysosomes), and the resulting short products are released back into the cytosol for reuse or, according to sometimes contested observations, possibly dispatched into the MIIC for ultimate processing and MHCII molecule loading for presentation to $CD4^+$ T cells[37,38]. In contrast to macroautophagy, microautophagy is characterized by direct lysosomal engulfment of cytosolic material into lysosomes, via the formation of characteristic invaginations of the lysosomal membrane. The third major form of autophagy is CMA, which involves the recognition of substrate proteins containing a KFERQ-like motif by a HSPA8/HSC70-containing complex (FIG. 1b). In CMA, two proteins have a key role: HSPA8 ensures the selectivity of proteins, which will be degraded via the CMA pathway; and LAMP2A translocates the targeted cytosolic proteins across the lysosomal membrane (reviewed elsewhere[7]). The terminal step of autophagy is called autophagic lysosome reformation, in which tubular proto-lysosomes are extruded from autolysosomes (containing lysosomal membrane components) and mature into functional lysosomes[39]. This step is not solely a lysosomal biogenesis process; it also includes a series of elements that are tightly correlated with the regulation of autophagy[40].

In combination with autophagy, lysosomes are involved in both innate and adaptive immune functions, including foreign material recognition (bacterial, parasitic and viral), activation of pattern recognition receptors (such as Toll-like receptors (TLRs) and nucleotide oligomerization domain-like receptor), antigen processing and presentation, especially in the context

Multiple sclerosis
(MS). A demyelinating disease in which the myelin sheaths wrapped around nerve fibres in the central nervous system are progressively destroyed by immune cells and possibly also by autoantibodies.

Parkinson disease
(PD). A neurodegenerative disorder with symptoms including slowness of movement and a loss of fine motor control, owing to the degeneration of dopamine-producing neurons in the substantia nigra.

Chaperone-mediated autophagy
(CMA). A selective autophagy pathway in which proteins that contain a signal KFERQ-like sequence are targeted by HSAP8/HSC70 chaperones and translocated into lysosomes via LAMP2A.

Transcription factor EB
(TFEB). A protein that plays a pivotal role in the regulation of basic cellular processes, such as lysosomal biogenesis and autophagy. It controls lysosomal function via the coordinated lysosomal expression and regulation (CLEAR) gene network (including genes coding for hydrolases, lysosomal membrane proteins and the proton pump v-ATPase complex), and additional lysosome-related processes such as autophagy, endocytosis and exocytosis.

Macroautophagy
A finely-regulated process during which the cell forms a double-membrane sequestering compartment named the phagophore, which matures into the autophagosome.

Autophagosome
A double membrane-bound vesicle, which encloses cellular constituents and fuses with lysosomes to form phagolysosomes where the engulfed material is digested or degraded and either released extracellularly via exocytosis or released intracellularly to undergo further processing.

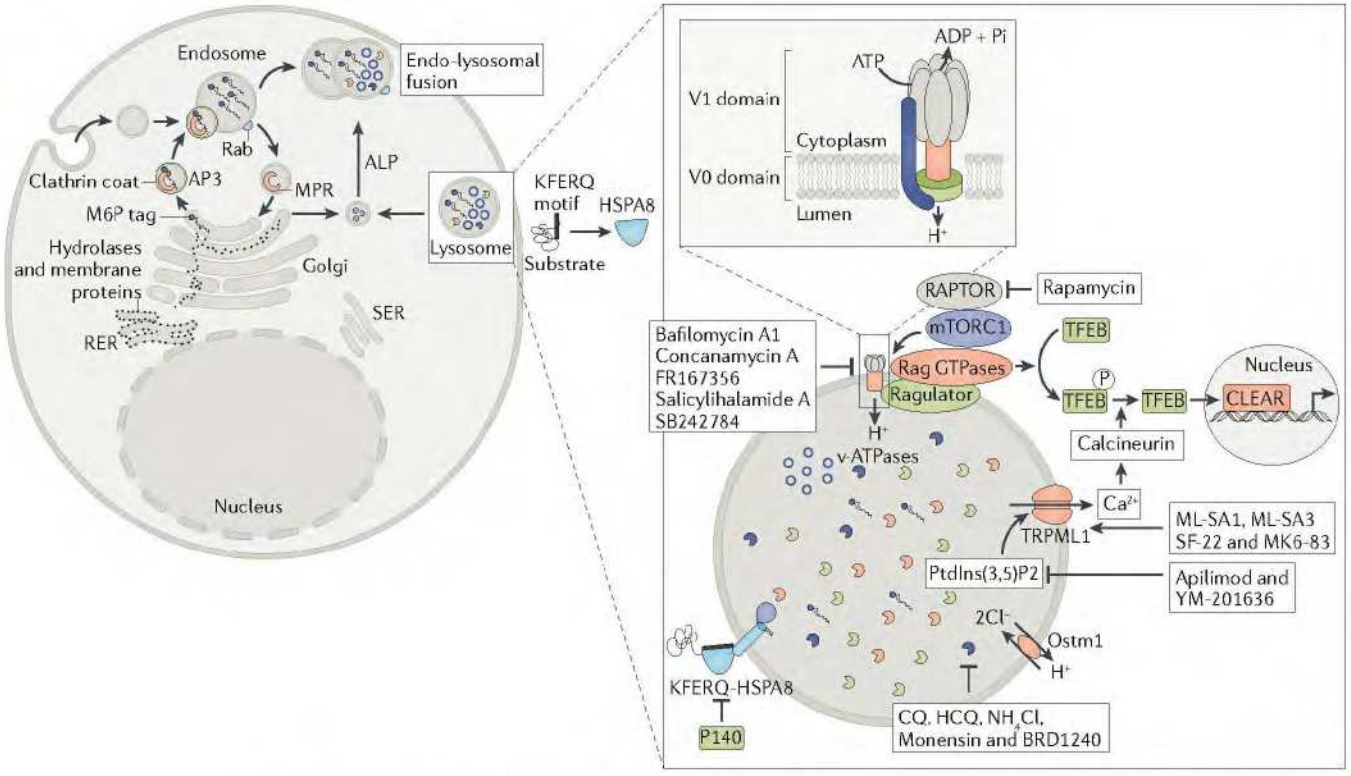


Fig. 2 | **Lysosomal molecular sites and processes as possible targets for therapeutic strategies.** After their synthesis in the rough endoplasmic reticulum (RER), the substrates (cargo) that are intended to be degraded through the endo-lysosomal pathway are transported to lysosomes via the *trans*-Golgi network (TGN). Among the key enzymatic systems that are involved in the lysosomal enzyme transportation of cargos from Golgi to lysosomes, the best studied is the mannose-6-phosphate (M6P) receptor (MPR) system, which binds newly synthesized lysosomal hydrolases in the TGN and delivers them to pre-lysosomal compartments. A few components synthesized in the late Golgi compartment are delivered directly to lysosomes via the 3-alkaline phosphatase (ALP) pathway. Lysosomal components, such as enzymes (lytic enzymes and kinases), membrane-bound proteins/complexes (mechanistic target of rapamycin (mTOR)), transporters and ion channels (vacuolar-type proton adenosine triphosphatase (v-ATPase), TRPML1 and osteopetrosis associated transmembrane protein 1 (Ostm1)) and chaperone-mediated transportation are the best-known targeting sites for lysosomal dysfunction. As depicted in the figure, many pharmacological antagonists and agonists exert activities that potentially correct lysosomal dysfunction and therefore represent potential effective pharmacological tools. CLEAR, coordinated lysosomal expression and regulation; CQ, chloroquine; HCQ, hydroxychloroquine; mTORC1, mTOR complex 1; PtdIns(3,5)P2, phosphatidylinositol-3,5-bisphosphate; RAPTOR, regulatory-associated protein of mTOR; SER, smooth endoplasmic reticulum; TFEB, transcription factor EB.

of MHCII molecules, T cell homeostasis, antibody production and induction of various immune signals (co-stimulation and cytokine secretion)[41]. Besides being a degradative organelle, the lysosome has recently been recognized as a cellular signalling platform[3,42]. It plays an important role in nutrient sensing through mTORC1 and other additional protein complexes, or the so-called 'lysosome nutrient sensing machinery'. The discovery of a stress-induced lysosome-to-nucleus signalling mechanism through TFEB further supports the key role of lysosomes in cellular signalling[36].

## Lysosome dysfunction in diseases

The lysosome occupies a central position in the maintenance of cellular homeostasis, being involved in the exclusion of infectious agents from penetrating host tissue and concomitantly promoting immune regulation. Lysosomes must therefore be able to respond quickly, with increased or decreased functions, to various metabolic conditions aimed at protecting cells from death or damage. Lysosomes are very diverse in size and shape. For reasons that are not totally understood — possibly according to their position in the cytosol[43] and/or their composition — some lysosomes in a single cell are more prone to act and defend cells. Given the wide range of functions of lysosomes in all metabolic compartments of the cell, any dysregulation of their activity could lead to the impairment of various elements of the cellular metabolic machinery (including the transport and biogenesis of sugar (glycolysis), lipids, proteins and nucleic acids) and of metabolic pathways, phagocytosis, endocytosis and autophagy. Although the underlying mechanisms are far from being fully deciphered, it has been seen that lysosomal dysfunction or defects in fusion with vesicles containing cargo are commonly observed abnormalities in proteinopathic neurodegenerative diseases. Dysfunctions of lysosomes can affect the proper activity of other organelles such as peroxisomes and

Mitophagy
A key process that selectively disrupts damaged mitochondria by autolysosomal degradation, preventing excessive reactive oxygen species and activation of cell death.

Huntingtin
(HTT). Discovered in 1993, HTT is a protein of 348 kDa that is widely expressed within the central nervous system. Its structure has been elucidated recently by cryo-electron microscopy. The protein is essential for embryonic development and neurogenesis. It is involved in transcription, vesicle transport, protein trafficking, endocytosis and autophagy.

Systemic lupus erythematosus
(SLE). A chronic, relapsing–remitting autoinflammatory syndrome that has multiple and heterogeneous symptoms, including arthralgia, swollen joints, fever, fatigue, chest pain, kidney inflammation, cardiovascular disease and neuropsychiatric complications. Its aetiology is mostly unknown.

mitochondria, leading to excessive production of reactive oxygen species with pathological features associated with ageing, cancer, chronic inflammation, neurological diseases, male infertility and infections.

Such dysregulation is thus central to LSDs, and also implicated in a wide range of other disorders, including autoimmune and neurological disorders, in which the autophagy–lysosomal network under the control of TFEB has attracted considerable attention.

### *Lysosomal storage disorders*

LSDs are a heterogeneous group of about 50 inherited metabolic disorders, which have an incidence of ~1 in 5,000 live births[44]. These disorders and their treatment have been reviewed extensively elsewhere[45,46], and so will only be covered relatively briefly here. The mutations responsible for most LSDs have been largely elucidated (TABLES 1,2), and many result in the dysfunction of a particular lysosomal hydrolase, leading to the accumulation of the substrate of that hydrolase. For example, in Gaucher disease, the sphingolipid glucocerebroside accumulates in cells (particularly macrophages) and organs, including the liver and spleen, owing to deficiency in the enzyme GCase[24,66]. In certain LSDs, the resultant pathology can be explained by the nature of molecules that accumulate (TABLES 1,2). Thus, the abundance of cerebrosides and gangliosides that deposit in the central nervous system (CNS) of patients with sphingolipid storage disorders, such as type II (acute infantile neuronopathic) Gaucher disease, underlies the severe neurological symptoms of such disorders[67,68]. In patients with Pompe disease, which is caused by α-glucosidase deficiency, the high levels of non-degraded glycogen that accumulate in muscles could explain the observed myopathy[69,70]. However, how the undegraded material accumulates and causes the observed cellular and organ pathology in many other LSDs remains unclear.

The accumulation of such undigested macromolecules or monomers in LSDs instigates the formation of secondary products, which ultimately escape from the endosomal–autophagic–lysosomal pathways[9,71] and lead to multiple consequences that affect most organs, including the brain, liver, spleen, heart, eyes, muscles and bone (TABLE 2). Most, if not all, organelles are altered in LSDs, including endosomes, autophagosomes and lysosomes, and their functions in lysosomal formation/reformation and fusion of endosomes or autophagosomes to lysosomes are abnormal. Alterations in several autophagy processes have also been described in LSDs. Thus, deregulated mitophagy, which results in the accumulation of damaged mitochondria, occurs in LSDs, leading to major inflammatory consequences in specific tissues[67,72]. Perturbations in mitochondrial dynamics are frequently observed, which have been linked to the increased production of reactive oxygen species, ATP production and $Ca^{2+}$ imbalance. In LSDs, reduced macroautophagy activity (with a decreased autophagic flux) rather than hyperactive autophagy processes, as seen in numerous autoimmune diseases, seems to be responsible for the accumulation of non-degraded cytoplasmic proteins such as α-synuclein, huntingtin (HTT) and others[73]. Mucolipidosis type IV (TABLE 2), a disease characterized by severe neurological and ophthalmological abnormalities, is caused by mutations in the *MCOLN1* gene and is inherited in an autosomal recessive manner. This gene encodes a non-selective cation channel, mucolipin 1, which has recently been shown to be required for efficient fusion of both late endosomes and autophagosomes with lysosomes[74,75]. Impaired autophagosome degradation results in the accumulation of autophagosomes in LSDs[76]. Microautophagy processes that do not involve de novo synthesis of nascent vacuoles also appear to be impaired in LSDs, and were notably revealed in primary myoblasts from patients with the muscle-wasting condition Pompe disease[77]. Finally, defective CMA components, such as LAMP2A, could also lead to lysosomal dysfunction. For example, mutations in the *LAMP2* gene have been claimed to cause Danon disease (inherited in an X-linked dominant pattern)[51]. Further investigations are needed to support this assertion.

Table 1 | **Approved enzyme replacement therapies for lysosomal storage disorders**

| Lysosomal storage disorder | Defective enzyme | Enzyme replacement therapies |
|---|---|---|
| Type 1 Gaucher disease | β-GCase | Imiglucerase, velaglucerase alfa and taliglucerase alfa |
| Fabry disease | α-Galactosidase A | Agalsidase beta and agalsidase alfa |
| Late infantile neuronal ceroid lipofuscinosis type 2 (CLN2 disease) | Tripeptidyl-peptidase 1 | Cerliponase alfa |
| MPS I (Hurler–Scheie and Scheie syndromes) | α-Iduronidase | Laronidase |
| MPS II (Hunter syndrome) | Iduronidase-2-sulfatase | Idursulfase and idursulfase beta |
| MPS IV (Morquio syndrome A) | *N*-acetylgalactosamine-6-sulfate sulfatase | Elosulfase |
| MPS VI (Maroteaux–Lamy syndrome) | *N*-acetylgalactosamine-4-sulfatase (arylsulfatase B) | Galsulfase |
| MPS VII (Sly syndrome) | β-Glucoronidase | Vestronidase alfa |
| Pompe disease | α-Glucosidase | Alglucosidase alfa |
| Wolman disease | Lysosomal acid lipase deficiency | Sebelipase alfa |

GCase, glucocerebrosidase; MPS, mucopolysaccharidosis.

### *Autoimmune disorders*

Lysosomes are involved in pathways central to the immune system, including the degradation of intracellular and extracellular material, plasma membrane repair, cell death signalling, cell homeostasis and death. Although the direct involvement of lysosomes in immunity is far from fully understood, it has long been expected that lysosome dysfunction will have a major impact in immune diseases (TABLE 2). Strikingly, however, this field has not been extensively explored. However, elevated levels of lysosomal enzyme activity have been reported to occur in several autoimmune diseases, such as RA, systemic lupus erythematosus (SLE), dermatomyositis and psoriasis[3,14,17,18,20–23].

As discussed, autophagosomes formed during the autophagy process must fuse with lysosomes to generate

Table 2 | **Selected diseases associated with lysosomal dysfunction**

| Disease | Lysosomal dysfunction | Observations/comments |
|---|---|---|
| ***Lysosomal storage disorder***[a] | | |
| Aspartylglucosaminuria | Aspartylglucosaminidase | Accumulation of unmodified aspartylglucosamine in lysosomes cause progressive mental health problems with skeletal and connective tissue abnormalities in humans[45,46] |
| α-Mannosidosis | α-D-Mannosidase | Caused by genetic mutation in the gene *MAN2B1* (REF.[47]) |
| | | Reduction of α-D-mannosidases causes reduced lysosomal breakdown of mannose-based oligosaccharides in many tissues[47] |
| | | Inherited LSD characterized by immune deficiency (susceptibility to infections including pulmonary infections), facial and skeletal abnormalities, hearing impairment and intellectual deficit[47] |
| Fabry disease | α-Galactosidase | Reduced lysosomal metabolism of α-galactosyl lipids, globotriaosylceramides, causes vascular diseases (cardio, cerebro and renal diseases) in patients[45,46] |
| Gaucher disease (types 1, 2 and 3) | β-GCase | Accumulation of glucosylceramides in leukocytes (especially in macrophages) leads to abnormalities in the visceral organs (type 1) and neurological defects in both children and adults (types 2 and 3)[45,46] |
| GM1 gangliosidosis | β-Galactosidase | Abnormal lysosomal storage of GM1-ganglioside (oligosaccharides) causes skeletal manifestations and neurological impairment in humans[45,46] |
| Krabbe disease (globoid cell leukodystrophy) | Galactocerebrosidase | Defects in the galactocerebrosidase provoke accumulation of galactosylceramide and galactosylsphingosine (psychosine). Patients' brain histology shows myelin loss, neuroinflammation and axonal degeneration[48] |
| Metachromatic leukodystrophy | Arylsulfatase A or saposin-B (activator protein; rare cases) | Defects in the enzymes lead to the accumulation of sulfogalactosylceramide in major organs. It affects the different age groups of humans with development signs and symptoms of the disease[45,46] |
| Mucopolysaccharidoses | Enzymes involved in mucopolysaccharide catabolism | Accumulation of mucopolysaccharides within lysosomes leads to skeletal and joint abnormalities in humans[45,46] |
| Multiple sulfatase deficiency | SUMF1 (formylglycine-generating enzyme needed to activate sulfatases) | Abnormal accumulation of multiple, including sulfated, glycosaminoglycans causes neurodegeneration and psychomotor retardation in humans[46] |
| Pompe disease | α-Glucosidase | Accumulated undegraded glycogen in the muscles and peripheral nerves was observed in humans[45,46] |
| Sandhoff disease | β-Hexosaminidase A and B | Enzyme defects cause GM2-ganglioside accumulation in lysosomes, which induces nervous system damage in humans[45,46] |
| Mucolipidosis (type II and III) | *N*-acetyl glucosamine phosphoryl transferase α/β | Enzyme deficiency results in accumulation of unphosphorylated glycoproteins, which causes motor function and neurological disorders in humans[45] |
| Mucolipidosis IV | Mucolipin-I | Defects in this lysosomal membrane protein ($Ca^{2+}$ channel) cause accumulation of mucopolysaccharides and lipids, thereby resulting in hepatosplenomegaly, dysmorphic features and neurological disorders in humans[45] |
| Cystinosis | Cystinosin (cysteine transporter) | Defects in this lysosomal transporter, cystinosin, cause accumulation of cystine in different organs, first in kidneys and later in other organs in humans[45,46] |
| Danon disease | LAMP2 | Defects in LAMP2 (especially LAMP2B) cause accumulation of glycogen and other autophagic components in cardiomyocytes of humans, which results in cardiac diseases[50] |
| | | LAMP2B is highly expressed in the brain, cardiac and skeletal muscles[51] |
| Free sialic acid storage disorder | Sialin | Defects in this sialic acid transporter cause accumulation of free sialic acid in organs, which ultimately leads to different disorders (muscular, cerebellar, CNS and other) in humans[52] |
| NPC1 | Membrane protein involved in lipid transport | Defects in Niemann–Pick C1 and C2 proteins lead to accumulation of cholesterol and glycosphingolipids in lysosomes and cause hepatic, pulmonary and neuropsychiatric disorders in humans[45,46] |
| NPC2 | Soluble cholesterol-binding protein | |
| ***Autoimmune diseases*** | | |
| SLE | Lysosomal maturation | Lysosome fragility in humans was observed[53] |
| | | Macrophages with impaired lysosomal maturation were observed in lupus (MRL/lpr) mice[54] |
| SjS | Abnormal elevated levels of lysosomal enzymes (glycosidases and proteases) | Observed in the leukocytes of patients with SjS[55] |
| | | Defective autophagy processes observed in SGs of MRL/lpr mice[56] |
| Crohn's disease | Abnormal lysosomal pH | Deregulation of proton-sensing G protein-coupled receptor (GPR65) was observed in both mice and human[57] |

Table 2 (cont.) | **Selected diseases associated with lysosomal dysfunction**

| Disease | Lysosomal dysfunction | Observations/comments |
|---|---|---|
| ***Autoimmune diseases (cont.)*** | | |
| Rheumatoid arthritis | Lysosomal hydrolases | In humans, different cathepsins, acid phosphatases and others are involved in the inflammation and joint damage[58] |
| CIDP | Alterations in the lysosomal CMA pathway | Increased LAMP2A expression was observed in mice sciatic nerves[59] |
| Multiple sclerosis | Lysosomal acidification | Defects in the lysosomal compartment lead to defects in lipid droplet degradation in human neuronal cells[60] |
| ALS | Defects in endo-lysosomal trafficking | Spinal cord motor neurons of sporadic patients with ALS were shown positive for autolysosomal inclusions[61] |
| | | Mouse spinal cord motor ($hSOD1^{G93A}$)-mimicking human disease model showed lysosomal defects and impaired mitophagy[61] |
| ***Neurodegenerative diseases*** | | |
| Alzheimer disease | Unbalanced lysosomal luminal pH | In humans, defective presenilin-1 dependent v-ATPase function was observed in the case of lysosomal acidification. Lysosomal non-specific cathepsins generate the β-amyloid protein and hyperphosphorylated tau proteins[62,63] |
| Parkinson disease | Alterations in the lysosomal CMA pathway | Selective loss of GCase in lysosomes relates to the decreased amount of LAMP2A and increased cathepsins A and D in humans[64] |
| Huntington disease | Alterations in the lysosomal transport pathway | Polyglutamine-expanded huntingtin protein accumulation changes the lysosomal enzyme activity and TFEB expression in mice. In addition, accumulation of lipofuscin (non-degradable intra-lysosomal polymer) in neuronal lysosomes prevents clearance[65] |

This list is not exhaustive; it highlights representative families of pathological indications in which lysosomal dysfunctions have been described. ALS, amytrophic lateral sclerosis; CIDP, chronic inflammatory demyelinating polyneuropathy; CMA, chaperone-mediated autophagy; CNS, central nervous system; GCase, glucocerebrosidase; LAMP2, lysosome-associated membrane protein 2; LSD, lysosomal storage disorder; MRL, Murphy Roths Large; NPC, Niemann–Pick disease type C; SG, salivary gland; SjS, Sjögren's syndrome; SLE, systemic lupus erythematosus; TFEB, transcription factor EB; v-ATPase, vacuolar-type proton adenosine triphosphatase. *The presentation of the successive sections follows the text, namely, LSDs, autoimmune diseases and neurodegenerative diseases.

peptide epitopes for further processing, clear possibly deleterious apoptotic debris, fuel the amino acid pool and produce energy (FIG. 1). Any deviation in this complex processing will affect crucial immune cell functions, such as the control of cytokine release, autoimmune cell anergy and programmed cell death of type I (apoptosis) and type II (autophagy). Secretory lysosomes regulate the release of both pro-inflammatory and anti-inflammatory cytokines, in a process that is dependent on the type of stimulation. In addition, lysosomes degrade glucocorticoid receptors, which are essential to bind glucocorticoids, although the reasons are not known[78]. In this complex system, lysosomes execute anti-inflammatory action via the phospholipase A2 and cyclooxygenase-2 pathways, and also induce inflammation through the IL-1β–caspase-1 pathway. In both conditions (pro-inflammatory and anti-inflammatory), lysosomes act as indirect precursors for autoimmunity. However, induction and suppression of inflammatory signals are stimulus dependent[78].

Lysosomal cathepsins have a central role in degrading biological macromolecules in the lysosomes and in the immune response. There are approximately 12 members in this large protease family, most of which are endopeptidases that can cleave peptide bonds of their protein substrates[79,80]. Cathepsins A and G are serine proteases, cathepsins D and E are aspartic proteases and cathepsins B, C, F, H, K, L, O, S, V, X and W are cysteine proteases. For example, cathepsin S is responsible for the degradation of antigens (and autoantigens) in antigen-presenting cells (dendritic cells, macrophages and B cells), and is therefore involved at an upstream level in the presentation of MHCII–(auto)antigenic peptide complexes to $CD4^+$ T cells[81]. Cathepsin L preferentially cleaves peptide bonds with aromatic residues in the P2 position and hydrophobic residues in the P3 position. It is central in antigen processing, bone resorption, tumour invasion and metastasis, and turnover of intracellular and secreted proteins involved in growth regulation. Cathepsin L-deficient mice display less adipose tissue, lower serum glucose and insulin levels, more insulin receptor subunits, more glucose transporter type 4 and more fibronectin than wild-type controls[82]. Cathepsin G is primarily known for its function in killing and digestion of engulfed pathogens[83]. It is also involved in connective tissue remodelling at sites of inflammation[84]. Anti-neutrophil cytoplasmic antibodies reacting with cathepsin G have been identified in some patients with SLE[85].

### *Lupus*

Abnormal antigen processing and presentation is known to be one of the upstream events that perturb immune responses in SLE[86]. Because this process is mediated through lysosomes, it was rational to speculate that lysosomal functions could be altered in lupus. Interestingly, hypotheses were raised in the 1960s on the 'lysosomal fragility' in lupus, but without much further pursuit[87]. The composition and fluidity of the lysosomal membrane are effectively crucial in the regulation of lysosomal fusion with other vesicular organelles and for lysosomal uptake of macromolecules. The integrity of the lysosomal membrane also ensures the prevention of release of lysosomal enzymes into the cytoplasm. Some lysosomal enzymes released from 'fragile' lysosomes were regarded potentially harmful in lupus[88].

Case 1:23-cv-00328-JLH-SRF Document 125 Filed 02/20/24 Page 9 of 73 PageID #: 4316

Lysosomes are abnormal in splenic B cells from Fas-deficient Murphy Roths Large (MRL)/lpr mice, a mouse model of lupus, compared with B cells from healthy CBA/J mice[89]. TFEB expression was increased, indicating an enhanced biogenesis of lysosomes, and the lysosomal volume was raised. The expression levels of LAMP1 and cathepsin D were also increased. These results reinforce previous data showing that the expression and activity of some lysosomal enzymes (such as cathepsins S, L and B) that play important roles in antigen processing are altered in lupus and other autoimmune diseases[90,91].

Substantial variations of the acidic endo-lysosomal pH also occur in MRL/lpr mice, being raised by 2 pH units in splenic B cells[53,92]. This pH change could dramatically influence the activity of soluble lysosomal hydrolases (such as cathepsins) as well as lysosomal membrane proteins (such as LAMPs) that are critical for lysosome activity. pH may also affect the elimination of immune complexes that accumulate in lupus as a result of deficits in complement, lower expression of scavenger receptors, increased expression of Fcγ receptors and other reasons[93]. These immune complexes, which contain non-selective IgG antibodies or autoantibodies associated with autoantigen (including some apoptotic debris), can initiate inflammation of tissues once deposited (for example, in the kidneys and the skin) and generate a cascade of deleterious effects, such as the release of harmful cytokines and chemokines[54].

Recent studies have highlighted the key role of mammalian target of rapamycin complex 2 (mTORC2) in the disruption of lysosome acidification that occurs in this process[94]. In normal conditions, the regulation of lysosomal acidification requires cleavage of the RAB small GTPase RAB39a, occurring on the surface of phagocytic vesicles by locally activated caspase-1[94]. This finely regulated process requires the association of cofilin with actin that surrounds the vesicle and recruits caspase-11, which then activates caspase-1 (REF.[94]). In lupus-prone macrophages, chronically active mTORC2 enhances cofilin phosphorylation, thereby hampering its association with actin and affecting the downstream cascade of events leading to the appropriate acidification of lysosomes[94]. The importance of mTORC1 and mTORC2 has been established earlier in lupus T cells, and in particular, in this context, mTORC1 activity was increased whereas mTORC2 activity was reduced[95].

In addition, lysosomal cathepsin K was seen to contribute to the pathological events that develop in *Fas*$^{lpr}$ mice, another model of lupus disease, in part through its activity in TLR-7 proteolytic processing and subsequent effects on regulatory T cells. Cathepsin K-deficiency in *Fas*$^{lpr}$ mice reduced all kidney pathological manifestations (glomerulus and tubulointerstitial scores, glomerulus complement C3 fraction and IgG deposition, chemokine expression and macrophage infiltration) and decreased the levels of potentially pathogenic serum autoantibodies[96].

In line with these internal alterations of lysosomes, notably those related to cathepsin functioning, deregulation of autophagy has been reported to contribute to lupus pathology[92,97–100]. Autophagy failures have been described in the lymphocytes of MRL/lpr mice and (NZBxNZW)F1 mice[56,92,97,101] (two spontaneous murine models of systemic autoimmunity of distinct genetic origins and that display different MHC haplotypes) as well as in T and B lymphocytes of patients with SLE[97,98,100]. Murine and human T cells from the peripheral blood showed a significant accumulation of autophagic vacuoles compared with normal[97]. The underlying reasons for the dysfunctions in autophagy observed in lupus are not clearly understood, but several independent investigations have identified risk loci spanning autophagy-linked genes in patients with lupus[102–106].

### *Sjögren's syndrome*

Recent studies have demonstrated an increase in the level of macroautophagy in salivary gland T lymphocytes and in tears and conjunctival epithelial cells of patients with primary Sjögren's syndrome (SjS)[107,108]. Alteration of CMA activity was also recently found to occur in the salivary glands of MRL/lpr mice that develop a secondary SjS-like disease[56]. Lysosomes, which as discussed are mechanistically involved at the downstream level of both macroautophagy and CMA, were found to be altered in salivary glands. Flow cytometry analyses revealed that the mean pH of acidic vesicles in MRL/lpr salivary glands was significantly higher compared with those in mouse control glands and the ATP content was significantly diminished in MRL/lpr salivary gland cells[56]. Furthermore, amounts of several leukocyte glycosidases and proteases were revealed to be increased in leukocytes of patients with SjS in comparison with healthy controls[55]. Notably, raised levels of the lysosomal enzymes glucosidase, β-glucuronidase and dipeptidyl peptidase I are involved in the tissue injury in SjS[55]. Increased expression of lacrimal gland cathepsin S was also reported, which may have application as a diagnostic tool in SjS[91]. Two members of the RAS oncogene family, RAB3D and RAB27, were found to be implicated in the regulation of cathepsin S secretion levels in SjS[109]. In vitro studies on lacrimal gland acinar cells suggested further that secreted IFNγ from acinar cells increases cathepsin S expression and that IFNγ stimulated the MHCII-mediated antigen presentation in ocular pathogenesis of SjS[110].

### *Rheumatoid arthritis*

Lysosomal cathepsins have important roles in the induction and diagnosis of RA, and levels of several cathepsins (B, D, G, K, L and S) that are present in the serum and synovial fluid of patients have been proposed as a basis for RA diagnosis[111–116]. Cathepsin S and cathepsin L are highly expressed in synovial macrophages and thymic cortical cells. They each exert essential roles in the positive selection of T cells and antigen presentation, respectively, and participate in the local inflammation and matrix degradation that occurs in joints[116]. Cathepsin B is involved in collagen degradation, which leads to joint destruction in RA[112,117]. Expression of cathepsin G, which participates in joint inflammation through its chemoattractant activity, has been shown to be raised in the synovial fluid of patients with RA when compared with individuals with osteoarthritis[115]. Autoantibodies

Sjögren's syndrome
(SjS). A multifactorial systemic autoimmune disorder characterized by lymphocytic infiltrates in exocrine organs. Symptoms include dry eyes, dry mouth and parotid enlargement, and serious complications include fatigue, chronic pain, neuropathies and lymphomas.


DEFS00023221

Myasthenia gravis
Caused by antibodies targeting the muscle acetylcholine receptor or other neuromuscular junction proteins such as muscle-specific kinase. These antibodies compromise communication between nerves and muscles, leading to muscular weakness and fatigue.

Chronic inflammatory demyelinating polyneuropathy
(CIDP). A progressive autoimmune disorder in which peripheral nerves (roots and trunks) and brachial plexuses are damaged owing to demyelination. It causes muscle weakness, sensory loss and reduced reflexes.

Neuromyelitis optica
Also known as Devic's syndrome, this disease is characterized by an inflammation and demyelination of the optic nerve (optic neuritis) and the spinal cord (myelitis). Antibodies reacting with aquaporin-4 water channels in the brains of patients are implicated in neuromyelitis optica.

Amyotrophic lateral sclerosis
(ALS). Also known as motor neuron disease, this disease generally starts with muscle twitching and weakness in a limb, or slurred speech. It can affect control of the muscles needed to move, speak, eat and breathe, and can be fatal.

reacting with cathepsin G were also identified in patients with RA[85]. Compared with patients with osteoarthritis, cathepsin K expression was found to be elevated in RA[113], and genetic deletion of this particular cathepsin was shown to reduce inflammation and bone erosion in RA conditions via TLR mediation[113].

### *Neurological autoimmune diseases*

MS, myasthenia gravis, Guillain–Barré syndrome, chronic inflammatory demyelinating polyneuropathy (CIDP), neuromyelitis optica and neuropsychiatric lupus are neurological diseases induced by abnormal autoimmunity[62,119–123]. Neurological autoimmunity against various proteins, such as myelin in MS or *N*-methyl-D-aspartate receptor in neuropsychiatric lupus[62,123,124], can affect various structures within the CNS and peripheral nervous system, with diverse consequences. Although the exact cause of amyotrophic lateral sclerosis (ALS) still remains unknown, studies support the existence of autoimmune mechanisms, and ALS is therefore also included in this section. Indeed, autoantibodies against ganglioside GM1 and GD1a, sulfoglucuronylparagloboside, neurofilament proteins, FAS/CD95 and voltage-gated $Ca^{2+}$ channels have all been reported in patients with ALS (reviewed elsewhere[125]).

In general, the origin of the breakdown in immune tolerance that occurs in this set of neurological diseases is not known. Only recently have investigations discovered that autophagy processes are altered in some of these diseases[59,62,126–130]. In MS and in experimental autoimmune encephalomyelitis, an experimental model of MS, upregulation of the protein kinase mTOR has been described, and treatment with rapamycin/sirolimus (an immunosuppressant that inhibits mTOR and consequently stimulates macroautophagy) ameliorates some clinical and histological signs of the disease[131]. Increased levels of macroautophagy markers were measured in the blood and brain of patients with MS[122,132]. However, impaired macroautophagy was found in the spinal cord of experimental autoimmune encephalomyelitis mice[133]. In a rat model mimicking human CIDP, both macroautophagy and CMA processes were found to be hyperactivated in lymphatic system cells and non-neuronal cells (sciatic nerves) of peripheral nervous system cells[59]. In ALS, current data are conflicted[62]. Some data suggest an activation of macroautophagy processes with an accumulation of autophagosomes in brain tissues of patients with ALS, or an increase of autophagic vacuoles, aggregated ubiquitin and SOD1 proteins associated with MAP1LC3B-II in motor neurons of mice developing an ALS-like disease[134,135]. In contrast, other data suggest a reduction of autophagy activity[136,137]. Mutations in SQSTM1, valosin-containing protein, dynactin (a protein complex that activates the dynein motor protein, enabling intracellular transport) and RAB7 (a member of small GTPases that is important in the process of endosomes and autophagosomes maturation) have also been described in ALS[138–141]. Further studies are required to better understand the type and extent of autophagy dysfunction in this family of complex diseases.

There are only a few published studies on lysosomal dysfunction in neurological autoimmune diseases (TABLE 2). These notably include lysosome fragility, which was observed in patients with MS in the white matter of cerebral tissue, an area of the CNS that is mainly made up of myelinated axons[142]. Lysosome fragility was also suspected in SLE (see above) and other rheumatic autoimmune diseases, albeit in other organs[53,58,92]. As noted above, significant variations in lysosomal pH have been measured in autoimmune conditions such as lupus and SjS, but to our knowledge such studies conducted in the brain or elements of the peripheral nervous system of patients or animal models with neurological autoimmune diseases have not been published[78].

In CIDP, it has been shown that Schwann cells dedifferentiate into immature states and that these dedifferentiated cells activate lysosomal and proteasomal protein degradation systems[143,144]. Based on these observations, Schwann cells have been claimed to actively participate in demyelinating processes via this dedifferentiation process, but the mechanism involved remains undefined[145]. In the rat model of CIDP mentioned above, it was shown that LAMP2A expression was drastically increased in the sciatic nerve macrophages and reduced macroautophagy was observed in Schwann cells and macrophages[59].

In MS, studies conducted on white matter demonstrated that lysosomes are involved in myelin sheath degeneration as well as in the fragmented protein formation. Lysosomal swelling was observed near the degenerated materials of astrocytes[146], and an accumulation of lipids was found[60]. It has been hypothesized that lysosomal swelling/permeabilization might cause the release of hydrolases in the cytosol, where they affect native proteins[147].

In ALS, patients also show dysfunctions in the endo/lysosomal pathways, which affect both lower and upper motor neurons (TABLE 2). Cathepsin B was particularly found to be involved in the motor neuron degeneration, whereas cathepsins H, L and D were not significantly affected[148]. A cDNA microarray analysis on post-mortem spinal cord specimens of four sporadic patients with ALS revealed major changes in the expression of mRNA in 60 genes including increased expression of cathepsins B and D[149]. Several disease-causing mutations in genes related to autophagy have been identified, such as *SOD1*, *TDP643*, *FUS*, *UBQLN2*, *OPTN*, *SQSTM1* and *C9orf72* (RFFS[61,150]), but none of them code for lysosomal proteins. So, a crucial remaining issue is to clearly determine whether the lysosomal abnormalities that are observed are linked to intrinsic defaults of lysosomes or result from upstream dysregulation in autophagosome formation and fusion[61,62,151].

### *Neurodegenerative disorders*

Insufficient clearance of neurotoxic proteins by the autophagy–lysosomal network has been implicated in numerous neurodegenerative disorders[152]. In disorders such as AD, Huntington disease (HD) and PD, modified or misfolded proteins abnormally accumulate in specific regions of the brain. Accumulation of aggregated proteins is also seen in ALS (see above). These abnormal proteins form deposits in intracellular inclusions or extracellular aggregates, which are characteristic for

each disease[153–155]. Although there has been substantial research in this field, it is still unclear why sophisticated 'quality-control' systems, such as the lysosome–autophagosome system in particular, fail in certain circumstances to protect the brain against such protein accumulation[156].

In AD, one of the most common neurodegenerative disorders, some alterations in the endo/lysosomal pathways have been described (reviewed elsewhere[157,158]). The amyloid precursor protein (APP) is cleaved by β- and γ-secretases into amyloid-β peptide (Aβ) fragments, particularly Aβ40 and Aβ42 (REF.[159]). These fragments are found in the amyloid plaques that are one of the hallmarks of AD (the other being neurofibrillary tangles containing phosphorylated tau), and have been widely considered to have an important role in AD pathogenesis[156,160]. Cell-based experiments have demonstrated that lysosomal cathepsins have a role in the generation of Aβ peptides (through cathepsins D and E) and the degradation of Aβ peptides (by cathepsin B)[161]. Lysosomal dysfunction has been observed in patients with AD[162,163], and accumulation of the Aβ42 fragment in neuronal cells was shown to lead to lysosomal membrane alterations, which cause neuronal cell death[63]. In this context, it is noteworthy that inhibition of cathepsin D, which is involved in the lysosomal dysfunction and notably in the cleavage of the tau protein into tangle-like fragments, diminishes its hyperphosphorylation in the brain of patients with AD[164]. In addition, patients with AD with an inherited form of the disease may carry mutations in the presenilin proteins (PSEN1 and PSEN2), APP or apolipoprotein E, resulting in increased production of the longer form of the Aβ fragment (reviewed elsewhere[165]). Mutation of PSEN1, for instance, leads to direct disruption of the lysosomal acidification due to impaired delivery of the V0A1 subunit of v-ATPase, a proton pump responsible for controlling the intracellular and extracellular pH of cells. The acidification deficit causes excessive release of lysosomal $Ca^{2+}$ through TRPML1 channels, which has numerous deleterious effects[166]. These findings strongly support the hypothesis that dysfunction of endo/lysosomal pathways is pivotal in AD.

Approximately 15% of patients with PD have a family history of the disorder, although the underlying molecular mechanisms remain unclear. In the context of lysosomal dysfunction, it is notable that the most common of the known PD genetic mutations are in *GBA1* (encoding the lysosomal β-GCAse) — the same gene that underlies Gaucher disease — which are present in up to 10% of patients with PD in the United States[167]. *GBA1* mutations are also associated with dementia with Lewy bodies[167]. Several other genes linked to PD are directly or indirectly related to the endo/lysosomal machinery, such as mutations in *SNCA* (coding for α-synuclein)[63,168]. A hallmark of PD is the presence in neurons of protein inclusions called Lewy bodies, which are mainly composed of fibrillar α-synuclein. The α-synuclein protein is normally degraded by the lysosomes through the CMA pathway, but macro-aggregates of α-synuclein mutants, which display a longer half-life compared with the non-aggregated wild-type protein, are not degraded by this pathway and, rather, would be degraded via the macroautophagy pathway[169–172]. It was further shown that the mutant proteins bind to LAMP2A and inhibit the translocation of other substrates and, therefore, their final degradation[170]. Biochemical analyses suggest that α-synuclein is mainly degraded by lysosomal proteases and notably by cathepsin D, rather than by non-lysosomal proteases (for example, calpain I)[173,174]. Accumulation of α-synuclein was observed in cathepsin D-deficient mice, whereas, conversely, the accumulation of α-synuclein aggregates was reduced in transgenic mice that overexpressed this cathepsin, resulting in protection of dopaminergic neuronal cells from damage[175].

HD is a rare autosomal-dominant neurodegenerative disease caused by an aberrant expansion of CAG trinucleotide repeats within exon 1 of the *HTT* gene, which results in the production of aggregation-prone HTT mutants (mHTT) that are detrimental to neurons[176,177]. Whereas HTT has a protective role against neuronal apoptosis, accumulation of mHTT, however, induces pathophysiological consequences including lysosomal and autophagy dysfunctions. Thus, mHTT perturbs post-Golgi trafficking to lysosomal compartments by delocalizing the optineurin/RAB8 complex, which, in turn, affects lysosomal function[177]. Excessive mHTT induces accumulation of clathrin adaptor complex 1 in the Golgi and an increase of clathrin-coated vesicles in the vicinity of Golgi cisternae[177]. The activity of several cathepsins such as B, D, E, L and Z has also been linked to HD[63,80,174,177–179]. Cathepsin D is responsible for full degradation of HTT but is less efficient at degrading mHTT, which is processed by cathepsin L[180,181]. Cathepsin Z also cleaves HTT and elongated polyglutamine tracts[182,183]. Thus, lysosomal modulators acting on cathepsin activity might have beneficial effects in the treatment of HD. Notably, hyperexpression of cathepsin D (and cathepsin B) was shown to protect primary neurons against mHTT toxicity[179]. Alterations in macroautophagy, mitophagy and CMA have also been implicated in HD[184,185]. CMA activity was increased in response to macroautophagy failure in the early stages of HD[186], a result supported by the findings that HSPA8 and LAMP2A have important roles in the clearance of HTT[187] and that shRNA-mediated silencing of LAMP2A increased the aggregation of mHTT[188]. Other studies focusing on the HTT secretory pathway revealed that mHTT secretion is mediated by the $Ca^{2+}$-dependent lysosomal exostosis mechanism via the synaptotagmin 7 sensor in neuro2A cells[189]. The extracellular release of mHTT was efficiently inhibited by the phosphoinositide 3-kinase and sphingomyelinase inhibitors Ly294002 and GW4869. HD-dependent perinuclear localization of lysosomes was also demonstrated[190].

Increasing evidence thus implicates lysosomal (and autophagy) dysfunction in the pathogenesis of neurodegenerative disorders[62,63,127,128,130,191,192]. TFEB has received particular attention in this regard[193–195], with recent data suggesting that TFEB is selectively lost in patients with AD (as well as ALS)[196]. Increasing TFEB activity might therefore prevent neuronal death and restore neuronal function in certain neurodegenerative diseases, including PD[194].

Tau
A major microtubule-associated protein of a mature neuron. Hyperphosphorylated tau accumulates with ubiquitin in ageing neurons as the neurofibrillary tangles that were identified in numerous neurodegenerative diseases called tauopathies that include Alzheimer disease.



DEFS00023223

## Lysosomes as therapeutic targets

Given the evidence discussed above, the various lysosomal pathways and their components could represent potential pharmacological targets for a wide range of diseases. When considering lysosomes as targets, it is important to note the need for specificity; that is, agents that will not target all lysosomes, but will specifically target those lysosomes/lysosomal proteins that are defective in certain organs, tissues or cells. In addition, inhibitors or activators of lysosomal components may be required, depending on the disease context.

There has been considerable interest in therapeutically targeting different autophagy pathways, including lysosome-dependent pathways, and progress in the discovery and development of small molecules and biologics that target these processes has been reviewed extensively[11,119–122,197,198]. However, very few therapies that specifically target lysosomal components have so far been generated and found to be effective in clinical trials, with one general exception — the development of ERTs and small-molecule drugs for LSDs (BOX 1). This topic has recently been comprehensively reviewed[46] and so will not be discussed in depth here.

It is important to target lysosomes and not the whole autophagy process for several reasons. First, regarding safety, the integral role of lysosomes in several key physiological processes means that therapeutic windows for pharmacological intervention with unacceptable side effects may be limited. For example, azithromycin, an antibiotic with anti-inflammatory properties that is used in the treatment of patients with chronic inflammatory lung diseases such as cystic fibrosis, was found to block autophagy in macrophages, inhibiting intracellular killing of mycobacteria within them and, thereby, increasing the risk of mycobacterial infection[204]. Second, in some diseases, autophagy may be enhanced in certain tissues or organs but compromised in others, for example in the spleen and salivary glands of MRL/lpr mice[56]. This phenomenon makes it highly challenging to identify a single drug able to correct a failure, unless a cell-specific targeting molecule could be incorporated into the autophagy activator/inhibitor to enable tissue specificity[205]. Again, the precise targeting of lysosomes in specialized cells may circumvent the complexity of dysregulation mechanisms of autophagy processes in pathophysiological settings[14,56,206,207].

As indicated, the current arsenal of lysosome-specific targeted drugs is small. In fact, many drugs claimed to target lysosomal components have also been found to be capable of interacting with several non-lysosomal receptors, limiting their efficacy and safety[12]. One example is provided by chloroquine (CQ), a 4-aminoquinoline compound, and its derivative hydroxychloroquine (HCQ), which are widely prescribed to patients with rheumatic diseases, and historically also for the prophylaxis and treatment of malaria (FIG. 3). CQ and HCQ are lysosomotropic agents and as such they raise intralysosomal pH, thereby affecting overall lysosomal function and impairing autophagic protein degradation (FIG. 2). Although the mechanism of action of these agents is not fully elucidated, it is well established that CQ and HCQ display pleiotropic activity[208–210] and have important deleterious properties. In certain settings, they have been claimed to operate by interacting directly with TLR ligands and not through an effect on the lysosomal pH, for example[211]. Toxicity of CQ/HCQ, in particular in the eye (cornea and macula) and the occurrence of cardiomyopathies[212], remains a major limitation. The observed ocular toxicity is related to the total cumulative dose rather than the daily dose; therefore, it becomes a serious potential problem in the cases of long-term use. Several HCQ analogues and mimics have been designed that aim to retain the therapeutic activity without secondary effects[213,214].

Furthermore, most, if not all, of the small molecules that have so far been identified and investigated as modulators of autophagy and/or lysosomal functions exhibit complex pleiotropic properties affecting the overall function of lysosomes, and also different autophagy pathways (for example, mTOR-dependent and mTOR-independent pathways), as well as other quality-control mechanisms that affect the cell life/death balance. As discussed below, several widely used molecules exert dual, sometimes opposite, effects on upstream and downstream molecular events of the autophagy–lysosomal network.

Several robust assays to characterize autophagy activators and inhibitors, as well as lysosomal effectors, are currently available and validated (TABLE 3). However, each assay has inherent biases, and so it is necessary to use several independent, in vitro and in vivo approaches to ascertain the reactivity and specificity of novel molecules able to modulate these pathways (BOX 2).

In this regard, the tremendous work in recent years to establish international guidelines for standardizing research in autophagy — and, in particular, to propose relevant methodologies for monitoring autophagy that are accepted by the whole community — is unique[231,232]. A better definition of terms and concepts has also

### Box 1 | Enzyme replacement therapies for lysosomal storage disorders

Enzyme replacement therapy (ERT) for lysosomal storage disorders (LSD) involves administration of a functional version of the defective enzyme in the particular LSD. Following administration, the enzyme is delivered to the target cells (typically mediated by mannose or mannose-6-phosphate receptors), where it breaks down its substrate in lysosomes, thereby ameliorating the LSD[46].

The approach was pioneered with the use of glucocerebrosidase (GCase) purified from placentae in the 1980s to treat patients with Gaucher disease, and a recombinant version of GCase was then introduced in the 1990s[199]. Following the success of this approach in treating Gaucher disease, other recombinant enzymes have been approved for other LSDs, including Fabry disease, mucopolysaccharidosis (MPS) I, MPS II, MPS VI and Pompe disease (TABLE 1), and many further ERTs for other LSDs are in clinical trials[200].

Although ERT has provided an effective treatment for patients with some LSDs, it has limitations. Recombinant enzymes administered by intravenous injection are not able to cross the blood–brain barrier, and so are not effective for central nervous system manifestations of LSDs[201]. Low expression of the receptors that mediate delivery on the cell surface of target cells can also be a challenge for the effectiveness of ERT for some LSDs[46]. For example, in Pompe disease, the level of expression of mannose receptors on skeletal muscle cells is low, necessitating high doses of ERT to achieve a therapeutic effect[202]. Numerous developments are being studied to address such limitations, with a focus on enzyme modifications that enable better access of enzymes to their receptors and on nanomaterials that enable safe and efficient delivery of enzymes via intra-cerebroventricular/intrathecal administration[10,46,200,203].

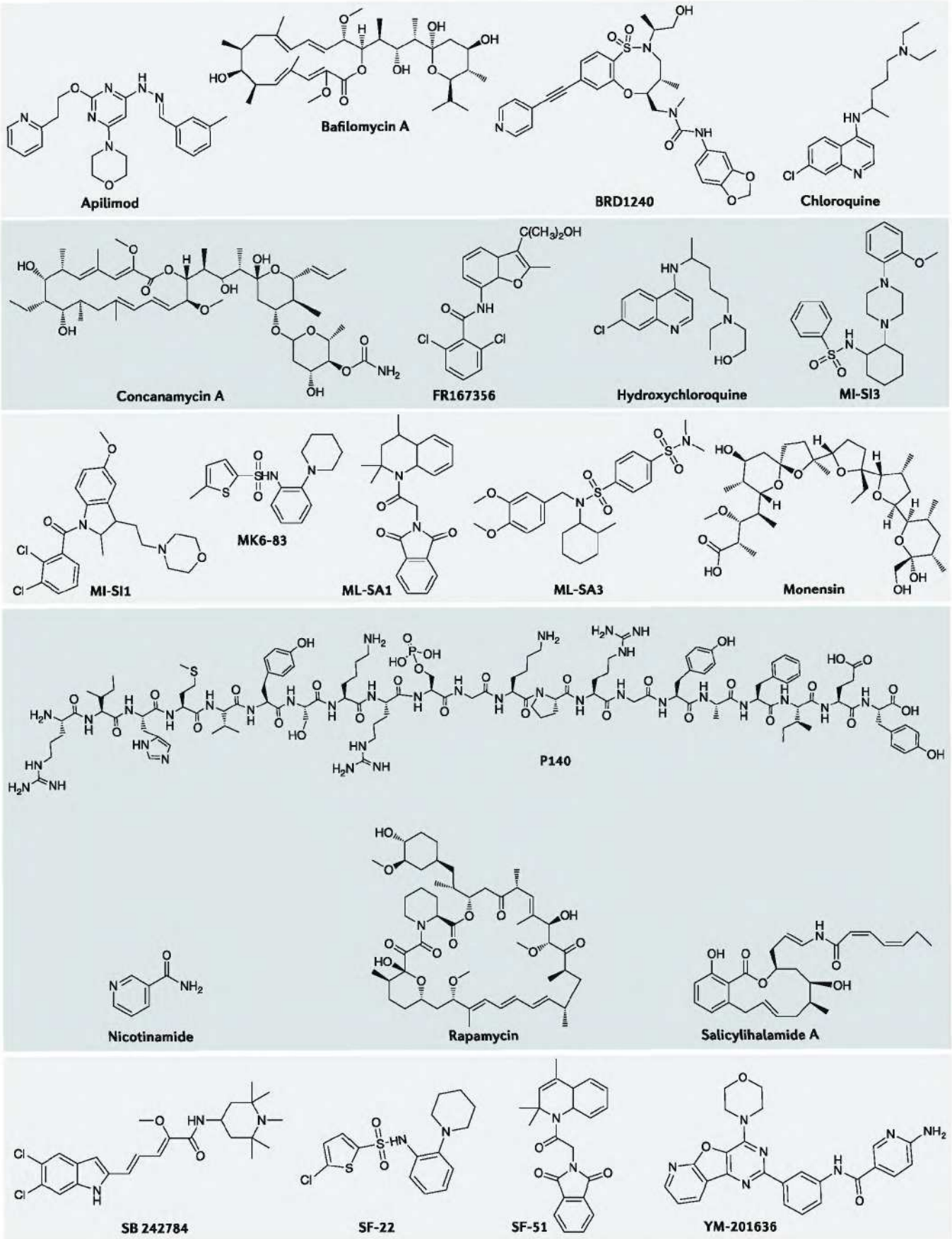
Apilimod
Bafilomycin A
BRD1240
Chloroquine
Concanamycin A
FR167356
Hydroxychloroquine
MI-SI3
MI-SI1
MK6-83
ML-SA1
ML-SA3
Monensin
P140
Nicotinamide
Rapamycin
Salicylihalamide A
SB 242784
SF-22
SF-51
YM-201636

Fig. 3 | **Structures of selected pharmacological molecules designed to correct lysosomal dysregulation in disease.** Small molecules and peptides highlighted in this figure are activators and inhibitors of lysosomal constituents targeting mechanistic target of rapamycin (mTOR), vacuolar-type proton adenosine triphosphatase (v-ATPase), TRPML1, PIK kinase and HSPA8. For details, see the text and accompanying tables.

been adopted by the community, leading to much easier understanding between researchers worldwide[233]. These guidelines and definitions should be used by investigators evaluating new molecules designed to selectively target key steps of autophagy or developing new high-throughput screening methods for autophagy-modulating pharmacological molecules. However, even the more sophisticated and detailed assays will not recapitulate the full complexity of integrated living systems, which can only be established in clinical trials.

### *Pharmacological regulators of lysosomal activity*

The pipeline of specific agonists and antagonists of autophagic activity is currently small, particularly for CMA (TABLES 4,5; FIGS 2,3). However, high-throughput screening programmes to identify such small molecules are ongoing, which should yield additional therapeutic targets and useful tools. Small molecules that specifically target lysosomes are even rarer (TABLE 4; FIG. 2). Small-molecule drugs developed specifically for particular LSDs, including substrate reduction therapies and small-molecule chaperones, have reached the market, but other small-molecule candidates for more common diseases are at an earlier stage of development. These molecules that more specifically act on lysosomes, some of which have been discovered by high-throughput screening, mostly target LAMP2A, various lysosomal enzymes such as cathepsins, acid sphingomyelinase, α-galactosidase A and acid β-glucocerebrosidase, and chaperones such as HSPA8 and β-*N*-acetyl hexosaminidase. Although not solely present in lysosomes, v-ATPase, a proton pump responsible for controlling the intracellular and extracellular pH of cells, and TRPML1, a cation channel located within endosomal and lysosomal membranes, are also pertinent targets.

Below and in TABLE 4, we summarize the availability of pharmacological tool compounds and progress in drug development, where applicable, for each broad target class.

***Substrate reduction therapies and small-molecule chaperones.*** In addition to ERTs for LSDs (BOX 1), drug discovery programmes have also focused on alternative small molecule-based approaches, which may be particularly relevant for LSDs that affect the CNS, due to the lack of blood–brain barrier penetration by ERTs[285].

Small molecules used in substrate reduction therapies prevent the accumulation of substrates of the defective enzymes in LSDs by inhibiting enzymes involved in substrate production[284]. Miglustat was the first such drug to be approved in the early 2000s by the US Food and Drug Administration and the European Medicines Agency for Gaucher disease and in 2009 for Niemann–Pick disease type C in Europe. This iminosugar inhibits glucosylceramide synthase (GCS), which catalyses the initial step in formation of many glycosphingolipids. Within cells, glycosphingolipids tend to localize to the outer leaflet of the plasma membrane; they cycle within the cell through endocytic pathways that involve the lysosome. Inhibition of GCS therefore reduces the deleterious accumulation of glycosphingolipids within lysosomes with potential therapeutic benefits in diseases like LSDs. Miglustat also inhibits disaccharidases in the gastrointestinal tract, resulting in diarrhoea as a side effect[285]. Eliglustat, another GCS inhibitor that does not penetrate the CNS, was also approved for Gaucher disease in 2014. Other GCS inhibitors in clinical development include lucerastat, a miglustat analogue with an improved safety profile that is currently in a phase III trial for Fabry disease (FD)[236,286], and ibiglustat, which penetrates the CNS. The latter is in clinical development for FD (phase II), for Gaucher disease type 3 (phase II) and for patients with PD who carry a mutation in *GBA* (phase II). Recent findings generated in a small number of patients have suggested a possible link between PD and FD[287], which also exists between patients with PD and Gaucher disease who have *GBA* mutations (see above). Finally, genistein, a pleotropic natural product that inhibits kinases involved in the regulation of proteoglycan biosynthesis and also affects TFEB function, is in a phase III trial for Sanfilippo syndrome[288].

Substrate mimetics that inhibit lysosomal enzymes have also been found to stabilize mutated enzymes in LSDs, thereby leading to restoration of some enzyme activity when suitable subinhibitory concentrations are used, as the enzyme remains stable and functional after dissociation of the inhibitor[46,283]. The pioneering example of this approach is migalastat, described above, that binds to the active site of α-galactosidase A, which is mutated in FD, and stabilizes the mutant enzyme. Other examples of this strategy include afegostat in Gaucher disease (which failed in a phase II clinical trial in 2009 due to lack of efficacy), pyrimethamine in Sandhoff disease and Tay–Sachs disease, and ambroxol in Gaucher disease with neurological symptoms (TABLE 4). Agents that are at earlier developmental stages include *N*-octyl-β-valienamine, a competitive inhibitor of β-glucosidase, for Gaucher disease; *N*-acetylcysteine for Pompe disease; α-lobeline, 3,4,7-trihydroxyisoflavone and azasugar in Krabbe disease; and *N*-octyl-4-epi-β-valienamine and 5*N*,6*S*-(*N*′-butyliminomethylidene)-6-thio-1-deoxygalactonojirimycin indicated in GM1 gangliosidosis[289]. The chemical structures of these pharmacological chaperones have been described recently[290,291]. Finally, an alternative strategy for stabilizing mutant enzymes, by binding away from the active site, is also being investigated. A promising example of this approach is NCGC607, a non-inhibitory small-molecule chaperone of GCase discovered by screening for molecules that improved the activity of the mutant enzyme[46,250]. Treatment with NCGC607 reduced lysosomal substrate storage and α-synuclein levels in dopaminergic neurons derived from induced pluripotent stem cells from patients with Gaucher disease with parkinsonism[46,250]. Further testing of NCGC607 in patients with PD and *GBA* mutations is awaited. Although promising, conflicting viewpoints still remain on the strength

Fabry disease
(FD). A progressive, X-linked inherited, multisystemic lysosomal storage disorder caused by *GLA* mutations, resulting in α-galactosidase deficiency and accumulation of lysosomal substrate.

of such small molecule-based approaches, primarily because these compounds bind to the catalytic site of enzymes, which may be a risk at high concentrations if they inhibit rather than increase activity[291,292]. More clinical trials are therefore required in order to analyse the robustness of this approach.

***Cathepsin modulators.*** Robust genetic and pharmacological preclinical investigations have consistently showed that regulating cathepsin activity can favourably improve pathological features in certain autoimmune and inflammatory diseases. Inhibitors of several cathepsins (B, D, L, K and S) have been described[174,293] and their activity has been evaluated in rheumatic autoimmune diseases (such as SLE, RA and SjS) and neurodegenerative disorders, notably in AD[294] (TABLE 4). Selective inhibition of cathepsin S with a potent active site inhibitor known as RO5461111 (Roche) mitigated disease in MRL/lpr lupus-prone mice, by reducing priming of T and B cells by dendritic cells, and plasma cell generation[262]. Promising data have also been generated in murine models, in the context of diabetic nephropathy and cardiovascular diseases[295]. Further studies based on cathepsin S inhibitors should evaluate the clinical safety and utility of treating patients affected by autoimmune and inflammatory diseases[295]. Cathepsin K, which is highly expressed by osteoclasts and very efficiently degrades type I collagen, the major component of the organic bone matrix, is also a potential target for modulating lysosomal dysfunction in some of the disorders discussed above, such as SLE[96]. Yet further investigations with selective cathepsin K inhibitors are required to determine whether this targeted strategy might apply in SLE and other inflammatory conditions in which articular manifestations are a major component (RA, ankylosing spondylitis, psoriatic arthritis and others). It should be noted, however, that various cathepsin K inhibitors have been pursued for postmenopausal osteoporosis, including odanacatib (Merck) which reached phase III trials[296]. Although odanacatib was effective, its development was discontinued in 2016 due to an increased risk of stroke in treated patients. Other cathepsin inhibitors and their context of clinical evaluation are listed in TABLE 4.

Despite multiple efforts to develop selective pharmacologic cathepsin modulators, important concerns still

Table 3 | **Measurements used to assess lysosomal dysfunction**

| Lysosomal characteristic | Methods | Comments |
|---|---|---|
| Total volume (number and size) | Fluorescence measurement (flow cytometry or fluorescence microscopy) of cellular staining of acidotropic dyes, such as LysoTracker dyes[92,215] | Simple to use but is not quantitative as stated by the manufacturer; can be adapted to clinical trial settings |
| | Western blot and fluorescence imaging of lysosomal markers such as LAMP1, LAMP2 etc.[216,217] | Simple but does not provide information on subcell populations[89]; can be adapted to clinical trial settings |
| | Electron microscopy[218] | Provides morphological information but laborious and semiquantitative |
| Biogenesis and activation status | Western blot and qPCR of TFEB (and also other family members)[219,220] | Simple but does not provide information on subcell populations; can be adapted to clinical trial settings |
| | Fluorescence imaging of the nuclear translocation of TFEB-GFP[219] | Limited usage in primary cells as they are hard to transfect |
| pH | Ratiometric fluorescence measurement with LysoSensor Yellow/Blue[92,221] or Oregon-Green 488 dye[222] | The dyes can have an alkalinizing effect on lysosomes and affect the accuracy of results[223] |
| Degradation ability | Fluorescence measurement of the degradation of labelled BSA (DQ-BSA Green/Red)[97] | Requires loading of BSA molecules to lysosomes by endocytosis and could potentially interfere with normal lysosomal function[224] |
| Protease expression | Western blot measurement of cathepsins[92], thiol reductase etc. | Simple but does not provide information on subcell populations; can be adapted to clinical trial settings |
| Protease activity | Fluorescence measurement of the cleavage of cathepsin substrates by Magic Red Cathepsin (B, K and L) kit[225] | N/A |
| Membrane stability | Membrane stability assay with acridine orange[226] | Phototoxic and stains nucleus as well[227] |
| Membrane integrity | Lysosomal galectin puncta assay[224] | N/A |
| | Cell fractionation to detect lysosomal content in cytosol[216] | Limited sensitivity as it fails to detect small amounts of lysosomal content[224] |
| Local calcium level | Live cell imaging of genetically encoded $Ca^{2+}$ indicator: GCaMP3-ML1[34] | Limited usage in primary cells as they are hard to transfect |

BSA, bovine serum albumin; LAMP, lysosome-associated membrane protein; N/A, not available; qPCR, quantitative PCR; TFEB, transcription factor EB.



DEFS00023227

**Box 2 | Methods to examine lysosomal dysfunction in disease**

Several parameters have been used to evaluate lysosomal functions (TABLE 2). Alteration of lysosomal volume is an important sign of lysosomal dysfunction; it has been observed in various diseases, such as autoimmune syndromes, cancers and lysosomal storage diseases[215]. It can be measured by staining cells with acidotropic dyes such as LysoTracker dyes and immunoblot of lysosomal membrane proteins such as lysosome-associated membrane protein 1 (LAMP1). Variation of lysosomal volume is often related to changes in lysosomal biogenesis, which can be assessed by the expression level and cellular location of transcription factor EB (TFEB). However, precise determination of lysosomal functions relies on measurement of lysosomal luminal pH and degradation activity. Several fluorescence probes that measure lysosomal pH (TABLE 2) are commercially available. Abnormal lysosomal pH affects lysosomal degradation activity, which can be followed, for example, by detecting the degradation of endocytosed fluorescence DQ-BSA[57]. In complement, the activity of specific enzymes, such as cathepsins B, D and L, can be tested using commercially available kits. Other lysosomal parameters can be evaluated to deepen the examination of lysosomal status, including lysosomal membrane stability and integrity and lysosomal $Ca^{2+}$ ion signalling, for example (TABLE 2). Lysosomal function is essentially linked with autophagy activity as autophagy is a lysosomal-dependent degradation pathway. Thus, a series of methods routinely applied for assessing macroautophagy in mouse models and patients with autoimmune diseases is summarized[89]. To ascertain the extent of autophagy defects, a combination of techniques, such as western blot and flow cytometry, measurement of autophagy makers, fluorescent imaging and electron microscopy, in the presence and absence of lysosomal protease inhibitors, is recommended. Several review articles have described reliable methods dedicated to the measurement of chaperone-mediated autophagy (CMA) activity[228–230]. Increased expression levels of LAMP2A and HSPA8, two key players in CMA, have been shown to occur in a mouse model of lupus[92]. However, it should be noted that increased expression levels of HSPA8 and LAMP2A starting from a total lysate is only indicative of CMA upregulation; this test is not sufficient to allow any firm conclusion, and it is necessary to examine their expression levels in purified lysosomes or in lysosome-enriched fractions.

remain with regard to off-target effects due to activity against other cathepsins or towards cathepsins present at non-relevant or unwanted sites. Nonetheless, the underlying biology and clinical effects of certain cathepsin inhibitors or activators remain of considerable interest and could guide future therapeutic approaches.

***v-ATPase inhibitors.*** As reported below, v-ATPase, a multisubunit ATP-driven proton pump, is best known for its role in acidification of endosomes and lysosomes. Regulating the function of v-ATPase may impact lysosomal activity and, hence, the acidification of specialized cells and diverse signalling pathways, such as autophagy. v-ATPase inhibitors like bafilomycin A1 and concanamycin A are non-selective compounds (TABLE 4; FIG. 3) that inhibit both mammalian and non-mammalian v-ATPases, which control the lysosomal pH of acidic vesicles via a manner that is not fully understood (FIG. 2). Through this mechanism, bafilomycin A1 inhibits autophagic flux by preventing the acidification of endosomes and lysosomes[297]. Bafilomycin and CQ also affect mitochondrial functions, as discovered recently using intact neurons[298]. Benzolactoneenamides (salicylihalamide A, lobatamides and oximidines; TABLE 4; FIGS 2,3) are much more selective v-ATPase inhibitors[299] than bafilomycin A1 and concanamycin A, but also much less potent. Further investigations into v-ATPase regulation of signalling pathways are needed to identify specific and safe molecules that regulate this vital proton pump[300].

***Ion channel modulators.*** As discussed above, lysosomal ion channels are master elements of lysosome activity and, thereby, of cell homeostasis. In the family of TRP channels, TRML1 is essential, being widely expressed in late endosomes and lysosomes, and preferentially associates with LAMP1 in the lysosomal membrane[22,301,302]. Genetic mutations leading to inactivation of TRPML1 cause a rare genetic disorder called mucolipidosis type IV (MLIV). Pharmacological activation of TRPML1 ameliorated some lysosomal functions that are classically associated with MLIV, NPCs and certain LSDs (TABLES 2,4; FIG. 2). Thus, the small molecule SF-22 (FIG. 3), which was identified in a screen for TRPML3 activators, was defined as an activator of both TRPML3 and TRPML1 (REF.[274]), and displayed an additive effect in combination with the endogenous activator phosphatidylinositol-3,5-bisphosphate (PtdIns(3,5)P2)[274,303]. An analogue of SF-22, in which chlorine on the thiophene had been replaced by a methyl group, showed greater efficacy on TRPML1 activation[303,304]. Another molecule called ML-SA1 (FIGS 2,3), acting as a mucolipin synthetic agonist, also showed an additive effect with endogenous PtdIns(3,5)P2 on TRPML1 channels[305]. It is important to note that in neurological diseases, as well as in other indications in which lysosomal acidification is defective (see above), interfering with TRML1 may have contraindications.

***Phosphatidylinositol kinase modulators.*** A central modulator of lysosomes is the lipid kinase FYVE finger-containing phosphoinositide kinase (PIKfyve), which converts phosphatidylinositol-3-phosphate into PtdIns(3,5)P2. The latter regulates $Ca^{2+}$ release from the lysosome lumen and is required for acidification by v-ATPase. Inactivation of PIKfyve leads to many pathophysiological problems including neurodegeneration and immune dysfunction, mostly related to impaired autophagic flux and alteration of lysosomes (trafficking, $Ca^{2+}$ transport, biogenesis and swelling)[306]. The small-molecule apilimod (FIG. 3; TABLE 4) was originally identified as an inhibitor of TLR-induced IL-12 and IL-23, and later found to be a highly specific inhibitor of PIKfyve[276]. Apilimod was evaluated in clinical trials involving several hundred patients with T helper 1 and T helper 17 cell-mediated inflammatory diseases such as Crohn's disease, RA and psoriasis[277,278]. It was well tolerated in more than 700 human subjects (normal healthy volunteers and patients with inflammatory disease), but the clinical trials did not meet their primary endpoints and further development was abandoned. Apilimod is currently being evaluated in a clinical trial (NCT02594384) aimed at defining a maximum tolerated dose in patients with B cell non-Hodgkin lymphoma and monitoring safety, pharmacokinetics, pharmacodynamics and preliminary efficacy[307]. YM-201636 is another selective inhibitor of PIKfyve (TABLE 4; FIG. 3). This inhibitor contains a FYVE-type zinc finger domain. YM-201636 was found to significantly reduce the survival of primary mouse hippocampal neurons in culture and reversibly impair endosomal trafficking in NIH3T3 cells, mimicking the effect produced by depleting PIKfyve with small interfering RNA. It was also found to block retroviral exit by budding

Table 4 | **Pharmacological modulators of lysosome functions: targets and disease indication**

| Pharmacological agent/company | Mechanism | Stage of development | Comments |
|---|---|---|---|
| ***LSD substrate reduction therapy*** | | | |
| Miglustat/Actelion | Inhibitor of GCS | Marketed | Used in various LSDs, Gaucher disease and NPC; therapeutic efficiency in long-term studies in Gaucher disease type 1 with adverse effects like gastrointestinal discomfort, tremors and weight loss[234] |
| Eliglustat/Genzyme | Inhibitor of GCS | Marketed | Does not cross the blood–brain barrier; used in non-neuronopathic Gaucher disease; superior efficacy to miglustat and other treatments in type 1 Gaucher disease[235] |
| Lucerastat/Idorsia Pharmaceuticals | Inhibitor of GCS | Phase III | Miglustat analogue with lesser side effects; 1,000 mg two times a day for 12 weeks was highly tolerable in patients with Fabry disease[236]; effective in a mouse model of GM2 gangliosidosis with improved neurological performance[237] |
| Ibiglustat/Genzyme | Inhibitor of GCS | Phase II | Clinically evaluated in Fabry disease, Gaucher disease type 3 and Parkinson disease; efficient in neuropathological and behavioural outcomes associated with Gaucher disease[238] |
| Genistein | Kinase inhibitor | Phase III | Inhibition of glycosaminoglycans in fibroblasts from patients with MPS III; improved hair morphology and cognitive functions in patients with MPS IIIA and IIIB[239]; TFEB function modulator[240] |
| Odiparcil (IVA336)/ Inventiva Pharma | Inhibitor of glycosaminoglycans accumulation | Phase II | Improved clinical symptoms in MPS VI mice[241]; superior biodistribution in comparison with enzyme replacement therapies[241]; phase II clinical trial in patients with MPS VI ongoing (NCT03370653) |
| ***LSD chaperone therapy*** | | | |
| Migalastat/Amicus Therapeutics | Assists α-galactosidase A conformation | Marketed | Oral chaperone therapy for Fabry disease by increasing catalytic enzyme activity; efficacious against mostly patients with *GLA* gene mutations |
| Afegostat (isofagomine)/ Amicus Therapeutics and Shire plc | Inhibitor of β-glucosidase | Failed in phase II | Binds to N370S glucocerebrosidase mutant; assists in the folding and transportation of enzymes from the endoplasmic reticulum to lysosomes[242]; pH-dependent activity |
| Pyrimethamine | Competitive inhibitor of β-hexosaminidase | Phase I | Effective in Sandhoff and Tay–Sachs diseases; binds selectively to the active site of domain II in β-hexosaminidase; side effects at >75 mg per day |
| Ambroxol (Mucoslovan)/ Boehringer Ingelheim | pH-dependent effect on β-glucosidase | Suspended phase I/II | Effective in Gaucher disease with improved neurological symptoms; a GCase chaperone, which also acts on other pathways, such as mitochondria, lysosomal biogenesis and the secretory pathway[243] |
| *N*-Octyl-β-valienamine | β-GCase inhibitor | Preclinical | Epimer of *N*-octyl-4-epi-β-valienamine for Gaucher disease |
| *N*-Acetylcysteine | Assists α-glucosidase in a pH- and temperature-dependent manner | Preclinical | Allosteric chaperone active in Pompe disease[244] |
| 5-(4-(4-Acetylphenyl) piperazin-1-ylsulfonyl)-6-chloroindolin-2-one | Inhibitor of acid α-glucosidase | Preclinical | Non-iminosugar chaperone; highest chaperone activity against acid α-glucosidase[245] |
| 1-Deoxynojirimycin/ Amicus Therapeutics | Inhibitor of acid α-glucosidase | Phase II | Effective against different mutant forms of acid α-glucosidase; roles in protein trafficking and stabilization of some mutant forms of acid α-glucosidase[246] |
| α-Lobeline and 3,4,7-trihydroxyisoflavone | β-Galactocerebrosidase | Preclinical | Effective in fibroblast cells from patients with Krabbe disease[247] |
| *N*-Octyl-4-epi-β-valienamine | Retains β-galactosidase catalytic activity | Preclinical | Effective in a mouse model of GM1 gangliosidosis[248] |
| 5*N*,6*S*-(*N*′-butylimino-methylidene)-6-thio-1-deoxygalactonojirimycin | Competitive inhibitor of β-galactosidase | Preclinical | *N*′-Butyl moiety selectively binds to the active site of β-galactosidase; protects the enzyme from degradation due to temperature fluctuation; used in GM1 gangliosidosis[249] |
| NCGC607 | Assists the conformation of GCase activity | Preclinical | Reduced lysosomal substrate storage and α-synuclein levels in cell-based assays[250] |
| ***Lysosomal acidification inhibitors*** | | | |
| Chloroquine | Inhibition of lysosomal acidification | Tool compound/ phase IV | Increases $T_{reg}$ cell expansion and alleviates EAE symptoms[251]; completed phase IV clinical trials in autoimmune hepatitis (NCT01980745) |

Table 4 (cont.) | **Pharmacological modulators of lysosome functions: targets and disease indication**

| Pharmacological agent/company | Mechanism | Stage of development | Comments |
|---|---|---|---|
| ***Lysosomal acidification inhibitors (cont.)*** | | | |
| Hydroxychloroquine | Inhibition of lysosomal acidification | Tool compound/ phase IV | Blocks the autoreactive T cell responses in SLE, RA, SjS and others[252]; ongoing end-stage clinical trials alone or in combination in SLE (NCT00413361), SjS (NCT01601028), RA (NCT03085940) and others |
| $NH_4Cl$ | Inhibition of lysosomal acidification | Tool compound | N/A |
| Monensin | Inhibition of lysosomal acidification | Tool compound | N/A |
| ***mTOR inhibitors*** | | | |
| Rapamycin/sirolimus | Antifungal metabolite produced by *Streptomyces hygroscopicus*; binds to the FK506-binding protein (FKBP12), resulting in allosteric mTOR inhibition | Tool compound | Used in the treatment of many diseases, including SLE[253] and RA[254] and others |
| ***Cathepsin inhibitors*** | | | |
| CA030, CA-074 and their analogues | Cathepsin B inhibitor | Preclinical | High amounts of cathepsin B in patients with RA compared with patients with osteoarthritis[132]; promising results in melanoma metastases in mice[255] |
| Pepstatin A | Cathepsin D inhibitor | Tool compound | Reduction of renal fibrosis in mouse models of CKD[256] |
| α1-Antichymotrypsin and phenylmethyl-sulfonyl fluoride | Cathepsin G inhibitor | Preclinical | Increased cathepsin G in patients with RA compared with patients with osteoarthritis[135]; monocyte chemotactic activity in the synovial fluid of patients with RA was directly proportional to cathepsin G expression |
| CLIK-148, CLIK-181 and CLIK-195 | Cathepsin L inhibitor | Preclinical | Inhibitors obtained as leads from in vitro and in vivo studies; high expression of cathepsin L in patients with RA compared with patients with osteoarthritis[257]; siRNA-mediated inhibition protected mice from autoimmune diabetes[258]; inhibition with oxocarbazate prevented virus (coronavirus and Ebola pseudotype virus) entry into cells[259] |
| LHVS and CLIK-60 | Cathepsin S inhibitor | Preclinical | Cathepsin S inhibitors (CLIK-6O) inhibited autoantigen presentation in mouse model of SjS[79,260]; cathepsin S-deficient mice are less susceptible to collagen-induced arthritis[261] |
| RO5461111/Roche | Cathepsin S inhibitor | Preclinical | Inhibition of cathepsin S has beneficial effects in SLE[262] and SjS[263] via inhibiting autoantigen presentation; cathepsin S, from tears of patients with SjS, enhanced the degradation of tear proteins[264] |
| CLIK-164 and SB-357114/ GlaxoSmithKline | Cathepsin K inhibitor | Preclinical | Inhibition of cathepsin K reduced collagen degradation in osteoporosis conditions[265,266] |
| L-006235 | Cathepsin K inhibitor | Preclinical | Inhibition of cathepsin K exerted analgesia in a rat model of osteoarthritis[267] |
| PADK, SD1002 and SD1003 | Cathepsin B and L inhibitor | Preclinical | Cathepsin B and L modulators decreased protein accumulation in Alzheimer disease via cathepsin upregulation[268] |
| ***v-ATPase inhibitors*** | | | |
| Bafilomycin A1 | A macrolide antibiotic isolated from *Streptomyces griseus*; a potent and selective inhibitor of v-ATPases, via the V0 c subunit in the lysosomal lumen | Tool compound | Reduced lymphoblastic leukaemia by inhibiting the autophagic process and activating the apoptosis pathway via mitochondria[269] |
| Concanamycin A | A macrolide antibiotic isolated from *Streptomyces diastatochromogenes*; a selective inhibitor of v-ATPases via V0 c subunit | Tool compound | N/A |
| FR167356 | A selective inhibitor of osteoclast v-ATPases and relatively less potent inhibitor of other v-ATPases | Preclinical | Effective in osteoporosis and metastatic bone disease[270] |
| Salicylihalamide A | First isolated from the marine sponge *Haliclona*; a selective inhibitor of mammalian v-ATPases via V0 domain | Tool compound/ preclinical | Anticancer activity via v-ATPase inhibition[271] |

Table 4 (cont.) | **Pharmacological modulators of lysosome functions: targets and disease indication**

| Pharmacological agent/company | Mechanism | Stage of development | Comments |
|---|---|---|---|
| ***v-ATPase inhibitors (cont.)*** | | | |
| Saliphenylhalamide | Synthetic molecule; inhibitor of v-ATPases | Preclinical | A derivative of salicylihalamide A with anticancer effects in cancer cell lines (including drug-resistant) |
| SB 242784/SmithKline Beecham Biologicals | Synthetic molecule; inhibitor of v-ATPases | Preclinical | Selectively inhibits osteoclast v-ATPases and alleviates the clinical signs of osteoporosis and metastatic bone disease[270,272] |
| BRD1240/Harvard University | Small molecule; exerts lysosomal acidification by inhibition of v-ATPases | Tool compound | Anticancer activity via inhibiting lysosomal enzymes[273] |
| ***Ion channel modulators*** | | | |
| ML-SA1 | TRPML1 agonist | Tool compound/ preclinical | Important role in lysosomal exocytosis[22]; induces secretion of lysosomal acid phosphatases and LAMP1 expression[22] |
| SF-22 | TRPML1/3 agonist | Preclinical | May have therapeutic uses in vaccines, autoimmune diseases and infectious diseases (WO2015118167A1)[274] |
| MK6-83 | TRPML1 agonist | Preclinical | N/A |
| ***PIK kinase modulators*** | | | |
| YM-201636 | PIKfyve kinase inhibitor | Preclinical | Used in antiretroviral therapy; inhibits glucose influx in adipocytes; dysregulated autophagy-induced cell death in neuronal cells[275] |
| Apilimod (LAM-002A (apilimoddimesylate)/ STA-5326)/AI Therapeutics | PIKfyve kinase inhibitor | Phase I | An inhibitor of T helper 1 and T helper 17 cell responses in autoimmune diseases[276–278]; under phase 1 study in subjects with relapsed or refractory B cell non-Hodgkin's lymphoma (NCT02594384) |
| ***Chaperone modulators*** | | | |
| P140 peptide (Lupuzor)/ ImmuPharma | CMA inhibitor | Phase III | Binds HSPA8 and blocks dysregulated chaperone-mediated activity in SLE[92,103], SjS[56] and CIDP[59] |
| VER-155008 | HSP70 inhibitor | Tool compound/ preclinical | Therapeutic effects in lung cancer[279] and Alzheimer disease[280] |
| Humanin | CMA activator | Preclinical | Mitochondria-associated peptide that binds HSP90 to facilitate substrate translocation[281] |
| ***Miscellaneous*** | | | |
| Lonafarnib/Eiger BioPharmaceuticals | Lysosomal activator | Preclinical | A known anticancer molecule; inhibits farnesyl transferase and reduces tauopathy in mice by activating lysosomal degradative process[282]; possible therapeutic option for neurodegenerative diseases |

CIDP, chronic inflammatory demyelinating polyneuropathy; CKD, chronic kidney disease; CLIK, cathepsin L inhibitor Katunuma; CMA, chaperone-mediated autophagy; EAE, experimental autoimmune encephalomyelitis; GCase, glucocerebrosidase; GCS, glucosylceramide synthase; LAMP1, lysosome-associated membrane protein 1; LSD, lysosomal storage disorder; LHVS, morpholinurea-leucine-homophenylalanin-vinyl phenyl-sulfone; MPS, mucopolysaccharidosis; mTOR, mechanistic target of rapamycin; N/A, not available; NPC, Niemann–Pick disease type C; PADK, Z-Phe-Ala-diazomethylketone; PIK, phosphatidylinositol-3-phosphate 5-kinase; PIKfyve, FYVE finger-containing phosphoinositide kinase; RA, rheumatoid arthritis; siRNA, small interfering RNA; SjS, Sjögren's syndrome; SLE, systemic lupus erythematosus; TFEB, transcription factor EB; $T_{reg}$ cell, regulatory T cell; v-ATPase, vacuolar-type proton adenosine triphosphatase.

from cells[275]. From a clinical perspective, although targeting PIKfyve is highly promising, further work is required to pave a way towards a future treatment.

***Farnesyl transferase inhibitors.*** Several molecules with farnesyl transferase inhibitory activity have been developed. However, some earlier compounds were found to have major side effects, and their development was discontinued. Lonafarnib (SCH66336; Eiger Biopharmaceuticals), a synthetic tricyclic halogenated carboxamide, has recently shown some promise in a transgenic mouse, which expresses human tau carrying a P301L mutation[282] (TABLE 4). These mice develop tangles in the hippocampus, amygdala, entorhinal cortex and cerebral cortex by 16 weeks, and about 60% of hippocampal neurons die at about 22 weeks. Compared with untreated mice, mice that received lonafarnib displayed less abnormal behaviour and half of the tangles in the hippocampi and cortices. Treatment also prevented brain atrophy that typically occurs in these transgenic mice, while reducing microgliosis in the hippocampus and tempering astrogliosis in the cortex. Mechanistic studies have shown in lonafarnib-treated mice that substrates were more efficiently delivered to lysosomes, their degradation products disappeared faster and the organelles were more readily degraded, specifically by improving lysosome efficiency. Knowing that lonafarnib is already approved for use in humans for other

indications (cancer, and ongoing evaluation for progeria and hepatitis delta virus infection), it might therefore be repurposed for use in patients with tauopathy. In this class of farnesyl transferase inhibitors, tipifarnib (R115777; Johnson & Johnson) might also display interesting therapeutic properties as it has been seen to block lysosomal-dependent degradation of bortezomib-induced aggresomes without inhibition of the early steps of autophagy. Kura-oncology in-licenced tipifarnib in 2014.

Table 5 | **Pharmacological modulators of lysosome functions: patents**

| Patent number | Assignee | Title | Year filed/ published/ granted | Composition | Target diseases |
|---|---|---|---|---|---|
| US8829204B2 | Vertex Pharmaceuticals Inc., Cambridge, MA (USA) | Modulators of ATP-binding cassette transporters | 2014 | Novel synthetic compounds | Sjögren's syndrome, LSD and many other diseases |
| US20140072540A1 | The Board of Trustees of the University of Illinois, Urbana, IL (USA) | Compositions and methods for the treatment of Krabbe and other neurodegenerative diseases | 2014 | Inhibitors, which modulate lysosomal function | Neurodegenerative diseases |
| US20160051629A1 (WO/2014/170892) | Yeda Research and Development Co. Ltd, Rehovot (Israel) | Inhibition of RIP kinases for treating lysosomal storage diseases | 2016 | RIP inhibitors are compounds or pharmaceutical compositions and some types of IL-1β antagonists | LSD |
| WO2018005713A1 | Liang Congxin, Palm Beach Gardens, FL 33418 (USA) | Piperazine derivatives as TRPML modulators | 2016 | Novel piperazine derivatives | Targets lysosomal dysfunction associated with TRPML |
| EP2744821B1 | University of Dundee (UK) | Inhibitors against endosomal/ lysosomal enzymes | 2016 | Protease inhibitor and conjugates | Diseases which need protease inhibition |
| US9265735B2 | The Research Foundation for Msta Hygiene, Inc., Menands, NY (USA) | Methods for screening to identify therapeutic agents for Alzheimer disease and use thereof | 2016 | Agents that modulate lysosomal function | Alzheimer disease |
| US9469683B2 | Biomarin Pharmaceutical Inc., Novato, CA (USA) | Lysosomal targeting peptides and uses thereof | 2016 | Peptides | LSD |
| US9717737B2 (WO2015/124120) | The University of Hong Kong, Hong Kong (China) | Vacuolin-1 as an inhibitor of autophagy and endosomal trafficking and the use thereof for inhibiting tumour progression | 2017 | Vacuolin-1 and structural analogue | Cancer and other diseases |
| WO2017040971A1 | Biomarin Pharmaceutical Inc., Novato, CA (USA) | Methods of using inhibitors of PIKfyve for the treatment of lysosomal storage disorders and neurodegenerative diseases | 2017 | Methods and chemicals which are pharmaceutically acceptable | LSD and neurodegenerative diseases |
| WO2006007560A3 | Icahn School of Medicine at Mount Sinai, New York, NY (USA); the Trustees of the University of Pennsylvania, Philadelphia, PA (USA) | Targeted protein replacement for the treatment of lysosomal storage disorders | 2017 | Compositions and methods for enzyme replacement therapies of LSDs | LSD |
| WO2018208630A1 | Calygene Biotechnology Inc., Camden, DE (USA) | Aryl-sulfonamide and aryl-sulfone derivatives as TRPML modulators | 2018 | Aryl or heteroaryl compounds | Diseases related to lysosomal functions |
| US20180110798A1 | The United States of America, as represented by the Secretary, Department of Health and Human Services, Rockville, MD (USA) | Cyclodextrin for the treatment of lysosomal storage diseases | 2018 | Cyclodextrin compounds | LSD |

The list of patents was generated by searching several databases (EPO (Espacenet), USPTO and others) from 2014 to early 2019 using keywords — lysosomal modulators or modulation, lysosomal protein inhibitors (mucolipin, vacuolins, and so forth), lysosomal enzyme inhibitors and lysosome function modulators — and selecting only the chemical modulators/inhibitors that act on lysosomal function. Patents are arranged based on the year filed, published or granted. LSD, lysosomal storage disorder; PIKfyve, FYVE finger-containing phosphoinositide kinase; RIP, receptor-interacting protein kinase; SjS, Sjögren's syndrome; TRPML, transient receptor potential mucolipin.

***Chaperone modulators.*** Molecules targeting chaperone proteins involved in lysosomal function have also been designed for potential therapeutic applications. One of these molecules is VER-155008, a small-molecule inhibitor of HSPA8, a key element of CMA[308,309]. VER-155008 binds to the nucleotide binding domain of HSPA8 and HSP70, and acts as an ATP-competitive inhibitor of ATPase and chaperone activity. In a mouse model of AD (5XFAD mice), intraperitoneal treatment with VER-155008 reduced the two main pathological features of AD (amyloid plaques and paired helical filament tau accumulation) and improved object recognition, location and episodic-like memory[280].

Another molecule, the 21-mer phosphopeptide P140 (TABLE 4; FIG. 3), was also shown to interact with HSPA8 (FIG. 2)[310] and lodge in the HSPA8 nucleotide binding domain[92,311]. P140 and VER-155008, however, do not have the same mechanism of action, and their effects were not additive[312]. P140 is a phosphorylated analogue of a nominal peptide that was initially spotted in a cellular screening assay using overlapping peptides covering the whole spliceosomal U1-70K protein and $CD4^+$ T cells collected from the lymph nodes of lupus-prone MRL/lpr mice[313]. P140 peptide enters B cells via a clathrin coat-dependent endocytosis process to reach early endosomes and then late endosomes/lysosomes[92]. It affects CMA that is hyperactivated in lupus, likely by hampering the CMA-mediating chaperone HSPA8 (REF.[101]). P140 peptide reduces the excessive expression of HSPA8 and LAMP2A observed in lupus mice, alters the (auto)antigen presentation by MHCII molecules in the MIIC compartment and, consequently, attenuates the activation of autoreactive T cells[92]. A significant diminution of MHC molecule expression at the surface of antigen-presenting cells was measured in mice that received the P140 peptide intravenously and on patient's peripheral cells treated ex vivo with the peptide[92,101,314]. As a downstream consequence, the activation of autoreactive B cells and their differentiation into autoantibody-secreting cells is repressed[101,314]. T cells from patients with lupus are no longer responders ex vivo to peptides encompassing $CD4^+$ T cell epitopes[315]. The effect of P140 on CMA was demonstrated in vitro, using a fibroblast cell line that stably expresses a CMA reporter[53,92]. P140, which selectively targets the CMA/lysosome process and has no effect on mitophagy[316], has been evaluated in murine models mimicking other rheumatic diseases with very promising results, notably in mice developing SjS features[56], in mice with neuropsychiatric lupus symptoms[62] and in rats that develop a CIDP-like disease with disturbance of both CMA and macroautophagy in sciatic nerves[59]. In clinical trials that included patients with SLE, P140 formulated in mannitol was found to be safe and non-immunogenic after several subcutaneous administrations of peptide[312,317,318]. P140 showed significant efficacy in a multicentre, double-blind, phase II trial[317]. This peptide is currently being evaluated in phase III trials in the United States, Europe and Mauritius. In continuation, an open-label trial including several hundred patients with lupus worldwide is planned.

Another peptide has been discovered that, in contrast to P140, activates CMA[319]. This 24-mer peptide called humanin was originally identified from surviving neurons in patients with AD, and was found to directly enhance CMA activity by increasing substrate binding and translocation into lysosomes. Humanin interacts with HSP90 and stabilizes the binding of this chaperone to CMA cargos as they bind to the lysosomal membrane. These results are important as humanin had been shown to possess some cardioprotective and neuroprotective properties in diseases such as AD, cardiovascular disease, stroke, myocardial infarction, diabetes and cancer[320].

### *Emerging potential lysosomal therapeutic targets*

In addition to the targets discussed above, there are a few emerging potential lysosomal therapeutic targets for which there is strong biological validation, but not yet any small molecules in development that target them. An example with likely pharmacological tractability is a lysosomal $K^+$ channel called TMEM175, which is important for maintaining the membrane potential and pH stability in lysosomes[321]. Deficiency in TMEM175 may play a critical role in PD pathogenicity[322]. Importantly, the structure of TMEM175 has been recently refined[323].

Another target for which ligands have not yet been validated is the KCNQ2/3 channel (also named M-channel or Kv7.2/7.3 channel). It has been shown in NPC1 disease that reduced cholesterol efflux from lysosomes aberrantly modifies neuronal firing patterns[324]. This disruption of lysosomal cholesterol efflux with decreases in PtdIns(4,5)P2-dependent KCNQ2/3 channel activity may lead to the aberrant neuronal activity. The cholesterol transporter and PtdIns(4,5)P2 floppase, ABCA1, is responsible for the decline in PtdIns(4,5)P2 that consequently modifies the electrical properties of NPC1 disease neurons. Dysfunction in the activity of KCNQ2/3 or altered levels of PtdIns(4,5)P2, due notably to genetic mutations, might also be involved in other neuropathies (for example, some forms of epilepsy, HD, PD, AD, ALS and Friedrich ataxia). Although further experiments are needed to validate the link discovered between hyperexcitability and cell death in NPC1 disease and other neurodegenerative diseases, small molecules such as retigabine, an anti-convulsant drug that keeps KCNQ2/3 channels open, might represent important therapeutic tools[324,325]. Other channel opener ligands of KCNQ2/Q3 include ICA-069673 and its derivatives.

Another promising therapeutic target is sphingomyelin phosphodiesterase 1 (SMPD1). Defects in the gene encoding SMPD1 cause Niemann–Pick disease type A and type B. SMPD1 converts sphingomyelin to ceramide, and also has phospholipase C activity. Reduced activity of acid sphingomyelinase, associated with a marked decrease in lysosomal stability, has been described in patients with Niemann–Pick disease, a phenotype that was corrected by treating cells with recombinant HSP70[326].

Finally, as LAMP2A, a specific lysosomal protein that displays a decisive role in CMA, has been shown to be overexpressed in certain pathological settings such as certain cancers and inflammatory diseases (autoimmune or non-autoimmune), downregulating its expression



DEFS00023233

might be therapeutically beneficial[53,327]. As mentioned above, however, in other indications there is a defect in LAMP2A. The latter can be due to reduced stability of the CMA receptor and not to decreased de novo synthesis (for example, in ageing)[328] or can result from aggregation to the lysosomal membrane of pathogenic proteins such as α-synuclein, ubiquitin carboxy-terminal hydrolase L1 (a deubiquitinating enzyme) and mutant tau, known to amass in neurodegenerative disorders (see above). Targeting LAMP2A therefore remains a challenge, although several strategies may be envisaged, for example by controlling de novo synthesis, by hampering its multimerization into lysosomes (possibly via HSP90 and/or other chaperones) or by regulating the degradation rate of LAMP2A monomers (for reuse) into lysosomes.

## Challenges and outlook

Current research into lysosomal function and dysfunction is revealing novel roles of lysosomes in disease pathogenesis and highlighting new opportunities to treat such lysosomal and autophagy-related diseases. As in the case of autophagy modulation[14,56,207], lysosomal activation or inhibition must be investigated with caution, as lysosomal activity can be abnormally reduced or enhanced in some organs or tissues and not in others, and, at another scale, lysosome activity can be altered in certain lysosomes and not in others within the same cell. Biodistribution studies in vivo must be undertaken to avoid accumulation of pharmaceuticals in healthy organs or tissues. There is an obvious requirement for safety, to ensure that a drug used as a lysosome modulator for a particular type of lysosomal disease does not increase vulnerability to another disease.

There is still much to be learned about the intimate working of lysosomes. This is due to the abundance of constitutive elements that comprise these vesicles, the added complexity resulting from their plasticity (ion channels and transporters, acidification and swelling) and the vast amount of proteins and peptides that are translocated into lysosomes and digested by lytic enzymes. Sensitive analysis methods have allowed important information to be generated about lysosomal membrane proteins, a large majority of which are transporters[8]. However, many questions remain related to how their expression is regulated and how they regulate their translocator and chaperoning activities. For example, certain cells only contain so-called secretory lysosomes (as in cytotoxic T cells), whereas other cell subsets contain both conventional and secretory lysosomes (as in platelets). Considering the large family of endo-lysosomal vesicles, the whole notion of 'secretory' and 'conventional' lysosomes remains a matter of debate. In many instances, lysosomes act as a basal cell metabolism organelle; whereas in other cases, they assist in the regulation of homeostasis through unconventional secretory pathways, known as lysosomal exocytosis, and different signalling mechanisms.

Although several assays used to measure the activity of lysosomes have been validated worldwide (BOX 2; TABLE 3), they have their limitations, including issues associated with reliability, performance and sensitivity, notably in vivo. Another level of complexity comes from the inherent organelle heterogeneity, which is an issue of tremendous importance. Unfortunately, with the tools and equipment we have in hand today, it is virtually impossible to examine what happens in the lysosomes of an individual patient. The introduction of microfluidic single-cell analysis technologies has enabled cellular populations to be characterized and huge advances to be performed. However, the level of precision has not yet been achieved at the level of lysosomes (0.2–0.5 μm). We know that lysosomes are heterogeneous in nature, composition and activity even in 'normal' settings; they are not all equally competent for autophagy or any other types of activity. Currently, this is obviously the focus of intense research.

Although a certain number of preclinical studies involving lysosomal regulators have been conducted over the years, only a small number of lysosome-targeted therapeutics have so far moved into clinical development. One of the biggest advances in developing such strategies would be the identification of a genetic signature that would allow those patients most likely to respond to a specific therapy to be selected. However, at this stage of our knowledge of specific lysosome-directed drugs and intrinsic lysosomal failures, genetic features that might predict potential responders are still lacking (with the exception of LSDs). Further investigations are required to achieve this level of knowledge, which obviously will also depend on the type of disease, heterogeneity and frequency.

Another issue associated with the development of lysosome-targeted therapeutics relates to delivery. The use of nanovectors represents an attractive delivery method, owing, in particular, to their unique ability to penetrate across cell barriers and, via the endo-lysosomal pathway, to preferentially home in on organelles such as lysosomes. Several nanoscale galenic forms have been developed to serve as vectors or carriers of proteins, peptides or nucleic acids, and a vast literature describes the many advantages of using such nanostructures in nanomedicine. However, safety is a concern as some carbon nanostructures have been claimed to induce nanotoxicity, accompanied by the induction of autophagy and lysosomal dysfunction[329–332] (reviewed elsewhere[333–336]).

The purpose of this Review is to gain awareness of the importance of lysosomes in disease, and to encourage the development of novel lysosomal targeted drugs. However, more research is needed to characterize components that are specifically linked to the lysosome, such as LAMP2A and HSPA8, and to more clearly define their specific involvement in lysosome biogenesis and metabolism. Special attention should be given to the mode of administration of lysosome-targeted medications in order to minimize toxicity and promote specific targeting. It is our hope that a large field of therapeutic applications could emerge from such investigations, encompassing rare and common autoimmune, neurodegenerative and metabolic diseases, as well as cancer, senescence and ageing.

Published online 2 September 2019

1. De Duve, C., Pressman, B. C., Gianetto, R., Wattiaux, R. & Appelmans, F. Tissue fractionation studies. 6. Intracellular distribution patterns of enzymes in rat-liver tissue. *Biochem. J.* **60**, 604–617 (1955).
2. Wang, F., Gomez-Sintes, R. & Boya, P. Lysosomal membrane permeabilization and cell death. *Traffic* **19**, 918–931 (2018).
3. Settembre, C., Fraldi, A., Medina, D. L. & Ballabio, A. Signals from the lysosome: a control centre for cellular clearance and energy metabolism. *Nat. Rev. Mol. Cell Biol.* **14**, 283–296 (2013).
4. Xu, H. & Ren, D. Lysosomal physiology. *Annu. Rev. Physiol.* **77**, 57–80 (2015).
**This article is an encyclopaedia of lysosomal physiology.**
5. Perera, R. M. & Zoncu, R. The lysosome as a regulatory hub. *Annu. Rev. Cell. Dev. Biol.* **32**, 223–253 (2016).
6. Pous, C. & Codogno, P. Lysosome positioning coordinates mTORC1 activity and autophagy. *Nat. Cell Biol.* **13**, 342–344 (2011).
7. Kaushik, S. & Cuervo, A. M. The coming of age of chaperone-mediated autophagy. *Nat. Rev. Mol. Cell Biol.* **19**, 365–381 (2018).
8. Saftig, P. & Klumperman, J. Lysosome biogenesis and lysosomal membrane proteins: trafficking meets function. *Nat. Rev. Mol. Cell Biol.* **10**, 623–635 (2009).
**This article presents a comprehensive review of lysosomal function.**
9. Ballabio, A. & Gieselmann, V. Lysosomal disorders: from storage to cellular damage. *Biochim. Biophys. Acta* **1793**, 684–696 (2009).
10. Desnick, R. J. & Schuchman, E. H. Enzyme replacement therapy for lysosomal diseases: lessons from 20 years of experience and remaining challenges. *Annu. Rev. Genom. Hum. Genet.* **13**, 307–335 (2012).
11. Fleming, A., Noda, T., Yoshimori, T. & Rubinsztein, D. Chemical modulators of autophagy as biological probes and potential therapeutics. *Nat. Chem. Biol.* **7**, 9–17 (2011).
12. Gros, F. & Muller, S. Pharmacological regulators of autophagy and their link with modulators of lupus disease. *Br. J. Pharmacol.* **171**, 4337–4359 (2014).
**Together with that by Fleming et al. (2011), this article lists chemical modulators of autophagy processes and lysosome activity.**
13. Dikic, I. & Elazar, Z. Mechanism and medical implications of mammalian autophagy. *Nat. Rev. Mol. Cell Biol.* **19**, 349–364 (2018).
14. Bonam, S. R., Wang, F. & Muller, S. Autophagy: a new concept in autoimmunity regulation and a novel therapeutic option. *J. Autoimmun.* **94**, 16–32 (2018).
15. Davidson, S. M. & Vander Heiden, M. G. Critical functions of the lysosome in cancer biology. *Annu. Rev. Pharmacol. Toxicol.* **57**, 481–507 (2017).
16. Lawrence, R. E. & Zoncu, R. The lysosome as a cellular centre for signalling, metabolism and quality control. *Nat. Cell Biol.* **21**, 133–142 (2019).
17. Di Ronza, A. et al. CLN8 is an endoplasmic reticulum cargo receptor that regulates lysosome biogenesis. *Nat. Cell Biol.* **20**, 1370–1377 (2018).
18. Griffiths, G., Hoflack, B., Simons, K., Mellman, I. & Kornfeld, S. The mannose 6-phosphate receptor and the biogenesis of lysosomes. *Cell* **52**, 329–341 (1988).
19. Malini, E. et al. Role of LIMP-2 in the intracellular trafficking of β-glucosidase in different human cellular models. *FEBS J.* **29**, 3839–3852 (2015).
20. Mindell, J. A. Lysosomal acidification mechanisms. *Annu. Rev. Physiol.* **74**, 69–86 (2012).
21. Forgac, M. Vacuolar ATPases: rotary proton pumps in physiology and pathophysiology. *Nat. Rev. Mol. Cell Biol.* **8**, 917–929 (2007).
22. Samie, M. et al. A TRP channel in the lysosome regulates large particle phagocytosis via focal exocytosis. *Dev. Cell* **26**, 511–524 (2013).
23. Zhang, X. et al. MCOLN1 is a ROS sensor in lysosomes that regulates autophagy. *Nat. Commun.* **7**, 12109 (2016).
24. Parenti, G., Andria, G. & Ballabio, A. Lysosomal storage diseases: from pathophysiology to therapy. *Annu. Rev. Med.* **66**, 471–486 (2015).
25. Jancic, C. et al. Rab27a regulates phagosomal pH and NADPH oxidase recruitment to dendritic cell phagosomes. *Nat. Cell Biol.* **9**, 367–378 (2007).
**This article describes the role of Rab27a, increased phagosome acidification, alteration of subsets of LROs and antigen degradation defects in antigen cross-presentation.**
26. Raposo, G. & Marks, M. S. Melanosomes—dark organelles enlighten endosomal membrane transport. *Nat. Rev. Mol. Cell Biol.* **8**, 786–797 (2007).
27. Luzio, J. P., Pryor, P. R. & Bright, N. A. Lysosomes: fusion and function. *Nat. Rev. Mol. Cell Biol.* **8**, 622–632 (2007).
**This review is one of the must-read introductions to the complex and dynamic systems of the lysosomal network.**
28. Marks, M. S., Heijnen, H. F. & Raposo, G. Lysosome-related organelles: unusual compartments become mainstream. *Curr. Opin. Cell Biol.* **25**, 495–505 (2013).
29. Patwardhan, A. et al. Routing of the RAB6 secretory pathway towards the lysosome related organelle of melanocytes. *Nat. Commun.* **8**, 15835 (2017).
30. Huizing, M., Helip-Wooley, A., Westbroek, W., Gunay-Aygun, M. & Gahl, W. A. Disorders of lysosome-related organelle biogenesis: clinical and molecular genetics. *Annu. Rev. Genomics Hum. Genet.* **9**, 359–386 (2008).
31. Settembre, C. et al. TFEB links autophagy to lysosomal biogenesis. *Science* **332**, 1429–1433 (2011).
**This article is the first research demonstrating that TFEB controls not only lysosomal biogenesis but also the autophagy network, making TFEB a highly attractive therapeutic target.**
32. Raben, N. & Puertollano, R. TFEB and TFE3: linking lysosomes to cellular adaptation to stress. *Annu. Rev. Cell. Dev. Biol.* **32**, 255–278 (2016).
33. Levine, B., Mizushima, N. & Virgin, H. W. Autophagy in immunity and inflammation. *Nature* **469**, 323–335 (2011).
**This review brought scientists' attention to the role of autophagy in immunity and inflammation, which prompted intense research into this topic.**
34. Medina, D. et al. Lysosomal calcium signalling regulates autophagy through calcineurin and TFEB. *Nat. Cell Biol.* **17**, 288–299 (2015).
35. Martina, J. A., Chen, Y., Gucek, M. & Puertollano, R. MTORC1 functions as a transcriptional regulator of autophagy by preventing nuclear transport of TFEB. *Autophagy* **8**, 903–914 (2012).
36. Settembre, C. et al. A lysosome-to-nucleus signalling mechanism senses and regulates the lysosome via mTOR and TFEB. *EMBO J.* **31**, 1095–1108 (2012).
37. Aichinger, M., Wu, C., Nedjic, J. & Klein, L. Macroautophagy substrates are loaded onto MHC class II of medullary thymic epithelial cells for central tolerance. *J. Exp. Med.* **210**, 287–300 (2013).
38. Blum, J. S., Wearsch, P. A. & Cresswell, P. Pathways of antigen processing. *Annu. Rev. Immunol.* **31**, 443–473 (2013).
39. Yu, L. et al. Termination of autophagy and reformation of lysosomes regulated by mTOR. *Nature* **465**, 942–946 (2010).
40. Chen, Y. & Yu, L. Development of research into autophagic lysosome reformation. *Mol. Cells* **41**, 45–49 (2018).
41. Levine, B. & Deretic, V. Unveiling the roles of autophagy in innate and adaptive immunity. *Nat. Rev. Immunol.* **7**, 767–777 (2007).
42. Lim, C. Y. & Zoncu, R. The lysosome as a command-and-control center for cellular metabolism. *J. Cell Biol.* **214**, 653–664 (2016).
43. Johnson, D. E., Ostrowski, P., Jaumouillé, V. & Grinstein, S. The position of lysosomes within the cell determines their luminal pH. *J. Cell Biol.* **212**, 677–692 (2016).
**This article highlights the heterogeneity of lysosomes in terms of cell positioning, motility and luminal pH, which all affect lysosomal functionality.**
44. Kroemer, G. & Jaattela, M. Lysosomes and autophagy in cell death control. *Nat. Rev. Cancer* **5**, 886–897 (2005).
45. Boustany, R. Lysosomal storage diseases—the horizon expands. *Nat. Rev. Neurol.* **9**, 583–598 (2013).
46. Platt, F. M. Emptying the stores: lysosomal diseases and therapeutic strategies. *Nat. Rev. Drug Discov.* **17**, 133–150 (2018).
47. Malm, D. & Nilssen, Ø. Alpha-mannosidosis. *Orphanet J. Rare Dis.* **3**, 21 (2008).
48. Mikulka, C. R. & Sands, M. S. Treatment for Krabbe's disease: finding the combination. *J. Neurosci. Res.* **94**, 1126–1137 (2016).
49. Sabourdy, F. et al. Natural disease history and characterisation of SUMF1 molecular defects in ten unrelated patients with multiple sulfatase deficiency. *Orphanet J. Rare Dis.* **10**, 31 (2015).
50. Fidzianska, A., Walczak, E. & Walski, M. Abnormal chaperone-mediated autophagy (CMA). *Folia Neuropathol.* **45**, 133–139 (2007).
51. Nishino, I. et al. Primary LAMP-2 deficiency causes X-linked vacuolar cardiomyopathy and myopathy (Danon disease). *Nature* **406**, 906–910 (2000).
52. Zielonka, M., Garbade, S. F., Kolker, S., Hoffmann, G. F. & Ries, M. A cross-sectional quantitative analysis of the natural history of free sialic acid storage disease—an ultra-orphan multisystemic lysosomal storage disorder. *Genet. Med.* **21**, 347–352 (2019).
53. Wang, F. & Muller, S. Manipulating autophagic processes in autoimmune diseases: a special focus on modulating chaperone-mediated autophagy, an emerging therapeutic target. *Front. Immunol.* **6**, 252 (2015).
54. Monteith, A. J. et al. Defects in lysosomal maturation facilitate the activation of innate sensors in systemic lupus erythematosus. *Proc. Natl Acad. Sci. USA* **113**, E2142–E2151 (2016).
55. Sohar, N., Sohar, I. & Hammer, H. Lysosomal enzyme activities: new potential markers for Sjögren's syndrome. *Clin. Biochem.* **38**, 1120–1126 (2005).
56. Li, B., Wang, F., Schall, N. & Muller, S. Rescue of autophagy and lysosome defects in salivary glands of MRL/lpr mice by a therapeutic phosphopeptide. *J. Autoimmun.* **90**, 132–145 (2018).
57. Lassen, K. G. et al. Genetic coding variant in GPR65 alters lysosomal pH and links lysosomal dysfunction with colitis risk. *Immunity* **44**, 1392–1405 (2016).
58. Weissmann, G. Lysosomes and joint disease. *Arthritis Rheum.* **9**, 834–840 (1966).
59. Brun, S. et al. An autophagy-targeting peptide to treat chronic inflammatory demyelinating polyneuropathies. *J. Autoimmun.* **92**, 114–125 (2018).
60. Kim, I., DeBartolo, D., Ramanan, S., Ponath, G. & Pitt, D. Excess lipid accumulation in cortical neurons in multiple sclerosis may lead to autophagic dysfunction and neurodegeneration. *Neurology* **84**, P5.237 (2015).
61. Ramesh, N. & Pandey, U. B. Autophagy dysregulation in ALS: when protein aggregates get out of hand. *Front. Mol. Neurosci.* **10**, 263 (2017).
62. Muller, S. et al. Autophagy in neuroinflammatory diseases. *Autoimmun. Rev.* **16**, 856–874 (2017).
63. Zhang, L., Sheng, R. & Qin, Z. The lysosome and neurodegenerative diseases. *Acta Biochim. Biophys. Sin.* **41**, 437–445 (2009).
64. Murphy, K. et al. Reduced glucocerebrosidase is associated with increased α-synuclein in sporadic Parkinson's disease. *Brain* **137**, 834–848 (2014).
65. Cortes, C. J. & La Spada, A. R. The many faces of autophagy dysfunction in Huntington's disease: from mechanism to therapy. *Drug Discov. Today* **19**, 963–971 (2014).
66. Neufeld, E. F. Lysosomal storage diseases. *Annu. Rev. Biochem.* **60**, 257–280 (1991).
67. Plotegher, N. & Duchen, M. R. Mitochondrial dysfunction and neurodegeneration in lysosomal storage disorders. *Trends Mol. Med.* **23**, 116–134 (2017).
68. Lee, J. S. et al. Diagnostic challenge for the rare lysosomal storage disease: late infantile GM1 gangliosidosis. *Brain Dev.* **40**, 383–390 (2018).
69. Perez-Lopez, J. et al. Delayed diagnosis of late-onset Pompe disease in patients with myopathies of unknown origin and/or hyperCKemia. *Mol. Genet. Metab.* **114**, 580–583 (2015).
70. Lukacs, Z. et al. Prevalence of Pompe disease in 3,076 patients with hyperCKemia and limb-girdle muscular weakness. *Neurology* **87**, 295–298 (2016).
71. Lee, J. & Ye, Y. The roles of endo-lysosomes in unconventional protein secretion. *Cells* **7**, 198 (2018).
72. Ezaki, J., Wolfe, L. S. & Kominami, E. Specific delay in the degradation of mitochondrial ATP synthase subunit c in late infantile neuronal ceroid lipofuscinosis is derived from cellular proteolytic dysfunction rather than structural alteration of subunit c. *J. Neurochem.* **67**, 1677–1687 (1996).
73. Settembre, C. et al. A block of autophagy in lysosomal storage disorders. *Hum. Mol. Genet.* **17**, 119–129 (2008).
74. Vergarajauregui, S. & Puertollano, R. Mucolipidosis type IV: the importance of functional lysosomes for efficient autophagy. *Autophagy* **4**, 832–834 (2008).
75. Takikita, S., Myerowitz, R., Zaal, K., Raben, N. & Plotz, P. H. Murine muscle cell models for Pompe disease and their use in studying therapeutic approaches. *Mol. Genet. Metab.* **96**, 208–217 (2009).
76. Lieberman, A. P. et al. Autophagy in lysosomal storage disorders. *Autophagy* **8**, 719–730 (2012).
77. Takikita, S. et al. The values and limits of an in vitro model of Pompe disease: the best laid schemes o'mice an'men .... *Autophagy* **5**, 729–731 (2009).
78. Ge, W., Li, D., Gao, Y. & Cao, X. The roles of lysosomes in inflammation and autoimmune diseases. *Int. Rev. Immunol.* **34**, 415–431 (2015).

79. Turk, V. et al. Cysteine cathepsins: from structure, function and regulation to new frontiers. *Biochim. Biophys. Acta* **1824**, 68–88 (2012).
80. Stoka, V., Turk, V. & Turk, B. Lysosomal cathepsins and their regulation in aging and neurodegeneration. *Ageing Res. Rev.* **32**, 22–37 (2016).
81. Tato, M. et al. Cathepsin S inhibition combines control of systemic and peripheral pathomechanisms of autoimmune tissue injury. *Sci. Rep.* **7**, 2775 (2017).
82. Yang, M. et al. Cathepsin L activity controls adipogenesis and glucose tolerance. *Nat. Cell Biol.* **9**, 970–977 (2007).
83. Shafer, W., Pohl, J., Onunka, V., Bangalore, N. & Travis, J. Human lysosomal cathepsin G and granzyme B share a functionally conserved broad spectrum antibacterial peptide. *J. Biol. Chem.* **266**, 112–116 (1991).
84. Janoff, A. & Scherer, J. Mediators of inflammation in leukocyte lysosomes: IX. Elastinolytic activity in granules of human polymorphonuclear leukocytes. *J. Exp. Med.* **128**, 1137–1155 (1968).
85. Tamiya, H. et al. Defensins and cathepsin G-ANCA in systemic lupus erythematosus. *Rheumatol. Int.* **27**, 147–152 (2006).
86. Zhu, J. et al. T cell hyperactivity in lupus as a consequence of hyperstimulatory antigen-presenting cells. *J. Clin. Invest.* **115**, 1869–1878 (2005).
87. Weissmann, G. & Thomas, L. Steroids, lysosomes and systemic lupus erythematosus. *Bull. N. Y. Acad. Med.* **38**, 779–787 (1962).
88. Kallenberg, C. et al. Autoimmunity to lysosomal enzymes: new clues to vasculitis and glomerulonephritis? *Immunol. Today* **12**, 61–64 (1991).
89. Wang, F., Li, B., Schall, N., Wilhelm, M. & Muller, S. Assessing autophagy in mouse models and patients with systemic autoimmune diseases. *Cells* **6**, 16 (2017).
90. Li, X. et al. Increased expression of cathepsins and obesity-induced proinflammatory cytokines in lacrimal glands of male NOD mouse. *Invest. Ophthalmol. Vis. Sci.* **51**, 5019–5029 (2010).
91. Hamm-Alvarez, S. F. et al. Tear cathepsin S as a candidate biomarker for Sjögren's syndrome. *Arthritis Rheumatol.* **66**, 1872–1881 (2014).
92. Macri, C. et al. Modulation of deregulated chaperone-mediated autophagy by a phosphopeptide. *Autophagy* **11**, 472–486 (2015).
**This study together with that of Wang et al. (2015) were the first to demonstrate in vivo that regulating CMA and lysosomal dysfunctions could provide potential therapeutic benefit for autoimmune diseases.**
93. Pickering, M., Botto, M., Taylor, P., Lachmann, P. & Walport, M. Systemic lupus erythematosus, complement deficiency, and apoptosis. *Adv. Immunol.* **76**, 227–324 (2000).
94. Monteith, A. J. et al. mTORC2 activity disrupts lysosome acidification in systemic lupus erythematosus by impairing caspase-1 cleavage of Rab39a. *J. Immunol.* **201**, 371–382 (2018).
95. Kato, H. & Perl, A. Mechanistic target of rapamycin complex 1 expands Th17 and IL-4$^+$ CD4$^-$CD8$^-$ double-negative T cells and contracts regulatory T cells in systemic lupus erythematosus. *J. Immunol.* **192**, 4134–4144 (2014).
96. Zhou, Y. et al. Cathepsin K deficiency ameliorates systemic lupus erythematosus-like manifestations in Fas$^{lpr}$ mice. *J. Immunol.* **198**, 1846–1854 (2017).
97. Gros, F. et al. Macroautophagy is deregulated in murine and human lupus T lymphocytes. *Autophagy* **8**, 1113–1123 (2012).
98. Alessandri, C. et al. T lymphocytes from patients with systemic lupus erythematosus are resistant to induction of autophagy. *FEBS J.* **26**, 4722–4732 (2012).
99. Li, B., Yue, Y., Dong, C., Shi, Y. & Xiong, S. Blockade of macrophage autophagy ameliorates activated lymphocytes-derived DNA induced murine lupus possibly via inhibition of proinflammatory cytokine production. *Clin. Exp. Rheumatol.* **32**, 705–714 (2014).
100. Clarke, A. J. et al. Autophagy is activated in systemic lupus erythematosus and required for plasmablast development. *Ann. Rheum. Dis.* **74**, 912–920 (2015).
101. Page, N. et al. HSC70 blockade by the therapeutic peptide P140 affects autophagic processes and endogenous MHCII presentation in murine lupus. *Ann. Rheum. Dis.* **70**, 837–843 (2011).
102. Lettre, G. & Rioux, J. D. Autoimmune diseases: insights from genome-wide association studies. *Hum. Mol. Genet.* **17**, R116–R121 (2008).
103. Orozco, G. et al. Study of the common genetic background for rheumatoid arthritis and systemic lupus erythematosus. *Ann. Rheum. Dis.* **70**, 463–468 (2011).
104. Ramos, P., Shaftman, S., Ward, R. & Langefeld, C. Genes associated with SLE are targets of recent positive selection. *Autoimmune Dis.* **2014**, 203435 (2014).
105. Yang, Z., Goronzy, J. J. & Weyand, C. M. Autophagy in autoimmune disease. *J. Mol. Med.* **93**, 707–717 (2015).
106. Lessard, C. J. et al. Identification of a systemic lupus erythematosus risk locus spanning ATG16L2, FCHSD2, and P2RY2 in Koreans. *Arthritis Rheumatol.* **68**, 1197–1209 (2016).
107. Alessandri, C. et al. CD4 T lymphocyte autophagy is upregulated in the salivary glands of primary Sjögren's syndrome patients and correlates with focus score and disease activity. *Arthritis Res. Ther.* **19**, 178 (2017).
108. Byun, Y. S., Lee, H. J., Shin, S. & Chung, S. H. Elevation of autophagy markers in Sjögren syndrome dry eye. *Sci. Rep.* **7**, 17280 (2017).
109. Meng, Z. et al. Imbalanced Rab3D versus Rab27 increases cathepsin S secretion from lacrimal acini in a mouse model of Sjögren's syndrome. *Am. J. Physiol. Cell Physiol.* **310**, C942–C954 (2016).
110. Meng, Z., Klinngam, W., Edman, M. C. & Hamm-Alvarez, S. F. Interferon-γ treatment in vitro elicits some of the changes in cathepsin S and antigen presentation characteristic of lacrimal glands and corneas from the NOD mouse model of Sjögren's syndrome. *PLOS ONE* **12**, e0184781 (2017).
111. Artmann, G., Fehr, K. & Boni, A. Cathepsin D agglutinators in rheumatoid arthritis. *Arthritis Rheumatol.* **20**, 1105–1113 (1977).
112. Hashimoto, Y. et al. Significance of cathepsin B accumulation in synovial fluid of rheumatoid arthritis. *Biochem. Biophys. Res. Commun.* **283**, 334–339 (2001).
113. Hou, W. S. et al. Comparison of cathepsins K and S expression within the rheumatoid and osteoarthritic synovium. *Arthritis Rheumatol.* **46**, 663–674 (2002).
114. Skoumal, M. et al. Serum cathepsin K levels of patients with longstanding rheumatoid arthritis: correlation with radiological destruction. *Arthritis Res. Ther.* **7**, R65–R70 (2005).
115. Miyata, J. et al. Cathepsin G: the significance in rheumatoid arthritis as a monocyte chemoattractant. *Rheumatol. Int.* **27**, 375–382 (2007).
116. Weitoft, T. et al. Cathepsin S and cathepsin L in serum and synovial fluid in rheumatoid arthritis with and without autoantibodies. *Rheumatology* **54**, 1923–1928 (2015).
117. Trabandt, A., Gay, R. E., Fassbender, H. G. & Gay, S. Cathepsin B in synovial cells at the site of joint destruction in rheumatoid arthritis. *Arthritis Rheumatol.* **34**, 1444–1451 (1991).
118. Hao, L. et al. Deficiency of cathepsin K prevents inflammation and bone erosion in rheumatoid arthritis and periodontitis and reveals its shared osteoimmune role. *FEBS Lett.* **589**, 1331–1339 (2015).
119. Yan, W. X., Taylor, J., Andrias-Kauba, S. & Pollard, J. D. Passive transfer of demyelination by serum or IgG from chronic inflammatory demyelinating polyneuropathy patients. *Ann. Neurol.* **47**, 765–775 (2000).
120. Cleveland, D. W. & Rothstein, J. D. From Charcot to Lou Gehrig: deciphering selective motor neuron death in ALS. *Nat. Rev. Neurosci.* **2**, 806–819 (2001).
121. Vincent, A. Unravelling the pathogenesis of myasthenia gravis. *Nat. Rev. Immunol.* **2**, 797–804 (2002).
122. Alirezaei, M. et al. Elevated ATG5 expression in autoimmune demyelination and multiple sclerosis. *Autophagy* **5**, 152–158 (2009).
123. Jeltsch-David, H. & Muller, S. Neuropsychiatric systemic lupus erythematosus: pathogenesis and biomarkers. *Nat. Rev. Neurol.* **10**, 579–596 (2014).
124. DeGiorgio, L. A. et al. A subset of lupus anti-DNA antibodies cross-reacts with the NR2 glutamate receptor in systemic lupus erythematosus. *Nat. Med.* **7**, 1189–1193 (2001).
125. Lall, D. & Baloh, R. H. Microglia and C9orf72 in neuroinflammation and ALS and frontotemporal dementia. *J. Clin. Invest.* **127**, 3250–3258 (2017).
126. Schneider, J. L. & Cuervo, A. M. Autophagy and human disease: emerging themes. *Curr. Opin. Genet. Dev.* **26**, 16–23 (2014).
127. Colacurcio, D. J. & Nixon, R. A. Disorders of lysosomal acidification—the emerging role of v-ATPase in aging and neurodegenerative disease. *Ageing Res. Rev.* **32**, 75–88 (2016).
128. Menzies, F. M. et al. Autophagy and neurodegeneration: pathogenic mechanisms and therapeutic opportunities. *Neuron* **93**, 1015–1034 (2017).
129. Brun, S., Schall, N., Jeltsch-David, H., Seze, J. D. & Muller, S. Assessing autophagy in sciatic nerves of a rat model that develops inflammatory autoimmune peripheral neuropathies. *Cells* **6**, 30 (2017).
130. Mc Donald, J. M. & Krainc, D. Lysosomal proteins as a therapeutic target in neurodegeneration. *Annu. Rev. Med.* **68**, 445–458 (2017).
131. Nicoletti, F., Fagone, P., Meroni, P., McCubrey, J. & Bendtzen, K. mTOR as a multifunctional therapeutic target in HIV infection. *Drug Discov. Today* **16**, 715–721 (2011).
132. Patergnani, S. et al. Autophagy and mitophagy elements are increased in body fluids of multiple sclerosis-affected individuals. *J. Neurol. Neurosurg. Psychiatry* **89**, 439–441 (2018).
133. Feng, X., Hou, H., Zou, Y. & Guo, L. Defective autophagy is associated with neuronal injury in a mouse model of multiple sclerosis. *Bosn. J. Basic Med. Sci.* **17**, 95–103 (2017).
134. Chen, S., Zhang, X., Song, L. & Le, W. Autophagy dysregulation in amyotrophic lateral sclerosis. *Brain Pathol.* **22**, 110–116 (2012).
135. Le, W. & Zhang, X. Autophagy dysregulation in amyotrophic lateral sclerosis. *J. Neurol. Sci.* **357**, e69–e71 (2015).
136. Farg, M. A. et al. C9ORF72, implicated in amytrophic lateral sclerosis and frontotemporal dementia, regulates endosomal trafficking. *Hum. Mol. Genet.* **23**, 3579–3595 (2014).
137. Soo, K. Y. et al. Rab1-dependent ER–Golgi transport dysfunction is a common pathogenic mechanism in SOD1, TDP-43 and FUS-associated ALS. *Acta Neuropathol.* **130**, 679–697 (2015).
138. Otomo, A., Pan, L. & Hadano, S. Dysregulation of the autophagy–endolysosomal system in amyotrophic lateral sclerosis and related motor neuron diseases. *Neurol. Res. Int.* **2012**, 12 (2012).
139. Barmada, S. J. et al. Autophagy induction enhances TDP43 turnover and survival in neuronal ALS models. *Nat. Chem. Biol.* **10**, 677–685 (2014).
140. Nassif, M. et al. Pathogenic role of BECN1/Beclin 1 in the development of amyotrophic lateral sclerosis. *Autophagy* **10**, 1256–1271 (2014).
**This pioneering work describes the role of Beclin 1 in the development of amyotrophic lateral sclerosis and highlights the complexity of predicting the effects of manipulating autophagy in a disease context.**
141. Bettencourt, C. & Houlden, H. Exome sequencing uncovers hidden pathways in familial and sporadic ALS. *Nat. Neurosci.* **18**, 611–613 (2015).
142. McKeown, S. R. & Allen, I. V. The fragility of cerebral lysosomes in multiple sclerosis. *Neuropathol. Appl. Neurobiol.* **5**, 405–415 (1979).
143. Pollard, J. D. & Armati, P. J. CIDP—the relevance of recent advances in Schwann cell/axonal neurobiology. *J. Peripher. Nerv. Syst.* **16**, 15–23 (2011).
144. Boerboom, A., Dion, V., Chariot, A. & Franzen, R. Molecular mechanisms involved in Schwann cell plasticity. *Front. Mol. Neurosci.* **10**, 38 (2017).
145. Kim, J., Lee, H. & Park, H. Two faces of Schwann cell dedifferentiation in peripheral neurodegenerative diseases: pro-demyelinating and axon-preservative functions. *Neural Regen. Res.* **9**, 1952–1954 (2014).
146. Arstila, A., Riekkinen, P., Rinne, U. & Laitinen, L. Studies on the pathogenesis of multiple sclerosis. *Eur. Neurol.* **9**, 1–20 (1973).
147. Smith, C. M., Mayer, J. A. & Duncan, I. D. Autophagy promotes oligodendrocyte survival and function following dysmyelination in a long-lived myelin mutant. *J. Neurosci.* **33**, 8088–8100 (2013).
148. Kikuchi, H. et al. Involvement of cathepsin B in the motor neuron degeneration of amyotrophic lateral sclerosis. *Acta Neuropathol.* **105**, 462–468 (2003).
149. Offen, D. et al. Spinal cord mRNA profile in patients with ALS: comparison with transgenic mice expressing the human SOD-1 mutant. *J. Mol. Neurosci.* **38**, 85–93 (2009).
150. Balch, W. E., Morimoto, R. I., Dillin, A. & Kelly, J. W. Adapting proteostasis for disease intervention. *Science* **319**, 916–919 (2008).
151. Wu, H. et al. Caspases: a molecular switch node in the crosstalk between autophagy and apoptosis. *Int. J. Biol. Sci.* **10**, 1072 (2014).
152. Boland, B. et al. Promoting the clearance of neurotoxic proteins in neurodegenerative disorders of ageing. *Nat. Rev. Drug Discov.* **17**, 660–688 (2018).

153. Ross, C. & Poirier, M. Protein aggregation and neurodegenerative disease. *Nat. Med.* **10**, S10–S17 (2004).
154. Takalo, M., Salminen, A., Soininen, H., Hiltunen, M. & Haapasalo, A. Protein aggregation and degradation mechanisms in neurodegenerative diseases. *Am. J. Neurodegener. Dis.* **2**, 1–14 (2013).
155. Kumar, V. et al. Protein aggregation and neurodegenerative diseases: from theory to therapy. *Eur. J. Med. Chem.* **124**, 1105–1120 (2016).
156. Eskelinen, E. L. & Saftig, P. Autophagy: a lysosomal degradation pathway with a central role in health and disease. *Biochim. Biophys. Acta* **1793**, 664–673 (2009).
157. Whyte, L. S., Lau, A. A., Hemsley, K. M., Hopwood, J. J. & Sargeant, T. J. Endo-lysosomal and autophagic dysfunction: a driving factor in Alzheimer's disease? *J. Neurochem.* **140**, 703–717 (2017).
158. Oikawa, N. & Walter, J. Presenilins and γ-secretase in membrane proteostasis. *Cells* **8**, 209 (2019).
159. Hampel, H. et al. Biomarkers for Alzheimer's disease: academic, industry and regulatory perspectives. *Nat. Rev. Drug Discov.* **9**, 560–574 (2010).
160. Corbett, A. et al. Drug repositioning for Alzheimer's disease. *Nat. Rev. Drug Discov.* **11**, 833–846 (2012).
161. Siman, R. et al. Processing of the beta-amyloid precursor. Multiple proteases generate and degrade potentially amyloidogenic fragments. *J. Biol. Chem.* **268**, 16602–16609 (1993).
162. Cataldo, A. M., Paskevich, P. A., Kominami, E. & Nixon, R. A. Lysosomal hydrolases of different classes are abnormally distributed in brains of patients with Alzheimer disease. *Proc. Natl Acad. Sci. USA* **88**, 10998–11002 (1991).
163. Cataldo, A. M. et al. Gene expression and cellular content of cathepsin D in Alzheimer's disease brain: evidence for early up-regulation of the endosomal-lysosomal system. *Neuron* **14**, 671–680 (1995).
164. Bi, X. et al. Novel cathepsin D inhibitors block the formation of hyperphosphorylated tau fragments in hippocampus. *J. Neurochem.* **74**, 1469–1477 (2000).
165. Lauritzen, I., Pardossi-Piquard, R., Bourgeois, A., Bécot, A. & Checler, F. Does intraneuronal accumulation of carboxyl terminal fragments of the amyloid precursor protein trigger early neurotoxicity in Alzheimer's disease? *Curr. Alzheimer Res.* **16**, 453–457 (2019).
166. Lee, J.-H. et al. Lysosomal proteolysis and autophagy require presenilin 1 and are disrupted by Alzheimer-related PS1 mutations. *Cell* **141**, 1146–1158 (2010).
167. Aflaki, E., Westbroek, W. & Sidransky, E. The complicated relationship between Gaucher disease and parkinsonism: insights from a rare disease. *Neuron* **93**, 737–746 (2017).
168. Dehay, B. et al. Lysosomal impairment in Parkinson's disease. *Mov. Disord.* **28**, 725–732 (2013).
169. Webb, J. L., Ravikumar, B., Atkins, J., Skepper, J. N. & Rubinsztein, D. C. α-Synuclein is degraded by both autophagy and the proteasome. *J. Biol. Chem.* **278**, 25009–25013 (2003).
170. Cuervo, A. M., Stefanis, L., Fredenburg, R., Lansbury, P. T. & Sulzer, D. Impaired degradation of mutant α-synuclein by chaperone-mediated autophagy. *Science* **305**, 1292–1295 (2004).
**This article discovered that α-synuclein, a protein associated with several neurodegenerative diseases, is degraded at least partially through CMA, making the latter a very attractive therapeutic target.**
171. Xilouri, M., Vogiatzi, T., Vekrellis, K., Park, D. & Stefanis, L. Abberant α-synuclein confers toxicity to neurons in part through inhibition of chaperone-mediated autophagy. *PLOS ONE* **4**, e5515 (2009).
172. Mak, S., McCormack, A., Manning-Bog, A., Cuervo, A. & Di Monte, D. A. Lysosomal degradation of alpha-synuclein in vivo. *J. Biol. Chem.* **285**, 13621–13629 (2010).
173. Sevlever, D., Jiang, P. & Yen, S. H. Cathepsin D is the main lysosomal enzyme involved in the degradation of α-synuclein and generation of its carboxy-terminally truncated species. *Biochemistry* **47**, 9678–9687 (2008).
174. Vidoni, C., Follo, C., Savino, M., Melone, M. A. & Isidoro, C. The role of cathepsin D in the pathogenesis of human neurodegenerative disorders. *Med. Res. Rev.* **36**, 845–870 (2016).
175. Cullen, V. et al. Cathepsin D expression level affects alpha-synuclein processing, aggregation, and toxicity in vivo. *Mol. Brain* **2**, 5–5 (2009).
176. Caron, N. S., Dorsey, E. R. & Hayden, M. R. Therapeutic approaches to Huntington disease: from the bench to the clinic. *Nat. Rev. Drug Discov.* **17**, 729–750 (2018).
177. Del Toro, D. et al. Mutant huntingtin impairs post-Golgi trafficking to lysosomes by delocalizing optineurin/Rab8 complex from the Golgi apparatus. *Mol. Biol. Cell* **20**, 1478–1492 (2009).
178. Nakanishi, H. et al. Age-related changes in activities and localizations of cathepsins D, E, B, and L in the rat brain tissues. *Exp. Neurol.* **126**, 119–128 (1994).
179. Liang, Q., Ouyang, X., Schneider, L. & Zhang, J. Reduction of mutant huntingtin accumulation and toxicity by lysosomal cathepsins D and B in neurons. *Mol. Neurodegener.* **6**, 37 (2011).
180. Qin, Z. H. et al. Autophagy regulates the processing of amino terminal huntingtin fragments. *Hum. Mol. Genet.* **12**, 3231–3244 (2003).
181. Kim, Y. J. et al. Lysosomal proteases are involved in generation of N-terminal huntingtin fragments. *Neurobiol. Dis.* **22**, 346–356 (2006).
182. Ratovitski, T., Chighladze, E., Waldron, E., Hirschhorn, R. & Ross, C. Cysteine proteases bleomycin hydrolase and cathepsin Z mediate N-terminal proteolysis and toxicity of mutant huntingtin. *J. Biol. Chem.* **286**, 12578–12589 (2011).
183. Bhutani, S., Das, A., Maheshwari, M., Lakhotia, S. & Jana, N. Dysregulation of core components of SCF complex in poly-glutamine disorders. *Cell Death Dis.* **3**, e428 (2012).
184. Ravikumar, B., Imarisio, S., Sarkar, S., O'Kane, C. J. & Rubinsztein, D. C. Rab5 modulates aggregation and toxicity of mutant huntingtin through macroautophagy in cell and fly models of Huntington disease. *J. Cell Sci.* **121**, 1649–1660 (2008).
185. Qi, L. & Zhang, X. D. Role of chaperone-mediated autophagy in degrading Huntington's disease-associated huntingtin protein. *Acta Biochim. Biophys. Sin.* **46**, 83–91 (2014).
186. Koga, H., Martinez-Vicente, M., Macian, F., Verkhusha, V. & Cuervo, A. A photoconvertible fluorescent reporter to track chaperone-mediated autophagy. *Nat. Commun.* **2**, 386 (2011).
187. Qi, L. et al. The role of chaperone-mediated autophagy in huntingtin degradation. *PLOS ONE* **7**, e46834 (2012).
188. Bauer, P. et al. Harnessing chaperone-mediated autophagy for the selective degradation of mutant huntingtin protein. *Nat. Biotechnol.* **28**, 256–263 (2010).
189. Trajkovic, K., Jeong, H. & Krainc, D. Mutant Huntingtin is secreted via a late endosomal/lysosomal unconventional secretory pathway. *J. Neurosci.* **37**, 9000–9012 (2017).
190. Erie, C., Sacino, M., Houle, L., Lu, M. L. & Wei, J. Altered lysosomal positioning affects lysosomal functions in a cellular model of Huntington's disease. *Eur. J. Neurosci.* **42**, 1941–1951 (2015).
191. Usenovic, M. & Krainc, D. Lysosomal dysfunction in neurodegeneration: the role of ATP13A2/PARK9. *Autophagy* **8**, 987–988 (2012).
192. Sweeney, P. et al. Protein misfolding in neurodegenerative diseases: implications and strategies. *Transl. Neurodegener.* **6**, 6 (2017).
193. Martini-Stoica, H., Xu, Y., Ballabio, A. & Zheng, H. The autophagy–lysosomal pathway in neurodegeneration: a TFEB perspective. *Trends Neurosci.* **39**, 221–234 (2016).
194. Torra, A. et al. Overexpression of TFEB drives a pleiotropic neurotrophic effect and prevents Parkinson's disease-related neurodegeneration. *Mol. Ther.* **26**, 1552–1567 (2018).
195. Cortes, C. J. & La Spada, A. R. TFEB dysregulation as a driver of autophagy dysfunction in neurodegenerative disease: molecular mechanisms, cellular processes, and emerging therapeutic opportunities. *Neurobiol. Dis.* **122**, 83–93 (2019).
196. Wang, H., Wang, R., Xu, S. & Lakshmana, M. Transcription factor EB is selectively reduced in the nuclear fractions of Alzheimer's and amyotrophic lateral sclerosis brains. *Neurosci. J.* **2016**, 4732837 (2016).
197. Vakifahmetoglu-Norberg, H., Xia, H. G. & Yuan, J. Pharmacologic agents targeting autophagy. *J. Clin. Invest.* **125**, 5–13 (2015).
198. Clarke, A. J. & Simon, A. K. Autophagy in the renewal, differentiation and homeostasis of immune cells. *Nat. Rev. Immunol.* **19**, 170–183 (2019).
199. Brady, R. O. Enzyme replacement for lysosomal diseases. *Annu. Rev. Med.* **57**, 283–296 (2006).
200. Jurecka, A. & Tylki-Szymanska, A. Enzyme replacement therapy: lessons learned and emerging questions. *Expert Opin. Orphan Drugs* **3**, 293–305 (2015).
201. Safary, A., Akbarzadeh Khiavi, M., Mousavi, R., Barar, J. & Rafi, M. A. Enzyme replacement therapies: what is the best option? *BioImpacts* **8**, 153–157 (2018).
202. Spada, M. et al. Early higher dosage of alglucosidase alpha in classic Pompe disease. *J. Pediatr. Endocrinol. Metab.* **31**, 1343–1347 (2018).
203. Lee, B. H. et al. A multicenter, open-label, phase III study of Abcertin in Gaucher disease. *Medicine (Baltimore)* **96**, e8492 (2017).
204. Renna, M. et al. Azithromycin blocks autophagy and may predispose cystic fibrosis patients to mycobacterial infection. *J. Clin. Invest.* **121**, 3554–3563 (2011).
205. Rubinsztein, D. C., Codogno, P. & Levine, B. Autophagy modulation as a potential therapeutic target for diverse diseases. *Nat. Rev. Drug Discov.* **11**, 709–730 (2012).
206. Yin, H. et al. The therapeutic and pathogenic role of autophagy in autoimmune diseases. *Front. Immunol.* **9** (2018).
207. Retnakumar, S. V. & Muller, S. Pharmacological autophagy regulators as therapeutic agents for inflammatory bowel diseases. *Trends Mol. Med.* **25**, 516–537 (2019).
208. Ziegler, H. K. & Unanue, E. R. Decrease in macrophage antigen catabolism caused by ammonia and chloroquine is associated with inhibition of antigen presentation to T cells. *Proc. Natl Acad. Sci. USA* **79**, 175–178 (1982).
209. Xiu, Y. et al. Chloroquine reduces osteoclastogenesis in murine osteoporosis by preventing TRAF3 degradation. *J. Clin. Invest.* **124**, 297–310 (2014).
210. Vomero, M. et al. Autophagy and rheumatoid arthritis: current knowledges and future perspectives. *Front. Immunol.* **9**, 1577 (2018).
211. Kuznik, A. et al. Mechanism of endosomal TLR inhibition by antimalarial drugs and imidazoquinolines. *J. Immunol.* **186**, 4794–4804 (2011).
212. Sumpter, M. D., Tatro, L. S., Stoecker, W. V. & Rader, R. K. Evidence for risk of cardiomyopathy with hydroxychloroquine. *Lupus* **21**, 1594–1596 (2012).
213. McAfee, Q. et al. Autophagy inhibitor Lys05 has single-agent antitumor activity and reproduces the phenotype of a genetic autophagy deficiency. *Proc. Natl Acad. Sci. USA* **109**, 8253–8258 (2012).
214. Maiuri, M. C. & De Stefano, D. Autophagy Networks in Inflammation (Springer, 2016).
215. Xu, M. et al. A phenotypic compound screening assay for lysosomal storage diseases. *J. Biomol. Screen.* **19**, 168–175 (2014).
216. Wang, F. et al. The biomolecular corona is retained during nanoparticle uptake and protects the cells from the damage induced by cationic nanoparticles until degraded in the lysosomes. *Nanomedicine* **9**, 1159–1168 (2013).
217. Bandyopadhyay, D., Cyphersmith, A., Zapata, J. A., Kim, Y. J. & Payne, C. K. Lysosome transport as a function of lysosome diameter. *PLOS ONE* **9**, e86847 (2014).
218. Valdor, R. et al. Chaperone-mediated autophagy regulates T cell responses through targeted degradation of negative regulators of T cell activation. *Nat. Immunol.* **15**, 1046–1054 (2014).
**This article is the first demonstration that CMA plays an important role in T cell immune regulation in vivo.**
219. Sardiello, M. et al. A gene network regulating lysosomal biogenesis and function. *Science* **325**, 473–477 (2009).
**This article reveals that a highly coordinated gene network, regulated by the master regulator TFEB, exists in lysosomes, and that regulating this gene network via TFEB may provide a potential therapeutic strategy.**
220. Martina, J. A., Diab, H. I., Li, H. & Puertollano, R. Novel roles for the MiTF/TFE family of transcription factors in organelle biogenesis, nutrient sensing, and energy homeostasis. *Cell. Mol. Life Sci.* **71**, 2483–2497 (2014).
221. Diwu, Z., Chen, C. S., Zhang, C., Klaubert, D. H. & Haugland, R. P. A novel acidotropic pH indicator and its potential application in labeling acidic organelles of live cells. *Chem. Biol.* **6**, 411–418 (1999).
222. Johnson, D. E., Ostrowski, P., Jaumouille, V. & Grinstein, S. The position of lysosomes within the cell determines their luminal pH. *J. Cell Biol.* **212**, 677–692 (2016).
223. Ma, L., Ouyang, Q., Werthmann, G. C., Thompson, H. M. & Morrow, E. M. Live-cell microscopy and fluorescence-based measurement of luminal pH in intracellular organelles. *Front. Cell Dev. Biol.* **5**, 71 (2017).

224. Aits, S. et al. Sensitive detection of lysosomal membrane permeabilization by lysosomal galectin puncta assay. *Autophagy* **11**, 1408–1424 (2015). **This article elegantly decsribes a novel, specific and practical tool to detect lysosomal membrane permeabilization.**
225. Zhou, J. et al. Activation of lysosomal function in the course of autophagy via mTORC1 suppression and autophagosome-lysosome fusion. *Cell Res.* **23**, 508–523 (2013).
226. Ono, K., Kim, S. O. & Han, J. Susceptibility of lysosomes to rupture is a determinant for plasma membrane disruption in tumor necrosis factor alpha-induced cell death. *Mol. Cell. Biol.* **23**, 665–676 (2003).
227. Pierzyńska-Mach, A., Janowski, P. A. & Dobrucki, J. W. Evaluation of acridine orange, LysoTracker Red, and quinacrine as fluorescent probes for long-term tracking of acidic vesicles. *Cytometry Part A* **85**, 729–737 (2014).
228. Kaushik, S. & Cuervo, A. Chaperone-mediated autophagy. *Methods Mol. Biol.* **445**, 227–244 (2008).
229. Kaushik, S. & Cuervo, A. Methods to monitor chaperone-mediated autophagy. *Methods Enzymol.* **452**, 297–324 (2009).
230. Patel, B. & Cuervo, A. Methods to study chaperone-mediated autophagy. *Methods* **75**, 133–140 (2015).
231. Klionsky, D. J. et al. Guidelines for the use and interpretation of assays for monitoring autophagy. *Autophagy* **8**, 445–544 (2012). **This article is a comprehensive and critical overview of the numerous methods and tools that are used for evaluating autophagy and lysosomal activity, and deciphers the complex mechanisms and pathways involved in the regulation of these processes.**
232. Bowes, J. et al. Reducing safety-related drug attrition: the use of in vitro pharmacological profiling. *Nat. Rev. Drug Discov.* **11**, 909–922 (2012).
233. Galluzzi, L. et al. Molecular mechanisms of cell death: recommendations of the Nomenclature Committee on Cell Death 2018. *Cell Death Differ.* **25**, 486–541 (2018).
234. Andrade, M. M. et al. Substrate reduction therapy with miglustat in type 1 Gaucher disease in Spain. Nine years outcomes update on ZAGAL Study. *Blood* **122**, 4713–4713 (2013).
235. Smid, B. E. et al. Biochemical response to substrate reduction therapy versus enzyme replacement therapy in Gaucher disease type 1 patients. *Orphanet J. Rare Dis.* **11**, 28 (2016).
236. Guerard, N. et al. Lucerastat, an iminosugar for substrate reduction therapy: tolerability, pharmacodynamics, and pharmacokinetics in patients with Fabry disease on enzyme replacement. *Clin. Pharmacol. Ther.* **103**, 703–711 (2018).
237. Guerard, N., Morand, O. & Dingemanse, J. Lucerastat, an iminosugar with potential as substrate reduction therapy for glycolipid storage disorders: safety, tolerability, and pharmacokinetics in healthy subjects. *Orphanet J. Rare Dis.* **12**, 9 (2017).
238. Marshall, J. et al. CNS-accessible inhibitor of glucosylceramide synthase for substrate reduction therapy of neuronopathic Gaucher disease. *Mol. Ther.* **24**, 1019–1029 (2016).
239. Piotrowska, E. et al. Genistin-rich soy isoflavone extract in substrate reduction therapy for Sanfilippo syndrome: an open-label, pilot study in 10 pediatric patients. *Curr. Ther. Res.* **69**, 166–179 (2008).
240. Moskot, M. et al. The phytoestrogen genistein modulates lysosomal metabolism and transcription factor EB (TFEB) activation. *J. Biol. Chem.* **289**, 17054–17069 (2014).
241. Entchev, E. V. et al. Odiparcil is a promising substrate reduction therapy in MPS VI murine model. *Mol. Genet. Metab.* **123**, S42–S43 (2018).
242. Steet, R. A. et al. The iminosugar isofagomine increases the activity of N370S mutant acid β-glucosidase in Gaucher fibroblasts by several mechanisms. *Proc. Natl Acad. Sci. USA* **103**, 13813–13818 (2006).
243. Magalhaes, J., Gegg, M. E., Migdalska-Richards, A. & Schapira, A. H. Effects of ambroxol on the autophagy–lysosome pathway and mitochondria in primary cortical neurons. *Sci. Rep.* **8**, 1385 (2018).
244. Porto, C. et al. Pharmacological enhancement of α-glucosidase by the allosteric chaperone *N*-acetylcysteine. *Mol. Ther.* **20**, 2201–2211 (2012).
245. Xiao, J. et al. Discovery of a novel noniminosugar acid α glucosidase chaperone series. *J. Med. Chem.* **55**, 7546–7559 (2012).
246. Flanagan, J. J. et al. The pharmacological chaperone 1-deoxynojirimycin increases the activity and lysosomal trafficking of multiple mutant forms of acid alpha-glucosidase. *Hum. Mutat.* **30**, 1683–1692 (2009).
247. Berardi, A. S. et al. Pharmacological chaperones increase residual β-galactocerebrosidase activity in fibroblasts from Krabbe patients. *Mol. Genet. Metab.* **112**, 294–301 (2014).
248. Matsuda, J. et al. Chemical chaperone therapy for brain pathology in GM1-gangliosidosis. *Proc. Natl Acad. Sci. USA* **100**, 15912–15917 (2003).
249. Takai, T. et al. A bicyclic 1-deoxygalactonojirimycin derivative as a novel pharmacological chaperone for GM1 gangliosidosis. *Mol. Ther.* **21**, 526–532 (2013).
250. Aflaki, E. et al. A new glucocerebrosidase chaperone reduces α-synuclein and glycolipid levels in iPSC-derived dopaminergic neurons from patients with Gaucher disease and parkinsonism. *J. Neurosci.* **36**, 7441–7452 (2016).
251. Thome, R. et al. Dendritic cells treated with chloroquine modulate experimental autoimmune encephalomyelitis. *Immunol. Cell Biol.* **92**, 124–132 (2014).
252. Danza, A., Grana, D., Goni, M., Vargas, A. & Ruiz-Irastorza, G. Hydroxychloroquine for autoimmune diseases. *Rev. Med. Chil.* **144**, 232–240 (2016).
253. Lai, Z. W. et al. Sirolimus in patients with clinically active systemic lupus erythematosus resistant to, or intolerant of, conventional medications: a single-arm, open-label, phase 1/2 trial. *Lancet* **391**, 1186–1196 (2018).
254. Shao, P., Ma, L., Ren, Y. & Liu, H. Modulation of the immune response in rheumatoid arthritis with strategically released rapamycin. *Mol. Med. Report.* **16**, 5257–5262 (2017).
255. Matarrese, P. et al. Cathepsin B inhibition interferes with metastatic potential of human melanoma: an in vitro and in vivo study. *Mol. Cancer* **9**, 207 (2010).
256. Fox, C. et al. Inhibition of lysosomal protease cathepsin D reduces renal fibrosis in murine chronic kidney disease. *Sci. Rep.* **6**, 20101 (2016).
257. Ikeda, Y. et al. Cathepsins B and L in synovial fluids from patients with rheumatoid arthritis and the effect of cathepsin B on the activation of pro-urokinase. *J. Med. Invest.* **47**, 61–75 (2000).
258. Yamada, A., Ishimaru, N., Arakaki, R., Katunuma, N. & Hayashi, Y. Cathepsin L inhibition prevents murine autoimmune diabetes via suppression of $CD8^+$ T cell activity. *PLOS ONE* **5**, e12894 (2010).
259. Shah, P. P. et al. A small-molecule oxocarbazate inhibitor of human cathepsin L blocks severe acute respiratory syndrome and ebola pseudotype virus infection into human embryonic kidney 293T cells. *Mol. Pharmacol.* **78**, 319–324 (2010).
260. Saegusa, K. et al. Cathepsin S inhibitor prevents autoantigen presentation and autoimmunity. *J. Clin. Invest.* **110**, 361–369 (2002).
261. Nakagawa, T. Y. et al. Impaired invariant chain degradation and antigen presentation and diminished collagen-induced arthritis in cathepsin S null mice. *Immunity* **10**, 207–217 (1999).
262. Rupanagudi, K. V. et al. Cathepsin S inhibition suppresses systemic lupus erythematosus and lupus nephritis because cathepsin S is essential for MHC class II-mediated CD4 T cell and B cell priming. *Ann. Rheum. Dis.* **74**, 452–463 (2015).
263. Hargreaves, P. et al. FRI0295 inhibition of cathepsin s leads to suppression of antigen specific T cells from patients with primary Sjögren syndrome. *Ann. Rheum. Dis.* **77**, 684–684 (2018).
264. Edman, M. C. et al. Increased cathepsin S activity associated with decreased protease inhibitory capacity contributes to altered tear proteins in Sjogren's syndrome patients. *Sci. Rep.* **8**, 11044 (2018).
265. Katunuma, N. et al. Structure-based development of pyridoxal propionate derivatives as specific inhibitors of cathepsin K in vitro and in vivo. *Biochem. Biophys. Res. Commun.* **267**, 850–854 (2000).
266. Stroup, G. B. et al. Potent and selective inhibition of human cathepsin K leads to inhibition of bone resorption in vivo in a nonhuman primate. *J. Bone Miner. Res.* **16**, 1739–1746 (2001).
267. Nwosu, L. N. et al. Analgesic effects of the cathepsin K inhibitor L-006235 in the monosodium iodoacetate model of osteoarthritis pain. *PAIN Rep.* **3**, e685 (2018).
268. Viswanathan, K. et al. Nonpeptidic lysosomal modulators derived from Z-Phe-Ala-diazomethylketone for treating protein accumulation diseases. *ACS Med. Chem. Lett.* **3**, 920–924 (2012).
269. Yuan, N. et al. Bafilomycin A1 targets both autophagy and apoptosis pathways in pediatric B-cell acute lymphoblastic leukemia. *Haematologica* **100**, 345–356 (2015).
270. Niikura, K., Takeshita, N. & Takano, M. A vacuolar ATPase inhibitor, FR167356, prevents bone resorption in ovariectomized rats with high potency and specificity: potential for clinical application. *J. Bone Miner. Res.* **20**, 1579–1588 (2005).
271. Lebreton, S., Jaunbergs, J., Roth, M. G., Ferguson, D. A. & De Brabander, J. K. Evaluating the potential of vacuolar ATPase inhibitors as anticancer agents and multigram synthesis of the potent salicylihalamide analog saliphenylhalamide. *Bioorg. Med. Chem. Lett.* **18**, 5879–5883 (2008).
272. Visentin, L. et al. A selective inhibitor of the osteoclastic V-H(+)-ATPase prevents bone loss in both thyroparathyroidectomized and ovariectomized rats. *J. Clin. Invest.* **106**, 309–318 (2000).
273. Aldrich, L. N. et al. Discovery of a small-molecule probe for V-ATPase function. *J. Am. Chem. Soc.* **137**, 5563–5568 (2015).
274. Grimm, C. et al. Small molecule activators of TRPML3. *Chem. Biol.* **17**, 135–148 (2010).
275. Martin, S. et al. Inhibition of PIKfyve by YM-201636 dysregulates autophagy and leads to apoptosis-independent neuronal cell death. *PLOS ONE* **8**, e60152 (2013).
276. Cai, X. et al. PIKfyve, a class III PI kinase, is the target of the small molecular IL-12/IL-23 inhibitor apilimod and a player in Toll-like receptor signaling. *Chem. Biol.* **20**, 912–921 (2013).
277. Sands, B. E. et al. Randomized, double-blind, placebo-controlled trial of the oral interleukin-12/23 inhibitor apilimod mesylate for treatment of active Crohn's disease. *Inflamm. Bowel Dis.* **16**, 1209–1218 (2010).
278. Krausz, S. et al. Brief Report: A phase IIa, randomized, double-blind, placebo-controlled trial of apilimod mesylate, an interleukin-12/interleukin-23 inhibitor, in patients with rheumatoid arthritis. *Arthritis Rheum.* **64**, 1750–1755 (2012).
279. Wen, W., Liu, W., Shao, Y. & Chen, L. VER-155008, a small molecule inhibitor of HSP70 with potent anti-cancer activity on lung cancer cell lines. *Exp. Biol. Med.* **239**, 638–645 (2014).
280. Yang, X. & Tohda, C. Heat shock cognate 70 inhibitor, VER-155008, reduces memory deficits and axonal degeneration in a mouse model of Alzheimer's disease. *Front. Pharmacol.* **9**, 48 (2018).
281. Gong, Z. et al. Humanin is an endogenous activator of chaperone-mediated autophagy. *J. Cell Biol.* **217**, 635–647 (2018).
282. Hernandez, I. et al. A farnesyltransferase inhibitor activates lysosomes and reduces tau pathology in mice with tauopathy. *Sci. Transl. Med.* **11**, eaat3005 (2019).
283. Lachmann, R. Treatments for lysosomal storage disorders. *Biochem. Soc. Trans.* **38**, 1465–1468 (2010).
284. Radin, N. S. Treatment of Gaucher disease with an enzyme inhibitor. *Glycoconjugate J.* **13**, 153–157 (1996).
285. Pineda, M., Walterfang, M. & Patterson, M. Miglustat in Niemann–Pick disease type C patients: a review. *Orphanet J. Rare Dis.* **13**, 140–140 (2018).
286. Hughes, D. A. et al. Oral pharmacological chaperone migalastat compared with enzyme replacement therapy in Fabry disease: 18-month results from the randomised phase III ATTRACT study. *J. Med. Genet.* **54**, 288–296 (2017).
287. Wise, A. H. et al. Parkinson's disease prevalence in Fabry disease: a survey study. *Mol. Genet. Metab. Rep.* **14**, 27–30 (2018).
288. Gaffke, L., Pierzynowska, K., Piotrowska, E. & Wegrzyn, G. How close are we to therapies for Sanfilippo disease? *Metab. Brain Dis.* **33**, 1–10 (2018).
289. Mohamed, F. E., Al-Gazali, L., Al-Jasmi, F. & Ali, B. R. Pharmaceutical chaperones and proteostasis regulators in the therapy of lysosomal storage disorders: current perspective and future promises. *Front. Pharmacol.* **8**, 448 (2017).
290. Ortolano, S., Vieitez, I., Navarro, C. & Spuch, C. Treatment of lysosomal storage diseases: recent patents and future strategies. *Recent Pat. Endocr. Metab. Immune Drug Discov.* **8**, 9–25 (2014).
291. Pereira, D. M., Valentao, P. & Andrade, P. B. Tuning protein folding in lysosomal storage diseases: the chemistry behind pharmacological chaperones. *Chem. Sci.* **9**, 1740–1752 (2018).
292. Beck, M. Treatment strategies for lysosomal storage disorders. *Dev. Med. Child Neurol.* **60**, 13–18 (2018).

293. Siklos, M., BenAissa, M. & Thatcher, G. R. Cysteine proteases as therapeutic targets: does selectivity matter? A systematic review of calpain and cathepsin inhibitors. *Acta Pharm. Sin. B* **5**, 506–519 (2015).
294. Lowry, J. R. & Klegeris, A. Emerging roles of microglial cathepsins in neurodegenerative disease. *Brain Res. Bull.* **139**, 144–156 (2018).
295. Sena, B. F., Figueiredo, J. L. & Aikawa, E. Cathepsin S as an inhibitor of cardiovascular inflammation and calcification in chronic kidney disease. *Front. Cardiovasc. Med.* **4**, 88 (2018).
296. Duong, L. T., Leung, A. T. & Langdahl, B. Cathepsin K inhibition: a new mechanism for the treatment of osteoporosis. *Calcif. Tissue Int.* **98**, 381–397 (2016).
297. Shacka, J. et al. Bafilomycin A1 inhibits chloroquine-induced death of cerebellar granule neurons. *Mol. Pharmacol.* **69**, 1125–1136 (2006).
298. Redmann, M. et al. Inhibition of autophagy with bafilomycin and chloroquine decreases mitochondrial quality and bioenergetic function in primary neurons. *Redox Biol.* **11**, 73–81 (2017).
299. Boyd, M. R. et al. Discovery of a novel antitumor benzolactone enamide class that selectively inhibits mammalian vacuolar-type (H+)-ATPases. *J. Pharmacol. Exp. Ther.* **297**, 114–120 (2001).
300. Pamarthy, S., Kulshrestha, A., Katara, G. K. & Beaman, K. D. The curious case of vacuolar ATPase: regulation of signaling pathways. *Mol. Cancer* **17**, 41 (2018).
301. Sterea, A., Almasi, S. & El Hiani, Y. The hidden potential of lysosomal ion channels: a new era of oncogenes. *Cell Calcium* **72**, 91–103 (2018).
302. Di Paola, S., Scotto-Rosato, A. & Medina, D. L. TRPML1: the Ca (2+) retaker of the lysosome. *Cell Calcium* **69**, 112–121 (2018).
303. Chen, C. C. et al. A small molecule restores function to TRPML1 mutant isoforms responsible for mucolipidosis type IV. *Nat. Commun.* **5**, 4681 (2014).
304. Waller-Evans, H. & Lloyd-Evans, E. Regulation of TRPML1 function. *Biochem. Soc. Trans.* **43**, 442–446 (2015).
305. Feng, X., Xiong, J., Lu, Y., Xia, X. & Zhu, M. X. Differential mechanisms of action of the mucolipin synthetic agonist, ML-SA1, on insect TRPML and mammalian TRPML1. *Cell Calcium* **56**, 446–456 (2014).
306. Choy, C. et al. Lysosome enlargement during inhibition of the lipid kinase PIKfyve proceeds through lysosome coalescence. *J. Cell Sci.* **131** (2018).
307. Gayle, S. et al. Identification of apilimod as a first-in-class PIKfyve kinase inhibitor for treatment of B-cell non-Hodgkin lymphoma. *Blood* **129**, 1768–1778 (2017).
308. Massey, A. J. et al. A novel, small molecule inhibitor of Hsc70/Hsp70 potentiates Hsp90 inhibitor induced apoptosis in HCT116 colon carcinoma cells. *Cancer Chemother. Pharmacol.* **66**, 535–545 (2010).
309. Schlecht, R. et al. Functional analysis of Hsp70 inhibitors. *PLOS ONE* **8**, e78443 (2013).
310. Page, N. et al. The spliceosomal phosphopeptide P140 controls the lupus disease by interacting with the HSC70 protein and via a mechanism mediated by γδ T cells. *PLOS ONE* **4**, e5273 (2009).
311. Wang, F. et al. Blocking nuclear export of HSPA8 after heat shock stress severely alters cell survival. *Sci. Rep.* **8**, 16820 (2018).
312. Schall, N. & Muller, S. Resetting the autoreactive immune system with a therapeutic peptide in lupus. *Lupus* **24**, 412–418 (2015).
313. Monneaux, F., Lozano, J. M., Patarroyo, M. E., Briand, J. P. & Muller, S. T cell recognition and therapeutic effect of a phosphorylated synthetic peptide of the 70K snRNP protein administered in MRL/lpr mice. *Eur. J. Immunol.* **33**, 287–296 (2003).
314. Wilhelm, M. et al. Lupus regulator peptide P140 represses B cell differentiation by reducing HLA class II molecule overexpression. *Arthritis Rheumatol.* **70**, 1077–1088 (2018).
315. Monneaux, F. et al. Selective modulation of CD4+ T cells from lupus patients by a promiscuous, protective peptide analog. *J. Immunol.* **175**, 5839–5847 (2005).
316. Bendorius, M. et al. The mitochondrion–lysosome axis in adaptive and innate immunity: effect of lupus regulator peptide P140 on mitochondria autophagy and NETosis. *Front. Immunol.* **9**, 2158 (2018).
317. Zimmer, R., Scherbarth, H., Rillo, O., Gomez-Reino, J. & Muller, S. Lupuzor/P140 peptide in patients with systemic lupus erythematosus: a randomised, double-blind, placebo-controlled phase IIb clinical trial. *Ann. Rheum. Dis.* **72**, 1830–1835 (2013).
318. Muller, S. & Wallace, D. The importance of implementing proper selection of excipients in lupus clinical trials. *Lupus* **23**, 609–614 (2014).
319. Gong, Z. et al. Humanin is an endogenous activator of chaperone-mediated autophagy. *J. Cell Biol.* **217**, 635–647 (2018).
320. Gong, Z. et al. Central effects of humanin on hepatic triglyceride secretion. *Am. J. Physiol. Endocrinol. Metab.* **309**, E283–E292 (2015).
321. Cang, C., Aranda, K., Seo, Y.-j., Gasnier, B. & Ren, D. TMEM175 is an organelle K+ channel regulating lysosomal function. *Cell* **162**, 1101–1112 (2015).
322. Jinn, S. et al. TMEM175 deficiency impairs lysosomal and mitochondrial function and increases α-synuclein aggregation. *Proc. Natl Acad. Sci. USA* **114**, 2389–2394 (2017).
323. Lee, C. et al. The lysosomal potassium channel TMEM175 adopts a novel tetrameric architecture. *Nature* **547**, 472–475 (2017).
324. Vivas, O., Tiscione, S. A., Dixon, R. E., Ory, D. S. & Dickson, E. J. Niemann–Pick type C disease reveals a link between lysosomal cholesterol and PtdIns(4,5)P2 that regulates neuronal excitability. *Cell Rep.* **27**, 2636–2648.e2634 (2019).
325. Ghezzi, F., Monni, L. & Nistri, A. Functional up-regulation of the M-current by retigabine contrasts hyperexcitability and excitotoxicity on rat hypoglossal motoneurons. *J. Physiol.* **596**, 2611–2629 (2018).
326. Kirkegaard, T. et al. Hsp70 stabilizes lysosomes and reverts Niemann–Pick disease-associated lysosomal pathology. *Nature* **463**, 549–553 (2010).
327. Kon, M. et al. Chaperone-mediated autophagy is required for tumor growth. *Sci. Transl. Med.* **3**, 109ra117 (2011).
328. Zhang, C. & Cuervo, A. M. Restoration of chaperone-mediated autophagy in aging liver improves cellular maintenance and hepatic function. *Nat. Med.* **14**, 959–965 (2008).
329. Stern, S. T. & Johnson, D. N. Role for nanomaterial–autophagy interaction in neurodegenerative disease. *Autophagy* **4**, 1097–1100 (2008).
330. Liu, H. et al. A functionalized single-walled carbon nanotube-induced autophagic cell death in human lung cells through Akt–TSC2-mTOR signaling. *Cell Death Dis.* **2**, e159 (2011).
331. Wu, L. et al. Tuning cell autophagy by diversifying carbon nanotube surface chemistry. *ACS Nano* **8**, 2087–2099 (2014).
332. Duan, J. et al. Silica nanoparticles enhance autophagic activity, disturb endothelial cell homeostasis and impair angiogenesis. *Part. Fibre Toxicol.* **11**, 50 (2014).
333. Stern, S. T., Adiseshaiah, P. P. & Crist, R. M. Autophagy and lysosomal dysfunction as emerging mechanisms of nanomaterial toxicity. *Part. Fibre Toxicol.* **9**, 20 (2012).
334. Peynshaert, K. et al. Exploiting intrinsic nanoparticle toxicity: the pros and cons of nanoparticle-induced autophagy in biomedical research. *Chem. Rev.* **114**, 7581–7609 (2014).
335. Bianco, A. & Muller, S. Nanomaterials, autophagy, and lupus disease. *ChemMedChem* **11**, 166–174 (2016).
336. Mohammadinejad, R., Ahmadi, Z., Tavakol, S. & Ashrafizadeh, M. Berberine as a potential autophagy modulator. *J. Cell. Physiol.* https://doi.org/10.1002/jcp.28325 (2019).

**Acknowledgements**
The authors apologize to all those whose work is not cited due to space limitations. They gratefully acknowledge Hélène Jeltsch-David for critically reading the manuscript. This research was funded by the French Centre National de la Recherche Scientifique, Région Alsace, the Laboratory of Excellence Medalis (ANR-10-LABX-0034), Initiative of Excellence (IdEx), Strasbourg University, and ImmuPharma France. S.M. is grateful to the University of Strasbourg Institute for Advanced Study (USIAS) for funding F.W., and acknowledges the support of the TRANSAUTOPHAGY COST Action (CA15138), the Club francophone de l'autophagie (CFATG) and the European Regional Development Fund of the European Union in the framework of the INTERREG V Upper Rhine programme.

**Author contributions**
All authors made substantial, direct and intellectual contribution to the work and approved it for publication.

**Competing interests**
S.M. discloses the following conflicts of interest: research funding (paid to institution) and a past consultant for ImmuPharma; co-inventor of CNRS-ImmuPharma patents on P140 peptide; owns ImmuPharma shares. The authors declare that the research was conducted in the absence of any commercial or financial relationships that could be construed as a potential conflict of interest. S.R.B. and F.W. declare no competing interests.

**Publisher's note**
Springer Nature remains neutral with regard to jurisdictional claims in published maps and institutional affiliations.



DEFS00023239

# EXHIBIT 2

0270-9139/89/0905-0763$02.00/0
HEPATOLOGY
Vol. 9, No. 5, pp. 763–784, 1989
Printed in U.S.A.
Copyright © 1989 by the American Association for the Study of Liver Diseases

Special Article

# The Liver and IgA: Immunological, Cell Biological and Clinical Implications

WILLIAM R. BROWN AND THOMAS M. KLOPPEL
*Department of Medicine, Veterans Administration Medical Center, and the University of Colorado School of Medicine, Denver, Colorado 80220*

**Secretory immunoglobulin A is the characteristic and predominant immunoglobulin of the mucosal immune system; it participates in immunological protection at the level of mucous membrane surfaces. During the past 10 to 15 years, a great deal of experimental and clinical evidence has shown that the liver is very much involved in the sIgA system.**

**In certain animals (rats, mice, rabbits), polymeric forms of IgA are efficiently cleared by the liver and transported into bile by a receptor-mediated vesicular pathway across hepatocytes. Taking advantage of this easily accessible pathway, investigators have defined many of the events in the external secretion of pIgA, including details about the synthesis and secretion of its receptor, secretory component. In the rat hepatocyte, secretory component is synthesized as a transmembrane glycoprotein and is expressed preferentially on the sinusoidal plasma membrane; circulating pIgA that binds to secretory component is internalized into endocytic vesicles and transported across the hepatocyte to the bile canalicular membrane, where the pIgA is released into bile as a soluble complex with a portion of the secretory component, the complex being secretory IgA. In some other animals (dog, guinea pig, sheep) as well as man, biliary epithelial cells, not hepatocytes, express secretory component and perform the transcytosis and secretion of pIgA into bile. In those species, much of the pIgA that reaches bile is synthesized locally in plasma cells that populate the biliary tree; this design is analogous to the release of sIgA into various mucosae in the body.**

**The major biological functions ascribed to the secretion of IgA into bile are enhancement of immunological defense of the biliary and upper intestinal tracts and the clearance of harmful antigens from the circulation as IgA-antigen complexes. However, the importance of biliary IgA antibodies is largely unclarified, and man lacks the capacity for effective clearance of IgA-antigen complexes via the secretory component-mediated transhepatocellular pathway; whether this deficit contributes to the propensity for man to develop IgA immune complex diseases should be clarified.**

**Among liver diseases, alcoholic disease is most closely linked to alterations in IgA metabolism. This association is manifested principally by the deposition of IgA along the sinusoids in the livers of the majority of alcoholics and in the renal mesangium of many. The IgA1 subclass of IgA predominates in the IgA deposits in both tissues; the possibility that this predominance is related to abnormalities in the removal of circulating IgA1 by asialoglycoprotein receptors on hepatocytes is an intriguing consideration.**

**Thus, the liver plays a unique role in mucosal immunity and in the physiology of IgA in normal and disease states. Further study of the associations between the liver and IgA, particularly in man, is clearly needed.**

IgA is the major and characteristic immunoglobulin of the mucosal immune system, that component of host immunological defenses specifically responsible for defense of mucous membrane surfaces against external agents (1). In the mid-1970's a group of Belgian workers (2), searching for an easily accessible and rich source of IgA in the rat, discovered that IgA was the major protein in bile; in second place was the glycoprotein secretory component (SC), the cellular receptor for the transport of IgA that is sometimes called the polymeric IgA (pIgA) receptor (3–6).

IgA also is present in human bile, but as we shall discuss, the source and transport pathways of biliary IgA in man are strikingly different from those in the rat. Clinically, relationships between IgA and liver diseases have long interested hepatologists. IgA often is deposited in the liver of patients with liver diseases, especially alcoholic liver diseases, and in the kidneys of some of these patients.

Our aim in this review is to analyze critically these various relationships between IgA and the liver, focusing especially on unresolved and controversial areas. First, we will present a brief overview of the secretory IgA immune system, then discuss the remarkable species differences in the hepatobiliary handling of IgA, the detailed cellular biology of IgA transport by the rat hepatocyte, the possible biological significance of the transport of IgA antibodies into bile and the relevance and possible mechanisms for the deposition of IgA in the liver and kidneys in disease states.

## OVERVIEW OF THE SECRETORY IgA SYSTEM

The delivery of immunoglobulins (primarily IgA) into external secretions involves a unique and complex series

This work was supported in part by the Veterans Administration.
Dr. Brown is a Medical Investigator of the Veterans Administration.
Address reprint requests to: William R. Brown, M.D., Professor of Medicine, Chief, Division of Gastroenterology, Veterans Administration Medical Center, 1055 Clermont St., Denver, Colorado 80220.



DEFS00021171
BTRAC_CP019_000000093

of inter- and intracellular events and the cooperation of at least two cell types [for reviews, see Refs. (6–14)]. In response to oral immunization, IgA-specific B cells, mostly in gut-associated lymphoid tissues, *i.e.* Peyer's patches, home to subepithelial layers of various mucosal tissues and differentiate into IgA-secreting plasma cells (11, 15, 16). In the plasma cells, precursor immunoglobulin heavy chains (alpha) and light chains (lambda or kappa) assemble to form monomeric IgA (mIgA) molecules; in the presence of an additional peptide, J (joining) chain, the monomeric units join to create dimers and other polymeric forms of IgA which are secreted from the cell into the connective tissue milieu (13, 17, 18). From there the IgA may diffuse in two directions: toward the epithelium or toward the draining lymphatics. Either route allows for the initiation of the second phase of the IgA delivery system, *i.e.* the interaction of the Fc portion of the pIgA molecule with SC on the surface of epithelial cells.

SC is synthesized as a transmembrane glycoprotein (mSC) by the epithelial cells of all external-secreting organs (intestine, breast, lung, etc.) as well as by the hepatocytes of some species (19–21). SC is expressed in a polar fashion on the basolateral (or sinusoidal) surface of the cells (22), where it is available to bind pIgA. Only polymeric forms of IgA have high affinity for SC (23, 24). After binding, the SC-pIgA complexes are internalized into endocytic vesicles, which are routed across the epithelial cells (transcytosis) to the apical pole, where the pIgA, still in complex with a portion of SC, is released from the cell into the external environment (1, 19, 25–28). This last step is accomplished by the proteolytic cleavage of mSC to yield a soluble SC-pIgA complex, or sIgA (29, 30). Interestingly, the intracellular movements of SC, including secretion, continue in the absence of IgA (31, 32). The proposed function of the secreted IgA is to act as a first line of defense against invading pathogens; the SC portion of the sIgA molecule serves to protect the IgA in the protease-rich external environment (33). See Figure 1 for a summary diagram of the IgA transcytotic pathway, as exemplified by the rat hepatocyte.

Several characteristics of the IgA delivery system have allowed cell biologists and immunologists to study this unique transfer of immunoglobulins from the inside to the outside of the body. For one, there is extensive species cross-affinity between pIgA and SC (34). Consequently, a preparation of IgA from one species can be used in studies of binding and transport with tissues or cultured cells from a different species. For another, free SC (not complexed with pIgA nor containing the membrane-anchoring domain of mSC) is easily purified from secretions such as milk and bile and is capable of binding pIgA *in vitro*; use of such free SC *in vitro* has allowed detailed kinetic analysis of the IgA-SC interactions (23, 35, 36). Finally, the discovery that, in some species, pIgA is cleared from the plasma by mSC on the sinusoidal surface of liver parenchymal cells (hepatocytes) and is delivered across the hepatocyte into bile has permitted detailed morphological examination and quantitation of the *in vivo* transcellular delivery pathway for pIgA, which has been difficult or impossible to define through studies of mucous membranes.

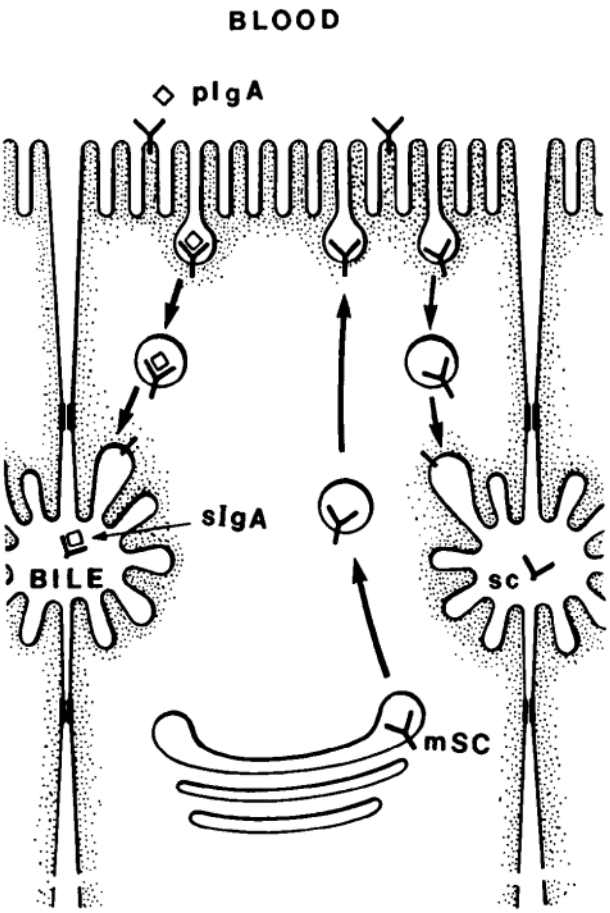


FIG. 1. Schematic representation of the transhepatocellular pathway for pIgA and SC, exemplified by the rat hepatocyte. SC is synthesized in hepatocytes as a transmembrane glycoprotein (mSC), then is transported in vesicles to the sinusoidal surface of the cell, where it is available to bind polymeric IgA (pIgA) from the circulation. As illustrated on the *left*, the pIgA-SC complex is internalized and transported by vesicles across the cell to the bile canalicular membrane of the hepatocyte. There, the transmembrane form of mSC is proteolytically processed to yield a smaller, soluble form of SC which remains complexed to pIgA. The pIgA-SC complex, now termed secretory IgA (sIgA), is released into the bile; the membrane-anchoring fragment is left behind. As illustrated on the *right*, the synthesis of mSC, expression of mSC on the sinusoidal membrane and secretion of free or uncomplexed SC into bile can proceed even in the absence of pIgA.

In man, unlike several other species, the majority of circulating IgA is in the monomeric form. Furthermore, there are two subclasses of human IgA: IgA1 and IgA2. IgA1 dominates in serum by a margin of about 4 to 1, whereas approximately equal amounts of IgA1 and IgA2 are found in secretions (37, 38). The possible role of these IgA subclasses in hepatic pathophysiology will be discussed.

## SPECIES DIFFERENCES IN THE HEPATOBILIARY PROCESSING OF IgA

The report of large amounts of sIgA and SC in rat hepatic bile (2) kindled new interest in the secretory IgA

15273350, 1989, 5, Downloaded from https://aasldpubs.onlinelibrary.wiley.com/doi/10.1002/hep.1840090518, Wiley Online Library on [11/04/2023]. See the Terms and Conditions (https://onlinelibrary.wiley.com/terms-and-conditions) on Wiley Online Library for rules of use; OA articles are governed by the applicable Creative Commons License

immune system. Several laboratories in addition to the group in Belgium began studying the mechanisms and biological relevance of the transport of IgA into bile. The results of several congruent studies established that, in the rat, biliary IgA is derived nearly entirely by the active hepatic transport of IgA polymers from the circulation and that the transport is an SC-mediated process. Initial reports demonstrated the rapid clearance of plasma pIgA by the liver and transport of the pIgA into bile against a strong concentration gradient. Those experiments used either radiolabeled (22, 39, 40) or unlabeled (22, 39, 41) rat or human myeloma pIgA in both the bile duct-cannulated animal (39, 40) and the liver perfused with synthetic medium (41). The transport of IgA was found to be far superior to that of IgG. In other experiments, ligation of the extrahepatic bile duct resulted in markedly reduced clearance of exogenous pIgA from serum (40) and a selective accumulation of sIgA and SC in the serum (42).

The role of SC in the hepatobiliary transport of IgA in the rat was conclusively established through the results of several studies: (a) pIgA was effectively transported, whereas there was minimal or no detectable transport of sIgA (prepared from breast fluids or bile) (43, 44), preformed complexes of pIgA with SC (22, 43) or mIgA (22, 43); (b) polymeric Fc fragments capable of binding *in vitro* to SC were actively transferred *in vivo* into bile, whereas the corresponding Fab fragments, which did not bind to SC, were not transported (44); (c) IgA polymers recovered from rat bile were entirely or mostly complexed with SC (41, 43); (d) heterologous IgG antibodies to rat SC injected into the circulation of rats were transported into bile, whereas control, nonimmune IgG was not (43, 44), and the transport of the anti-SC antibodies was diminished by competition from simultaneously injected purified rat SC or human pIgA (44); (e) pIgA immune complexes were transported into bile, and the transport could be inhibited by preincubation of the complexes with SC (45); (f) IgA antibodies obtained from thoracic duct lymph were much more rapidly cleared from plasma than were the same antibodies that had traversed the liver and acquired SC (biliary sIgA) (46).

The early reports on the hepatic transport of IgA in the rat were followed by similar studies conducted on several other species, with very remarkable differences being recorded. It soon became clear that although the rabbit, like the rat, could transport much pIgA from plasma into bile (47–50), the guinea pig (49–51), dog (47) and sheep (49–51) could not transfer the immunoglobulin nearly as efficiently. Man fell into the category of the inefficient hepatic transporters of IgA (52–54). The mouse was difficult to categorize and for a time was believed to have relatively little capacity for hepatic transport of IgA (55–57), but more recent results have indicated that the mouse liver transports IgA quite effectively, although with slower kinetics than those of the rat liver (58, 59). An example of the differences in hepatic transfer of pIgA among various species are the calculated relative (to albumin) coefficient of biliary excretion of pIgA; values of 97 and 22 were obtained for dog and man, respectively, compared to 1,096 and 310 for rats and rabbits, respectively (48).

The results of studies from various laboratories on the hepatic transfer of IgA are somewhat difficult to compare because of several variables or technical problems: various homologous and heterologous forms of IgA with unknown or various degrees of affinity for SC have been used; differences in kinetics of the transport, despite similarities in total transport, have sometimes been observed; the methods of collection of hepatic bile have been difficult (mouse) or variable (sheep) (60, 61). We (62), for example, have observed that minor reductions in bile flow dramatically reduce the IgA content of the bile. The influence of the state of the IgA on affinity of hepatic transport of IgA was also evident in our studies, where about only 40% of $^{125}$I-rat myeloma pIgA was transported (22), whereas more than 95% of a highly purified $^{3}$H-labeled rat hybridoma pIgA was transported (63). Despite the difficulties in comparing studies, sufficient reliable data are available to establish persuasively the striking species differences in hepatobiliary transport of IgA, as summarized in Table 1.

The explanation for the species differences in hepatic transport of pIgA is fascinating, incomplete and elusive. One point seems clear, however: transport is related to the locations of SC in hepatobiliary tissues. In those species in which transport of pIgA is moderate or high (rat, rabbit, mouse), SC, when searched for immunohistochemically, has been found on hepatocytes (see Table 2). Moreover, our immunoelectron microscopic examinations revealed that the SC is expressed on the external surface of the sinusoidal plasma membrane of the hepatocytes (22), ideally situated to serve as a receptor for IgA polymers circulating in sinusoidal blood. The cellular site of transport of pIgA in the chicken liver is as yet undefined, but pIgA in that species is transported in association with a molecule that is a functional homolog of mammalian SC (77). In contrast to the above species, those that transport IgA poorly from blood to bile (man, dog, guinea pig) do not express SC on hepatocytes; rather, they express it on intrahepatic and extrahepatic biliary epithelium (see Table 2). We first observed this species distinction when comparing human liver (69) to rat liver (22). Except for an early study (78) and a report in abstract only (79), all immunohistochemical studies on the location of SC in human liver have found it only in biliary epithelium (11, 14, 48, 53, 69–75).

Immunohistochemical and autoradiographic studies also have documented that the binding and transport of pIgA occur selectively by the cells that contain and express SC. For example, specific binding of pIgA to the sinusoidal surface of rat hepatocytes was demonstrated by immunofluorescence and autoradiography (20, 26, 80, 81), and a vesicular transport mechanism for pIgA in rat hepatocytes was implicated in studies that used cell fractionation and ultracentrifugation (26, 52, 81–83), then firmly documented by immunoelectron microscopic monitoring of the migration of native pIgA across rat hepatocytes (22). Similarly, in the mouse, the presence of SC (66) and the binding and uptake of pIgA (73) were localized to the same cells. By contrast with those species,

15273350, 1989, 5, Downloaded from https://aasldpubs.onlinelibrary.wiley.com/doi/10.1002/hep.1840090518, Wiley Online Library on [11/04/2023]. See the Terms and Conditions (https://onlinelibrary.wiley.com/terms-and-conditions) on Wiley Online Library for rules of use; OA articles are governed by the applicable Creative Commons License

Case 1:23-cv-00328-JLH-SRF Document 125 Filed 02/20/24 Page 32 of 73 PageID #: 4339



TABLE 1. Transport of pIgA from plasma to bile in various species

| pIgA injected into | % of injected dose recovered in bile (hr) and reference: pIgA obtained from | | | | | | | | | |
|---|---|---|---|---|---|---|---|---|---|---|
| | Rat | | Mouse | | Human | | Sheep | | Dog | |
| Rat | 30 (5–7) | 49, 50 | 15 (5–7) | 50 | 35 (5–7) | 49, 50 | 20 (5) | 50 | | |
| | 25 (3) | 40 | 60 (5) | 58 | 52 (6) | 39 | | | | |
| | 15–27 (3–5) | 43 | 33 (3) | 48 | | | | | | |
| | 95 (2) | 63 | 41 (3) | 44 | | | | | | |
| | 42 (3) | 44 | | | | | | | | |
| | 40 (3) | 22 | | | | | | | | |
| | 50 (2) | 46 | | | | | | | | |
| Rabbit | 35 (5–7) | 49, 50 | | | 35 (5–7) | 49, 50 | | | | |
| | | | | | 37–69 (3) | 47 | | | | |
| Chicken | | | | | 40 (5–7) | 50 | | | | |
| | | | | | 43 (7) | 64 | | | | |
| Mouse | 24 (5) | 58 | —[a] | 57 | —[a] | 56 | | | | |
| | 25 (3) | 59 | | | | | | | | |
| Man | | | | | <3 (24) | 53, 54 | | | | |
| | | | | | <1 (8) | 52 | | | | |
| Dog | | | | | <3 (8) | 48 | | | <1 (8) | 48 |
| Guinea pig | <1 (5) | 49, 50 | | | <1 (5) | 49, 50 | | | | |
| | <1 (3) | 51 | | | <1 (3) | 51 | | | | |
| Sheep | 20 (5) | 50 | | | | | 5 (5–7) | 50 | | |
| | | | | | | | 5 (5) | 60 | | |
| | | | | | | | 4 | 61 | | |

[a] Percent transport not given, but selective transport observed.

TABLE 2. Relationship between capacity for hepatobiliary transfer of pIgA and predominant cellular location of secretory component in hepatobiliary tissues

| Species | Capacity for plasma-to-bile transfer of pIgA | Location of SC | Reference for location of SC |
|---|---|---|---|
| Rat | Large | Hepatocytes | 22, 65–68 |
| Rabbit | Large | Hepatocytes | 66 |
| Chicken | Large | Unknown | |
| Mouse | Moderate | Hepatocytes | 66 |
| Human | Small | Biliary epithelium | 11, 14, 48, 53, 69–75 |
| Monkey | Small | Unknown (not on hepatocytes) | 76 |
| Dog | Small | Biliary epithelium | 48, 66 |
| Guinea pig | Small | Biliary epithelium | 66 |
| Sheep | Small to moderate | Unknown | |

in man, immunoelectron microscopy demonstrated a vesicular pathway for pIgA across intrahepatic and extrahepatic biliary epithelial cells only (69). The results of studies by other techniques have corroborated these morphological studies: the synthesis of SC by cultured rat hepatocytes has been demonstrated (20, 84, 85), whereas in studies on the human liver, although mIgA and pIgA specifically bound to particulate fractions of homogenates and Hep G2 cells, the binding was mediated by the asialoglycoprotein receptor (ASGPR), not SC (70, 76).

The pathway for the relatively small amount of pIgA that is transferred from plasma to bile in man has been examined by immunoelectron microscopy, to the extent possible from static photographs (60). Evidence compatible with the migration of IgA across the endothelium of periductular vessels to the basolateral surfaces of biliary ductular epithelial cells, and of IgA and SC within typical endocytic and transport vesicles in the epithelial cells, was found. Occasionally, IgA has been seen by electron microscopy in human hepatocytes, but this IgA seems to be associated with acid phosphatase-containing structures; thus, the IgA might be following a degradative (lysosomal) pathway rather than a transport pathway into bile (69; Nagura H, personal communication).

The fascinating species differences in the locations of SC in hepatobiliary tissues so far have defied logical explanation. Whereas rat and mouse express SC on hepatocytes, another rodent, the guinea pig, expresses it on the biliary epithelium. Some animals that have gallbladders (guinea pig, man, dog) have the biliary ductular cell pattern of SC expression, whereas others that have gallbladders (rabbit, mouse) have the hepatocyte pattern of expression, *i.e.* like the rat, which has no gallbladder.

There does not seem to be a correlation either between the amount of pIgA entering the circulation from sites of synthesis in the intestinal mucosa and the hepatobiliary cellular locations of SC (and related capacity for hepatic clearance of pIgA). The concentrations of IgA in mesenteric or thoracic duct lymph are reportedly several times higher than in the serum of rats (86, 87), mice (87), guinea pigs (86) and dogs (87), even though only the rat and mouse have the hepatobiliary mechanism for effectively transferring the excess IgA into bile. We (88) and others (87, 89) have found that, in man, thoracic duct lymph is not enriched for pIgA compared to plasma, nor is much pIgA contributed to the systemic circulation by portal vein blood (88, 90). Interestingly, in man, the amount of IgA synthesized each day by various mucosal sites exceeds production of all other immunoglobulin isotypes combined, and the amount of IgA entering the

15273350, 1989, 5, Downloaded from https://aasldpubs.onlinelibrary.wiley.com/doi/10.1002/hep.1840090518, Wiley Online Library on [11/04/2023]. See the Terms and Conditions (https://onlinelibrary.wiley.com/terms-and-conditions) on Wiley Online Library for rules of use; OA articles are governed by the applicable Creative Commons License

DEFS00021174
BTRAC_CP019_000000093

plasma compartment daily is similar to the amount of IgG (91). However, since the plasma half-life of IgA is considerably shorter than IgG (3 to 6 days vs. 21 days, respectively), the serum concentration of IgA is several-fold less than IgG (91–93). The sites of catabolism of the serum IgA are unknown, although the liver presumably plays a major role, as serum levels of IgA often are elevated in liver disease (93–95). Thus, in the rat, serum IgA is integrally linked with biliary or mucosal IgA, whereas in man, it appears that the serum compartment of IgA is distinct and separate from mucosal IgA.

The species differences in capacity for transport of pIgA by the liver result in marked differences in the amount of IgA delivered into the intestine from hepatic blood by way of bile. Probably the most reliable comparative data on this point come from the Belgian group, who, using similar methods of measurement among species, found the biliary excretion of pIgA to be about 35 mg per kg per day in rats and rabbits, 8.8 mg per kg per day in mice and only on the order of 1 mg per kg per day in man, guinea pig and dog (48, 53, 59). Results of estimates of the concentration of IgA in human hepatic bile in our laboratory (69) and another (94) would suggest more secretion of IgA by the liver than estimated by the Belgians, but given the difficulties and variabilities in accurately measuring IgA in secretions, the differences probably are not worth debating; the rat clearly wins out over man on this score. Indeed, cannulation of the rat bile duct reduced the amount of IgA recovered in upper intestinal washings by about 90% (96), whereas persuasive data from studies in man on relative amounts of pIgA entering the intestinal lumen via direct secretion by the bowel mucosa vs. hepatic bile suggest that the direct route is quantitatively far more important (97).

The proportions of biliary IgA that are derived from clearance of plasma pIgA vs. synthesis within the hepatobiliary tissues also vary among species. For example, whereas around 90% of biliary pIgA in the rat and mouse is derived from the plasma (59), the corresponding figure in man is about 50% (53, 54). The source of the remaining pIgA in human hepatic bile has not been directly identified. Normally, not many IgA-containing lymphoid cells are present in the human liver (69, 98, 99). However, we (100) have found large numbers of plasma cells containing IgA and J chain surrounding the accessory glands in the extrahepatic bile ducts and just beneath the luminal surface epithelium of the ducts. At the ultrastructural level, IgA and SC in the biliary epithelial cells had the characteristic features of SC-mediated endocytic transport of IgA. We suspect that biliary duct mucosa is the source of much of the IgA that is secreted into human hepatic bile. Recently, Carter et al. (101, 102) demonstrated in the rat that oral administration of an antigen induced specific IgA-secreting plasma cells to home to the liver. Whether man responds in a similar manner remains to be determined.

The differences in the sources and transport pathways for pIgA in various species can be reflected also in dramatic differences in the levels of IgA and SC in serum during biliary duct obstruction. Thus, ligation of the bile duct in the rat and rabbit results in increases in serum levels of IgA on the order of 8- to 14-fold within 24 to 48 hr (42, 47, 59, 103), whereas similar treatment of dogs and guinea pigs causes practically no change in the serum level of pIgA (48, 51, 66). The mouse, predictably, falls into an intermediate range, with about a 2- to 4-fold increase in serum IgA within 24 to 48 hr after bile duct ligation (51, 59, 104). Early reports suggested that in patients who had extrahepatic biliary obstruction, serum levels of IgA were specifically and significantly elevated (105, 106), but studies in our laboratories (Brown WR, et al., unpublished observations) and others (53, 59, 93, 107, 108) were nonconfirmatory, dashing hopes that measurement of serum levels of pIgA or SC might be useful in the differential diagnosis of obstructive jaundice.

Thus far, our discussion has been directed toward hepatic bile. But in man, the gallbladder may contribute much if not most of the IgA that reaches the intestinal lumen via bile (109–112). Evidence of selective secretion of IgA into gallbladder bile recently was published (109), an observation that is congruent with reports of numerous IgA-containing lymphoid cells in the gallbladder mucosa (11, 113). Moreover, we have found immunoelectron microscopic evidence of typical endocytic, SC-mediated transport of IgA across gallbladder epithelial cells (Brown WR, et al., unpublished observations).

From the results of the extensive studies on the synthesis and secretion of pIgA by intestinal and hepatobiliary tissues in various species, we have constructed a scheme for the pathways for IgA in an animal (rat) that is characterized by very efficient hepatic clearance and biliary secretion of pIgA compared to the pathways in humans, with their very limited capacity for clearance and biliary secretion (Fig. 2).

A subject of some uncertainty with regard to the mechanism of hepatic transport of IgA is whether, to a limited extent, monomeric IgA, even though it does not have affinity for SC, also is preferentially (as compared to IgG) transported into bile. Vaerman and Lemaitre-Coelho (39) found evidence for preferential transport of mIgA in the rat, whereas Fisher et al. (43) did not. This difference might be related to the use of human myeloma IgA by the former laboratory (39) but not by the latter (43). Since, as we shall discuss in the following section, the IgA1 subclass of human IgA apparently can bind to the ASGPR on hepatocytes (70, 114–116), a portion of the IgA1 used in such experiments might have reached bile via the asialoglycoprotein pathway. The human liver also has been shown to transport some monomeric IgA into bile (117), and recent studies suggest that this could be the result of binding of IgA1 to the asialoglycoprotein receptor on hepatocytes (70).

There has been some interest in whether IgM also is selectively transported into bile. The concentration of IgM in the bile of rats normally is very low,but IgM was easily detected in bile from rats bearing an IgM plasmacytoma, and the concentration of IgA in the same samples was about one-half the normal level; most of the IgM was complexed with SC (118). Thus, when concentrations of IgM in the blood are sufficiently high relative to those of IgA, IgM may be capable of undergoing transhepatic transport by the same route as pIgA. Some of the IgM in the rat bile also might be produced locally

15273350, 1989, 5, Downloaded from https://aasldpubs.onlinelibrary.wiley.com/doi/10.1002/hep.1840090518, Wiley Online Library on [11/04/2023]. See the Terms and Conditions (https://onlinelibrary.wiley.com/terms-and-conditions) on Wiley Online Library for rules of use; OA articles are governed by the applicable Creative Commons License

Case 1:23-cv-00328-JLH-SRF Document 125 Filed 02/20/24 Page 34 of 73 PageID #: 4341



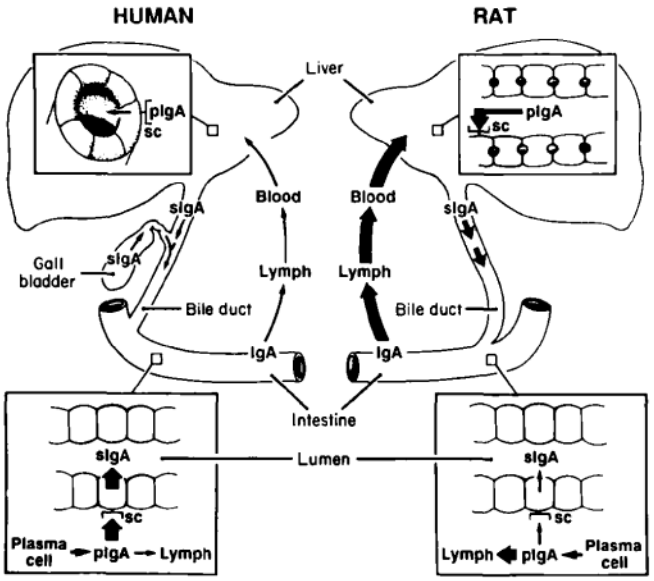


FIG. 2. Illustration of species differences in the transport of IgA into the intestinal lumen. In the rat, only a small proportion of the pIgA that is synthesized by plasma cells in the intestinal mucosa enters the intestinal lumen directly, by way of the SC-mediated transport pathway across intestinal epithelial cells; the majority of pIgA enters the mesenteric lymph, then the blood circulation, and is cleared by transport into bile, by way of SC-mediated transport across hepatocytes. About 90% of the total IgA that enters the intestine of rats is derived from the hepatic clearance of plasma pIgA. In man, large amounts of pIgA synthesized in the intestinal mucosa enter the intestine directly via the SC-mediated transport across intestinal epithelial cells. A minority of the pIgA enters the mesenteric lymph and the blood circulation; this pIgA probably is cleared via a pathway across periductular capillaries, then the epithelium of biliary ductules in the liver. In addition, pIgA synthesized in the mucosa of the extrahepatic biliary ducts and the gallbladder is secreted across the epithelium of those structures and enters the bile. The result of these transport pathways in man is that most of the pIgA that enters the intestine is secreted directly across the intestinal wall; a minority comes from bile, and probably most of that fraction is derived from local synthesis in the biliary ducts and gallbladder mucosa, rather than by clearance of plasma pIgA.

within the liver (119). Very little IgM is present in human hepatic bile (54, 69), but this IgM appears to be transported actively (69).

The species differences in hepatic transport of IgA are of more than academic interest. As we shall discuss later, IgA-liver relationships in man doubtless are important pathophysiologically and therefore deserve much additional study, to some extent in an animal model. The animal(s) chosen for these kinds of study should reflect man in their hepatobiliary handling of IgA. Thus, the rat, rabbit and mouse are not appropriate; the dog and guinea pig (48) may be. Unfortunately, immunoglobulins of the dog and guinea pig have not been nearly as well characterized as those of the other animals.

## CELL BIOLOGICAL ASPECTS OF IgA TRANSPORT IN THE LIVER

This section will focus on (i) the biosynthesis, post-translational modifications and expression of mSC; (ii) the targeting role of SC in the transhepatocellular transport of IgA and IgA-antigen complexes from blood to bile; (iii) the effects of age, hormones, bile flow and other factors on the IgA transport pathway, and (iv) the relationships between the IgA transcellular pathway and the asialoglycoprotein degradation pathway.

***Biosynthesis and Expression of mSC.*** mSC, like most integral plasma membrane proteins, is synthesized in the rough endoplasmic reticulum, processed in the Golgi and transported to the plasma membrane. However, since SC is a soluble protein in secretions as well as a cell-surface receptor for pIgA, it follows a complicated intracellular biosynthetic pathway. Mostov et al. (19), using mRNA isolated from rabbit mammary gland, first showed *in vitro* that SC is synthesized as a molecule larger than that form secreted into milk; the membrane form of SC, which was cotranslationally inserted into dog pancreas microsomes in an asymmetric fashion and core glycosylated through asparagine residues, was capable of binding pIgA. Kuhn and Kraehenbuhl (27) purified SC by means of affinity absorption from rabbit mammary gland and liver membranes, and documented that the membrane forms of SC were larger than comparable forms present in milk and bile, respectively; importantly, those workers showed that the larger, membrane forms were structurally related to the secreted forms. Using HT29 (human colonic adenocarcinoma cell line), Mostov and Blobel (28) demonstrated by means of biosynthetic pulse labeling/chase experiments that the secreted form of SC (77 kD) is derived from the $NH_2$-terminus of a larger, transmembrane form of SC (95 kD). Results obtained from studies in rabbit mammary gland similarly suggested a precursor-product relationship between the membrane and secreted forms of SC (6).

A more complete understanding of the structure of SC was attained when the gene for rabbit mSC was cloned and sequenced (120). The deduced amino acid sequence indicated that the mSC molecule contains a leader sequence of 18 amino acids, an extracytosolic domain of 630 amino acids, a membrane-spanning domain of 23 amino acids and a cytosolic tail of 102 amino acids. The extracytosolic portion contains five 100- to 115-amino acid domains which are homologous to each other and to immunoglobulin kappa chain variable regions (120); similar homologous domains also were observed in human free SC (121). Interestingly, rabbit SC, unlike human and rat SC, is comprised of a family of proteins; this heterogeneity results from a combination of multiple alleles and mRNA processing; the latter produces deletions of certain intramolecular domains of the extracytosolic portion of SC (122–124).

The discovery that IgA can be transported across hepatocytes into bile in some species, particularly the rat, prompted additional studies on the biosynthesis of SC and the transcellular routing of IgA during secretion. The ability of cultured rat hepatocytes to synthesize and secrete SC was demonstrated initially by Socken et al. (20) and Zevenbergen et al. (84). At about the same time, Mullock et al. (82) showed in whole rats that biosynthetically labeled, immunorecognizable SC appeared sequentially in the Golgi, in the plasma membrane and finally in the bile. Sztul et al. (21) first showed that rat liver Golgi contained membrane forms of SC that were larger than biliary forms of SC. We (29) also identified

15273350, 1989, 5, Downloaded from https://aasldpubs.onlinelibrary.wiley.com/doi/10.1002/hep.1840090518, Wiley Online Library on [11/04/2023]. See the Terms and Conditions (https://onlinelibrary.wiley.com/terms-and-conditions) on Wiley Online Library for rules of use; OA articles are governed by the applicable Creative Commons License

DEFS00021176
BTRAC_CP019_000000093

forms of SC in rat liver membranes that were larger (~115 and ~105 kD) than the immunologically related biliary form of SC (~85 kD) and found evidence for proteolytic processing of membrane SC to yield the soluble form. In pulse-labeling and subcellular fractionation experiments in rat liver, Sztul et al. (125, 126) demonstrated that mSC was synthesized first as a 105-kD Endo H-sensitive form in the rough endoplasmic reticulum, then was processed to a 116-kD and, eventually, to a 120-kD Endo H-resistant form in the Golgi; both the 116-kD and 120-kD forms were transported to the sinusoidal plasma membrane, where presumably some additional conversion of the 116-kD form to the 120-kD form occurred. Radioactivity initially observed in larger membrane forms of SC was subsequently found in biliary SC (21). Solari et al. (127, 128), using subcellular fractionation and immunoblotting in the rat liver, obtained similar results: an Endo H-sensitive 105-kD SC band in the rough endoplasmic reticulum and an Endo H-resistant 115-kD SC band in the Golgi.

From the sinusoidal membrane, mSC is routed across the hepatocyte to the canalicular plasma membrane, where it is proteolytically converted to the smaller (~80 kD), soluble form that is secreted into the bile (21, 29; see sections below on exocytosis and sorting of SC). Solari et al. (128), using a monoclonal antibody directed against the cytoplasmic tail of SC, observed the presence of a 34-kD peptide in both Golgi and bile that they believed to be the cytoplasmic anchoring remnant of mSC.

Recently, it has been reported that mSC is phosphorylated. Larkin et al. (129) showed that, in intact liver, the 120-kD form of mSC is phosphorylated at serine residue(s) located within the cytosolic tail of the molecule; consequently, the biliary form of SC is not phosphorylated. Musil and Baenziger (130) demonstrated, in cultured primary rat hepatocytes, that two species of mSC (105 and 109 kD) that were resistant to Endo-H digestion were phosphorylated; these latter experiments suggest that phosphorylation of SC does not require the presence of ligand (pIgA). Scharer et al. (131) observed Golgi forms of SC that were phosphorylated; some were phosphorylated at tyrosine residues. Consequently, the status of the phosphorylation of mSC is incomplete and will require more study. The possible role of phosphorylation or other posttranslational processing events in the intracellular sorting of SC remains to be clarified.

***Binding of IgA to mSC.*** The first step in the transcytosis of IgA is the binding of pIgA to mSC (132). This binding, which was first studied *in vitro* with purified preparations of IgA and free or membrane-associated SC, is a saturable, reversible and time-dependent process; the stoichiometry is one polymer of IgA for one molecule of SC. The affinity binding constant for pIgA and free SC is $10^8$ $M^{-1}$; for pIgA and mSC it is $10^9$ $M^{-1}$; this difference suggests that the interaction of pIgA with mSC is slightly the stronger (36, 133). It is important to stress that only polymeric forms of IgA are capable of interacting with SC with high affinity (23, 24, 34, 134, 135). The J chain, which links IgA monomers together (136, 137) via disulfide bonds, is required for the binding of IgA to SC and subsequent transport of IgA (138), although SC does not bind directly to the J chain. The $NH_2$-terminal first homologous domain of SC is necessary for binding pIgA (139), and a tyrosine residue in the pIgA molecule may play a role in the binding of pIgA to SC, since binding and transcellular transport of IgA often are decreased after iodination of the IgA (140–142; Brown WR, et al., unpublished observations).

At the surface of the transporting cell, IgA first interacts with SC noncovalently (35); later, disulfide interchange between a reactive sulfhydryl group on the IgA molecule and a disulfide bond on SC occurs, thereby forming a single covalent disulfide bond between one IgA heavy chain and SC [143–148; for review of the disulfide bonding between J chain, SC and IgA, see Ref. (9)]. Interestingly, even though there is great species cross-affinity between IgA and SC (34), the ability of IgA from one species to bond covalently to SC of different species is quite variable (149).

As described in detail in the preceding section, IgA that is transported into bile is either synthesized locally in plasma cells along the biliary tree and bound and transported by bile duct epithelium (predominant pathway in man) or is cleared from the plasma by mSC on the sinusoidal surface of hepatocytes and delivered to the bile canaliculus (predominant pathway in rats). However, Delacroix and Vaerman (53) found that 50% of pIgA and all of mIgA in human bile comes from plasma. These latter data suggest that alternative routes (other than SC) accomplish the transport of at least some IgA into human bile. Indeed, the interaction of IgA with other receptors on the hepatocyte has been documented. Stockert et al. (114) first showed that both human pIgA1 and mIgA1 could bind to the rat ASGPR. Recently it was shown that IgA1, sIgA and asialo-IgA2 bind to human hepatocytes (Hep G2 cell line) or human liver membranes via the ASGPR (70). Although Tomana et al. (70) showed that most of the IgA thus bound was internalized and degraded, a missorting pathway that can direct internalized asialoglycoproteins into bile has been described (140, 141). Interestingly, the plasma clearance of mIgA1 was better than pIgA1 in the rat, presumably due to the greater affinity for the ASGPR (141, 142).

In the rat, most of the circulating pIgA is cleared by hepatocytes and delivered into the bile. This clearance probably reflects two attributes of the IgA: (i) an ability to bind mSC and (ii) an appropriate size to penetrate the fenestrae in the endothelium of the hepatic sinusoids. For example, smaller polymers of IgA and Fc$\alpha$ fragments reportedly are cleared from the plasma more quickly than are larger polymers (150). Additionally, pentameric IgM and large IgA immune complexes are generally transported less efficiently into bile than IgA dimers (43, 45). Consequently, if the IgA polymer is of the appropriate size and capable of interacting with SC, the IgA should be cleared rapidly from the blood and delivered quantitatively into bile. Indeed, recent results from our laboratories document that all of a biosynthetically labeled rat hybridoma pIgA, injected intravenously, is cleared from the plasma within 5 min and all of the injected

15273350, 1989, 5, Downloaded from https://aasldpubs.onlinelibrary.wiley.com/doi/10.1002/hep.1840090518, Wiley Online Library on [11/04/2023]. See the Terms and Conditions (https://onlinelibrary.wiley.com/terms-and-conditions) on Wiley Online Library for rules of use; OA articles are governed by the applicable Creative Commons License

material is recovered in bile within 60 to 90 min (Brown WR, et al., unpublished observations).

***Endocytosis and Transcellular Routing of IgA-mSC Complexes.*** A direct vesicular pathway from blood to bile across the hepatocyte was initially demonstrated by Renston et al. (151, 152), simultaneously using horseradish peroxidase as a fluid-phase marker and $^{125}$I-labeled insulin as a physiological ligand. The movement of IgA across the hepatocyte follows a route similar to that described by Renston et al. (151) for horseradish peroxidase and is analogous to the transport of IgA across the enterocyte (17, 26). Circulating IgA binds to mSC, which is located diffusely along and in invaginations of the plasma membrane (22) that often appear to be coated (153, 154). In isolated hepatocytes, the binding of IgA induces clustering of mSC-IgA complexes; the clustering is sensitive to agents like cytochalasin B, which can disrupt microfilaments (154).

After pIgA binds mSC on the sinusoidal surface of the hepatocyte, the IgA-mSC complexes are internalized into coated endocytic vesicles (22, 153, 155). Soon after endocytosis, the IgA-mSC complexes are localized in a vesicular-tubular network (153). In this network [CURL (compartment for uncoupling ligand and receptor) (153)], the sorting of IgA from other endocytosed ligands presumably occurs. The sorted, IgA-mSC containing vesicles then migrate across the cell, avoiding interaction with lysosomes, and fuse with the bile canalicular membrane (22, 156, 157). The IgA transport vesicles are smooth-coated and vary in size from 100 to 160 nm, with larger vesicles than those present in the canalicular area (157). The transcellular migration appears to involve discrete vesicles, as opposed to a continuous intracellular tubule (157), and depends upon functioning microtubules, since treatment with colchicine abolishes the transport of IgA (25, 158, 159). Mullock et al. (160) isolated the IgA transport vesicles and characterized them as approximately 140 nm in diameter, with a density of 1.07 to 1.08 gm per ml. Detailed biochemical characterization of the IgA transport vesicle still is needed.

***Exocytosis of IgA-SC Complexes into Bile.*** The culmination of the IgA delivery pathway involves the proteolytic solubilization of the IgA-mSC complex at the bile canalicular pole of the hepatocyte. At this step, mSC is proteolytically processed to yield two proteins: a soluble form of SC that is released into bile still in complex with IgA, and a transmembrane anchoring fragment that contains the cytoplasmic tail of mSC and remains with the membrane. The exact mechanism and location of this proteolytic event (in the transport vesicle or at the lumen of the canalicular membrane) remain obscure. Immunohistochemical studies have shown an accumulation of pIgA and SC at or near the bile canalicular membrane (22, 154); this observation suggests that the fusion of the transport vesicle with the bile canalicular membrane or the proteolysis of mSC is the limiting step in the pathway. It was also observed that membranes or membrane fragments containing IgA or SC appear to be shed into the bile (22). Through the use of monoclonal antibodies specific for the cytoplasmic tail of mSC, it has been shown that the tail (or slightly degraded fragments) also is (are) released into the bile, as opposed to being degraded intracellularly (128).

Musil and Baenziger (30) recently demonstrated, in cultures of primary rat hepatocytes, that the cleavage of the membrane form of SC to the secreted form occurs at the surface of the cell and is a direct result of the action of a thiol protease. However, since those studies utilized nonpolar cells, the specific site of the proteolysis of mSC is unknown, although it is likely to be at the canalicular membrane. Interestingly, in the small intestine, we (161) observed that solubilized, secreted SC is proteolytically processed a second time by a metalloprotease present on the brush border plasma membrane that appears to have high specificity for SC.

***Clearance and Biliary Secretion of IgA-Antigen Complexes.*** The discovery that IgA-antigen complexes could be removed from the circulation and delivered into bile suggested an additional role for the SC-mediated hepatic transport of IgA. The availability of a myeloma pIgA (MOPC 315) with antibody specificity for proteins haptenated with dinitrophenyl (DNP) or trinitrophenyl (TNP) allowed many investigators to examine the transhepatocellular transport of IgA-antigen complexes. Table 3 presents many of the contributions that have documented the plasma clearance of IgA-immune complexes by liver cells and, in some cases, transport of these immune complexes into bile. Taken together, these studies imply that IgA-antigen complexes as well as other immune complexes may be cleared by a variety of receptors on many different cells in the liver. However, it appears that only clearance of pIgA-immune complexes by mSC on the sinusoidal surface of the hepatocyte promotes transcytosis of the IgA-antigen-mSC complexes and their secretion into bile. The physiological role of other hepatic receptors for IgA and for immune complexes composed of other immunoglobulin isotopes requires more study.

***Intracellular Sorting of mSC.*** A unique aspect of the IgA delivery pathway is that the receptor and transporter for IgA, SC, does not require the presence of IgA for its biosynthesis, intracellular transport or secretion into bile. Both in liver perfusion studies (31, 32) and experiments with cultured cells (19, 130, 175–178), SC in the absence of IgA followed its usual intracellular route: synthesis of the larger membrane form of SC, expression of the mSC at the cell surface (basolateral domain in polarized cells), internalization and transcytosis of the mSC to the canalicular (apical) pole and exocytosis of a smaller, soluble SC into bile or tissue culture medium. That SC is properly routed within the cell in the absence of IgA strongly suggests that determinants of the complex intracellular sorting mechanisms for SC reside within the mSC molecule. Indeed, recent elegant studies by Mostov and colleagues (3), using expression of a normal or mutated mSC gene in cultured, polarized epithelial cells [Madrin Darby canine kidney cells (MDCK)], have begun to define regions in the mSC molecule that may contain information that directs proper intracellular sorting. Those workers' studies showed that mSC could be synthesized from the trans-

15273350, 1989, 5, Downloaded from https://aasldpubs.onlinelibrary.wiley.com/doi/10.1002/hep.1840090518, Wiley Online Library on [11/04/2023]. See the Terms and Conditions (https://onlinelibrary.wiley.com/terms-and-conditions) on Wiley Online Library for rules of use; OA articles are governed by the applicable Creative Commons License

Case 1:23-cv-00328-JLH-SRF Document 125 Filed 02/20/24 Page 37 of 73 PageID #: 4344



**TABLE 3. Uptake of immune complexes by liver cells and secretion into bile**

| Antibody | Antigen | Species (cell type) | Biliary transport | Comments | Reference |
|---|---|---|---|---|---|
| MOPC 315 | DNP[a]-ovalbumin | Mouse (?) | ? | Rapid plasma clearance of Ag | 162 |
| Anti-idiotype | Human IgA | Rat (?) | Yes | 18% transported in 6 hr | 163 |
| MOPC 315 | TNP-albumin | Rat (?) | Yes | Inhibited by incubation with SC; IgG immune complexes not transported | 45, 164 |
| MOPC 315 | DNP-HSA | Mice (?) | Yes | Immune complexes intact in bile | 55 |
| Endogenous anti-CGG | CGG | Rats (?) | Yes | 22% in 24 hr; Ag complexed with SC and IgA in bile | 165 |
| Polymeric MOPC 315 | DNP-HSA | Mice (?) | Yes | mIgA not transported; complement and macrophages not involved | 166 |
| MOPC 315 | DNP-BSA | Rat (?) | Yes | Immune complexes formed *in vivo*, then transported into bile | 167 |
| MOPC 315 | DNP-albumin | Mice (?) | Yes | Not transported into saliva, milk, urine, lung or gut | 168 |
| MOPC 315 tumor | DNP-HSA | Mice (?) | ? | Tumor Ab prevented uptake of Ag from gut | 169 |
| Endogenous IgA | Endogenous Type III polysaccharide + C carbohydrate | Mice (?) | Yes | IgG and IgM complexes not transported | 170 |
| MOPC 315 | RBC-TNP | Mice, *in vitro* (Kupffer cells) | | IgA immune complexes bound to Kupffer cells | 171 |
| MOPC 315 | DNP | Mice (nonparenchymal cells) | ? | Larger complexes were cleared better | 172 |
| Human myeloma pIgA and mIgA | Unknown | Mice, *in vitro* (hepatocytes and Kupffer cells) | | Both cell types have receptors different from SC | 115, 173 |
| Anti-idiotype | IgA | Mice (?) | Yes | IgM immune complexes not transported | 174 |

[a] DNP = dinitrophenyl; Ag = antigen; Ab = antibody; RBC = red blood cell; BSA = bovine serum albumin; HSA = human serum albumin; TNP = trinitrophenyl; CGG = chicken γ-globulin.

fected normal gene, expressed on the basolateral surface of the MDCK cells and was capable of binding and transporting IgA across the cell to the apical domain, where the IgA-SC complex was secreted (3). Subsequent studies showed that the deletion of the cytoplasmic domain of mSC prevented its localization to the basolateral surface and thereby endocytosis of IgA; the tail-minus mutant was targeted directly to the apical membrane, where it was secreted (5). Similarly, deletion of the membrane anchor and cytosolic tail produced a soluble SC protein which was primarily routed to the apical pole of the cell and secreted into the apical medium (4). The results of these experiments suggest that the cytoplasmic portion of mSC is responsible for the initial targeting of mSC to the basolateral (sinusoidal) domain of the cell, whereas the extracytosolic portion of mSC (or SC) contains the appropriate signals for routing mSC to the apical domain of the cell. The mechanisms that operate to utilize these sorting domains remain to be determined.

The intracellular sorting dilemmas brought on by the entry of IgA-SC complexes into the hepatocyte can be further appreciated by the fact that multiple ligands are simultaneously internalized at the sinusoidal surface. In fact, one study suggests that both asialoglycoproteins, internalized via the ASGPR, and acid hydrolases, internalized via the mannose-6-phosphate receptor, are present in the same endocytic vesicle with pIgA and mSC (153). However, most ligands that enter the hepatocyte via receptor-mediated endocytosis are targeted to lysosomes for degradation and their receptors are recycled to the cell surface to undergo additional rounds of endocytosis [for review, see Ref. (65)], whereas pIgA, in complex with SC, is routed to the biliary pole of the cell for exocytosis (comparisons between the IgA pathway and the ASGPR pathway are presented below). The intracellular sorting maneuvers that accomplish the proper routing of IgA into bile exemplify the complexity of the hepatocyte and remain an exciting area for study.

***Relationships between the IgA Pathway and the ASGPR Pathway.*** Although the transport of pIgA into bile in several species, like the rat, depends on the interaction between mSC on hepatocytes and circulating pIgA, biliary secretion of pIgA in man remains incompletely defined and may in part involve hepatic receptors other than mSC. In particular, the ASGPR may be involved in the uptake of IgA1. IgA1 contains a galactose terminated, *O*-linked oligosaccharide in the hinge region of the molecule (179, 180) that may allow the IgA1 to interact with the ASGPR (114). Tomana et al. (116) demonstrated in mice that sIgA and IgA1 are cleared from the serum by the ASGPR. These studies were extended recently (70) to show that sIgA, SC and IgA1

15273350, 1989, 5, Downloaded from https://aasldpubs.onlinelibrary.wiley.com/doi/10.1002/hep.1840090518, Wiley Online Library on [11/04/2023]. See the Terms and Conditions (https://onlinelibrary.wiley.com/terms-and-conditions) on Wiley Online Library for rules of use; OA articles are governed by the applicable Creative Commons License

DEFS00021179
BTRAC_CP019_000000093

bind to and are taken up by Hep G2 cells. The uptake of sIgA and SC are thought to occur through the galactose-terminated oligosaccharides present on SC (181). Normally, circulating asialoglycoproteins that bind to the ASGPR, which are located on the sinusoidal membrane of hepatocytes [182–185; for review, see Ref. (186)], are internalized into clathrin-coated endocytic vesicles (187–190) (see Fig. 3 for comparison of the IgA and ASGPR pathways). Shortly after internalization, the clathrin coat is lost, and the lumen of the smooth endocytic vesicle, now termed an endosome, is acidified through the action of a proton-translocating ATPase (194, 195).

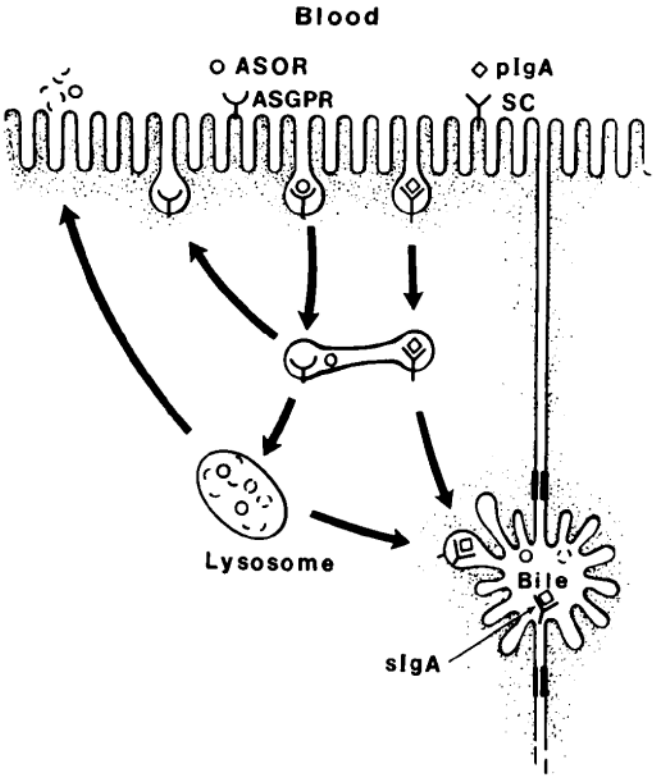


FIG. 3. Comparisons between the pathways for the handling of IgA and asialoglycoproteins by the rat hepatocyte. Both mSC and the ASGPR are expressed on the sinusoidal surface of the hepatocyte, where they are available to bind pIgA and asialoglycoproteins, respectively [for demonstration, an asialoglycoprotein, asialoorosomucoid (ASOR), is shown]. pIgA is internalized in complex with mSC into an endocytic vesicle and is transported across the cell to the bile canalicular membrane, where, via a proteolytic event, the solubilized pIgA-SC complex (sIgA) is released into bile. ASOR is internalized by the ASGPR into endocytic vesicles; soon after endocytosis, the lumen of the endocytic vesicle is acidified. The low-pH environment promotes the dissociation of the ASOR from ASGPR. The ASGPR is then recycled to the cell surface to undergo additional rounds of internalization; the ASOR is directed to a lysosome for degradation. The products of degradation within lysosomes are released into both the blood and the bile. Recent evidence suggests that pIgA and ASOR travel through a common intracellular sorting compartment (141, 153, 155); this close association might permit some pIgA to be accidentally targeted to lysosomes and, conversely, some ASOR to be routed to the bile; both of these possibilities have been observed (see text; 140, 191–193). The mechanisms that provide for the proper intracellular sorting of pIgA and ASOR, and the biochemical reactions that take place in gallbladder mucosa, rather than by clearance of plasma pIgA.
the sorting compartment, require additional study.

Since the interaction between an asialoglycoprotein and ASGPR is sensitive to reduction in pH, the acidified environment promotes the dissociation of asialoglycoprotein from the ASGPR (196). At this point, the asialoglycoprotein and ASGPR are segregated from one another (153, 188, 197); the asialoglycoprotein is targeted to a lysosome for degradation and the ASGPR is recycled to the cell surface to undergo additional rounds of endocytosis (198–201). Thus, presumably, ligands that enter the hepatocyte via the ASGPR are destined for destruction. However, some ligands that enter via this pathway are not degraded, but are either returned to the cell surface via a pathway termed diacytosis (83, 197, 202) or are transcytosed and released intact into the bile; the fraction of internalized ligand that follows the latter pathway generally is fairly small, 0.5 to 5% (140, 191, 192).

Recently, it has been suggested that in rat hepatocytes, which have both the ASGPR and mSC, human pIgA1 can be internalized via the ASGPR, and once inside the cell, dissociates from the ASGPR because of the low pH, then binds to mSC and is routed into the bile (141). In this regard, a common sorting compartment that contains mSC and ASGPR has been identified morphologically (153). Limet et al. (155) reported that IgA and galactosylated bovine serum albumin are sorted from each other in an intermediate membranous compartment, with a density of 1.13 gm per ml, between 5 and 15 min after injection. However, in those studies, only 64% of the injected rat pIgA reached the bile in 3 hr; thus, it is possible that some denatured, nontransportable pIgA was colocalized with the galactose-albumin. Presumably, the sorting of asialoglycoprotein from ASGPR, and of IgA from these and other ligands, occurs in a prelysosomal sorting compartment that is slightly acidified; the low-pH environment promotes the dissociation of many ligands from the receptors, thereby allowing the individual processing of each. However, since the interaction between pIgA and SC is stable at low pH (35), the pIgA-SC complex survives the environment of the sorting compartment and proceeds along the pathway to bile. In experiments in which animals are treated with weak bases, like chloroquine, vesicle acidification is blocked and degradation of internalized asialoglycoprotein is subsequently inhibited; under these conditions, the transport of IgA into bile continues (155, 203; Brown WR, et al., unpublished observations), which implies that vesicle acidification is not required for successful transport of IgA. Similarly, we (191) observed secretion of SC into bile in the perfused rat liver treated with monensin. Thus, while it is possible that some forms of IgA may be internalized by the ASGPR, the amount of IgA that is transcytosed and secreted into bile via this route is minimal. The role of the ASGPR, as well as other hepatic receptors, in the biliary secretion of IgA in man remains to be established.

***Influence of Hormones, Aging, Bile Flow and Other Factors on SC Expression and IgA Transport.*** The synthesis and expression of mSC appear to be regulated during the development of the organism and during cellular differentiation. In the rat intestine, immunorecognizable SC appears in enterocytes between 10

15273350, 1989, 5, Downloaded from https://aasldpubs.onlinelibrary.wiley.com/doi/10.1002/hep.1840090518, Wiley Online Library on [11/04/2023]. See the Terms and Conditions (https://onlinelibrary.wiley.com/terms-and-conditions) on Wiley Online Library for rules of use; OA articles are governed by the applicable Creative Commons License

and 15 days after birth, a time corresponding to the appearance of IgA-producing plasma cells in the lamina propria (204), and reaches adult levels of expression by 40 days (205). In contrast, in man, SC was observed in fetal tissues prior to the appearance of IgA or IgA plasma cells (206). In the intestine, SC expression is dominant in the cells from the lower two-thirds of the crypt and is diminished in the more differentiated cells at the villus tip (205, 207, 208). Interestingly, the expression of SC is often diminished in carcinomas, and the level of its expression often correlates with the degree of malignancy (208–210). Schmucker et al. (211) have shown in the rat that the transport of IgA into bile decreases with age, as a direct result of an age-related decrease in the expression of SC on hepatocytes (212).

The regulation of the expression of mSC, and consequently the delivery of pIgA into external secretions, as well as the induction of the secretory immune response in general, may depend on specific hormonal and other chemical influences and may be tissue specific (213–216). For example, the amount of SC synthesized by uterine or lacrimal cells may be influenced by sex steroids (217, 218), whereas in hepatocytes, glucocorticoids perform a regulating function (219); the alterations in the expression of SC apparently reside at the levels of both transcription and translation (219–221). Additionally, the synthesis and secretion of SC by HT-29 cells can be increased by treatment with $\gamma$-interferon (70, 222) or tumor necrosis factor $\alpha$ (223), or by growing the cells in glucose-free, galactose-substituted medium (224). The physiological consequences of these increases in SC expression and the related effect on the delivery of IgA into secretions remain to be explored.

The transport of IgA into bile also is affected by agents that affect bile flow. Even cannulation of the bile duct can affect the delivery pathway. For example, Hinton et al. (225) reported that the concentration if IgA in bile decreased to about 75% of the initial concentration within 3 hr after bile duct cannulation; this decrease was not due to interruption of enterohepatic circulation of IgA, since no such pathway normally exists. Seo et al. (226) similarly reported that IgA levels fell to 25% of normal after 4.5 hr of bile duct cannulation, and Rank and Wilson (103) showed that chronic retardation of bile flow decreased the biliary concentration of IgA, although not affecting other biliary proteins. We (62) demonstrated that transient bile duct ligation (2 hr) dramatically decreased the ability of the liver to transport IgA in the period subsequent to ligation, although not affecting the biliary secretion of other proteins, including SC. In the rat, pharmacological doses of estradiol, which retard bile flow, decreased the plasma clearance and biliary secretion of IgA (227). The mechanisms that link IgA transport to bile flow are unknown, but perhaps when understood, they will aid our understanding of the transhepatocellular delivery of IgA from blood to bile.

## BIOLOGICAL ACTIVITIES OF IgA ANTIBODIES IN BILE

Two major biological benefits have been proposed for the secretion of IgA antibodies into bile: enhanced immunological protection of the biliary and upper gastrointestinal tracts and the clearance of harmful antigens from the circulation in the form of IgA-antigen complexes. Critical analysis of both of these propositions is indicated.

***Immunological Protection of the Biliary and Upper Intestinal Tracts.*** Specific IgA antibodies in bile have been demonstrated after experimental immunization as well as in the "natural" state. Table 4 is a list of many of the antibodies that have been induced or detected in bile and, in experimental circumstances, the methods used to induce the secretion of antibodies.

Natural antibodies are those that are present without intentional immunization. Environmental antigens, particularly those within the intestinal tract, would be expected to produce a secretory IgA antibody response (as well as an IgG and IgM response in the serum). Thus, it is not surprising that the natural IgA antibodies detected in rat and human bile are specific for bacteria that likely are encountered in the intestine. Direct documentation of the origins of natural biliary IgA antibodies was provided by Manning et al. (241), who caused a dramatic (75%) reduction in specific IgA antibody content of bile in rats by cannulation of the thoracic duct; the remaining portion of antibodies presumably were synthesized by immune cells within the liver. Most attempts to induce the secretion of IgA antibodies into bile have taken advantage of the well-documented observation that administration of an antigen either into the gut lumen or directly into intestinal lymphoid tissues, such as the Peyer's patches, activates the mucosal immune system (9). It was shown in some experiments (229, 230) that the synthesis of bile-destined antibodies was initiated in the mesenteric lymph nodes, from which site lymphoid cells presumably matured and migrated to the intestinal lamina propria. However, antibodies originating from other sites might also reach bile, as the secretion of antibodies into bile after the removal of mesenteric nodes, drainage of thoracic duct lymph and intrathoracic injection of antigen has been observed (238, 240). Under certain circumstances, the liver itself might be the source of a large portion of the antibodies secreted into bile: in response to intestinal administration of cholera toxin, which may induce a generalized systemic immune response in addition to a mucosal immune response, large numbers of specific antibody-forming cells appeared in the liver during the early priming period and after boosting (245). Similarly, immunization by various routes with horse erythrocytes has resulted in the appearance of specific antibody-forming IgA cells in the liver (121, 102). The experiments we have just described, as well as others concerned with immunological memory in the mucosal immune system (229, 235, 239, 245), are examples of how the secretion of IgA antibodies into bile can be used to define events in the regulation of the entire immune system.

Whereas it has been relatively easy to demonstrate the presence of specific IgA antibodies in bile, it is quite another matter to show that the antibodies are effective in protecting either the biliary tract or the upper gastrointestinal tract. Any discussion of this type raises the issue of what the roles of IgA antibodies in secretions are in general, an issue not yet fully clarified [for review, see

15273350, 1989, 5, Downloaded from https://aasldpubs.onlinelibrary.wiley.com/doi/10.1002/hep.1840090518, Wiley Online Library on [11/04/2023]. See the Terms and Conditions (https://onlinelibrary.wiley.com/terms-and-conditions) on Wiley Online Library for rules of use; OA articles are governed by the applicable Creative Commons License

Case 1:23-cv-00328-JLH-SRF Document 125 Filed 02/20/24 Page 40 of 73 PageID #: 4347



TABLE 4. IgA antibodies that have been demonstrated in bile

| Species | Antigen | Method of inducing antibodies | Reference |
|---|---|---|---|
| Rat | *B. abortus*[a], *S. typhi*, *C. parvum*, allogeneic erythrocytes | Injection into PP[b] | 46, 228–230 |
| Rat | *G. lamblia* | Intestinal inoculation | 231 |
| Rat | Cholera toxin | Intraduodenal inoculation | 232 |
| Rat | Cholera toxin | i.g. inoculation; injection into PP | 233 |
| Rat | *V. cholerae* | Intestinal inoculation | 234, 235 |
| Rat | Allogeneic erythrocytes | i.p. or i.g. inoculation | 96 |
| Rat | Diphenylated pneumococcus | s.c., i.v., i.g. inoculation | 236, 237 |
| Rat | *B. abortus* sheep erythrocytes | Intrathoracic or i.p. inoculation | 238 |
| Rat | Chicken γ-globulin | Injection into PP | 165 |
| Rat | *E. coli* horse spleen ferritin | Injection into PP | 239, 240 |
| Rat | *Lactobacillus* sp., *S. aureus* | "Natural" | 241 |
| Rat | Horse erythrocytes | Injection into PP, i.v. | 101 |
| Rat | *N. brasiliensis* | Intestinal inoculation | 242 |
| Man | *E. coli* | "Natural" | 119 |
| Man | *V. cholerae* cell walls | Oral inoculation | 243 |
| Monkey | *V. cholerae*, *B. abortus* | Intestinal infection | 244 |

[a] *B. abortus* = *Brucella abortus*; *S. typhi* = *Salmonella typhi*; *C. parvum* = *Corynebacterium parvum*; *G. lamblia* = *Giardia lamblia*; *V. cholerae* = *Vibrio cholerae*; *E. coli* = *Escherichia coli*; *S. aureus* = *Staphylococcus aureus*; *N. brasiliensis* = *Nippostrongylus brasiliensis*.

[b] PP = Peyer's patches; i.g. = intragastric; i.p. = intraperitoneal; s.c. = subcutaneous; i.v. = intravenous.

Ref. (246)]. Probably a major role of secreted IgA antibodies is to prevent the attachment or penetration of injurious agents, including certain microorganisms, into mucous membranes. sIgA antibodies also are capable of neutralizing certain viruses and enterotoxins. Although IgA antibodies are not very effective in opsonization or in activating complement via the classic pathway, and therefore usually are not bactericidal, they may mediate the killing of some bacteria via antibody-dependent cytotoxicity reactions. It is also proposed that IgA antibodies, by binding antigens that might otherwise combine with antibodies of other immunoglobulin isotypes and thereby activate complement pathways, prevent untoward or excessive immunological reactions in or on mucosal surfaces.

Whatever the activities of IgA antibodies in secretion, they are but one of the numerous components of the mucosal defense system, and the singular absence of sIgA antibodies from secretions usually is not accompanied by an increased frequency of pyogenic infections (247). Thus, it is not surprising that biliary tract infections are apparently uncommon in selectively IgA-deficient persons (247), although the finding of gallstones or biliary sludge in eight of 13 IgA-deficient children prompted the suggestion that predisposition to gallbladder infection was responsible (248). Moreover, biliary diversion in man does not result in a marked increase in intestinal infections; a partial explanation for this point might lie in the observation that diversion of anti-*Vibrio cholerae* antibody-containing bile from the intestine of immunized rats did not diminish the levels of antibodies in the intestinal mucus, presumably because the biliary antibodies were replaced by antibodies from serum or the intestinal mucosa itself (235).

Experimental evidence has given some clues, though, about how IgA antibodies in bile might help defend the biliary and intestinal tracts. Human hepatic and gallbladder bile containing anti-*Escherichia coli* antibodies inhibited the attachment of the bacteria to epithelial cells, although, interestingly, low-molecular-weight nonimmunoglobulin components in the bile had similar inhibitory activity (119). IgA antibodies in the bile of rats that had been inoculated with *Giardia lamblia* trophozoites were bound to flagella and surfaces of the trophozoites; perhaps the presence of such antibodies can facilitate clearance of the organisms from the intestinal lumen (231). We (233) and another laboratory (232) have reported that IgA antibodies in rat bile can neutralize cholera toxin and prevent an intestinal secretory response to the toxin (Fig. 4); thus, it appears that sIgA antibodies can retain certain immunological effectiveness even in the detergent milieu of bile.

***Clearance of Circulating Antigens into Bile.*** As we discussed in the previous section, the hepatic transport of circulating IgA-antigen complexes into bile via the SC-mediated pathway has been frequently demonstrated in the rat and the mouse. This observation has prompted much speculation that the disposal of such complexes represents a major role of the liver in protecting the host from harmful antigens, in particular those that might have inadvertently violated mucosal barriers (249). We are concerned, however, that this kind of speculation has not sufficiently taken into account the species differences in hepatic transport of IgA and that, in particular, conclusions from studies in the rat or mouse have been uncritically extrapolated to man (249, 250). Since the efficiency of hepatic transport of IgA-antigen complexes is directly related to the transport of IgA itself (45, 164), the human liver probably is not very effective in clearing IgA-antigen complexes into bile via the SC-mediated pathway. This is not to say that the human liver does not utilize other mechanisms for the

15273350, 1989, 5, Downloaded from https://aasldpubs.onlinelibrary.wiley.com/doi/10.1002/hep.1840090518, Wiley Online Library on [11/04/2023]. See the Terms and Conditions (https://onlinelibrary.wiley.com/terms-and-conditions) on Wiley Online Library for rules of use; OA articles are governed by the applicable Creative Commons License

Case 1:23-cv-00328-JLH-SRF Document 125 Filed 02/20/24 Page 41 of 73 PageID #: 4348



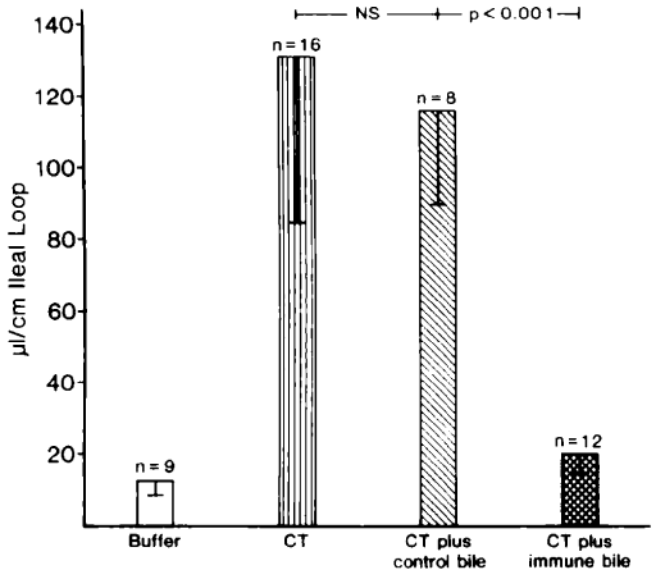


FIG. 4. Specific inhibition of cholera toxin-induced secretion by IgA. The secretory response of *in situ* rat ileal loops after the instillation of buffer, cholera toxin (CT), CT plus control bile containing no anti-CT antibodies or CT plus bile containing IgA anti-CT antibodies (immune bile) are illustrated. Whereas the control bile had no effect on CT-induced secretion, immune bile almost completely inhibited the secretion. Reprinted by permission from: IgA antibodies in rat bile inhibit cholera toxin-induced secretion in ileal loops in situ. By T. Tamaru and W. R. Brown. Immunology, Volume 55, No. 4, pp. 597–583. Copyright © 1985 by Blackwell Scientific Publications.

disposal of IgA-antigen complexes in the liver, for example, via the ASGPR pathway (70) or by uptake into reticuloendothelial (Kupffer) cells; but it raises the possibility that, in man, the lack of an effective SC-mediated pathway for the disposal of IgA-antigen complexes through hepatocytes is a handicap. Might this "defect" render the human species more prone to the development of the numerous diseases that involve the deposition of IgA or IgA immune complexes in tissue?

## IgA IN HEPATOBILIARY DISEASES

Among the numerous immunological abnormalities that have been investigated in liver diseases, those involving IgA physiology have been among the most popular. Alterations in the concentration, subclass distribution and molecular configuration of serum IgA, and in the deposition of IgA in various tissues have been examined in detail. The most extensively studied association of IgA and liver disease has been that of alcoholic disease (ALD), which lately has been referred to as an IgA-associated disorder (251).

***IgA and ALD.*** Elevated levels of total serum IgA in ALD have been reported often (74, 94, 95, 105, 252–258). Usually the elevations are modest (on the order of 2-fold) and overall are not specific for ALD (93, 94, 105, 253, 255). It is noteworthy, though, that when the histopathological abnormalities in a liver disease are severe, serum IgA concentrations may be increased irrespective of the cause of the disease, but when the abnormalities are only mild, as in steatosis, the concentrations are increased only in ALD (251, 253, 259). More refined characterization of IgA in the serum has not increased the ability to distinguish ALD from other liver diseases. For example, the proportion of serum IgA present as pIgA, although significantly increased in ALD compared to that in normal subjects, is not increased in comparison to diseases such as primary biliary cirrhosis, chronic active liver disease and acute hepatitis (93–95, 237, 244, 251, 253, 258, 259). A shift in the ratio of serum IgA1 to IgA2 in favor of the latter has been observed in alcoholic cirrhosis (93, 253, 260), but the magnitude of the change is small. The suggestion has been made that the shift toward IgA2 in ALD reflects either increased stimulation of IgA2 production by plasma cells in the intestinal mucosa or impaired secretion of IgA2 into the intestinal lumen, with "spillover' into the circulation (93). In addition, the proportion of serum IgA present as sIgA often is increased in ALD, but, again, the elevation is not specific (71, 93, 94, 105, 106, 253, 256, 260–265).

The subject of sIgA elevations in ALD and other liver diseases, though, has attracted a great deal of attention because of the implications for the metabolism of pIgA and the hepatobiliary source of SC. Ordinarily, the concentration of circulating sIgA is only on the order of 10 to 40 µg per ml (251, 261); but years ago it was recognized that higher concentrations were present in many conditions, especially in diseases of the liver. Among the liver diseases, highest sIgA values were generally recorded in extrahepatic biliary obstruction or primary biliary cirrhosis (105, 106, 262, 266). On the basis of these results, it was suspected that the SC portion of the sIgA was derived principally from biliary ductule tissues, a suspicion supported by the finding of a strong correlation between serum sIgA levels and serum alkaline phosphatase and leucine aminopeptidase levels (261). However, Delacroix and associates (75, 261) also found very high levels of circulating sIgA in patients with acute hepatitis and during certain stages of fulminant hepatitis, prompting them to suggest that the site of origin of SC in the liver is hepatocytes. Later, however, those workers found that high sIgA levels in the recovery phase of fulminant hepatitis corresponded to the appearance of large numbers of proliferating cholangiocytes containing SC (75), and they concluded that the increased level of sIgA in the serum in acute hepatitis is due either to regurgitation of sIgA from bile as a result of disturbed hepatic architecture, or release of SC from biliary ductule cells into the serum, perhaps by reversal in the normal pathway for secretion of SC, which then complexes with pIgA. The results of two immunohistochemistry studies have supported the view of those authors: Chandy et al. (74) and Fukuda et al. (71) found evidence favoring passage of sIgA from biliary canaliculi via interhepatocyte tight junctions, as well as leakage of SC from bile ductules into portal spaces during cholestatic diseases. By electron microscopy, Fukuda et al. (71) found no support for the possibility of retrograde vesicular passage of sIgA through hepatocytes, a phenomenon that had been observed after the infusion of pIgA or sIgA into the bile duct of rats (267).

The factors responsible for elevated levels of serum IgA in ALD have been partially explored. A selective and significant reduction in the fractional catabolic rate of

15273350, 1989, 5, Downloaded from https://aasldpubs.onlinelibrary.wiley.com/doi/10.1002/hep.1840090518, Wiley Online Library on [11/04/2023]. See the Terms and Conditions (https://onlinelibrary.wiley.com/terms-and-conditions) on Wiley Online Library for rules of use; OA articles are governed by the applicable Creative Commons License

DEFS00021183
BTRAC_CP019_000000093

pIgA, together with an increase in the synthetic rate of pIgA, have been recorded in cirrhotic patients (53, 93). It has been proposed that the reduced catabolism of pIgA in cirrhosis reflects impaired removal of some pIgA from the plasma by a non-SC-mediated mechanism through hepatocytes (93). Several investigations of the IgA-producing capacity of peripheral blood mononuclear cells in ALD have found increased spontaneous production of IgA (258, 268–270); this finding suggests a state of *in vivo* activation of B lymphocytes dedicated to IgA synthesis. Searches for an immunoregulatory defect accounting for the increased IgA synthesis in ALD have been conflicting: T cell immunoregulatory function was found to be normal by some investigators (270), but decreased suppressor activity for IgA was reported by others (269).

Analysis of the specific antibody content of circulating immunoglobulins in ALD has regularly revealed increased amounts of antibodies to dietary (271, 272) or microbial antigens (273–276). It has been suggested that this increase is a consequence of an inhibitory influence of ethanol on macrophages (274) and the decreased Kupffer cell activity that has been observed in alcoholic hepatitis (277). However, increased levels of serum antibodies to dietary antigens also have been observed in children with chronic liver diseases (278). In one study of ALD, the number of positive reactions to *E. coli* O antigens was significantly correlated with serum IgA concentrations (274). In addition, the levels of anti-*E. coli* O antibodies were higher in cirrhosis with associated alcoholic hepatitis than without this association (274); this observation supports the hypothesis that the liver in ALD fails to extract circulating antigens and gut-derived endotoxins, and that alcoholic hepatitis and high levels of IgA are related to the presence of *E. coli* endotoxins in the liver and systemic circulation.

Circulating IgA immune complexes in ALD have been demonstrated repeatedly (260, 279–283). Often, the presence of complexes and the severity of disease are correlated, which suggests that alcoholism *per se* does not cause the formation of complexes. Another observation is that IgG as well as IgA complexes often are present in ALD, whereas other IgA-associated diseases (Henoch-Schönlein purpura and primary IgA nephropathy) seem to have a more selective IgA response; the meaning of this difference is unclear. The antigen(s) associated with IgA when immune complexes are present often has (have) not been defined (280, 282), but complexes of IgA with IgG (IgA rheumatoid factor) (281), alkaline phosphatase (279) and γ-glutamyltransferase (283) have been identified. The presence of circulating IgA immune complexes in ALD may be independent of the presence of associated glomerular deposits of IgA (280), and circulating IgA immune complexes have been found in primary IgA nephropathy (no associated liver disease) (284). Both IgA1 and IgA2 have been represented in circulating IgA immune complexes in ALD (280).

Far more interesting and potentially important than alterations in serum IgA in ALD are the deposits of IgA in the liver, skin and kidneys of such patients. IgA deposition in the liver in ALD has been recognized for many years. Hopf and associates (73, 285) found IgA associated with hepatocytes isolated from the livers of patients with various liver diseases; IgA was bound to hepatocytes from nearly all of the ALD patients, but was also often found in cells from patients with chronic active hepatitis, fatty liver or even normal liver. Compared to those studies, immunohistological examination of liver sections has generally yielded a stronger correlation of IgA deposits with ALD. Moreover, the IgA in ALD usually is deposited in a characteristic continuous pattern along the sinusoidal margins. Kater et al. (72) reported that alcohol was the presumed cause of the liver disease in 50 of 66 liver specimens with a continuous pattern of IgA deposition, whereas alcoholism was involved in only eight of 254 patients who had scanty or no IgA deposits. In other reports (253, 286–288), ALD has been associated with a continuous pattern of IgA deposition on the order of 75% of the time compared to less than 10% in non-ALD. Others (71, 74, 289), though, have reported the common occurrence of IgA deposits in a continuous pattern in nonalcoholic liver disease, especially chronic hepatitis. Whether the disparity in these reports is due to differences in histological interpretation of the pattern of IgA deposition, nonspecific fixation of IgA present in sinusoidal blood or differences in the diseases examined deserves clarification. We conclude that the continuous pattern of IgA deposition is at least very common in ALD, if not specific for it. This pattern of IgA deposition in ALD has been associated with a higher likelihood of progressive hepatic injury in ALD than has an initial discontinuous pattern (290), an observation that raises the question of whether the IgA deposits reflect a role of the IgA in the liver injury, even though mediation of tissue injury is not generally perceived as an important pathological function of IgA antibodies.

Characterization of the IgA deposited in the liver in ALD has been regarded as important in determining the source of the IgA and the cause of the deposition. One group (287) reported that the IgA is mostly of the IgA2 subclass and therefore likely is derived from the gastrointestinal tract. However, by the use of monclonal antibodies, others (253, 289, 291) have found the IgA far more often to be IgA1 and therefore not necessarily from a mucosal source. In attempts to determine whether the IgA deposits in ALD are polymeric or in complex with SC, there also has been disagreement; some investigators (287) found SC antigenic determinants to be present, but others (289, 291) found them lacking and observed that in less than 20% of the ALD specimens the IgA contained J chain and was capable of binding SC *in vitro* (291). We conclude that the IgA deposited along the sinusoids in ALD is most often IgA1 and mostly monomeric; therefore it probably is not mucosal in origin. Electron microscopic immunocytochemistry of ALD in Japanese patients has shown that the IgA1 is deposited along the plasma membrane of hepatocytes in mild disease, but when fibrosis is present, the IgA1 seems to be excluded from the hepatocyte proper and lies in adjacent collagenous fibers and along endothelial cells (Nagura H, personal communication). The electron micrographs have also shown some IgA1 in endocytic vacuoles of Kupffer cells; IgA2 was never seen on or adjacent to hepatocytes but was

15273350, 1989, 5, Downloaded from https://aasldpubs.onlinelibrary.wiley.com/doi/10.1002/hep.1840090518, Wiley Online Library on [11/04/2023]. See the Terms and Conditions (https://onlinelibrary.wiley.com/terms-and-conditions) on Wiley Online Library for rules of use; OA articles are governed by the applicable Creative Commons License

present in Kupffer cells. These results probably explain why the IgA1 deposits appear to be continuous or smooth by light microscopy, whereas the IgA2 deposits appear more granular and discontinuous.

The issue of whether IgA deposition in ALD is due to the effects of alcohol on the liver or, rather, to some alteration in circulating IgA or the histological alterations present in ALD has been examined carefully (253). Clearly, the deposits are not simply the consequence of elevated concentrations of circulating IgA, because they are not seen in IgA myeloma and other conditions associated with high levels of serum IgA or in liver diseases of nonalcoholic cause (253). Neither can the deposits be attributed to a shift toward IgA1 in the circulation, because of the opposite tendency in ALD (93, 253, 260). Finally, the deposits are about equally common in all histological expressions of ALD (steatosis, fibrosis, hepatitis and cirrhosis) (253, 291); thus, some workers have concluded that the deposition of IgA is a consequence of alcohol-induced changes to the liver *per se*. Van de Wiel (251, 259), in fact, has advocated the use of immunohistochemistry for the detection of hepatic IgA deposits to aid in the diagnosis of alcoholism and liver disease of uncertain cause.

We come then to the fundamental question of why IgA is deposited so readily in the liver of alcoholics. The answer, it seems, must lie in some alteration of the hepatocyte surface induced by alcohol. Moreover, that alteration must induce a change that allows for deposition preferentially of IgA1. As we have discussed, IgA1 differs from IgA2 by the presence of terminal galactose residues; this structure permits the IgA1 to bind to the hepatocyte asialoglycoprotein receptor (70, 114). Therefore, it seems likely that the effect of alcohol on the liver allowing for IgA to be deposited is an alteration in the expression or function of the ASGPR. Conceivably, the amount or availability of the cell-surface receptor, or the ability of the receptor to bind, internalize and facilitate the intracellular degradation of IgA1 might be altered. Alternatively, alcohol might alter the molecular conformation of IgA, making the galactose-terminated oligosaccharide more available for interaction with the ASGPR. We anxiously await experiments to determine the effects of alcohol on the handling of IgA1 by human hepatocytes.

The presence of IgA deposits in the kidneys of patients with ALD has prompted much investigation; only the salient features of the extensive literature on this subject can be reviewed here. ALD is one of several diseases associated with IgA nephropathy; others include Henoch-Schönlein purpura and systemic lupus erythematosus [for review, see Ref. (292)]. Liver diseases besides ALD also may have associated IgA renal deposits, but ALD seems to be responsible most frequently. The reported frequency of the deposits in ALD varies from greater than 50% (293, 294) to less than 20% (295), and the severity of the disease also varies, from a latent, asymptomatic state to a very active, proliferative condition. A wide range of glomerular pathological changes, from minimal to diffuse sclerosing glomerulonephritis, can be seen. Whether experimental, geographic or genetic differences account for these differences in expression of disease is unclear. The IgA may be deposited in the kidney alone or in association with IgG, IgM, C3 and fibrinogen. The prevailing opinion is that the deposits represent complexes of IgA with various antigens (260), but no consistent association with identifiable antigens has been established. Some workers (296) have found the deposited IgA to contain J chain and to be capable of binding SC, as is characteristic of pIgA, but others (297) have published contrary results. Most workers have failed to find SC associated with the IgA deposits (292), so the IgA probably is not sIgA. As in the liver, the renal deposits of IgA were first reported to be IgA2 subclass (298, 299), but later studies using monoclonal antibodies convincingly demonstrated that the IgA is IgA1 (296, 297).

The fact that the deposited IgA is IgA1 deserves emphasis. Is it possible that a disturbance in the activity of an asialoglycoprotein receptor-mediated mechanism in the liver for the removal of IgA1 or IgA-antigen complexes results in the accumulation of this subclass of IgA in the serum and consequent deposition in the kidney? This very important issue should receive intensive study, not only to the extent possible in man, but perhaps also in experimental models. If models are to be used, the choice of animal may be critical. Experimental models of IgA deposition in the rat kidney in association with carbon tetrachloride-induced cirrhosis have been described (300, 301), but a closer representation of the human disease might be produced in animals that resemble man in the hepatic handling of IgA (*e.g.* guinea pig), as we have already discussed.

***IgA and Primary Biliary Cirrhosis.*** We have mentioned that elevations of serum sIgA concentrations are common in primary biliary cirrhosis (105, 106, 262, 266). Recently, markedly elevated values in this condition have been described (256, 263–265), and values greater than 118 mg per ml have even been called specific for the disease (263). On the basis of combined results of several studies, though, it does not appear that measurement of serum sIgA in primary biliary cirrhosis, even if it were to become a practical test, would reliably discriminate between that disease and other cholestatic diseases. An interesting question had been whether the biliary ductule damage that characterizes primary biliary cirrhosis can be related to abnormalities in IgA. Any speculation of this kind was laid to rest by the reports of the disease in patients with selective and severe IgA deficiency (302; Logan RF. Gastroenterology 1987; 92:270–271, Correspondence), an observation which indicates that the pathogenesis of primary biliary cirrhosis does not require IgA-dependent immune mechanisms. The association of IgA deficiency with this disease might be due to chance alone, although it is consistent with the recognized association of IgA deficiency with various kinds of autoimmune diseases (247). With respect to relationships between IgA and biliary epithelium, it has recently been reported that IgA stimulates the growth of extrahepatic bile duct epithelium in mice (303); we await confirmation of this very provocative observation.

***IgA and Obstructive Biliary Tract Disease.*** Although early reports suggested that measurement of IgA, especially sIgA, in the serum would be

15273350, 1989, 5, Downloaded from https://aasldpubs.onlinelibrary.wiley.com/doi/10.1002/hep.1840090518, Wiley Online Library on [11/04/2023]. See the Terms and Conditions (https://onlinelibrary.wiley.com/terms-and-conditions) on Wiley Online Library for rules of use; OA articles are governed by the applicable Creative Commons License

useful in diagnosing extrahepatic biliary obstruction (105, 106), it is now clear that it is not (93, 94). In an unreported study, we and Mestecky's group in Birmingham were unable to detect any significant change in the serum levels of IgA in patients who had severe extrahepatic biliary obstruction, either during the obstruction or in response to surgical relief of the obstruction. A marked elevation of SC in the serum reportedly is a prominent feature of biliary obstruction as well as primary biliary cirrhosis. The SC levels are not correlated with levels of pIgA (93); the circulating SC is bound both to pIgA and IgM (93, 304) probably because of the release of SC from biliary epithelium into the circulation, where it can bind to the polymeric immunoglobulins.

## CONCLUDING STATEMENT

The fascinating, close relationships between IgA and the liver deserve intensified research. Such investigation likely will further enhance our understanding of the secretory immune system, the bile secretory apparatus and general cell biological principles regarding the synthesis and expression of cell membrane receptors and the cellular transport of macromolecules. Moreover, resolution of the mysteries surrounding the abnormalities in IgA-liver relationships in liver diseases, especially in alcoholic disease, might clarify not only the pathogenesis of those diseases but of IgA-associated renal diseases as well.

## REFERENCES


1. Tomasi TB, Tan EM, Solomon A, et al. Characteristics of an immune system common to certain external secretions. J Exp Med 1965; 121:101–124.
2. Lemaitre-Coelho I, Jackson GDF, Vaerman JP. Rat bile as a convenient source of secretory IgA and free secretory component. Eur J Immunol 1977; 7:588–590.
3. Mostov KE, Deitcher DL. Polymeric immunoglobulin receptor expressed in MDCK cells transcytoses IgA. Cell 1986; 46:613–621.
4. Mostov KE, Breitfeld P, Harris JM. An anchor-minus form of the polymeric immunoglobulin receptor is secreted predominantly apically in Madrin-Darby canine kidney cells. J Cell Biol 1987; 105:2031–2036.
5. Mostov KE, Kops AD, Deitcher DL. Deletion of the cytoplasmic domain of the polymeric immunoglobulin receptor prevents basolateral localization and endocytosis. Cell 1986; 47:359–364.
6. Solari R, Kraehenbuhl JP. The biosynthesis of secretory component and its role in the transepithelial transport of IgA dimer. Immunol Today 1985; 6:17–20.
7. Ahnen DJ, Brown WR, Kloppel TM. Secretory component. The polymeric immunoglobulin receptor. What's in it for the hepatologist and gastroenterologist. Gastroenterology 1985; 89:667–682.
8. Ahnen DJ, Brown WR, Kloppel TM. Secretory component. The polymeric immunoglobulin receptor. In: Conn M, ed. The receptors, Vol. III. Orlando, Florida: Academic Press, 1986: 2–52.
9. Mestecky J, McGhee JR. Immunoglobulin A (IgA): molecular and cellular interactions involved in IgA biosynthesis and immune response. Adv Immunol 1987; 40:153–245.
10. Mestecky J, Russell MW, Jackson S, et al. The human IgA system: a reassessment. Clin Immunol Immunopathol 1986; 40:105–114.
11. Brandtzaeg P, Valnes K, Scott H, et al. The human gastrointestinal secretory immune system in health and disease. Scand J Gastroenterol 1985; 20(Suppl. 114):17–38.
12. Underdown BJ, Schiff JM. Immunoglobulin A: strategic defense initiative at the mucosal surface. Annu Rev Immunol 1986; 4:389–417.
13. Mestecky J, Schrohenholer RE, Kulhavy R, et al. Association of S-IgA subunits. In: Mestecky J, Lawton AR, eds. The immunoglobulin A system. New York: Plenum Press, 1974: 99–109.
14. Brandtzaeg P. Role of J chain and secretory component in receptor-mediated glandular and hepatic transport of immunoglobulins in man. Scand J Immunol 1985; 22:111–146.
15. Mestecky J, Preud'homme JL, Crago SS, et al. Presence of J chain in human lymphoid cells. Clin Exp Immunol 1980; 39:371–385.
16. Bienenstock J. Gut and bronchus-associated lymphoid tissue: an overview. Adv Exp Med Biol 1982; 149:417–477.
17. Nagura H, Nakane PK, Brown WR. Ultrastructural localization of J-chain in human intestinal mucosa. J Immunol 1979; 123:1044–1050.
18. Brandtzaeg P. Immunohistochemical characterization of intracellular J chain and binding site for secretory component (SC) in the human immunoglobulin (Ig)-producing cells. Mol Immunol 1983; 20:941–966.
19. Mostov KE, Kraehenbuhl JP, Blobel G. Receptor-mediated transcellular transport of immunoglobulin: synthesis of secretory component as multiple and larger transmembrane forms. Proc Natl Acad Sci USA 1980; 77:7257–7261.
20. Socken DJ, Jeejeebhoy KN, Bazin H, et al. Identification of secretory component as an IgA receptor on rat hepatocytes. J Exp Med 1979; 150:1538–1548.
21. Sztul ES, Howell KE, Palade GE. Intracellular and transcellular transport of secretory component and albumin in rat hepatocytes. J Cell Biol 1983; 97:1582–1591.
22. Takahashi I, Nakane PK, Brown WR. Ultrastructural events in the translocation of polymeric IgA by rat hepatocytes. J Immunol 1982; 128:1181–1187.
23. Weicker J, Underdown BJ. A study of the association of human secretory component with IgA and IgM proteins. J Immunol 1975; 114:1337–1344.
24. Vaerman JP, Heremans JF, Bazin H, et al. Identification and some properties of rat secretory component. J Immunol 1975; 114:265–269.
25. Nagura H, Nakane PK, Brown WR. Translocation of dimeric IgA through neoplastic colon cells in vitro. J Immunol 1979; 123:2359–2368.
26. Renston RH, Jones AL, Christiansen WD, et al. Evidence for a vesicular transport mechanism in hepatocytes for biliary secretion of immunoglobulin A. Science 1980; 208:1276–1278.
27. Kuhn LC, Kraehenbuhl JP. The membrane receptor for polymeric immunoglobulin is structurally related to secretory component. Isolation and characterization of membrane secretory component from rabbit liver and mammary gland. J Cell Biol 1981; 256:12490–12495.
28. Mostov K, Blobel G. A transmembrane precursor of secretory component. J Biol Chem 1982; 257:11816–11821.
29. Klopper TM, Brown WR. Rat liver membrane secretory component is larger than free secretory component in bile. Evidence of proteolytic conversion of the membrane form to the free form. J Cell Biochem 1984; 24:307–318.
30. Musil LS, Baenziger JU. Cleavage of membrane secretory component of soluble secretory component occurs on the cell surface of rat hepatocyte monolayers. J Cell Biol 1987; 104:1725–1733.
31. Mullock BM, Jones RS, Hinton RH. Movement of endocytic shuttle vesicles from the sinusoidal to the bile canalicular face of hepatocytes does not depend on the occupation of receptor sites. FEBS Lett 1980; 113:201–205.
32. Kloppel TM, Brown WR, Reichen J. Mechanisms of secretion of proteins into bile. Studies in the perfused rat liver. Hepatology 1986; 6:587–594.
33. Brown WR, Newcomb RW, Ishizaka K. Proteolytic degradation of exocrine and serum immunoglobulins. J Clin Invest 1970; 49:1374–1380.
34. Mach JP. In vitro combination of human and bovine free secretory component with IgA of various species. Nature 1970; 228:1278–1282.
35. Lindh E, Bjork I. Binding of secretory component to dimers of immunoglobulin A in vitro. Eur J Biochem 1976; 62:263–270.
36. Kuhn LC, Kraehenbuhl JP. Role of secretory component, a secreted glycoprotein, in the specific uptake of IgA dimer by epithelial cells. J Biol Chem 1979; 254:11072–11081.
37. Mestecky J, Russell MW. IgA subclasses. Monogr Allergy 1986; 19:277–301.


15273350, 1989, 5, Downloaded from https://aasldpubs.onlinelibrary.wiley.com/doi/10.1002/hep.1840090518, Wiley Online Library on [11/04/2023]. See the Terms and Conditions (https://onlinelibrary.wiley.com/terms-and-conditions) on Wiley Online Library for rules of use; OA articles are governed by the applicable Creative Commons License

Case 1:23-cv-00328-JLH-SRF Document 125 Filed 02/20/24 Page 45 of 73 PageID #: 4352




38. Delacroix DL, Dive C, Rambaud JC, et al. IgA subclasses in various secretions and in serum. Immunology 1982; 47:383–385.
39. Vaerman JP, Lemaitre-Coelho I. Transfer of circulating human IgA across the rat liver into the bile. In: Hemmings WA, ed. Protein transmission through living membranes. Amsterdam: Elsevier/North Holland Biomedical Press, 1979: 383–398.
40. Orlans E, Peppard J, Reynolds J, et al. Rapid active transport of immunoglobulin A from blood to bile. J Exp Med 1978; 147:588–592.
41. Jackson GDF, Lemaitre-Coelho I, Vaerman JP, et al. Rapid disappearance from serum of intravenously injected rat myeloma IgA and its secretion into bile. Eur J Immunol 1978; 8:123–126.
42. Lemaitre-Coelho I, Jackson GDF, Vaerman J-P. High levels of secretory IgA and free secretory component in the serum of rats with bile duct obstruction. J Exp Med 1978; 147:934–939.
43. Fisher MM, Nagy B, Bazin H, et al. Biliary transport of IgA. Role of secretory component. Proc Natl Acad Sci USA 1979; 76:2008–2012.
44. Lemaitre-Coelho I, Altamirano GA, Barranco-Acosta C, et al. In vivo experiments involving secretory component in the rat hepatic transfer of polymeric IgA from blood into bile. Immunology 1981; 43:261–270.
45. Socken DJ, Simms ES, Nagy BR, et al. Secretory component-dependent hepatic transport of IgA antibody-antigen complexes. J Immunol 1981; 127:316–319.
46. Reynolds J, Gyure L, Andrew E, et al. Studies of the transport of polyclonal IgA antibody from blood to bile in rats. Immunology 1980; 39:463–467.
47. Delacroix DL, Denef AM, Acosta GA, et al. Immunoglobulins in rabbit hepatic bile: selective secretion of IgA and IgM and active plasma-to-bile transfer of polymeric IgA. Scand J Immunol 1982; 16:343–350.
48. Delacroix DL, Furtado-Barreira G, de Hemptinne B, et al. The liver in the IgA secretory immune system. Dogs, but not rats and rabbits, are suitable models for human studies. Hepatology 1983; 3:980–988.
49. Hall JG, Gyure LA, Payne AWR. Comparative aspects of the transport of immunoglobulin A from blood to bile. Immunology 1980; 41:899–902.
50. Orlans E, Peppard JV, Payne AWR, et al. Comparative aspects of the hepatobiliary transport of IgA. Ann NY Acad Sci 1983; 409:411–427.
51. Vaerman JP, Lemaitre-Coelho I, Limet J, et al. Hepatic transter of polymeric IgA from plasma to bile in rats and other mammals. A survey. In: Strober W, Hanson LA, Sell KW, eds. Recent advances in mucosal immunity. New York: Raven Press, 1982: 233–250.
52. Dooley JS, Potter BJ, Thomas HC, et al. A comparative study of the biliary secretion of human dimeric and monomeric IgA in the rat and in man. Hepatology 1982; 2:323–327.
53. Delacroix DL, Vaerman JP. Function of the human liver in IgA homeostasis in plasma. Ann NY Acad Sci 1983; 409:383–401.
54. Delacroix DL, Hodgson HJF, McPherson A, et al. Selective transport of polymeric immunoglobulin A in bile. J Clin Invest 1982; 70:230–241.
55. Russell MW, Brown TA, Mestecky J. Role of serum IgA. Hepatobiliary transport of circulating antigen. J Exp Med 1981; 153:968–976.
56. Phillips JO, Russell MW, Brown TA, et al. Selective hepatobiliary transport of human polymeric IgA in mice. Mol Immunol 1984; 21:907–914.
57. Jackson GDF, Lemaitre-Coelho I, Vaerman J-P. Transfer of MOPC-315 IgA to secretions in MOPC-315 tumour-bearing and normal BALB/c mice. Prot Biol Fluids 1977; 25:919–922.
58. Koertge TE, Butler JE. Dimeric mouse IgA is transported into rat bile five times more rapidly than into mouse bile. Scand J Immunol 1986; 24:567–574.
59. Delacroix DL, Malburny GN, Vaerman JP. Hepatobiliary transport of plasma IgA in the mouse: contribution to clearance of intravascular IgA. Eur J Immunol 1985; 15:893–899.
60. Scicchitano R, Husband AJ, Cripps AW. Biliary transport of serum IgA in sheep. Immunology 1984; 53:121–129.
61. Sheldrake RF, Scicchitano R, Husband AJ. The effect of lactation on the transport of serum-derived IgA into bile of sheep. Immunology 1985; 54:471–477.
62. Kloppel TM, Hoops TC, Gaskin C, et al. Uncoupling of the biliary secretory pathways for IgA and its receptor, secretory component, by brief periods of cholestasis. Am J Physiol 1987; 253:G232–G240.
63. Kloppel TM, Mysan L. Transport of IgA into bile in the rat may depend on proper bile salt traffic (Abstract). J Cell Biol 1987; 105:233a.
64. Rose ME, Orlans E, Payne AWR, et al. The origin of IgA in chicken bile: its rapid active transport from blood. Eur J Immunol 1981; 11:561–564.
65. Geuze HJ, Van Der Donk HA, Simmons CF, et al. Receptor-mediated endocytosis in liver parenchymal cells. Int Rev Exp Pathol 1986; 29:113–171.
66. Delacroix DL, Furtado-Barreira G, Rahier J, et al. Immunohistochemical localization of secretory component in the liver of guinea pigs and dogs versus rats, rabbits, and mice. Scand J Immunol 1984; 19:425–434.
67. Wilson ID, Wong M, Erlandsen SL. Immunohistochemical localization of IgA and secretory component in rat liver. Gastroenterology 1980; 79:924–930.
68. Orlans E, Peppard J, Fry JF, et al. Secretory component as the receptor for polymeric IgA on rat hepatocytes. J Exp Med 1979; 150:1577–1581.
69. Nagura H, Smith PD, Nakane PK, et al. IgA in human bile and liver. J Immunol 1981; 126:587–595.
70. Tomana M, Kulhavy R, Mestecky J. Receptor-mediated binding and uptake of immunoglobulin A by human liver. Gastroenterology 1988; 94:762–770.
71. Fukuda Y, Nagura H, Asai J, et al. Possible mechanisms of elevation of serum secretory immunoglobulin A in liver diseases. Am J Gastroenterol 1986; 81:315–324.
72. Kater L, Jobsis AC, de la Faille-Kuyper EH, et al. Alcoholic hepatic disease. Specificity of IgA deposits in liver. Am J Clin Pathol 1979; 71:51–57.
73. Hopf U, Brandtzaeg P, Hutteroth TH, et al. In vivo and in vitro binding of IgA to the plasma membrane of hepatocytes. Scand J Immunol 1978; 8:543–549.
74. Chandy KG, Hubscher SG, Elias E, et al. Dual role of the liver in regulating circulating polymeric IgA in man: studies on patients with liver disease. Clin Exp Immunol 1983; 52:207–218.
75. Delacroix DL, Courtoy PJ, Rahier J, et al. Localization and serum concentration of secretory component during massive necrosis of human liver. Gastroenterology 1984; 86:521–531.
76. Daniels CK, Schmucker DL. Secretory component-dependent binding of immunoglobulin A in the rat, monkey and human: a comparison of intestine and liver. Hepatology 1987; 7:517–521.
77. Peppard JV, Rose ME, Hesketh P. A functional homologue of mammalian secretory component exists in chickens. Eur J Immunol 1983; 13:566–570.
78. Hsu SM, Hsu PL. Determination of IgA and secretory component in human hepatocytes. Gut 1980; 21:985–989.
79. Foss-Bowman C, Jones AL, Dejbakhsh S, et al. Immunofluorescent and immunocytochemical localization of secretory component and immunoglobulins in human livers (Abstract). Ann NY Acad Sci 1983; 409:822–823.
80. Birbeck MSC, Cartwright P, Hall JG, et al. The transport by hepatocytes of immunoglobulin A from blood to bile visualized by autoradiography and electron microscopy. Immunology 1979; 37:477–484.
81. Jones AL, Hradek GT, Schmucker DL. Intracellular processing of human vs rat immunoglobulin A in the rat liver. Hepatology 1985; 5:1172–1178.
82. Mullock BM, Hinton RH, Peppard J, et al. Distribution of secretory component in hepatocytes and its model of transfer into bile. Biochem J 1980; 190:819–826.
83. Tolleshaug H, Brandtzaeg P, Holte K. Quantitative study of the uptake of IgA by isolated rat hepatocytes. Scand J Immunol 1981; 13:47–56.
84. Zevenbergen JL, May C, Wanson JC, et al. Synthesis of secretory component by rat hepatocytes in culture. Scand J Immunol 1980; 11:93–97.
85. Limet JN, Schneider YJ, Vaerman JP, et al. Interaction of rat IgA with cultured rat hepatocytes: binding site, drug effects. Toxicology 1980; 18:187–194.
86. Vaerman J-P, Andre C, Bazin H, et al. Mesenteric lymph as a


2723350, 1989, 5, Downloaded from https://aasldpubs.onlinelibrary.wiley.com/doi/10.1002/hep.1840090518, Wiley Online Library on [11/04/2023]. See the Terms and Conditions (https://onlinelibrary.wiley.com/terms-and-conditions) on Wiley Online Library for rules of use; OA articles are governed by the applicable Creative Commons License

DEFS00021187
BTRAC_CP019_000000093

major source of serum IgA in guinea pigs and rats. Eur J Immunol 1973; 3:580–584.
87. Kaartinen J, Imir R, Klokars M, et al. IgA in blood and thoracic duct lymph: concentration and degree of polymerization. Scand J Immunol 1978; 7:229–232.
88. Brown WR, Smith PD, Lee E, et al. A search for an enriched source of polymeric IgA in human thoracic duct lymph, portal vein blood and aortic blood. Clin Exp Immunol 1982; 48:85–90.
89. Cruchard A, Lapperrouza C, Megevand R. Agammaglobulinemia in monozygous twins: therapeutical prospects. Birth Defects 1968; 4:315–327.
90. Challacombe SJ, Greenall C, Stoker TAM. A comparison of IgA in portal and peripheral venous blood. Immunology 1987; 60:111–116.
91. Conley ME, Delacroix DL. Intravascular and mucosal immunoglobulin A: two separate but related systems of immune defense. Ann Intern Med 1987; 106:892–899.
92. Waldmann TA, Strober W. Metabolism of immunoglobulins. Prog Allergy 1969; 13:1–110.
93. Delacroix DL, Elkon KB, Geubel AP, et al. Changes in size, subclass, and metabolic properties of serum immunoglobulin A in liver diseases and in other diseases with high serum immunoglobulin A. J Clin Invest 1983; 71:358–367.
94. Kutteh WH, Prince BJ, Phillips JO, et al. Properties of immunoglobulin A in serum of individuals with liver diseases and in hepatic bile. Gastroenterology 1982; 82:184–193.
95. Newkirk MM, Klein MH, Katz A, et al. Estimation of polymeric IgA in human serum: an assay based on binding of radiolabeled human secretory component with applications in the study of IgA nephropathy, IgA monoclonal gammopathy, and liver disease. J Immunol 1983; 130:1176–1181.
96. Lemaitre-Coelho I, Jackson GDF, Vaerman JP. Relevance of biliary IgA antibodies in rat intestinal immunity. Scand J Immunol 1978; 8:459–461.
97. Jonard PP, Rambaud JC, Dive C, et al. Secretion of immunoglobulins and plasma proteins from the jejunal mucosa. J Clin Invest 1984; 74:525–535.
98. Paronetto F, Rubin E, Popper H. Local formation of gammaglobulin in the diseased liver, and its relation to hepatic necrosis. Lab Invest 1962; 11:150–158.
99. Hadziyannis S, Feizi T, Scheuer PJ, et al. Immunoglobulin-containing cells in the liver. Clin Exp Immunol 1969; 5:499–514.
100. Nagura H, Tsutsumi Y, Hasegawa H, et al. IgA plasma cells in biliary mucosa. A likely source of locally synthesized IgA in human bile. Clin Exp Immunol 1983; 54:671–680.
101. Carter L, Jackson GDF. Antibody synthesis in the rat liver: a source of biliary IgM, IgA and IgG following injection of horse erythrocytes into the intestine or Peyer's patches. Adv Exp Med Biol 1987; 216b:1147–1156.
102. Carter L, Barrington PJ, Cooper GN, et al. Antibody synthesis in the rat liver: an association between antibody-forming cells in the liver and biliary antibodies following intravenous injection of horse erythrocytes. Int Arch Allergy Appl Immunol 1987; 82:153–158.
103. Rank J, Wilson ID, Changes in IgA following varying degrees of biliary obstruction in the rat. Hepatology 1983; 3:241–247.
104. Vaerman JP, Lemaitre-Coelho I, Jackson GDF. The secretory IgA system and the liver. Ric Clin Lab 1978; 8(Suppl. 1):281–286.
105. Thompson RA, Carter R, Stokes RP, et al. Serum immunoglobulins, complement component levels and autoantibodies in liver disease. Clin Exp Immunol 1973; 14:334–346.
106. Goldblum RM, Powell GK, Van Sickle G. Secretory IgA in the serum of infants with obstructive jaundice. J Pediatr 1980; 97:33–36.
107. Hodgson HJF. Gut-liver interactions in the IgA system. Scand J Gastrointest 1985; 20:39–44.
108. Mestecky J, Kutteh WH, Brown TA, et al. Function and biosynthesis of polymeric IgA. Ann NY Acad Sci 1983; 409:292–306.
109. Vuitton DA, Seilles E, Claude P, et al. Gall bladder: the predominant source of bile IgA in man? Clin Exp Immunol 1985; 62:185–192.
110. Chodirker WB, Tomasi TB. Gamma globulins: quantitative relationships in human serum and nonvascular fluids. Science 1963; 142:1080–1081.
111. Chen ST, Tobe T. Cellular sites of immunoglobulins. V. An immunological study of the human gall bladder. Digestion 1974; 10:184–190.
112. Danon YL, Garty B, Weiss H, et al. Immunoglobulin content of human hepatic bile: selective IgA concentration in bile. Isr J Med Sci 1986; 22:414–415.
113. Green FHY, Fox H. An immunofluorescent study of the distribution of immunoglobulin-containing cells in the normal and inflamed human gall bladder. Gut 1972; 13:379–384.
114. Stockert RJ, Kressner MB, Collins JC, et al. IgA interaction with the asialoglycoprotein receptor. Proc Natl Acad Sci USA 1982; 79:6229–6231.
115. Sancho J, Gonzalez E, Egido J. The importance of the Fc receptors for IgA in the recognition of IgA by mouse liver cells: its comparison with carbohydrate and secretory component receptors. Immunology 1986; 57:37–42.
116. Tomana M, Phillips JO, Kulhavy R, et al. Carbohydrate-mediated clearance of secretory IgA from the circulation. Mol Immunol 1985; 22:887–892.
117. Dive CH, Heremans JF. Nature and origin of the proteins of bile. I. A comparative analysis of serum and bile proteins in man. Eur J Clin Invest 1974; 4:235–238.
118. Peppard JV, Jackson LE, Hall JG. The occurrence of secretory IgM in the bile of rats. Clin Exp Immunol 1983; 53:623–626.
119. Dahlgren UIH, Svanvik J, Eden CS. Antibodies to *Escherichia coli* and anti-adhesive activity in paired serum, hepatic and gall bladder bile samples. Scand J Immunol 1986; 24:251–260.
120. Mostov KE, Friedlander M, Blobel G. The receptor for transepithelial transport of IgA and IgM contains multiple immunoglobulin-like domains. Nature 1984; 308:37–43.
121. Eiffert H, Quentin E, Decker J, et al. Die primarstruktur der menschlichen freien sekretkomponente und die anordung der disulfidbrucken. Hoppe-Seyler's Z Physiol Chem 1984; 365:1489–1495.
122. Knight KL, Rosenzweig M, Lichter EA, et al. Rabbit secretory IgA: identification and genetic control of two allotypes of secretory component. J Immunol 1974; 112:877–882.
123. Kuhn LC, Kocher HP, Hanly WC, et al. Structural and genetic heterogeneity of the receptor mediating translocation of immunoglobulin A dimer antibodies across epithelia in the rabbit. J Biol Chem 1983; 258:6653–6659.
124. Frutiger S, Hughes GJ, Hanly WC, et al. The amino-terminal domain of rabbit secretory component is responsible for noncovalent binding of immunoglobulin A dimers. J Biol Chem 1986; 261:16673–16681.
125. Sztul ES, Howell KE, Palade GE. Biogenesis of the polymeric IgA receptor in rat hepatocytes. I. Kinetic studies of its intracellular forms. J Cell Biol 1985; 100:1248–1254.
126. Sztul ES, Howell KE, Palade GE. Biogenesis of the polymeric IgA receptor in rat hepatocytes. II. Localization of its intracellular forms by cell fractionation studies. J Cell Biol 1985; 100:1255–1261.
127. Solari R, Kraehenbuhl JP. Biosynthesis of the IgA antibody receptor: a model for the transepithelial sorting of a membrane glycoprotein. Cell 1984; 36:61–71.
128. Solari R, Racine L, Tallichet C, et al. Distribution and processing of the polymeric immunoglobulin receptor in the rat hepatocyte: morphological and biochemical characterization of subcellular fractions. J Histochem Cytochem 1986; 34:17–23.
129. Larkin JM, Sztul ES, Palade GE. Phosphorylation of the rat hepatic polymeric IgA receptor. Proc Natl Acad Sci USA 1986; 83:4759–4763.
130. Musil LS, Baenziger JU. Intracellular transport and processing of secretory component in cultured rat hepatocytes. Gastroenterology 1987; 93:1194–1204.
131. Scharer E, Verry F, Riezman H, et al. Cloning of the higher and lower molecular weight forms of the polymeric immunoglobulin receptor and its expression in yeast (Abstract). J Cell Biol 1986; 103:339a.
132. Brown WR, Isobe K, Nakane PK, et al. Studies on translocation of immunoglobulins across intestinal epithelium. IV. Evidence for binding of IgA and IgM to secretory component in intestinal epithelium. Gastroenterology 1977; 73:1333–1339.
133. Kuhn LC, Kraehenbuhl JP. Interaction of rabbit secretory component with rabbit IgA dimer. J Biol Chem 1979; 254:11066–11071.

15273350, 1989, 5, Downloaded from https://aasldpubs.onlinelibrary.wiley.com/doi/10.1002/hep.1840090518, Wiley Online Library on [11/04/2023]. See the Terms and Conditions (https://onlinelibrary.wiley.com/terms-and-conditions) on Wiley Online Library for rules of use; OA articles are governed by the applicable Creative Commons License

134. Radl J, Klein F, van den Berg P. Binding of secretory piece to polymeric IgA and IgM paraproteins in vitro. Immunology 1971; 20:843–852.
135. Underdown BJ, Socken DJ. A comparison of secretory component-immunoglobulin interactions amongst different species. Adv Exp Med Biol 1978; 107:503–511.
136. Halpern MS, Koshland ME. Novel subunit in secretory IgA. Nature 1970; 228:1276–1278.
137. Garcia-Pardo A, Lamm ME, Plaut AG, et al. J chain is covalently bound to both monomer subunits in human secretory IgA. J Biol Chem 1981; 256:11734–11738.
138. Brandtzaeg P, Prydz H. Direct evidence for an integrated function of J chain and secretory component in epithelial transport. Nature 1984; 311:71–73.
139. Frutiger S, Hughes GJ, Fonck C, et al. High and low molecular weight rabbit secretory components. Evidence for the deletion of the second and third domains in the smaller peptide. J Biol Chem 1987; 262:1712–1715.
140. Schiff JM, Fisher MM, Underdown BJ. Receptor-mediated biliary transport of immunoglobulin A and asialoglycoprotein: sorting and missorting of ligands revealed by two radiolabeling methods. J Cell Biol 1984; 98:79–89.
141. Schiff JM, Fisher MM, Jones AL, et al. Human IgA as a heterovalent ligand: switching from the asialoglycoprotein receptor to secretory component during transport across the rat hepatocyte. J Cell Biol 1986; 102:920–931.
142. Schiff JM, Fisher MM, Underdown BJ. Secretory component as the mucosal transport receptor: separation of physiochemically analogous human IgA fractions with different receptor-binding capacities. Mol Immunol 1986; 23:45–56.
143. Lindh E, Bjork I. Relative rates of the non-covalent and covalent binding of secretory component to an IgA dimer. Acta Pathol Microbiol Scand Sect C 1977; 85:449–453.
144. Brandtzaeg P. Human secretory component. VI. Immunoglobulin binding properties. Immunochemistry 1977; 14:179–188.
145. Underdown BJ, De Rose J, Plaut A. Disulfide bonding of secretory component to a single monomer subunit in human secretory IgA. J Immunol 1977; 118:1816–1821.
146. Murkofsky NA, Lamm ME. Effect of a disulfide interchange enzyme on the assembly of human secretory immunoglobulin A from immunoglobulin A and free secretory component. J Biol Chem 1979; 254:12181–12184.
147. Garcia-Pardo A, Lamm ME, Plaut AG, et al. Secretory component is covalently bound to a single sub-unit in human secretory IgA. Mol Immunol 1979; 16:477–482.
148. Hanly CW, Chang CH, Schiffer M. A model for secretory component-IgA interactions (Abstract). Fed Proc 1985; 44:1299.
149. Socken DJ, Underdown BJ. Comparison of human, bovine and rabbit secretory component-immunoglobulin interactions. Immunochemistry 1978; 15:499–506.
150. Schiff JM, Endo Y, Kells DIC, et al. Kinetic differences in hepatic transport of IgA polymers reflect molecular size. (Abstract). Fed Proc 1983; 42:1341.
151. Renston RH, Maloney DG, Jones AL, et al. Bile secretory apparatus: evidence for a vesicular transport for proteins in the rat, using horseradish peroxidase and [$^{125}$I]-insulin. Gastroenterology 1980; 78:1373–1388.
152. Jones AL, Schmucker DL, Renston RH, et al. The architecture of bile secretion; a morphological perspective of physiology. Dig Dis Sci 1980; 25:609–629.
153. Geuze HJ, Slot JW, Strous GJAM, et al. Intracellular receptor sorting during endocytosis: comparative immunoelectron microscopy of multiple receptors in rat liver. Cell 1984; 37:195–204.
154. Gebhardt R, Robenek H. Ligand-dependent redistribution of the IgA receptor on cultured rat hepatocytes and its disturbance by cytochalasin B. J Histochem Cytochem 1987; 35:301–309.
155. Limet JN, Quintart J, Schneider Y-J, et al. Receptor-mediated endocytosis of polymeric IgA and galactosylated serum albumin in rat liver. Evidence for intracellular ligand sorting and identification of distinct endosomal compartments. Eur J Biochem 1985; 146:539–548.
156. Courtoy PJ, Limet JN, Quintart J, et al. Transfer of IgA into rat bile: ultrastructure demonstration. Ann NY Acad Sci 1983; 409:799–802.
157. Hoppe CA, Connolly TP, Hubbard AL. Transcellular transport of polymeric IgA in the rat hepatocyte: biochemical and morphological characterization of the transport pathway. J Cell Biol 1985; 101:2113–2123.
158. Mullock BM, Jones RS, Peppard J, et al. Effect of colchicine on the transfer of IgA across hepatocytes into bile in isolated perfused livers. FEBS Lett 1980; 120:278–282.
159. Goldman IS, Jones AL, Hradek GT, et al. Hepatocyte handling of immunoglobulin A in the rat: the role of microtubules. Gastroenterology 1983; 85:130–140.
160. Mullock BM, Luzio JP, Hinton RH. Preparation of a low-density species of endocytic vesicle containing immunoglobulin A. Biochem J 1983; 214:823–827.
161. Ahnen DJ, Singleton JR, Hoops TC, et al. Posttranslational processing of secretory component in the rat jejunum by a brush border metalloprotease. J Clin Invest 1986; 77:1841–1848.
162. Stokes CR, Swarbrick ET, Soothill JF. Immune elimination and enhance antibody responses: functions of circulating IgA. Immunology 1980; 40:455–458.
163. Peppard J, Orlans E, Payne AW, et al. The elimination of circulating complexes containing polymeric IgA by excretion in the bile. Immunology 1981; 42:83–89.
164. Socken DJ, Simms ES, Nagy B, et al. Transport of IgA antibody-antigen complexes by the rat liver. Mol Immunol 1981; 18:345–348.
165. Peppard JV, Orlans E, Andrew E, et al. Elimination into bile of circulating antigen by endogenous IgA antibody in rats. Immunology 1982; 45:467–472.
166. Brown TA, Russell MW, Mestecky J. Hepatobiliary transport of IgA immune complexes: molecular and cellular aspects. J Immunol 1982; 128:2183–2186.
167. Harmatz PR, Kleinman RE, Bunnell BW, et al. Hepatobiliary clearance of IgA immune complexes formed in the circulation. Hepatology 1982; 2:328–333.
168. Brown TA, Russell MW, Kulhavy R, et al. IgA-mediated elimination of antigens by the hepatobiliary route. Fed Proc 1983; 42:3218–3221.
169. Skogh T, Edebo L, Stendahl O. Gastrointestinal uptake and blood clearance of antigen in the presence of IgA antibodies. Immunology 1983; 50:175–180.
170. Russell MW, Brown TA, Claflin JL, et al. Immunoglobulin A-mediated hepatobiliary transport constitutes a natural pathway for disposing of bacterial antigens. Infect Immunol 1983; 42:1041–1048.
171. Fernandez-Tello DS, Frommel D. In vitro uptake of IgA complexes by Kupffer cells. Liver 1983; 3:71–78.
172. Rifai A, Mannik M. Clearance kinetics and fate of mouse IgA immune complexes prepared with monomeric or dimeric IgA. J Immunol 1983; 130:1826–1832.
173. Sancho J, Gonzalez E, Egido J. Handling of IgA immune aggregates by liver cells. Contr Nephrol 1984; 40:93–98.
174. Phillips JO, Stohrer R, Russell MW, et al. Analysis of the hepatobiliary transport of IgA with monoclonal anti-idiotype and anti-allotype antibodies. Mol Immunol 1986; 23:339–346.
175. Limet JN, Schneider YJ, Vaerman JP, et al. Binding, uptake and intracellular processing of polymeric rat immunoglobulin A by cultured rat hepatocytes. Eur J Biochem 1982; 125:437–443.
176. Gebhardt R. Primary cultures of rat hepatocytes as a model of canalicular development, biliary secretion, and intrahepatic cholestasis. III. Properties of the biliary transport of immunoglobulin A as revealed by immunofluorescence. Gastroenterology 1983; 84:1462–1470.
177. Jones AL, Huling S, Hradek GT, et al. Uptake and intracellular disposition of IgA by rat hepatocytes in monolayer culture. Hepatology 1982; 2:769–776.
178. Deitcher DL, Neutra MR, Mostov KE. Functional expression of the polymeric immunoglobulin receptor from cloned cDNA in fibroblasts. J Cell Biol 1986; 102:911–919.
179. Baenziger J, Kornfeld S. Structure of the carbohydrate units of IgA1 immunoglobulin. I. Composition, glycopeptide isolation, and structure of the asparagine-linked oligosaccharide units. J Biol Chem 1974; 249:7260–7269.
180. Baenziger J, Kornfeld S. Structure of the carbohydrate units of IgA1 immunoglobulin. II. Structure of the O-linked oligosaccharide units. J Biol Chem 1974; 249:7270–7281.
181. Mizoguchi A, Mizuochi T, Kobata A. Structure of the carbohy-


15273350, 1989, 5, Downloaded from https://aasldpubs.onlinelibrary.wiley.com/doi/10.1002/hep.1840090518, Wiley Online Library on [11/04/2023]. See the Terms and Conditions (https://onlinelibrary.wiley.com/terms-and-conditions) on Wiley Online Library for rules of use; OA articles are governed by the applicable Creative Commons License

drate moieties of secretory component purified from human milk. J Biol Chem 1982; 257:9612–9621.
182. Bridges K, Harford J, Ashwell G, et al. Fate of receptor and ligand during endocytosis of asialoglycoproteins by isolated hepatocytes. Proc Natl Acad Sci USA 1982; 79:350–354.
183. Geuze HJ, Slot JW, Strous GJAM, et al. Immunocytochemical localization of the receptor for asialoglycoprotein in rat liver cells. J Cell Biol 1982; 92:865–870.
184. Mizuno M, Kloppel TM, Nakane PK, et al. Cellular distribution of the asialoglycoprotein receptor in rat liver. Gastroenterology 1984; 84:142–149.
185. Mizuno M, Brown WR, Vierling JM. Ultrastructural immunocytochemical localization of the asialoglycoprotein receptor in rat hepatocytes. Gastroenterology 1984; 87:763–769.
186. Ashwell G, Harford J. Carbohydrate-specific receptors of the liver. Annu Rev Biochem 1982; 51:531–534.
187. Stockert RJ, Haimes HB, Morell AG, et al. Endocytosis of asialoglycoprotein-enzyme conjugates by hepatocytes. Lab Invest 1980; 43:556–563.
188. Geuze HJ, Slot JW, Strous GJAM, et al. The pathway of the asialoglycoprotein receptor-ligand during receptor-mediated endocytosis: a morphological study with colloidal gold ligand in the human hepatoma cell line, Hep G2. Eur J Cell Biol 1983; 32:38–44.
189. Wall DA, Wilson G, Hubbard AL. The galactose-specific recognition system of mammalian liver: the route of ligand internalization in rat hepatocytes. Cell 1980; 21:79–93.
190. Weigle PH, Oka JA. Endocytosis and degradation mediated by the asialoglycoprotein receptor in isolated rat hepatocytes. J Biol Chem 1982; 257:1201–1207.
191. Kloppel TM, Brown WR, Reichen R. Effects of monensin vesicular transport pathways in the perfused rat liver. J Cell Biochem 1986; 32:235–245.
192. Thomas P, Summers JW. The biliary secretion of circulating asialoglycoproteins in the rat. Biochem Biophys Res Commun 1978; 80:335–339.
193. Finck MH, Reichen J, Vierling JM, et al. Hepatic uptake and disposition of polymeric IgA in the perfused rat liver. Evidence for incomplete biliary excretion and intrahepatic degradation. Am J Physiol 1985; 248:G450–G455.
194. Stone DK, Xie XS, Racker E. An ATP-driven proton pump in clathrin-coated vesicles. J Biol Chem 1983; 258:4059–4062.
195. Yamashiro DJ, Fluss SR, Maxfield FR. Acidification of endocytic vesicles by an ATP-dependent proton pump. J Cell Biol 1983; 97:929–934.
196. Harford J, Bridges K, Ashwell G, et al. Intracellular dissociation of receptor-bound asialoglycoproteins in cultured hepatocytes: a pH-mediated non-lysosomal event. J Biol Chem 1983; 258:3191–3197.
197. Weigle PH, Oka JA. The large intracellular pool of asialoglycoprotein receptors functions during the endocytosis of asialoglycoproteins by isolated rat hepatocytes. J Biol Chem 1983; 258:5095–5102.
198. Hubbard AL, Stukenbrok H. An electron microscope autoradiographic study of the carbohydrate recognition systems in rat liver. II. Intracellular fates of the $^{125}$I-ligands. J Cell Biol 1979; 83:65–81.
199. Weigle PH. Characterization of the asialoglycoprotein receptor on isolated rat hepatocytes. J Biol Chem 1980; 255:6111–6120.
200. Steer CJ, Ashwell G. Studies on a mammalian hepatic binding protein specific for asialoglycoproteins: evidence for receptor recycling in isolated hepatocytes. J Biol Chem 1980; 255:3008–3013.
201. Baenziger JU, Fiete D. Recycling of the hepatocyte asialoglycoprotein receptor does not require delivery of ligand to lysosomes. J Biol Chem 1982; 257:6007–6009.
202. Regoeczi E, Chindemi PA, Debanne MT, et al. Dual nature of the hepatic lectin pathway for human asialotransferrin type 3 in the rat. J Biol Chem 1982; 257:5431–5436.
203. Underdown BJ, Schiff JM, Nagy B, et al. Differences in processing polymeric IgA and asialoglycoproteins by the rat liver. Ann NY Acad Sci 1983; 409:402–410.
204. Nagura H, Nakane PK, Brown WR. Breast milk IgA binds to jejunal epithelium in suckling pets. J Immunol 1978; 120:1333–1337.
205. Buts JP, Delacroix D. Oncogenic changes in secretory component expression by villous and crypt cells of rat small intestine. Immunology 1985; 54:181–187.
206. Ogra SS, Ogra PL, Lippes J, et al. Immunohistologic localization of immunoglobulins, secretory component, and lactoferrin in the developing human fetus. Proc Soc Exp Biol Med 1972; 139:570–574.
207. Brown WR, Isobe Y, Nakane PK. Studies on translocation of immunoglobulins across intestinal epithelium. II. Immunoelectron microscopic localization of immunoglobulins and secretory component in human intestinal mucosa. Gastroenterology 1976; 71:985–995.
208. Ahnen DJ, Nakane PK, Brown WR. Ultrastructural localization of carcinoembryonic antigen in normal intestine and colon cancer. Abnormal distribution of CEA on the surfaces of colon cancer cells. Cancer 1982; 49:2077–2090.
209. Poger ME, Hirsch BR, Lamm ME. Synthesis of secretory component by colonic neoplasms. Am J Pathol 1976; 82:327–339.
210. Rognum T, Brandtzaeg P, Orjasaeter H, et al. Immunohistochemical study of secretory component, secretory IgA and carcinoembryonic antigen in large bowel carcinomas. Pathol Res Pract 1980; 170:126–145.
211. Schmucker DL, Gilbert R, Jones AL, et al. Effect of aging on the hepatobiliary transport of dimeric immunoglobulin A in the male Fischer rat. Gastroenterology 1985; 88:436–443.
212. Daniels CK, Schmucker DL, Jones AL. Age-dependent loss of dimeric immunoglobulin A receptors in the liver of the Fischer 344 rat. J Immunol 1985; 134:3855–3858.
213. Wira CR, Sandoe CP. Sex steroid hormone regulation of IgA and IgG in rat uterine secretions. Nature 1977; 268:534–536.
214. Weisz-Carrington P, Roux ME, McWilliams M, et al. Hormonal induction of the secretory immune system in the mammary gland. Proc Natl Acad Sci USA 1978; 75:2928–2932.
215. McDermott MR, Clark DA, Bienenstock J. Influence of the estrous cycle on B immunoblast migration into genital and intestinal tissues. J Immunol 1980; 124:2536–2539.
216. Sullivan DA, Wira CR. Variations in the levels of free secretory component in rat mucosal secretions. J Immunol 1983; 130:1330–1335.
217. Sullivan DA, Wira CR. Estradiol regulation of secretory component in the female reproductive tract. J Steroid Biochem 1981; 15:439–444.
218. Sullivan DA, Bolch KJ, Allansmith MR. Hormonal influence on the secretory immune system of the eye: androgen regulation of secretory component levels in rat tears. J Immunol 1984; 132:1130–1135.
219. Wira CR, Colby E. Regulation of secretory component by glucocorticoids in primary cultures of rat hepatocytes. J Immunol 1985; 134:1744–1748.
220. Sullivan DA, Underdown BJ, Wira CR. Steroid hormone regulation of free secretory component in the rat uterus. Immunology 1983; 49:379–386.
221. Wira CR, Stern J, Colby E. Estradiol regulation of secretory component in the uterus of the rat: evidence for involvement of RNA synthesis. J Immunol 1984; 133:2624–2628.
222. Sollid DM, Kvale D, Brandtzaeg P, et al. Synthesis of cytoplasmic and functional membrane SC induced by gamma interferon. Adv Exp Med Biol 1987; 216B:1109–1116.
223. Kvale D, Lovhaug D, Sollid LM, et al. Tumor necrosis factor-alpha up-regulates expression of secretory component, the epithelial receptor for polymeric Ig. J Immunol 1988; 140:3086–3089.
224. Rao CK, Kaetzel CS, Lamm ME. Induction of secretory component synthesis in colonic epithelial cells. Adv Exp Med Biol 1987; 216B:1071–1077.
225. Hinton RH, Ah-Sing E, Jones RS, et al. Enterohepatic circulation of IgA does not occur in rats. Biosci Rep 1981; 1:575–580.
226. Seo JK, Grant KE, Sullivan DA, et al. Biliary IgA content following common duct cannulation in the rat. Adv Exp Med Biol 1987; 216B:1133–1138.
227. Goldsmith MA, Jones AL, Underdown BJ, et al. Alterations in protein transport events in rat liver after estrogen treatment. Am J Physiol 1987; 253:G195–G200.
228. Hall J, Orlans E, Reynolds J, et al. Occurrence of specific antibodies of the IgA class in the bile of rats. Int Arch Allergy Appl

15273350, 1989, 5, Downloaded from https://aasldpubs.onlinelibrary.wiley.com/doi/10.1002/hep.1840090518, Wiley Online Library on [11/04/2023]. See the Terms and Conditions (https://onlinelibrary.wiley.com/terms-and-conditions) on Wiley Online Library for rules of use; OA articles are governed by the applicable Creative Commons License

Case 1:23-cv-00328-JLH-SRF Document 125 Filed 02/20/24 Page 49 of 73 PageID #: 4356



Immunol 1979; 59:75–84.
229. Andrew E, Hall JG. IgA antibodies in the bile of rats. I. Some characteristics of the primary response. Immunology 1982; 45:169–175.
230. Andrew E, Hall JG. IgA antibodies in the bile of rats. II. Evidence for immunological memory in secretory immunity. Immunology 1982; 45:177–182.
231. Loftness TJ, Erlandsen SL, Wilson ID, et al. Occurrence of specific secretory immunoglobulin A in bile after inoculation of *Giardia lamblia* trophozoites into rat duodenum. Gastroenterology 1984; 87:1022–1029.
232. Vaerman JP, Derijck-Langendries A, Rits M, et al. Neutralization of cholera toxin by rat bile secretory IgA antibodies. Immunology 1985; 54:601–603.
233. Tamaru T, Brown WR. IgA antibodies in rat bile inhibit cholera toxin-induced secretion in ileal loops in situ. Immunology 1985; 55:579–583.
234. Cooper GN, McNab CE, Walker PG, et al. Intestinal antibodies in rats following exposure to live *Vibrio cholerae*. Aust J Exp Biol Med Sci 1984; 62:465–477.
235. Jackson GDF, Cooper GN. Immune response of rats to live *Vibrio cholerae*: secretion of antibodies in bile. Parasite Immunol 1981; 3:127–135.
236. Montgomery PC, Lemaitre-Coelho IM, Vaerman JP. Molecular diversity of secretory IgA anti-DNP antibodies elicited in rat bile. J Immunol 1980; 125:518–522.
237. Montgomery PC, Lemaitre-Coelho IM, Vaerman JP. The induction and expression of IgA anti-DNP antibodies in rat bile and secretions. Scand J Immunol 1981; 13:587–595.
238. Spencer J, Gyure LA, Hall JG. IgA antibodies in the bile of rats. III. The role of intrathoracic lymph nodes and the migration pattern of their blast cells. Immunology 1983; 48:687–693.
239. Dahlgren UIH, Halstedt S, Hanson LA. The localization of the antibody response in milk or bile depends on the nature of the antigen. J Immunol 1987; 138:1397–1402.
240. Dahlgren U, Ahlstedt S, Andersson T, et al. IgA antibodies in rat bile are not solely derived from thoracic duct lymph. Scand J Immunol 1983; 17:569–574.
241. Manning RJ, Walker PG, Carter L, et al. Studies on the origins of biliary immunoglobulins in rats. Gastroenterology 1984; 87:173–179.
242. Brown PJ, Charley-Poulain J, Pery P. *Nippostrongylus brasiliensis* infection in the rat: 1. Production of bile IgA and serum IgG antibodies by adult rats. Vet Immunol Immunopathol 1981; 2:343–352.
243. Champsaur H, Iscaki S, Bernard O, et al. Induction of *Vibrio cholerae* specific biliary antibodies after oral immunization with a cholera cell wall fraction. Lancet 1985; 1:1276–1277.
244. Keclik M, Wolf RH, Felsenfeld O, et al. Immunoglobulins and antibodies in gallbladder bile. Am J Gastroenterol 1970; 54:19–29.
245. Altorfer J, Hardesty SJ, Scott JH, et al. Specific antibody synthesis and biliary secretion by the rat liver after intestinal immunization with cholera toxin. Gastroenterology 1987; 93:539–549.
246. Strober W, Brown W. The mucosal immune system. In: Samter W, Talmage D, eds. Immunological diseases, Ed. 4. Boston: Little, Brown, 1988: 79–139.
247. Brown WR, Butterfield D, Savage D, et al. Clinical, microbiological, and immunological studies in patients with immunoglobulin deficiencies and gastrointestinal disorders. Gut 1972; 13:441–449.
248. Danon YL, Dinari G, Garty BZ, et al. Cholelithiasis in children with immunoglobulin A deficiency: a new gastrointestinal syndrome. J Pediatr Gastroenterol Nutr 1983; 2:663–666.
249. Kleinman RE, Harmatz PR, Walker WA. The liver: an integral part of the enteric mucosal immune system. Hepatology 1982; 2:379–384.
250. Richter G. IgA mesangial nephropathy. Cont Nephrol 1984; 40:1–3.
251. Van de Wiel A, Valentijn RM, Schuurman HJ, et al. Alcoholic liver disease: an IgA-associated disorder. Scand J Gastroenterol 1987; 22:1025–1030.
252. Wilson ID, Onstad G, Williams RC Jr. Serum immunoglobulin concentrations in patients with alcoholic liver disease. Gastroenterology 1969; 57:59–67.
253. Van de Wiel A, Delacroix DL, van Hattum J, et al. Characteristics of serum IgA and liver IgA deposits in alcoholic liver disease. Hepatology 1987; 7:95–99.
254. Pelletier G, Briantais MJ, Buffet C, et al. Serum and intestinal secretory IgA in alcoholic cirrhosis of the liver. Gut 1982; 23:475–480.
255. Iturriaga H, Pereda T, Estevez A, et al. Serum immunoglobulin A changes in alcoholic patients. Ann Clin Res 1977; 9:39–43.
256. Fukuda Y, Imoto M, Hayakawa T. Serum levels of secretory immunoglobulin A in liver disease. Am J Gastroenterol 1985; 80:237–241.
257. Martin DM, Vroon DH, Nasrallah SM. Value of serum immunoglobulins in the diagnosis of liver disease. Liver 1984; 4:214–218.
258. Kalsi J, Delacroix DL, Hodgson HJ. IgA in alcoholic cirrhosis. Clin Exp Immunol 1983; 52:499–504.
259. Van de Wiel A, van Hattum J, Schuurman H-J, et al. Immunoglobulin A in the diagnosis of alcoholic liver disease. Gastroenterology 1988; 94:457–462.
260. Sancho J, Egido J, Sanchez-Crespo M, et al. Detection of monomeric and polymeric IgA containing immune complexes in serum and kidney from patients with alcoholic liver disease. Clin Exp Immunol 1982; 47:327–335.
261. Delacroix DL, Reynaert M, Pauwels S, et al. High serum levels of secretory IgA in liver disease. Possible liver origin of the circulating secretory component. Dig Dis Sci 1982; 27:333–348.
262. Iscaki S, Buffet C. Secretory IgA increase in sera of patients with liver diseases. Ric Clin Lab 1978; 8:287–291.
263. Homburger HA, Casey M, Jacob GL, et al. Measurement of secretory IgA in serum by radioimmunoassay in patients with chronic nonalcoholic liver disease or carcinoma. Am J Clin Pathol 1984; 81:569–574.
264. Kvale D, Schrumpf E, Brandtzaeg P, et al. Circulating secretory immunoglobulins of the A and M isotypes in chronic liver disease. J Hepatol 1987; 4:229–235.
265. Soppi E, Granfors K, Leino R. Serum secretory IgA, IgA1 and IgA2 subclasses in inflammatory bowel and chronic liver diseases. J Clin Lab Immunol 1987; 23:15–17.
266. Waldman RH, Rowe DS, Mach JP. Secretory IgA levels in serum of patients with various disorders. Clin Med 1973; 80:11–13.
267. Jones AL, Hradek GT, Schmucker DL, et al. The fate of polymeric secretory immunoglobulin A after retrograde infusion into the common bile duct in rats. Hepatology 1984; 4:1173–1183.
268. Van de Wiel A, Seifert WF, Van der Linden JA, et al. Spontaneous IgA synthesis by blood mononuclear cells in alcoholic liver disease. Scand J Immunol 1987; 25:181–187.
269. Nouri-Aria KT, Alexander GJ, Portmann BC, et al. T and B cell function in alcoholic liver disease. J Hepatol 1986; 2:195–207.
270. McKeever U, O'Mahony C, Whelan CA, et al. Helper and suppressor T lymphocyte function in severe alcoholic liver disease. Clin Exp Immunol 1985; 60:39–48.
271. Russell MW, Spotswood MF, Julian BA, et al. Detection of food antigen-specific IgA immune complexes in human sera. Adv Exp Med Biol 1987; 216A:813–820.
272. Volta U, Bonazzi C, Bianchi FB, et al. IgA antibodies to dietary antigens in liver cirrhosis. Ric Clin Lab 1987; 17:235–242.
273. Nolan JP, DeLissio MG, Camara DS, et al. IgA antibody to lipid A in alcoholic liver disease. Lancet 1986; 1:176–179.
274. Staun-Olsen P, Bjorneboe M, Prytz H, et al. *Escherichia coli* antibodies in alcoholic liver disease. Scand J Gastroenterol 1983; 18:889–896.
275. Bjorneboe M, Prytz H, Orskov F. Antibodies to intestinal microbes in serum of patients with cirrhosis of the liver. Lancet 1972; 1:58–60.
276. Triger DR, Wright R. Hypergammaglobulinemia in liver disease. Lancet 1973; 1:1494–1496.
277. Lahnborg G, Friman L, Bergman L. Reticuloendothelial function in patients with alcoholic cirrhosis. Scand J Gastroentero 1981; 16:481–489.
278. Lerner A, Park BH, Rossi TM, et al. Increased serum antibody levels against cow's milk proteins in children with chronic liver disease. Hepatology 1985; 5:488–491.
279. Maekawa M, Sudo K, Kanno T. Characteristics of the complex between alkaline phosphatase and immunoglobulin A in human serum. Clin Chim Acta 1985; 30:185–195.

2573350, 1989, 5, Downloaded from https://aasldpubs.onlinelibrary.wiley.com/doi/10.1002/hep.1840090518, Wiley Online Library on [11/04/2023]. See the Terms and Conditions (https://onlinelibrary.wiley.com/terms-and-conditions) on Wiley Online Library for rules of use; OA articles are governed by the applicable Creative Commons License

DEFS00021191
BTRAC_CP019_000000093

280. Coppo R, Arico S, Piccoli G, et al. Presence and origin of IgA1- and IgA2-containing circulating immune complexes in chronic alcoholic liver diseases with and without glomerulonephritis. Clin Immunol Immunopathol 1985; 35:1–8.
281. Czerkinsky C, Koopman WJ, Jackson S, et al. Circulating immune complexes and immunoglobulin A rheumatoid factor in patients with mesangial immunoglobulin A nephropathies. J Clin Invest 1986; 77:1931–1938.
282. Penner E, Albini B, Milgrom F. Detection of circulating immune complexes in alcoholic liver disease. Clin Exp Immunol 1978; 34:28–31.
283. Artur Y, Wellman-Bednawska M, Jacquier A, et al. Complexes of serum gamma-glutamyltransferase with apolipoproteins and immunoglobulin A. Clin Chem 1984; 30:631–633.
284. Lesavre P, Digeon M, Bach JF. Analysis of circulating IgA and detection of immune complexes in primary IgA nephropathy. Clin Exp Immunol 1982; 48:61–69.
285. Hopf U, Meyer zum Buschenfelde KH, Dierich MP. Demonstration of binding sites for IgG and Fc and the third complement component (C3) on isolated hepatocytes. J Immunol 1976; 117:639–645.
286. Swerdlow MA, Chowdhury LN, Horn T. Patterns of IgA deposition in liver tissues in alcoholic liver disease. Am J Clin Pathol 1982; 77:259–266.
287. Swerdlow MA, Chowdhury LN. IgA subclasses in liver tissues in alcoholic liver disease. Am J Clin Pathol 1983; 80:283–289.
288. Goldin RD, Cattle S, Boylston AW. IgA deposition in alcoholic liver disease. J Clin Pathol 1986; 39:1181–1185.
289. Amano K, Tsukada K, Takeuchi T, et al. IgA deposition in alcoholic liver disease. An immunoelectron microscopic study. Am J Clin Pathol 1988; 89:22–28.
290. Swerdlow MA, Chowdhury LN. IgA deposition in liver in alcoholic liver disease. An index of progressive injury. Arch Pathol Lab Med 1984; 108:416–419.
291. Van de Wiel A, Schuurman HJ, van Riessen D, et al. Characteristics of IgA deposits in liver and skin of patients with liver disease. Am J Clin Pathol 1986; 86:724–730.
292. Sinniah R. IgA mesangial nephropathy: Berger's disease. Am J Nephrol 1985; 5:73–83.
293. Woodroffe AJ. IgA, glomerulonephritis and liver disease. Aust NZ J Med 1981; 11:109–111.
294. Berger J, Yaneva H, Nabarra B. Glomerular changes in patients with cirrhosis of the liver. Adv Nephrol 1977; 7:3–14.
295. Montoliu J, Darnell A, Torras A, et al. Glomerular disease in cirrhosis of the liver: low frequency of IgA deposits. Am J Nephrol 1986; 6:199–205.
296. Lomax-Smith JD, Zabrowarny LA, Howarth GS, et al. The immunochemical characterization of mesangial IgA deposits. Am J Pathol 1983; 113:359–364.
297. Russell MW, Mestecky J, Julian BA, et al. IgA-associated renal diseases: antibodies to environmental antigens in sera and deposition of immunoglobulins and antigens in glomeruli. J Clin Immunol 1986; 6:74–86.
298. Andre C, Berthoux FC, Andre F, et al. Prevalence of IgA2 deposits in IgA nephropathies: a clue to their pathogenesis. N Engl J Med 1980; 303:1343–1346.
299. Bene MC, Faure G, Levy M, et al. Identification de la sous-classe IgA1 et/ou IgA2 des depots mésangiaux d'IgA. Nouv Presse Med 1982; 11:2639–2640.
300. Gormly AA, Smith PS, Seymour AE, et al. IgA glomerular deposits in experimental cirrhosis. Am J Pathol 1981; 104:50–54.
301. Iida H, Izumino K, Matsumoto M, et al. Glomerular deposition of IgA in experimental hepatic cirrhosis. Acta Pathol Jpn 1985; 35:561–567.
302. James SP, Jones EA, Schafer DF, et al. Selective immunoglobulin A deficiency associated with primary biliary cirrhosis in a family with liver disease. Gastroenterology 1986; 90:283–288.
303. Fallon-Friedlander S, Boscamp JR, Morecki R, et al. Immunoglobulin A stimulates growth of the extrahepatic bile duct in BALB/c mice. Proc Natl Acad Sci USA 1987; 84:3244–3248.
304. Delacroix DL, Jonard P, Dive C, et al. Serum IgM-bound secretory component (sIgM) in liver diseases: comparative molecular state of the secretory component in serum and bile. J Immunol 1982; 129:133–138.

15273350, 1989, 5, Downloaded from https://aasldpubs.onlinelibrary.wiley.com/doi/10.1002/hep.1840090518, Wiley Online Library on [11/04/2023]. See the Terms and Conditions (https://onlinelibrary.wiley.com/terms-and-conditions) on Wiley Online Library for rules of use; OA articles are governed by the applicable Creative Commons License

# EXHIBIT 3

Bioconjugate Chemistry

Review

pubs.acs.org/bc

# Well-Defined Multivalent Ligands for Hepatocytes Targeting via Asialoglycoprotein Receptor

Xiangang Huang,[§] Jean-Christophe Leroux,*[,§] and Bastien Castagner*[,‡]

[§]Institute of Pharmaceutical Sciences, Department of Chemistry and Applied Biosciences, ETH Zurich, Vladimir-Prelog-Weg 1-5/10, 8093 Zurich, Switzerland

[‡]Department of Pharmacology and Therapeutics, McGill University, 3655 Prom. Sir-William-Osler, Montréal, Québec H3G 1Y6, Canada

**ABSTRACT:** Targeted delivery of therapeutic agents to hepatocytes is a particularly attractive strategy for the treatment of hepatocellular carcinoma and other liver diseases. The asialoglycoprotein receptor (ASGP-R) is abundantly expressed on hepatocytes and minimally found on extra-hepatic cells, making it an ideal entry gateway for hepatocyte-targeted therapy. Numerous multivalent ligands have been developed to target ASGP-R, among which well-defined multivalent ligands display especially high binding affinity to the receptor. Recently, several gene delivery systems based on such ligands for ASGP-R showed encouraging clinical results, drawing increasing interest in the scientific community and eventually promoting the improvement of current treatment for liver diseases. Here, we review ASGP-R targeting with a special emphasis on well-defined systems and properties such as the linker's length, hydrophilic−hydrophobic balance of the linker, and the spatial geometry of the scaffold. The present manuscript provides important guidelines for the design of multivalent ligands for ASGP-R.

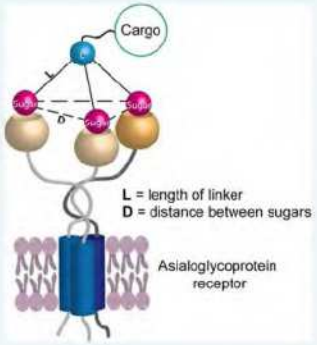


## 1. INTRODUCTION

The liver's role in the metabolism of toxic substances implies that liver cells are frequently exposed to drugs, microbes, and toxic materials that can lead to various liver diseases. Hepatocellular carcinoma (HCC) is the fifth most common neoplasm in the world and the third most mortal cancer.[1,2] Two main types of hepatitis viruses, namely, hepatitis viruses B and C (HBV and HCV), are associated with the development of HCC. HBV infects approximately 2 billion people worldwide and is estimated to result in 320 000 deaths annually,[3] while HCV infection affects about 170 million people worldwide.[4,5] Since HCC and other liver diseases such as fibrosis and cirrhosis[6] mainly affect hepatocytes, targeted delivery of therapeutic agents to these cells is an attractive approach. In order to design hepatocyte-directed delivery system, a target receptor that is abundantly expressed on the surface of hepatocytes but minimally expressed by extrahepatic cells was sought. The asialoglycoprotein receptor (ASGP-R) fits this expression pattern, positioning itself as an ideal target for the delivery of therapeutic agents to hepatocytes.[7]

Monovalent and multivalent ligands have been proposed to target ASGP-R. This Review discusses the design of synthetic multivalent ligands for ASGPR-mediated hepatocyte delivery. Well-defined multivalent ligands are uniquely positioned to inform the design of optimal targeting systems. Here, important properties such as linker length, hydrophilic−hydrophobic balance, and spatial geometry of well-defined ligands will be discussed in detail. In addition, the different synthesis routes of the ligands are presented and compared in terms of synthetic complexity. Monovalent or natural ligand for ASGP-R have been recently reviewed by D'Souza et al.[8] and Ahmed et al.[9] and has thus not been included here.

## 2. ASIALOGLYCOPROTEIN RECEPTOR

**2.1. General Characteristics.** The ASGP-R was the first mammalian lectin to be identified[10] and was originally discovered by Ashwell, Morell, and their co-workers in the 1960s during their studies on the metabolism of plasma glycoproteins in mammals.[11−13] The main function of ASGP-R is to maintain the homeostasis of serum glycoproteins by mediating the recognition and endocytosis of a broad range of desialylated glycoproteins that carry terminal galactose (Gal) or *N*-acetyl galactosamine (GalNAc) residues.[14] These desialylated glycoproteins are endocytosed via clathrin-coated pits, and once in the acidic endosomal compartment they dissociate from the receptor, followed by trafficking to the lysosomes for degradation. Notably, ASGP-R belongs to the recycling receptors group and is endocytosed and recycled constitutively about every 15 min, with or without the ligands.[15−18] The ASGP-R is predominantly expressed on the surface of liver parenchymal cells, which contain $(1-5) \times 10^5$ binding sites per cell.[14,19,20] In addition, ASGP-R plays a role in infectious diseases since viruses like hepatitis A and B, as well as Marburg virus were shown to bind to it, thus facilitating hepatic infections.[21−24]

**2.2. Structure.** The mammalian ASGP-R is composed of two homologous major and minor subunits that are encoded by

Received: November 8, 2016
Revised: December 12, 2016
Published: December 14, 2016

ACS Publications © 2016 American Chemical Society



DOI: 10.1021/acs.bioconjchem.6b00651
Bioconjugate Chem. 2017, 28, 283−295

two distinct genes.[10,25] In humans, the major subunit H1 and the minor subunit H2 are 46 and 50 kDa in size, respectively, and the combination of various ratios of the subunits forms functional homo- and hetero-oligomers with different receptor configurations. Among all the identified configurations of ASGP-R, the trimer composed of two H1 and one H2 is the most abundant one and shows the highest binding affinity to the ligand asialoorosomucoid (ASOR) (Figure 1).[26−35]

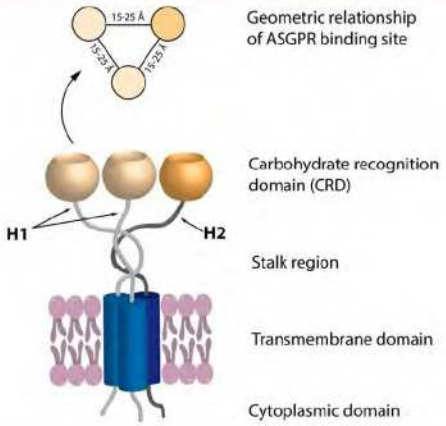


**Figure 1.** Schematic representation of the ASGP-R, illustrating the hetero-oligomer composed of two H1 and one H2 subunit, each of them containing four domains.[42] The geometric relationship of the ASGP-R binding sites is also indicated.[38−41]

Both H1 and H2 are type II single-spanning membrane proteins with 58% sequence identity, and the most relevant difference between them is an 18-amino-acid insert included only in the cytoplasmic domain of H2.[36] The general structure of H1 and H2 subunits includes a 40-amino-acid N-terminal cytoplasmic domain, a ~20-amino-acid single-pass transmembrane domain, an ~80-amino-acid extracellular stalk region, and an ~140-amino-acid functional calcium-dependent carbohydrate recognition domain (CRD) (Figure 1).[37,38] The stalk region, composed of heptad repeats characteristic of $\alpha$-helical coiled-coil structure, mediates the protein oligomerization.[28] Importantly, cell lines expressing only H1 or H2 are unable to bind or internalize the ligand ASOR since the coexpression of both subunits is required for endocytosis of the ligand.[43]

In addition to human, ASGP-R has also been isolated from hepatocytes of other mammals including rabbit,[44] mouse,[45] and rat,[46] although the size and number of subunits that constitute the receptor vary slightly among species. Despite the species-dependent composition of the receptor, the protein sequences for a given subunit are highly conserved and probably originate from the same ancestral gene.[35,36] For example, there is 80% homology between the human H1 and the rat hepatic lectin 1 (RHL1), and 62% between the H2 and the RHL2.[47]

**2.3. Carbohydrate Recognition Domain (CRD).** The carbohydrate recognition domain (CRD) of the ASGP-R subunits belongs to the C-type ($Ca^{2+}$-dependent) superfamily.[48] Most C-type CRDs preferentially bind to D-mannose (Man), D-glucose (Glu) and their derivatives (Man-type ligands), or to D-Gal and its derivatives (Gal-type ligands). The monosaccharide ligands bind to these CRDs by direct coordination to a calcium ion.[49] The first study involving the CRD of ASGP-R was performed by Weis and Kolatkar,[50] where the active site of a related CRD was mutated from a Man-binding protein (MBP) to that of ASGP-R. The mutated protein termed QPDWG was obtained with the mutations $Glu^{185} \rightarrow Gln^{185}$, $Asn^{187} \rightarrow Asp^{187}$, and $His^{189} \rightarrow Trp^{189}$ and the insertion of a Gly-rich loop. The binding specificity for Man was converted to Gal with an affinity almost identical to that of the CRD of ASGP-R. Moreover, NMR measurements revealed similar modes of Gal binding by mutant QPDWG and ASGP-R, confirming that the mutant QPDWG could be used as a model to investigate ligand binding to ASGP-R.[51] This QPDWG mutant was a good model for the binding mode of Gal to ASGP-R, but it could not explain the fact that ASGP-R always displays preferential binding to GalNAc compared to Gal. Therefore, further mutations were performed on QPDWG ($Thr^{202} \rightarrow His^{202}$) to create the mutant QPDWGH for the selective binding of GalNAc.[52] The molecular basis of selective GalNAc recognition by CRD was revealed by the crystal structure of QPDWGH complexed with GalNAc (Figure 2a). The $Ca^{2+}$ binds to the CRD by the coordination to residues $Gln^{185}$, $Asp^{187}$, $Glu^{198}$, $Asn^{210}$, and $Asp^{211}$, and GalNAc binds directly to the $Ca^{2+}$ with its 3-OH and 4-OH groups, replacing two water molecules. In addition, the sugar also forms hydrogen bonds with the residues $Gln^{185}$, $Asp^{187}$, $Glu^{198}$, $Asn^{210}$, and $Asp^{211}$. Furthermore, the apolar face (C3, C4, C5, and C6) of the sugar exhibits hydrophobic interaction with the plane of the side-chain of Trp189. The histidine residue ($His^{202}$) plays a key role by direct coordination with the 2-acetamido methyl group of GalNAc (Figure 2b). This crystallographic analysis of

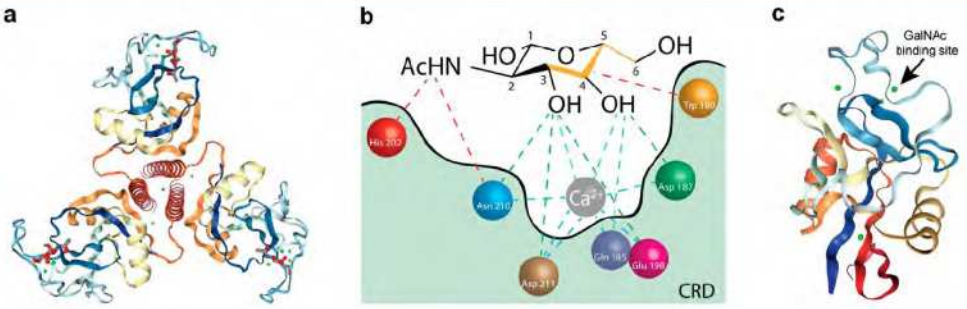


**Figure 2.** (a) QPDWGH mutant of MBP cocrystallized with GalNAc (PDB: 1BCH[52]); calcium is represented by green spheres and GalNAc by the ball and stick model in gray and red. Figure are prepared by NGL Viewer.[53,54] (b) GalNAc binds to the CRD of the QPDWGH mutant of MBP. Coordination and hydrogen bonds are represented by blue and green dashed lines, while the hydrophobic interaction is represented by red dashed lines. Apolar face of GalNAc is depicted in orange.[52] (c) Crystal structure of the H1-CRD, the ligand GalNAc binds to calcium ion from calcium-binding site 2 (PDB: 1DV8[55]). Calcium is represented by the green spheres.



DOI: 10.1021/acs.bioconjchem.6b00651
*Bioconjugate Chem.* 2017, 28, 283−295

GalNAc bound to the CRD of QPDWGH provides a model for the binding mode of GalNAc to ASGP-R.

The first crystal structure of the H1 subunit of the CRD of ASGP-R was determined by Meier et al. (Figure 2c).[55] The CRD contains several calcium-binding sites and the binding site 2 is essential for sugar binding. Although the CRD was cocrystallized with lactose, no lactose ligand was visible at the sugar binding site. Therefore, the straightforward data such as crystal structure of Gal binding to the CRD of ASGP-R are still missing. However, at the sugar binding site, the $Ca^{2+}$ is coordinated to five residues, $Gln^{239}$, $Asp^{241}$, $Glu^{252}$, $Asp^{265}$, and $Asn^{264}$, which are the same residues mediating $Ca^{2+}$ binding to the mutant MBP. Hence, it is reasonable to assume that Gal binding to the CRD of ASGP-R and to the CRD of mutant MBP are likely to happen in an analogous fashion.

## 3. WELL-DEFINED MULTIVALENT LIGANDS FOR ASGP-R

In contrast to a monovalent ligand, multivalent ligands show dramatically enhanced binding affinity toward the ASGP-R. The binding hierarchy of multivalent ligands to the rabbit ASGP-R was tetra- > tri- ≫ bi- ≫ monoantennary according to the half-maximum inhibitory concentration ($IC_{50}$) of $10^{-9}$, $5 \times 10^{-9}$, $10^{-6}$, and $10^{-3}$ M, respectively.[56,57] The addition of sugar beyond triantennary only gave a modest increase of the binding affinity. This is probably related to the fact that the trimer with three sugar-binding sites is the most abundant receptor conformation, as mentioned already.

In the last two decades, multivalent ligands based on different scaffolds have been developed with the aim of achieving optimal ASGP-R targeting.[58−60] Since the sugar binding sites of the receptor are estimated to be 15−25 Å apart in a triangle spatial geometry (Figure 1),[61] properties like linker length, hydrophilic−hydrophobic balance of the linker, and spatial geometry of the scaffold are important factors to consider in the design of multivalent ligands.

**3.1. Bivalent Glycoclusters (BG).** *3.1.1. Length of Linker.* Despite the fact that the most prevalent presentation of the ASGP-R is the trivalent one, simple divalent targeting ligands have been reported, such as the BG1 based on a benzaldehyde scaffold (Figure 3a).[62] A BG1-oligonucleotide conjugate was prepared for the targeted delivery of the transcription factor nuclear erythroid 2-related factor 2 (Nrf2) to the liver. In this conjugate, BG1 enhanced the uptake of oligonucleotides that were bound to the transcription factor, and a hydrophobic membrane-disruptive chain helped the complex escape the endosomes. Indeed, the BG1-oligonucleotide conjugate enhanced the delivery efficiency of the transcription factor to the liver; however, the contribution of BG1 was proved to be low since BG1-oligonucleotide conjugate without the hydrophobic membrane-disruptive chain was unable to delivery Nrf2 in vivo. The generally low targeting effect of BG1 should be ascribed to the short linker. With a linker length of 11 Å, BG1 displays its sugars 17 Å apart from each other, a distance that would seem too short for bivalent binding to ASGP-R (Figure 3b). One advantage of this benzaldehyde scaffold is that the acid-labile acetal linkage between the linker and the backbone can be cleaved at the acidic endosomal pH, exposing the hydrophobic membrane-disruptive domain only upon endocytosis, which was demonstrated to be critical for the delivery efficiency.

To achieve bivalent binding to ASGP-R, BG2 was prepared based on a dimethylglutamate scaffold using a longer linker than the one employed with BG1 (Figure 3a).[63] The length of

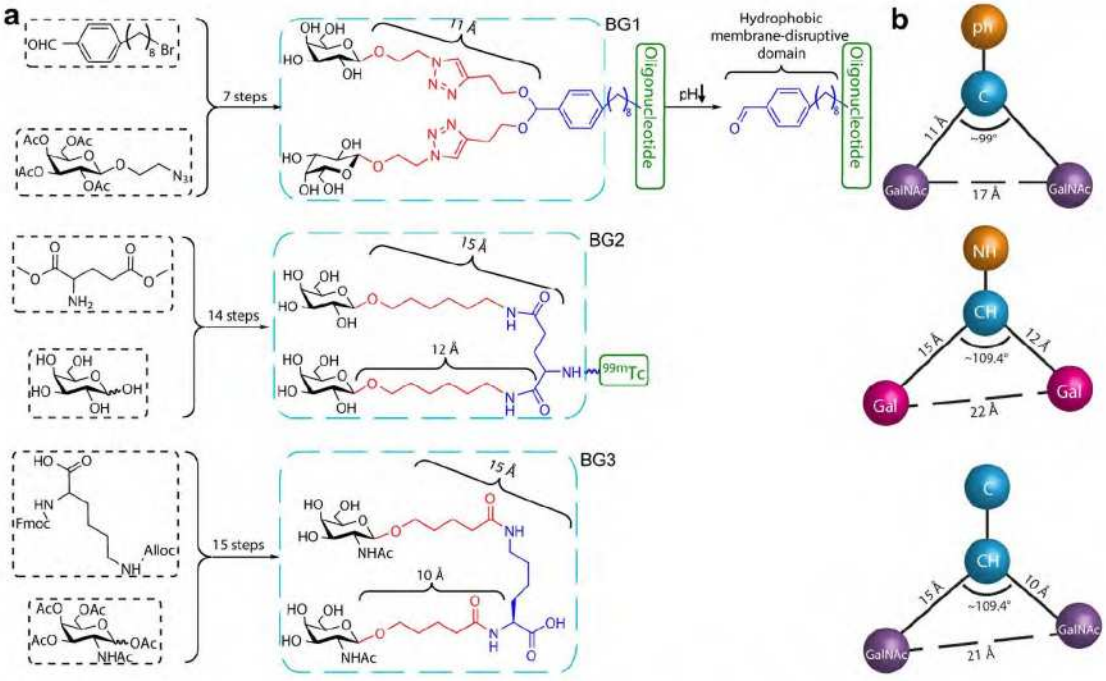


**Figure 3.** (a) BG1: Oligonucleotide-conjugated BG1 was obtained from a benzaldehyde moiety with Ac-Gal-azide in 7 steps.[62] Ac is Acetyl group. BG2: Radionuclide-labeled BG2 was obtained from dimethylglutamate with Gal in 14 steps.[63] BG3: The BG3 was obtained from Fmoc-Lys(Alloc)-OH and Ac-GalNAc in 15 steps.[64] (b) Geometry of the sugar moieties. Using the ChemBio3D 12.0 software, the extended length of the linker ($L$) was estimated through an MM2 molecular mechanics energy minimization and the angle between the two linkers was obtained. The distance between sugars ($D$) was then calculated by applying the cosine rule to triangles.



DOI: 10.1021/acs.bioconjchem.6b00651
Bioconjugate Chem. 2017, 28, 283−295

the linkers of BG2 were 15 and 12 Å, respectively, which separated the sugars 22 Å apart from each other and allowed bivalent binding to ASGP-R (Figure 3b). Indeed, BG2 displayed 10-fold higher binding affinity for the ASGP-R on HepG2 cells compared to a monovalent ligand ($IC_{50}$, 0.47 mM vs >4 mM). The administration of $^{99m}$Tc-labeled BG2 to hepatic fibrosis mice resulted in significantly different pharmacokinetic parameters (derived from microSPECT/CT imaging) compared to the normal mice, whereas no difference was observed for mice injected with $^{99m}$Tc-labeled monovalent ligand.

Another example with an appropriate linker length that achieved bivalent binding effect was BG3, which was based on a lysine scaffold (Figure 3a).[64] BG3 showed high binding affinity ($K_i$ = 30 nM) to ASGP-R in rat hepatocytes, as determined by a competition assay with $^{125}$I-ASOR. The high binding affinity of BG3 is likely due to the fact that the distance between the sugars of 21 Å is appropriate for a bivalent binding mode (Figure 3b). The BG3 was further conjugated to several systems for targeted delivery of the drug antiviral nucleoside phosphonate 9-(2-phosphonylmethoxyethyl)adenine (PMEA)[65] and the antisense peptide nucleic acid (asPNA)[66] to the liver of mice and rats.

*3.1.2. Spatial Geometry of Scaffold.* The effect of the scaffold's spatial geometry on the targeting efficacy to ASGP-R was investigated in a coiled-coil scaffold platform aimed at determining the distances between the sugar-binding sites of ASGP-R.[67] The coiled-coil folding motif was tailored by attaching ligands at specific sites along the axis. Glycopeptides that differed in the number of displayed ligands, their position on the peptide sequence, and the distance between peptide backbone and ligands were prepared. Among the different glycopeptides prepared, BG4 (Figure 4) showed the best targeting potential according to an uptake experiment in HepG2 cells. BG4 had a 14 Å (according to our calculation method, the authors evaluate it at 18 Å) distance between peptide backbone and Gal, and 13 Å in between the functionalized amino acids on the peptide chain. Altering the distance between the peptide backbone and Gal to 0 Å or to 30 Å resulted in a dramatic loss of uptake efficiency. Furthermore, adding a third Gal moiety to BG4 barely changed the uptake efficiency, which was probably due to the fact that the rigid coiled-coil backbone displayed the three Gal in a brush-like geometry that did not match that of ASGP-R. This study showed that the scaffold's geometry should be taken into consideration in the design of multivalent ligands to achieve maximum binding to ASGP-R.

**3.2. Trivalent Glycoclusters (TG).** *3.2.1. Length of Linker.* An elegant study about the influence of the linker length of trivalent glycoclusters on the targeting efficacy to ASGP-R was first conducted by Biessen et al.[59] In this study, a series of trivalent glycoclusters based on Tris scaffold was prepared with various linker lengths for ASGP-R targeting. In a competition assay against $^{125}$I-ASOR for binding to rat parenchymal liver cells, the TG1 with a 20 Å linker (Figure 5) showed the strongest binding affinity ($K_i$ = 200 nM) to ASGP-R. This was at least 2000-fold higher than the TG with a 4 Å linker and 6-fold higher than the TG with a 10 Å linker. This study demonstrated that including a linker of appropriate length between the Gal residues and the branching point of the trivalent glycoclusters was necessary to obtain a high binding affinity to ASGP-R. The TG1 with a linker length of 20 Å displayed its Gal moieties at a distance of 32 Å, thus allowing trivalent binding to ASGP-R. A TG1-cholesterol conjugate was shown to directly associate with both low-density lipoprotein (LDL) and high-density lipoprotein (HDL), and its introduction into $^{125}$I-lipoprotein dramatically accelerated the serum decay and enhanced the liver uptake of these lipoproteins in rats.[68,69] The enhancement of hepatic uptake was probably mediated by ASGP-R, since the uptake decreased by about 80% in the presence of free GalNAc.

A nitro-triacid scaffold-based conjugate (TG2-ASO, Figure 5) was also optimized in terms of linker length, showing a quite promising binding affinity ($K_i$ = 6.2 nM) to primary mouse hepatocytes.[60] One advantage of TG2 was that the use of nitro-triacid scaffold reduced significantly the synthetic complexity. Notably, when the linker length of TG2 was varied in the range of 13−21 Å, the measured binding affinity remained high ($K_i$ = 6.2−10.3 nM), while decreasing it to 10 Å resulted in more than a 2-fold decrease of binding affinity ($K_i$ = 26 nM).

The studies cited showed that there was a minimal linker length required for multivalent binding of trivalent glycoclusters. However, the existence of a maximal linker length remained to be investigated. A lysine scaffold-based TG3 was prepared for targeted delivery of magnetic nanoparticles to HepG2 cancer cells (Figure 5) with one linker of 12 Å and two linkers of 13 Å.[70] Given that TG3 had at least two sugar moieties displayed at a distance of 21 Å, bivalent or trivalent binding to ASGP-R was expected. The uptake of TG3-magnetic nanoparticles by HepG2 was attributed to their interaction with ASGP-R based on the observation that HeLa cells, which do not express ASGP-R, did not internalize the particles. In addition, since the uptake of the TG3-magnetic nanoparticles by HepG2 cells was more efficient than the uptake of particles decorated with monovalent Gal, TG3 was suggested to bind to ASGP-R in a multivalent mode. Prolonging the linker length of TG3 from 13 to 19 Å caused a significant loss of the uptake efficiency. TG3 was also used for targeting delivery of the

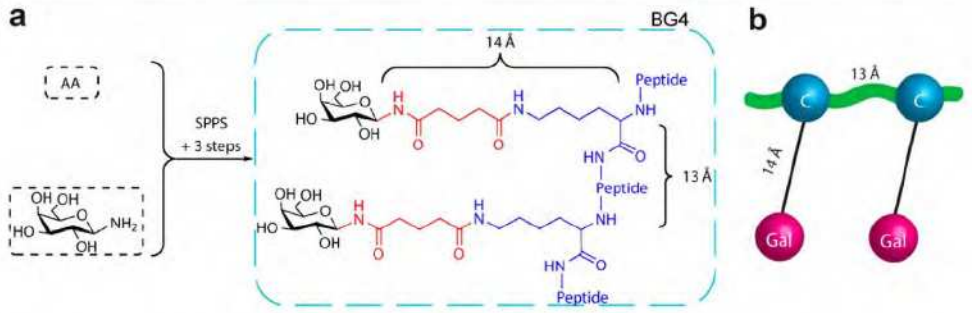


**Figure 4.** (a) Peptide sequence was first produced by solid phase peptide synthesis (SPPS). BG4 was obtained by coupling Gal to the side chains of lysines (at position 3 and position 10) of a peptide sequence, via glutaric anhydride in 3 steps.[67] (b) Geometry of the Gal moieties.



DOI: 10.1021/acs.bioconjchem.6b00651
*Bioconjugate Chem.* 2017, 28, 283−295

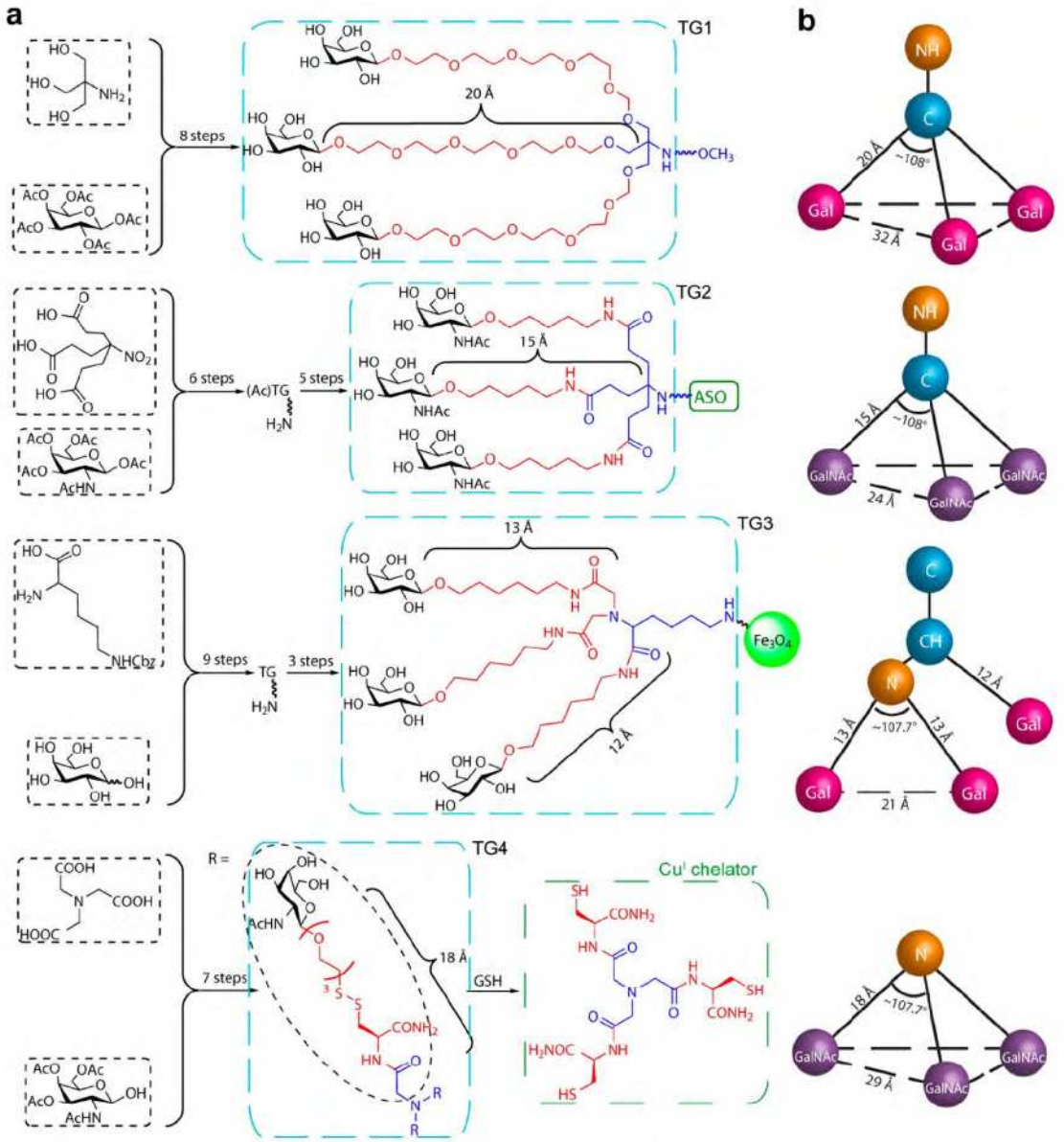


**Figure 5.** (a) (Ac)TG: Acetyl protected TG. TG1: The TG1 was obtained from Tris and Ac-Gal in 8 steps.[59] TG2: (Ac)TG-$NH_2$ was obtained from nitromethanetrispropionic acid (nitro-triacid) and Ac-GalNAc in 6 steps. The coupling of trivalent glycoclusters to ASO finally produced the TG2-ASO conjugates.[60,75] TG3: TG-$NH_2$ was obtained from Z-Lys-OH and Gal in 9 steps, reacting the trivalent glycoclusters to $Fe_3O_4$ nanoparticles produced the final TG3-magnetic ($Fe_3O_4$) nanoparticles.[70] TG4: The TG4 was obtained from nitrilotriacetic acid (triacid) and Ac-GalNAc in 8 steps.[73] In the presence of Glutathione (GSH), the cleavage of disulfide bonds of TG4 produced the functional $Cu^I$ chelator. (b) Geometry of the sugar moieties.

anticancer drug paclitaxel (PTX) to the HepG2 cells.[71] However, in another study where Gal was replaced by GalNAc, the prolongation of the linker from 13 to 16 Å by introducing a glycine lead to a 12-fold increase of the binding affinity to rat hepatocytes.[72] It is possible that a linker length of 19 Å but not of 16 Å would separate the sugars too much from each other, hindering the ligand's multivalent binding to ASGP-R. Therefore, it can be concluded that there is a maximal linker length for multivalent binding of trivalent glycoclusters, which for this asymmetric lysine scaffold-based ligand should be below 19 Å.

One delivery system that benefited from an optimal linker length was a triacid scaffold-based TG4 that was prepared with the aim of specifically decreasing the copper concentration in hepatic cells. Upon its internalization into the hepatic cells via ASGP-R-mediated uptake, TG4 was converted by the reducing agent glutathione (GSH) into an efficient $Cu^I$ chelator, which ultimately decreased the free copper concentration in the hepatic cells (Figure 5).[73] A dye-labeled TG4 was taken up by the ASGP-R-expressing hepatic cells HepG2 and WIF-B9 but not by the ASGP-R-lacking HeLa cells, suggesting an ASGP-R-mediated uptake mechanism. Incubation of TG4 with the WIF-B9 cells containing a high intracellular level of copper ions resulted in dramatic decrease of the copper concentration. To achieve an optimal ASGP-R recognition, the linker of TG4 was designed to be 18 Å in length. Indeed, this length was able to present the three GalNAc moieties approximately 29 Å apart from each other. Monestier et al.[74] further investigated the impact of ligand valency of the chelator on its uptake by



DOI: 10.1021/acs.bioconjchem.6b00651
Bioconjugate Chem. 2017, 28, 283−295

HepG2 cells and found that the uptake of the multivalent chelator was significantly higher than the monovalent one, revealing the multivalent binding mode between the trivalent ligand and ASGP-R. A pentaerythritol scaffold was also used for the preparation of trivalent glycoclusters, but in this case multivalent binding was not expected due to the short linker length.[76,77]

*3.2.2. Hydrophilic–Hydrophobic Balance of Linker.* The influence of the linker's hydrophilic–hydrophobic balance on the targeting effect to ASGP-R was studied by Biessen and co-workers by introducing two important modifications to the linker of TG1.[78] The methylene acetals connecting the linker to Tris were replaced by acid stable ether bonds, and an alkyl chain containing two amide bonds was used for the linker instead of the oligo(ethylene glycol). In a competition experiment with $^{125}$I-ASOR binding to rat parenchymal liver cells, the newly obtained TG5 (Figure 6) showed slightly higher binding affinity ($K_i$ = 93 nM) compared to TG1 ($K_i$ = 200 nM). Replacing the linker of TG5 with a new linker (linker 1, Figure 6) did not change the binding affinity. Moreover, liposomes with 5% (w/w) of TG5-lipid conjugate showed efficient liver uptake in mice, and since preinjection with asialofetuin nearly completely inhibited the uptake, the liposomes were proposed to be recognized by ASGP-R. Therefore, trivalent glycoclusters containing a hydrophilic–hydrophobic balanced linker, such as an alkyl chain with two amides, bind more strongly to ASGP-R than trivalent glycoclusters containing very hydrophilic linkers like oligo(ethylene glycol). Different reasons could account for this. For instance, it is possible that the hydrophobic linker would enhance the interactions between the linker and the protein surface. Alternatively, the hydrophilic linker could form aggregates and therefore suppress the multivalent binding.[79–81]

Early work established that the binding affinity of trivalent glycoclusters toward ASGP-R could be greatly improved by up to 60-fold in rat hepatocytes by replacing the Gal moieties for GalNAc.[82] Based on these findings, Biessen and co-workers[83] modified TG5 and generated a new GalNAc-terminated TG6 (Figure 6) that displayed 50-fold higher binding affinity ($K_i$ = 2 nM) to ASGP-R compared to TG5. The linker of TG6 contained a short oligo(ethylene glycol) chain and an amide bond, which provided a new option for preparing the hydrophilic–hydrophobic balanced linker. A TG6-lipid conjugate was able to associate with plasma lipoproteins, and intravenous injection of this glycolipid containing lipoproteins lead to an efficient dose-dependent uptake of lipoproteins by the liver. The involvement of ASGP-R in the uptake was confirmed by competition experiments performed with preinjection of asialoorosomucoid, which significantly inhibited the uptake of TG6-lipid conjugate. In addition, intravenous injection of the TG6-lipid conjugate to hyperlipidemic low-density lipoprotein receptor-deficient mice resulted in an efficient cholesterol-lowering effect.

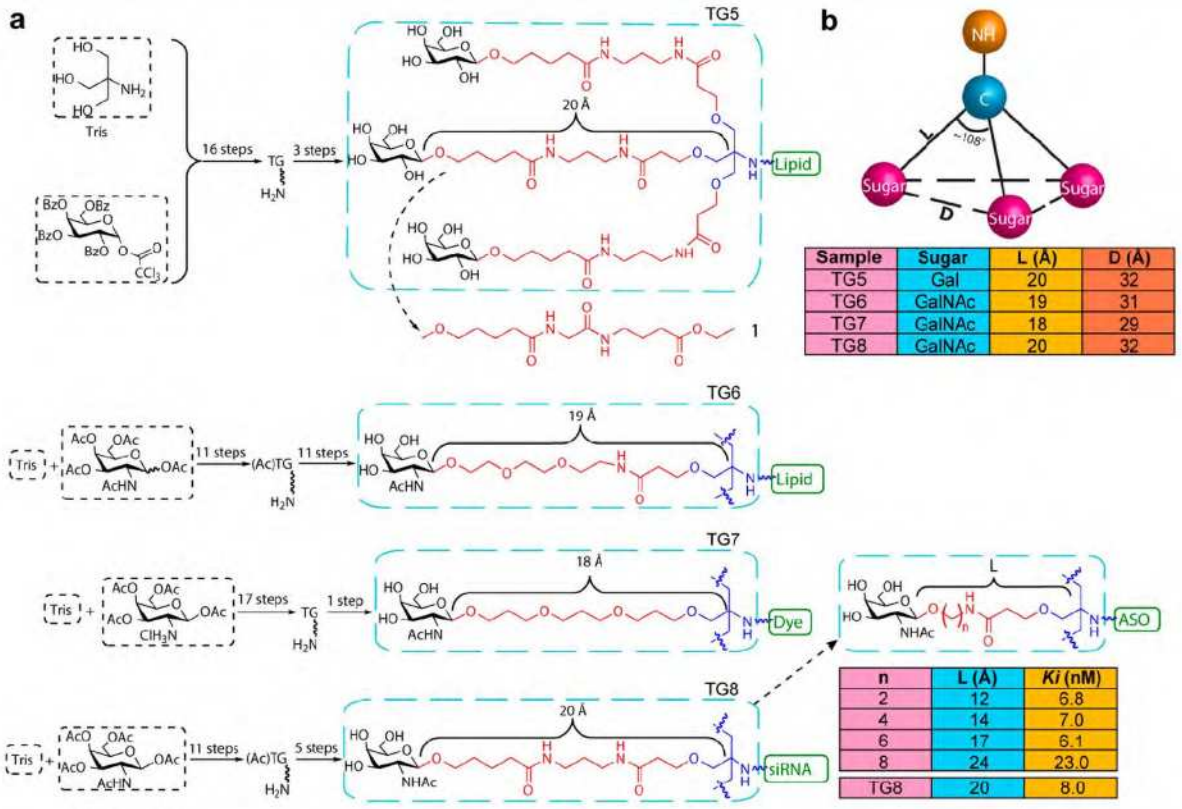


**Figure 6.** (a) TG5: (Ac)TG-$NH_2$ was obtained from Tris and Bz-Gal in 16 steps; the coupling of trivalent glycoclusters to the lipid gave the final TG5-lipid conjugates.[78] TG6: (Ac)TG-$NH_2$ was obtained from Tris and Ac-Gal in 11 steps. The coupling of trivalent glycoclusters to the lipid gave TG6-lipid conjugates.[86] TG7: (Ac)TG-$NH_2$ was obtained from Tris and Ac-Gal in 17 steps, coupling the trivalent glycoclusters to the dye gave the final fluorescently labeled TG7.[42] TG8: (Ac)TG-$NH_2$ was obtained from Tris and Ac-GalNAc in 11 steps, coupling the trivalent glycoclusters to siRNA produced the final TG8-siRNA conjugates.[85] The binding affinity of TG8-ASO conjugates with various linker lengths for ASGP-R is reported in the inset table.[60] (b) Geometry of the sugar moieties.



DOI: 10.1021/acs.bioconjchem.6b00651
*Bioconjugate Chem.* 2017, 28, 283–295

DEFS00020364

Another attempt to optimize the hydrophilic−hydrophobic balance of the linker was carried out by Ernst and co-workers,[42] who replaced the more frequently used ethylene glycol-based linker by a propylene glycol-based linker regarded as a good combination of flexibility and hydrophilic−hydrophobic balance. The obtained TG7 (Figure 6) had linker length of 18 Å and distance between the sugars of 29 Å. The fluorescently labeled TG7 was selectively internalized by HepG2 via ASGP-R, as demonstrated by fluorescence microscopy and flow cytometry analysis. However, it is difficult to compare TG7 with other ligands since its binding affinity to ASGP-R was not measured.

Finally, Alnylam Pharmaceuticals developed a new TG8 which was described in a 2012 patent[84] and was quite similar to TG5 except for the inclusion of GalNAc instead of Gal (Figure 6).[85] The binding affinity of TG8 to ASGP-R on freshly isolated mouse hepatocytes was quite strong ($K_d$ = 2.3 nM), as determined by flow cytometry.[87] Its efficacy was demonstrated using TG8-decorated ionizable lipid nanoparticles.[88]

In addition to the TG8-lipid nanoparticles, a TG8-siRNA conjugate is also under investigation at Alnylam Pharmaceuticals. The conjugation of TG8 to siRNA remarkably increased the uptake of siRNA by primary mouse hepatocytes.[85] This enhanced uptake was largely inhibited in the presence of free TG8 or the calcium binder EGTA (ethylene glycol-bis(β-aminoethyl ether)-*N,N,N′,N′*-tetraacetic acid), indicating that the uptake was mediated by specific binding of the TG8 ligand to ASGP-R. The ability of the TG8-siRNA to silence gene expression was further evaluated in vivo using a siRNA that specifically targeted rodent TTR. Upon subcutaneous administration of a single 25 mg/kg dose to mice, more than 80% TTR mRNA in the liver was suppressed after 24 h. Chronic weekly administration of the conjugates over 9 months resulted in sustained dose-dependent gene silencing without any adverse effect in rodents. Based on TG8-siRNA conjugate, a nucleic acid drug under the name of ALN-PCSsc for the treatment of hypercholesterolemia showed promising results in phase 1 and phase 2 clinical trials (NCT02314442, NCT02963311). In addition to the conjugate and targeted nanoparticle formulation described earlier, a series of TG8-based nucleic acid drugs are currently under development at Alnylam Pharmaceuticals for the treatment of rare diseases, cardiovascular and metabolic diseases, and hepatic infectious diseases. Thus, the TG8 is currently the most advanced trivalent ligand for ASGP-R targeting.

Due to the robust ASGP-R-targeting effect of TG8, the ligand was also used for the delivery of short interfering ribonucleic neutrals (siRNN),[89] antisense oligonucleotides (ASO),[90] and anti-microRNA therapeutics[91] to the liver of mice and humans. Interestingly, altering the linker length of a TG8-ASO conjugate in the range of 12−20 Å showed a high binding affinity ($K_i$ = 6.2−8.0 nM), while introducing a longer hydrophobic alkyl chain (27 Å) resulted in almost a 3-fold decrease of binding affinity ($K_i$ = 23 nM) (Figure 6).[60] This loss of binding affinity could be ascribed to the hydrophobicity of the scaffold, which would disrupt the hydrophilic−hydrophobic balance.

The effect of the linker's hydrophilic−hydrophobic balance on the targeting effect of trivalent glycoclusters was also studied in a lysine scaffold-based system. TG9 (Figure 7) showed very strong binding affinity ($K_i$ = 4 nM) to ASGP-R on rat hepatocytes, as determined by a competition assay with $^{125}$I-ASOR. In this system, the replacement of GalNAc by Gal also caused a significant decrease of the binding affinity ($K_i$ = 650 nM).[64] In an early study, Gal and oligo(ethylene glycol) linker were used instead of GalNAc and alkyl linker, but this early version of TG9 only showed micromolar binding affinity,[92,93] demonstrating once again that a more hydrophobic linker resulted in enhanced affinity.

*3.2.3. Spatial Geometry of Scaffold.* The scaffolds of trivalent glycoclusters need to have an appropriate spatial geometry that matches the one of ASGP-R in order to achieve trivalent binding. This was illustrated by the BG4 ligand discussed before, where the addition of a third Gal moiety barely changed the uptake efficiency due to the brush-like geometry that did not match that of ASGP-R. In 1987, Lee and co-workers[94] used a glutamic acid-based scaffold to produce the multivalent ligand TG10 for ASGP-R (Figure 8). The binding affinity of TG10 to ASGP-R of rat hepatocytes was in the subnanomolar level ($IC_{50}$ = 0.2 nM) as determined by an inhibition assay with $^{125}$I-ASOR. The removal of one GalNAc residue from TG10 caused a 15-fold decrease of the binding affinity to ASGP-R, suggesting a trivalent binding mode for TG10. In a later study, a lower binding affinity was obtained for TG10 ($IC_{50}$ = 10 nM), according to a modified inhibition assay in which Eu-labeled ASOR was employed instead of $^{125}$I-ASOR and surface-immobilized hepatocytes were used instead of suspended ones.[72] The binding affinity of TG10 was 10-fold lower than that of the new version of TG3 (GalNAc, 16 Å),

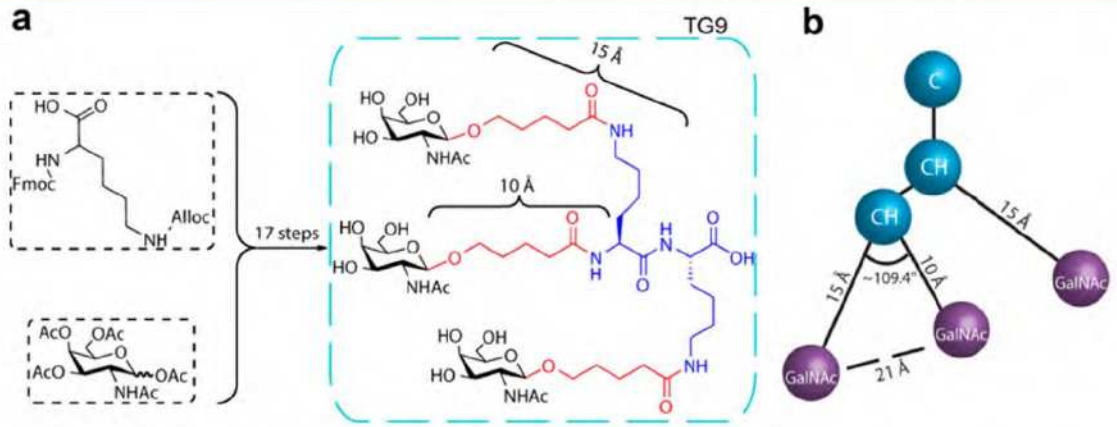


**Figure 7.** (a) TG9 was obtained from Fmoc-Lys(Alloc)-OH and Ac-GalNAc in 17 steps.[64] (b) Geometry of the sugar moieties.



DOI: 10.1021/acs.bioconjchem.6b00651
*Bioconjugate Chem.* 2017, 28, 283−295

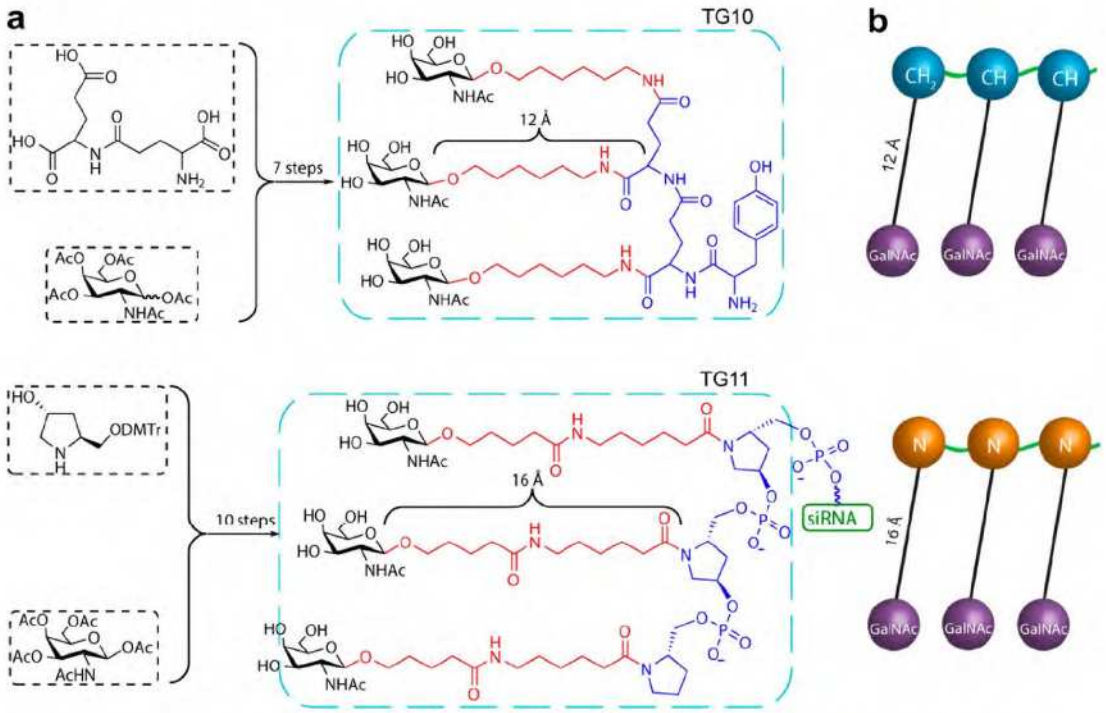


**Figure 8.** (a) TG10: TG10 was obtained from γ-L-glutamyl-L-glutamic acid and Ac-GalNAc in 7 steps.[94] TG11: TG11-siRNA conjugates were obtained from hydroxyprolinol and Ac-GalNAc in 10 steps.[95] (b) Geometry of the sugar moieties.

which was likely related to the brush-like geometry of the scaffold that did not fit the triangle geometry of ASGP-R, therefore hinders TG10 from reaching the maximal binding affinity to ASGP-R. TG10 was then used for targeting delivery of several nucleic acid drugs to hepatocytes.[58,96−98] Lee and co-workers also made an attempt to replace the glutamic acid scaffold with other amino acids such as aspartic acid. The new aspartic acid scaffold-based trivalent glycocluster displayed a similar binding affinity to the TG10,[99] which is not surprising since the spatial geometry was in fact the same for both ligands.

More recently, Alnylam Pharmaceuticals attempted to produce several ligands based on TG8 with brush-like spatial geometry, but unfortunately none of them could further improve the binding of TG8. Hydroxyprolinol scaffold-based TG11 was one of these ligands produced. A TG11-siRNA conjugate was prepared for hepatocyte-specific delivery in which GalNAc was conjugated to the 3′-end of the sense strand of the siRNA by a phosphodiester linkage (Figure 8).[95] Compared to the previously reported TG8-siRNA conjugates (optimal range of linker length: 12−20 Å), TG11-siRNA had the same optimal sugar valency and was in the same optimal range of linker length, but required fewer synthetic steps (10 steps vs 15 steps). In a fluorescence-based assay, the binding affinity of TG11-siRNA ($K_i$ = 37.6 nM) to primary mouse hepatocytes was demonstrated to be 2-fold lower than that of the TG8-siRNA ($K_i$ = 18.9 nM). In conclusion, although TG11 implied a lower synthetic complexity, it also displayed lower binding affinity to ASGP-R compared to TG8, which was probably because the brush-like geometry of the scaffold did not fit that of ASGP-R. Similarly, trivalent glycoclusters based on nucleosides also failed to outperform TG8 in terms of binding affinity. These trivalent glycoclusters displayed GalNAc in a row along the scaffold with a similar spatial geometry as TG11.[100] Therefore, the brush-like geometry of the ligand scaffold would not be the ideal one, and optimal binding effect was usually achieved by ligands with the triangular geometry.

**3.3. Tetravalent Glycoclusters (TeG).** *3.3.1. Valency.* The effect of valency on the binding affinity of multivalent ligands to ASGP-R was first studied by Lee et al.[56] in an inhibition experiment, which demonstrated that the binding affinity to rabbit ASGP-R increased dramatically from monovalent to trivalent ligand, but only slightly from trivalent to tetravalent ligand. More recently, the effect of valency was studied in a cyclic peptide scaffold-based system. TeG1 was prepared with the aim of selectively decreasing copper concentration in hepatocytes (Figure 9),[101] and it displayed a controlled conformation with the upper face presenting a cluster of ligands for the ASGP-R targeting and the lower face presenting thiolates for copper complexation. Experiments in hepatic cell lines demonstrated that TeG1 was internalized by the HepG2 and WIF-B9 cells after as early as 2 h incubation time, and that it was able to lower the free intracellular copper concentration. The removal of one sugar moiety from TeG1 only resulted in less than 2-fold decease of binding affinity to ASGP-R.[74] Therefore, the contribution of the fourth sugar moiety of tetravalent glycoclusters on the binding affinity was very low, which would be expected given the fact that ASGP-R with 3 binding sites is the most prevalent configuration.

*3.3.2. Anomeric Carbon Configuration of Sugar.* The impact of the anomeric carbon configuration (α and β) of the sugar on the uptake by hepatic cells was also studied by Monestier et al.[74] (Figure 9), revealing no significant difference between the uptake efficiency of tetravalent glycoclusters bearing β-GalNAc and α-GalNAc.

**3.4. Other Multivalent Glycoclusters (MG).** *3.4.1. Multivalency.* Dendrimer[103,104] and polymer-based scaffolds have been widely used to prepare multivalent ligands to target ASGP-R. These ligands with high valency display enhanced



DOI: 10.1021/acs.bioconjchem.6b00651
Bioconjugate Chem. 2017, 28, 283−295

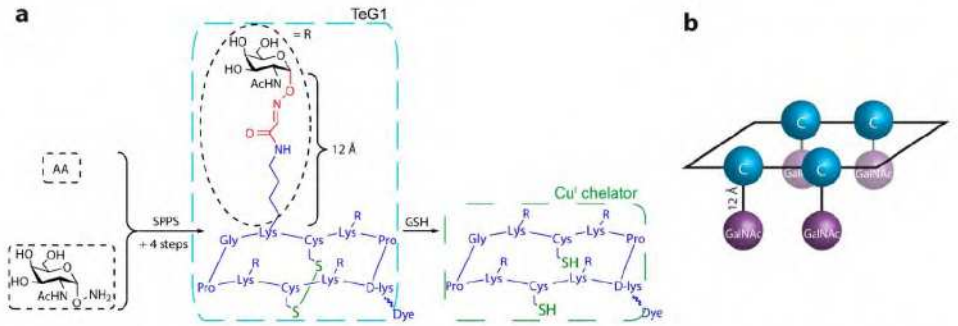


**Figure 9.** (a) Cyclic peptide was first prepared by multisteps of SPPS from amino acids (AA), and then the TeG1 was obtained by coupling GalNAc to the side chains of lysines.[101] In the presence of glutathione (GSH), the cleavage of the disulfide bonds of TeG1 released the functional $Cu^{I}$ chelator. (b) Geometry of the GalNAc moieties.

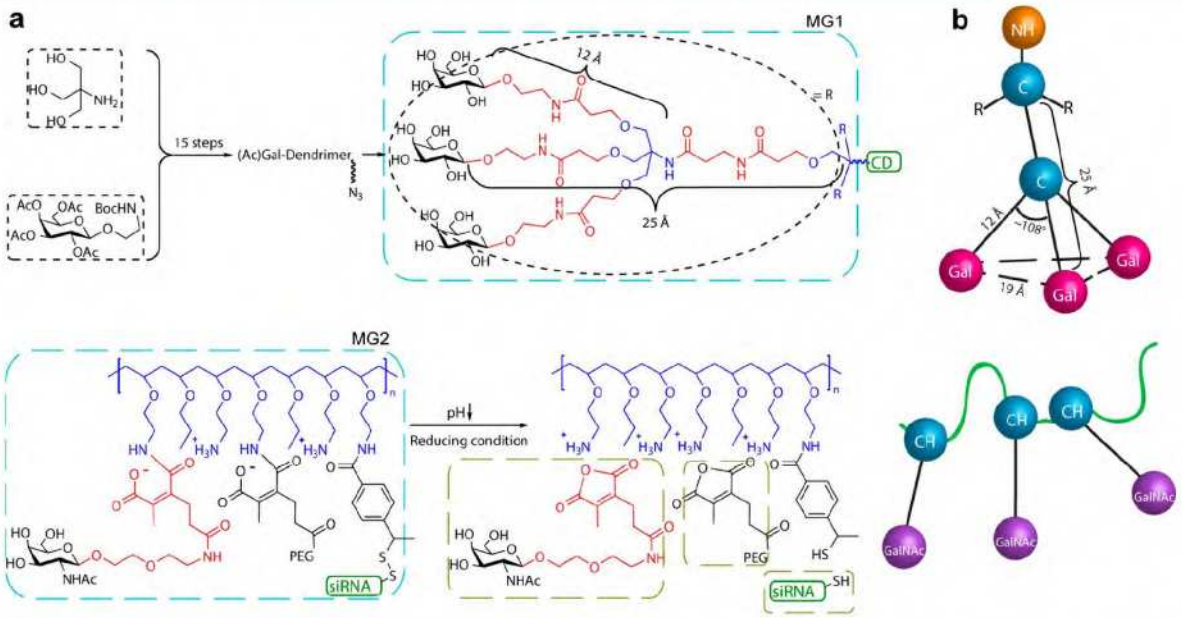


**Figure 10.** (a) MG1: Ac-Gal dendrimer was prepared from Tris and Ac-Gal in 15 steps, then MG1-$\beta$-cyclodextrin ($\beta$CD) conjugate was obtained by coupling the dendrimer to $\beta$CD.[102] MG2: Dynamic polyconjugates MG2. The synthesis route of DPC has not been described in detail in the literature, probably because this system is proprietary technology.[106] (b) Geometry of the sugar moieties.

binding activity compared to the corresponding monovalent ligands, a phenomenon termed "cluster glycoside effect".[79] MG1-$\beta$-cyclodextrin ($\beta$CD) conjugate is a dendrimer scaffold-based platform for targeted delivery of drugs to hepatocytes (Figure 10a).[102] In an uptake experiment with HepG2 cells, the rhodamine B-loaded MG1-$\beta$CD displayed significantly enhanced uptake efficiency compared to the Man-functionalized $\beta$CD control. From a structural point of view, MG1 can be considered as a combination of 3 trivalent glycoclusters with a 12-Å-long linker that can separate the sugars 19 Å apart, enabling a multivalent binding mode (Figure 10b). However, it was not clear whether the targeting effect resulted from single trivalent glycoclusters or from the synergistic effect of 3 trivalent glycoclusters. Therefore, it would be interesting to compare the uptake of MG1-$\beta$CD with a single trivalent glycocluster-$\beta$CD conjugate to investigate the impact of multivalency.[103,104]

One of the most clinically advanced polymer scaffold-based systems for ASGP-R targeting is the dynamic polyconjugate MG2 (Figure 10),[105] which was prepared with the aim of treating liver diseases by targeting hepatocytes with GalNAc ligands. The MG2 contained a membrane-disrupting polymer PBAVE (polyconjugate of butyl and amino vinyl ethers), a shielding polymer PEG, a targeting ligand GalNAc, and a therapeutic siRNA, which were reversibly conjugated to the backbone polymer PBAVE. Upon GalNAc-mediated cellular uptake and subsequent exposure to the low pH of endosomes and the reducing conditions of cytosol, the reversible bonds in the polyconjugate would break, releasing the siRNA into the cytoplasm of the target cell. MG2 proved to be able to deliver siRNA to hepatocytes in vitro and in mice, probably thanks to the cluster glycoside effect since MG2 has high ligand valency. In this case, it would be very interesting to investigate the binding affinity of MG2 to ASGP-R, so that it can be compared with the well-defined trivalent ligands, which are already at the nanomolar level. A drug candidate ARC-520 based on a new generation of MG2 is being developed by Arrowhead Research Corporation for the treatment of Hepatitis B disease, and is currently in Phase 2 clinical trials (NCT02065336). In this new generation of MG2, two important chemical modifications were introduced, the original backbone PBAVE was replaced with melittin-like peptide (MLP), siRNA cargo was modified with cholesterol but not covalently linked to the backbone.



DOI: 10.1021/acs.bioconjchem.6b00651
Bioconjugate Chem. 2017, 28, 283−295

In the end, the MLP-modified MG2 and cholesterol-modified siRNA were coinjected to the animals or humans.[107]

## 4. SUMMARY AND OUTLOOK

The type of sugar used in the multivalent ligands was found to play an important role in the binding to ASGPR. The monovalent GalNAc showed a 60-fold stronger binding affinity to ASGP-R than Gal,[82] similarly to what was observed for multivalent ligands where replacing the Gal with GalNAc remarkably enhanced the binding affinity. Interestingly, although the impact of the sugar's anomeric carbon configuration on the interaction with ASGP-R was rarely reported, the $\beta$ configuration was predominantly used for multivalent ligands. However, a recent study found that this was not a significant parameter. In contrast, the length of the linker was found to be the most decisive factor for the binding affinity of the multivalent ligands to ASGP-R. Since the sugar binding sites of ASGP-R are estimated to be 15−25 Å apart, the ideal linker should display the ligands within this range of distance to prevent the loss of binding affinity. Indeed, numerous published studies confirmed that optimal binding affinity was obtained when the distance between the sugars was 19−32 Å. Another property that has been investigated in detail is the hydrophilic−hydrophobic balance of the linker. In early studies, hydrophilic linkers such as oligo(ethylene glycol) were often chosen, but these were deemed suboptimal after more recent studies revealed that ligands containing linkers with appropriate hydrophilic−hydrophobic balance displayed better binding affinity to ASGP-R. In addition, the compatibility between the scaffold's spatial geometry and that of the ASGP-R was found to be an important factor in achieving a strong binding (Figure 1). This would explain why many attempts to make brush-like geometry of the sugar ligands failed to obtain optimal binding affinities. So far, the best fitting geometry of the sugar ligands proved to be the symmetric or asymmetric triangle with a side length between 19 and 32 Å.

The parameters that were highlighted in this Review are of crucial importance for the design of a multivalent ligand for efficient ASGP-R targeting. It is very encouraging to see that several gene delivery systems associated with the multivalent ligands for liver diseases targeting are undergoing clinical trials. The success of these systems will prompt the scientific community to generate multivalent ligands, with increasingly higher binding affinity and less synthetic complexity. The experience and knowledge obtained from the design and preparation of the multivalent ligands for ASGP-R should provide a guide for the synthesis of multivalent ligand for other receptors.

## AUTHOR INFORMATION


### Corresponding Authors

*E-mail: jleroux@ethz.ch.

*E-mail: bastien.castagner@mcgill.ca.

### ORCID

Xiangang Huang: 0000-0001-8948-7879


### Notes

The authors declare no competing financial interest.

## ACKNOWLEDGMENTS

This work was supported by a China Scholarship Council (CSC) (No. [2012]3013) scholarship to X.G. Huang and a NSERC discovery grant (RGPIN-2015-05364). B.C. is supported by a Canada Research Chair in Therapeutic Chemistry. The authors would like to acknowledge Jong Ah Kim for reading the manuscript.

## REFERENCES


(1) Llovet, J. M., Burroughs, A., and Bruix, J. (2003) Hepatocellular carcinoma. *Lancet 362*, 1907−1917.

(2) Farazi, P. A., and DePinho, R. A. (2006) Hepatocellular carcinoma pathogenesis: from genes to environment. *Nat. Rev. Cancer 6*, 674−687.

(3) Lavanchy, D. (2004) Hepatitis B virus epidemiology, disease burden, treatment, and current and emerging prevention and control measures. *J. Viral Hepat. 11*, 97−107.

(4) Chisari, F. V. (2005) Unscrambling hepatitis C virus-host interactions. *Nature 436*, 930−932.

(5) de Jong, Y. P., Rice, C. M., and Ploss, A. (2011) Evaluation of combination therapy against hepatitis C virus infection in human liver chimeric mice. *J. Hepatol. 54*, 848−850.

(6) Eisenberg, C., Seta, N., Appel, M., Feldmann, G., Durand, G., and Feger, J. (1991) Asialoglycoprotein receptor in human isolated hepatocytes from normal liver and its apparent increase in liver with histological alterations. *J. Hepatol. 13*, 305−309.

(7) Poelstra, K., Prakash, J., and Beljaars, L. (2012) Drug targeting to the diseased liver. *J. Controlled Release 161*, 188−197.

(8) D'Souza, A. A., and Devarajan, P. V. (2015) Asialoglycoprotein receptor mediated hepatocyte targeting-Strategies and applications. *J. Controlled Release 203*, 126−139.

(9) Ahmed, M., and Narain, R. (2015) Carbohydrate-based materials for targeted delivery of drugs and genes to the liver. *Nanomedicine 10*, 2263−2288.

(10) Weigel, P. H., and Yik, J. H. (2002) Glycans as endocytosis signals: the cases of the asialoglycoprotein and hyaluronan/chondroitin sulfate receptors. *Biochim. Biophys. Acta, Gen. Subj. 1572*, 341−363.

(11) Ashwell, G., and Harford, J. (1982) Carbohydrate-specific receptors of the liver. *Annu. Rev. Biochem. 51*, 531−554.

(12) Ashwell, G., and Morell, A. G. (2006) The role of surface carbohydrates in the hepatic recognition and transport of circulating glycoproteins. *Adv. Enzymol. Relat. Areas Mol. Biol. 41*, 99−128.

(13) Morell, A. G., Irvine, R. A., Sternlieb, I., Scheinberg, I. H., and Ashwell, G. (1968) Physical and chemical studies on ceruloplasmin V. Metabolic studies on sialic acid-free ceruloplasmin in vivo. *J. Biol. Chem. 243*, 155−159.

(14) Hubbard, A. L., Wilson, G., Ashwell, G., and Stukenbrok, H. (1979) An electron microscope autoradiographic study of the carbohydrate recognition systems in rat liver. I. Distribution of $^{125}$I-ligands among the liver cell types. *J. Cell Biol. 83*, 47−64.

(15) Spiess, M. (1990) The asialoglycoprotein receptor: a model for endocytic transport receptors. *Biochemistry 29*, 10009−10018.

(16) Geffen, I., and Spiess, M. (1993) Asialoglycoprotein receptor. *Int. Rev. Cytol. 137*, 181−181.

(17) Schwartz, A., Fridovich, S., and Lodish, H. (1982) Kinetics of internalization and recycling of the asialoglycoprotein receptor in a hepatoma cell line. *J. Biol. Chem. 257*, 4230−4237.

(18) Bider, M. D., and Spiess, M. (1998) Ligand-induced endocytosis of the asialoglycoprotein receptor: evidence for heterogeneity in subunit oligomerization. *FEBS Lett. 434*, 37−41.

(19) Weigel, P., and Oka, J. (1983) The large intracellular pool of asialoglycoprotein receptors functions during the endocytosis of asialoglycoproteins by isolated rat hepatocytes. *J. Biol. Chem. 258*, 5095−5102.

(20) Monroe, R. S., and Huber, B. E. (1994) The major form of the murine asialoglycoprotein receptor: cDNA sequence and expression in liver, testis and epididymis. *Gene 148*, 237−244.

(21) Dotzauer, A., Gebhardt, U., Bieback, K., Göttke, U., Kracke, A., Mages, J., Lemon, S. M., and Vallbracht, A. (2000) Hepatitis A virus-specific immunoglobulin A mediates infection of hepatocytes with hepatitis A virus via the asialoglycoprotein receptor. *J. Virol. 74*, 10950−10957.




DOI: 10.1021/acs.bioconjchem.6b00651
*Bioconjugate Chem.* 2017, 28, 283−295

(22) Treichel, U., Meyer zum Büschenfelde, K.-H., Stockert, R. J., Poralla, T., and Gerken, G. (1994) The asialoglycoprotein receptor mediates hepatic binding and uptake of natural hepatitis B virus particles derived from viraemic carriers. *J. Gen. Virol. 75*, 3021−3029.
(23) Becker, S., Spiess, M., and Klenk, H.-D. (1995) The asialoglycoprotein receptor is a potential liver-specific receptor for Marburg virus. *J. Gen. Virol. 76*, 393−399.
(24) Treichel, U., zum Büschenfelde, K.-H. M., Dienes, H.-P., and Gerken, G. (1997) Receptor-mediated entry of hepatitis B virus particles into liver cells. *Arch. Virol. 142*, 493−498.
(25) Paietta, E., Stockert, R., and Racevskis, J. (1992) Alternatively spliced variants of the human hepatic asialoglycoprotein receptor, H2, differ in cellular trafficking and regulation of phosphorylation. *J. Biol. Chem. 267*, 11078−11084.
(26) Grewal, P. K. (2010) Chapter Thirteen-The Ashwell-Morell Receptor, in *Methods in Enzymology* (Minoru, F., Ed.) pp 223−241, Academic Press.
(27) Bider, M. D., Cescato, R., Jenö, P., and Spiess, M. (1995) High-affinity ligand binding to subunit H1 of the asialoglycoprotein receptor in the absence of subunit H2. *Eur. J. Biochem. 230*, 207−212.
(28) Bider, M. D., Wahlberg, J. M., Kammerer, R. A., and Spiess, M. (1996) The oligomerization domain of the asialoglycoprotein receptor preferentially forms 2:2 heterotetramers in vitro. *J. Biol. Chem. 271*, 31996−32001.
(29) Braiterman, L. T., Chance, S., Porter, W., Lee, Y., Townsend, R., and Hubbard, A. (1989) The major subunit of the rat asialoglycoprotein receptor can function alone as a receptor. *J. Biol. Chem. 264*, 1682−1688.
(30) Hardy, M. R., Townsend, R. R., Parkhurst, S., and Lee, Y. C. (1985) Different modes of ligand binding to the hepatic galactose/N-acetylgalactosamine lectin on the surface of rabbit hepatocytes. *Biochemistry 24*, 22−28.
(31) Henis, Y. I., Katzir, Z., Shia, M. A., and Lodish, H. F. (1990) Oligomeric structure of the human asialoglycoprotein receptor: nature and stoichiometry of mutual complexes containing H1 and H2 polypeptides assessed by fluorescence photobleaching recovery. *J. Cell Biol. 111*, 1409−1418.
(32) Ruiz, N. I., and Drickamer, K. (1996) Differential ligand binding by two subunits of the rat liver asialoglycoprotein receptor. *Glycobiology 6*, 551−559.
(33) Saxena, A., Yik, J. H., and Weigel, P. H. (2002) H2, the minor subunit of the human asialoglycoprotein receptor, trafficks intracellularly and forms homo-oligomers, but does not bind asialoorosomucoid. *J. Biol. Chem. 277*, 35297−35304.
(34) Bischoff, J., and Lodish, H. F. (1987) Two asialoglycoprotein receptor polypeptides in human hepatoma cells. *J. Biol. Chem. 262*, 11825−11832.
(35) Spiess, M., Schwartz, A., and Lodish, H. (1985) Sequence of human asialoglycoprotein receptor cDNA. An internal signal sequence for membrane insertion. *J. Biol. Chem. 260*, 1979−1982.
(36) Spiess, M., and Lodish, H. F. (1985) Sequence of a second human asialoglycoprotein receptor: conservation of two receptor genes during evolution. *Proc. Natl. Acad. Sci. U. S. A. 82*, 6465−6469.
(37) Chiacchia, K., and Drickamer, K. (1984) Direct evidence for the transmembrane orientation of the hepatic glycoprotein receptors. *J. Biol. Chem. 259*, 15440−15446.
(38) Stefanescu, R., Born, R., Moise, A., Ernst, B., and Przybylski, M. (2011) Epitope structure of the carbohydrate recognition domain of asialoglycoprotein receptor to a monoclonal antibody revealed by high-resolution proteolytic excision mass spectrometry. *J. Am. Soc. Mass Spectrom. 22*, 148−157.
(39) Stockert, R. J. (1995) The asialoglycoprotein receptor: relationships between structure, function, and expression. *Physiol. Rev. 75*, 591−610.
(40) Baenziger, J. U., and Maynard, Y. (1980) Human hepatic lectin. Physiochemical properties and specificity. *J. Biol. Chem. 255*, 4607−4613.
(41) Baenziger, J. U., and Fiete, D. (1980) Galactose and N-acetylgalactosamine-specific endocytosis of glycopeptides by isolated rat hepatocytes. *Cell 22*, 611−620.
(42) Khorev, O., Stokmaier, D., Schwardt, O., Cutting, B., and Ernst, B. (2008) Trivalent, Gal/GalNAc-containing ligands designed for the asialoglycoprotein receptor. *Bioorg. Med. Chem. 16*, 5216−5231.
(43) Shia, M. A., and Lodish, H. F. (1989) The two subunits of the human asialoglycoprotein receptor have different fates when expressed alone in fibroblasts. *Proc. Natl. Acad. Sci. U. S. A. 86*, 1158−1162.
(44) Kawasaki, T., and Ashwell, G. (1976) Carbohydrate structure of glycopeptides isolated from an hepatic membrane-binding protein specific for asialoglycoproteins. *J. Biol. Chem. 251*, 5292−5299.
(45) Hong, W., Van Le, A., and Doyle, D. (1988) Identification and characterization of a murine receptor for galactose-terminated glycoproteins. *Hepatology 8*, 553−558.
(46) Drickamer, K., Mamon, J., Binns, G., and Leung, J. (1984) Primary structure of the rat liver asialoglycoprotein receptor. Structural evidence for multiple polypeptide species. *J. Biol. Chem. 259*, 770−778.
(47) Park, E. I., and Baenziger, J. U. (2004) Closely related mammals have distinct asialoglycoprotein receptor carbohydrate specificities. *J. Biol. Chem. 279*, 40954−40959.
(48) Weis, W. I., Taylor, M. E., and Drickamer, K. (1998) The C-type lectin superfamily in the immune system. *Immunol. Rev. 163*, 19−34.
(49) Weis, W. I., Drickamer, K., and Hendrickson, W. A. (1992) Structure of a C-type mannose-binding protein complexed with an oligosaccharide. *Nature 360*, 127−134.
(50) Kolatkar, A. R., and Weis, W. I. (1996) Structural basis of galactose recognition by C-type animal lectins. *J. Biol. Chem. 271*, 6679−6685.
(51) Iobst, S. T., Wormald, M. R., Weis, W. I., Dwek, R. A., and Drickamer, K. (1994) Binding of sugar ligands to Ca (2+)-dependent animal lectins. I. Analysis of mannose binding by site-directed mutagenesis and NMR. *J. Biol. Chem. 269*, 15505−15511.
(52) Kolatkar, A. R., Leung, A. K., Isecke, R., Brossmer, R., Drickamer, K., and Weis, W. I. (1998) Mechanism of N-acetylgalactosamine binding to a C-type animal lectin carbohydrate-recognition domain. *J. Biol. Chem. 273*, 19502−19508.
(53) Rose, A. S., and Hildebrand, P. W. (2015) NGL Viewer: a web application for molecular visualization. *Nucleic Acids Res. 43*, W576.
(54) Rose, A. S., Bradley, A. R., Valasatava, Y., Duarte, J. M., Prlić, A., and Rose, P. W. (2016) *Proceedings of the 21st International Conference on Web3D Technology*, pp 185−186, ACM.
(55) Meier, M., Bider, M. D., Malashkevich, V. N., Spiess, M., and Burkhard, P. (2000) Crystal structure of the carbohydrate recognition domain of the H1 subunit of the asialoglycoprotein receptor. *J. Mol. Biol. 300*, 857−865.
(56) Lee, Y. C., Townsend, R., Hardy, M. R., Lönngren, J., Arnarp, J., Haraldsson, M., and Lönn, H. (1983) Binding of synthetic oligosaccharides to the hepatic Gal/GalNAc lectin. Dependence on fine structural features. *J. Biol. Chem. 258*, 199−202.
(57) Connolly, D. T., Townsend, R., Kawaguchi, K., Bell, W., and Lee, Y. C. (1982) Binding and endocytosis of cluster glycosides by rabbit hepatocytes. Evidence for a short-circuit pathway that does not lead to degradation. *J. Biol. Chem. 257*, 939−945.
(58) Merwin, J. R., Noell, G. S., Thomas, W. L., Chiou, H. C., DeRome, M. E., McKee, T. D., Spitalny, G. L., and Findeis, M. A. (1994) Targeted delivery of DNA using YEE $(GalNAcAH)_3$, a synthetic glycopeptide ligand for the asialoglycoprotein receptor. *Bioconjugate Chem. 5*, 612−620.
(59) Biessen, E. A. L., Beuting, D. M., Roelen, H. C. P. F., van de Marel, G. A., Van Boom, J. H., and Van Berkel, T. J. C. (1995) Synthesis of Cluster Galactosides with High Affinity for the Hepatic Asialoglycoprotein Receptor. *J. Med. Chem. 38*, 1538−1546.
(60) Prakash, T. P., Yu, J., Migawa, M. T., Kinberger, G. A., Wan, W. B., Østergaard, M. E., Carty, R. L., Vasquez, G., Low, A., Chappell, A., et al. (2016) Comprehensive structure-activity relationship of triantennary *N*-acetylgalactosamine conjugated antisense oligonucleo-



DOI: 10.1021/acs.bioconjchem.6b00651
*Bioconjugate Chem.* 2017, 28, 283−295

tides for targeted delivery to hepatocytes. *J. Med. Chem. 59*, 2718–2733.

(61) Lee, Y. C., Lee, R. T., Ernst, B., Hart, G. W., and Sinaý, P. (2008) Interactions of Oligosaccharides and Glycopeptides with Hepatic Carbohydrate Receptors, in *Carbohydrates in Chemistry and Biology*, pp 549–561, Wiley-VCH Verlag GmbH.

(62) Lee, K., Rafi, M., Wang, X., Aran, K., Feng, X., Lo Sterzo, C., Tang, R., Lingampalli, N., Kim, H. J., and Murthy, N. (2015) In vivo delivery of transcription factors with multifunctional oligonucleotides. *Nat. Mater. 14*, 701–706.

(63) Chang, W.-Y., Kao, H.-W., Wang, H.-E., Chen, J.-T., Lin, W.-J., Wang, S.-J., and Chen, C.-L. (2013) Synthesis and biological evaluation of technetium-99m labeled galactose derivatives as potential asialoglycoprotein receptor probes in a hepatic fibrosis mouse model. *Bioorg. Med. Chem. Lett. 23*, 6486–6491.

(64) Valentijn, A. R. P., van der Marel, G. A., Sliedregt, L. A., van Berkel, T. J., Biessen, E. A., and van Boom, J. H. (1997) Solid-phase synthesis of lysine-based cluster galactosides with high affinity for the asialoglycoprotein receptor. *Tetrahedron 53*, 759–770.

(65) Biessen, E., Valentijn, A., De Vrueh, R., Van De Bilt, E., Sliedregt, L., Prince, P., Bijsterbosch, M., Van Boom, J., Van Der Marel, G., and Abrahams, P. (2000) Novel hepatotrophic prodrugs of the antiviral nucleoside 9-(2-phosphonylmethoxyethyl) adenine with improved pharmacokinetics and antiviral activity. *FASEB J. 14*, 1784–1792.

(66) Biessen, E. A., Sliedregt-Bol, K., 'T Hoen, P. A. C., Prince, P., Van der Bilt, E., Valentijn, A. R. P., Meeuwenoord, N. J., Princen, H., Bijsterbosch, M. K., Van der Marel, G. A., et al. (2002) Design of a targeted peptide nucleic acid prodrug to inhibit hepatic human microsomal triglyceride transfer protein expression in hepatocytes. *Bioconjugate Chem. 13*, 295–302.

(67) Zacco, E., Hütter, J., Heier, J. L., Mortier, J., Seeberger, P. H., Lepenies, B., and Koksch, B. (2015) Tailored presentation of carbohydrates on a coiled coil-based scaffold for asialoglycoprotein receptor targeting. *ACS Chem. Biol. 10*, 2065–2072.

(68) Biessen, E. A., Vietsch, H., and Van Berkel, T. J. (1994) Cholesterol derivative of a new triantennary cluster galactoside directs low-and high-density lipoproteins to the parenchymal liver cell. *Biochem. J. 302*, 283–289.

(69) Biessen, E., Broxterman, H., Van Boom, J., and Van Berkel, T. J. (1995) The cholesterol derivative of a triantennary galactoside with high affinity for the hepatic asialoglycoprotein receptor: a potent cholesterol lowering agent. *J. Med. Chem. 38*, 1846–1852.

(70) Lai, C. H., Lin, C. Y., Wu, H. T., Chan, H. S., Chuang, Y. J., Chen, C. T., and Lin, C. C. (2010) Galactose encapsulated multifunctional nanoparticle for HepG2 cell internalization. *Adv. Funct. Mater. 20*, 3948–3958.

(71) Lin, C.-C., Lai, C.-H., Chuang, Y.-J., Tzou, D.-L. M., and Chang, T.-C. (2013) Stepwise Orthogonal Click Chemistry toward Fabrication of Paclitaxel/Galactose Functionalized Fluorescent Nanoparticles for HepG2 cell Targeting and Delivery. *Bioconjugate Chem. 24*, 1698–1709.

(72) Lee, R. T., Wang, M.-H., Lin, W.-J., and Lee, Y. C. (2011) New and more efficient multivalent glyco-ligands for asialoglycoprotein receptor of mammalian hepatocytes. *Bioorg. Med. Chem. 19*, 2494–2500.

(73) Pujol, A. M., Cuillel, M., Jullien, A. S., Lebrun, C., Cassio, D., Mintz, E., Gateau, C., and Delangle, P. (2012) A sulfur tripod glycoconjugate that releases a high-affinity copper chelator in hepatocytes. *Angew. Chem., Int. Ed. 51*, 7445–7448.

(74) Monestier, M., Charbonnier, P., Gateau, C., Cuillel, M., Robert, F., Lebrun, C., Mintz, E., Renaudet, O., and Delangle, P. (2016) ASGPR-mediated uptake of multivalent glycoconjugates for drug delivery in hepatocytes. *ChemBioChem 17*, 590–4.

(75) Migawa, M. T., Prakash, T. P., Vasquez, G., Wan, W. B., Yu, J., Kinberger, G. A., Østergaard, M. E., Swayze, E. E., and Seth, P. P. (2016) A convenient synthesis of 5′-triantennary N-acetyl-galactosamine clusters based on nitromethanetrispropionic acid. *Bioorg. Med. Chem. Lett. 26*, 2194–2197.

(76) Lubineau, A., Malleron, A., and Le Narvor, C. (2000) Chemoenzymatic synthesis of oligosaccharides using a dendritic soluble support. *Tetrahedron Lett. 41*, 8887–8891.

(77) Symens, N., Méndez-Ardoy, A., Díaz-Moscoso, A., Sánchez-Fernández, E., Remaut, K., Demeester, J., Fernández, J. M. G. a., De Smedt, S. C., and Rejman, J. (2012) Efficient transfection of hepatocytes mediated by mRNA complexed to galactosylated cyclodextrins. *Bioconjugate Chem. 23*, 1276–1289.

(78) Sliedregt, L. A., Rensen, P. C., Rump, E. T., van Santbrink, P. J., Bijsterbosch, M. K., Valentijn, A. R. P., van der Marel, G. A., van Boom, J. H., van Berkel, T. J., and Biessen, E. A. (1999) Design and synthesis of novel amphiphilic dendritic galactosides for selective targeting of liposomes to the hepatic asialoglycoprotein receptor. *J. Med. Chem. 42*, 609–618.

(79) Lundquist, J. J., and Toone, E. J. (2002) The cluster glycoside effect. *Chem. Rev. 102*, 555–578.

(80) Lundquist, J. J., Debenham, S. D., and Toone, E. J. (2000) Multivalency effects in protein-carbohydrate interaction: the binding of the shiga-like toxin I binding subunit to multivalent c-linked glycopeptides. *J. Org. Chem. 65*, 8245–8250.

(81) Teixeira, J. M. C., Dias, D. M., Cañada, F. J., Martins, J. A., André, J. P., Jiménez-Barbero, J., and Geraldes, C. F. G. C. (2011) The interaction of $La^{3+}$ complexes of DOTA/DTPA glycoconjugates with the RCA120 lectin: a saturation transfer difference NMR spectroscopic study. *JBIC, J. Biol. Inorg. Chem. 16*, 725–734.

(82) Iobst, S. T., and Drickamer, K. (1996) Selective sugar binding to the carbohydrate recognition domains of the rat hepatic and macrophage asialoglycoprotein receptors. *J. Biol. Chem. 271*, 6686–6693.

(83) Rensen, P. C., Sliedregt, L. A., Ferns, M., Kieviet, E., van Rossenberg, S. M., van Leeuwen, S. H., van Berkel, T. J., and Biessen, E. A. (2001) Determination of the upper size limit for uptake and processing of ligands by the asialoglycoprotein receptor on hepatocytes *in vitro* and *in vivo*. *J. Biol. Chem. 276*, 37577–37584.

(84) Manoharan, M., Rajeev, K. G., Narayanannair, J. K., and Maier, M. U.S. Patent No. 8,106,022, 31 Jan. 2012.

(85) Nair, J. K., Willoughby, J. L. S., Chan, A., Charisse, K., Alam, M. R., Wang, Q., Hoekstra, M., Kandasamy, P., Kel'in, A. V., Milstein, S., et al. (2014) Multivalent *N*-acetylgalactosamine-conjugated siRNA localizes in hepatocytes and elicits robust RNAi-mediated gene silencing. *J. Am. Chem. Soc. 136*, 16958–16961.

(86) Rensen, P. C., van Leeuwen, S. H., Sliedregt, L. A., van Berkel, T. J., and Biessen, E. A. (2004) Design and synthesis of novel N-acetylgalactosamine-terminated glycolipids for targeting of lipoproteins to the hepatic asialoglycoprotein receptor. *J. Med. Chem. 47*, 5798–5808.

(87) Severgnini, M., Sherman, J., Sehgal, A., Jayaprakash, N. K., Aubin, J., Wang, G., Zhang, L., Peng, C. G., Yucius, K., Butler, J., et al. (2012) A rapid two-step method for isolation of functional primary mouse hepatocytes: cell characterization and asialoglycoprotein receptor based assay development. *Cytotechnology 64*, 187–195.

(88) Akinc, A., Querbes, W., De, S., Qin, J., Frank-Kamenetsky, M., Jayaprakash, K. N., Jayaraman, M., Rajeev, K. G., Cantley, W. L., and Dorkin, J. R. (2010) Targeted delivery of RNAi therapeutics with endogenous and exogenous ligand-based mechanisms. *Mol. Ther. 18*, 1357–1364.

(89) Meade, B. R., Gogoi, K., Hamil, A. S., Palm-Apergi, C., van den Berg, A., Hagopian, J. C., Springer, A. D., Eguchi, A., Kacsinta, A. D., Dowdy, C. F., et al. (2014) Efficient delivery of RNAi prodrugs containing reversible charge-neutralizing phosphotriester backbone modifications. *Nat. Biotechnol. 32*, 1256–1261.

(90) Prakash, T. P., Graham, M. J., Yu, J., Carty, R., Low, A., Chappell, A., Schmidt, K., Zhao, C., Aghajan, M., Murray, H. F., et al. (2014) Targeted delivery of antisense oligonucleotides to hepatocytes using triantennary N-acetyl galactosamine improves potency 10-fold in mice. *Nucleic Acids Res. 42*, 8796–8807.

(91) *Regulus* (2014) http://ir.regulusrx.com/releasedetail.cfm?ReleaseID=877462.



DOI: 10.1021/acs.bioconjchem.6b00651
*Bioconjugate Chem.* 2017, 28, 283–295

(92) Kichler, A., and Schuber, F. (1995) Versatile synthesis of bi-and tri-antennary galactose ligands: interaction with the Gal/GalNAc receptor of human hepatoma cells. *Glycoconjugate J. 12*, 275−281.
(93) Frisch, B., Carrière, M., Largeau, C., Mathey, F., Masson, C., Schuber, F., Scherman, D., and Escriou, V. (2004) A new triantennary galactose-targeted PEGylated gene carrier, characterization of its complex with DNA, and transfection of hepatoma cells. *Bioconjugate Chem. 15*, 754−764.
(94) Lee, R. T., and Lee, Y. C. (1987) Preparation of cluster glycosides of N-acetylgalactosamine that have subnanomolar binding constants towards the mammalian hepatic Gal/GalNAc-specific receptor. *Glycoconjugate J. 4*, 317−328.
(95) Rajeev, K. G., Nair, J. K., Jayaraman, M., Charisse, K., Taneja, N., O'Shea, J., Willoughby, J. L., Yucius, K., Nguyen, T., and Shulga-Morskaya, S. (2015) Hepatocyte-specific delivery of siRNAs conjugated to novel non-nucleosidic trivalent *N*-acetylgalactosamine elicits robust gene silencing *in vivo*. *ChemBioChem 16*, 903−908.
(96) Hangeland, J. J., Levis, J. T., Lee, Y. C., and Tso, P. O. (1995) Cell-type specific and ligand specific enhancement of cellular uptake of oligodeoxynucleoside methylphosphonates covalently linked with a neoglycopeptide, YEE(ah-GalNAc)$_3$. *Bioconjugate Chem. 6*, 695−701.
(97) Hangeland, J. J., Flesher, J. E., Deamond, S. F., Lee, Y. C., TS'O, P. O., and Frost, J. J. (1997) Tissue distribution and metabolism of the [$^{32}$P]-labeled oligodeoxynucleoside methylphosphonate-neoglycopeptide conjugate, [YEE(ah-GalNAc)$_3$]-SMCC-AET-pUmp T7, in the mouse. *Antisense Nucleic Acid Drug Dev. 7*, 141−149.
(98) Jiaang, W.-T., Tseng, P.-H., and Chen, S.-T. (2000) Facile solid phase synthesis of YEE(ah-GalNAc)$_3$, a ligand with known high affinity for the asialoglycoprotein receptor. *Synlett 2000*, 0797−0800.
(99) Lee, R. T., and Lee, Y. C. (1997) Facile synthesis of a high-affinity ligand for mammalian hepatic lectin containing three terminal N-acetylgalactosamine residues. *Bioconjugate Chem. 8*, 762−765.
(100) Matsuda, S., Keiser, K., Nair, J. K., Charisse, K., Manoharan, R. M., Kretschmer, P., Peng, C. G., V. Kel'in, A., Kandasamy, P., Willoughby, J. L., et al. (2015) siRNA conjugates carrying sequentially assembled trivalent N-acetylgalactosamine linked through nucleosides elicit robust gene silencing in vivo in hepatocytes. *ACS Chem. Biol. 10*, 1181−1187.
(101) Pujol, A. s. M., Cuillel, M., Renaudet, O., Lebrun, C., Charbonnier, P., Cassio, D., Gateau, C., Dumy, P., Mintz, E., and Delangle, P. (2011) Hepatocyte targeting and intracellular copper chelation by a thiol-containing glycocyclopeptide. *J. Am. Chem. Soc. 133*, 286−296.
(102) Bernardes, G. J., Kikkeri, R., Maglinao, M., Laurino, P., Collot, M., Hong, S. Y., Lepenies, B., and Seeberger, P. H. (2010) Design, synthesis and biological evaluation of carbohydrate-functionalized cyclodextrins and liposomes for hepatocyte-specific targeting. *Org. Biomol. Chem. 8*, 4987−4996.
(103) Arima, H., Yamashita, S., Mori, Y., Hayashi, Y., Motoyama, K., Hattori, K., Takeuchi, T., Jono, H., Ando, Y., Hirayama, F., et al. (2010) *In vitro* and *in vivo* gene delivery mediated by lactosylated dendrimer/$\alpha$-cyclodextrin conjugates (G2) into hepatocytes. *J. Controlled Release 146*, 106−117.
(104) Medina, S. H., Tekumalla, V., Chevliakov, M. V., Shewach, D. S., Ensminger, W. D., and El-Sayed, M. E. (2011) N-acetylgalactosamine-functionalized dendrimers as hepatic cancer cell-targeted carriers. *Biomaterials 32*, 4118−4129.
(105) Rozema, D. B., Lewis, D. L., Wakefield, D. H., Wong, S. C., Klein, J. J., Roesch, P. L., Bertin, S. L., Reppen, T. W., Chu, Q., Blokhin, A. V., et al. (2007) Dynamic PolyConjugates for targeted in vivo delivery of siRNA to hepatocytes. *Proc. Natl. Acad. Sci. U. S. A. 104*, 12982−12987.
(106) Yin, H., Kanasty, R. L., Eltoukhy, A. A., Vegas, A. J., Dorkin, J. R., and Anderson, D. G. (2014) Non-viral vectors for gene-based therapy. *Nat. Rev. Genet. 15*, 541−555.
(107) Wooddell, C. I., Rozema, D. B., Hossbach, M., John, M., Hamilton, H. L., Chu, Q., Hegge, J. O., Klein, J. J., Wakefield, D. H., Oropeza, C. E., et al. (2013) Hepatocyte-targeted RNAi therapeutics for the treatment of chronic hepatitis B virus infection. *Mol. Ther. 21*, 973−985.



DOI: 10.1021/acs.bioconjchem.6b00651
*Bioconjugate Chem.* 2017, 28, 283−295

# EXHIBIT 4

Vol. 6, 765–772, March 2000 

*Advances in Brief*

# Antibody-directed Enzyme Prodrug Therapy: Efficacy and Mechanism of Action in Colorectal Carcinoma[1]

**M. P. Napier, S. K. Sharma, C. J. Springer, K. D. Bagshawe, A. J. Green, J. Martin, S. M. Stribbling, N. Cushen, D. O'Malley, and R. H. J. Begent[2]**

Cancer Research Campaign Targeting and Imaging Group, Department of Oncology, Royal Free and University College London Medical School, London NW3 2PF [M. P. N., S. K. S., K. D. B., A. J. G., N. C., D. O., R. H. J. B.], with the Cancer Research Campaign Phase I/II Trials Committee, and Cancer Research Campaign Centre for Cancer Therapeutics, Institute of Cancer Research, 15 Cotswold Road Sutton, Surrey SM2 5NG [C. J. S., J. M., S. M. S.], United Kingdom

## Abstract

**In antibody-directed enzyme prodrug therapy, an enzyme conjugated to an antitumor antibody is given i.v. and localizes in the tumor. A prodrug is then given, which is converted to a cytotoxic drug selectively in the tumor. Ten patients with colorectal carcinoma expressing carcinoembryonic antigen received antibody-directed enzyme prodrug therapy with A5B7 F(ab′)$_2$ antibody to carcinoembryonic antigen conjugated to carboxypeptidase G2 (CPG2). A galactosylated antibody directed against the active site of CPG2 (SB43-gal) was given to clear and inactivate circulating enzyme. A benzoic acid mustard-glutamate prodrug was given when plasma enzyme levels had fallen to a predetermined safe level, and this was converted by CPG2 in the tumor into a cytotoxic form. Enzyme levels derived from quantitative gamma camera imaging and from direct measurements in plasma and tumor biopsies showed that the median tumor:plasma ratio of enzyme exceeded 10000:1 at the time of prodrug administration. Enzyme concentrations in the tumor (median, 0.47 units g$^{-1}$) were sufficient to generate cytotoxic levels of active drug. The concentration of prodrug needed for optimal conversion ($K_m$) of 3 μM was achieved. Prodrug conversion to drug was shown by finding detectable levels of drug in plasma. There was evidence of tumor response; one patient had a partial response, and six patients had stable disease for a median of 4 months after previous tumor progression (one of these six had a tumor marker response). Manageable neutropenia and thrombocytopenia occurred. Conditions for effective antitumor therapy were met, and there was evidence of tumor response in colorectal cancer.**

## Introduction

Systemic cancer therapy is limited by a lack of tumor selectivity and by drug resistance; ADEPT[3] is designed to overcome both problems (1). An antibody directed against a tumor-associated antigen is linked to an enzyme and given i.v., resulting in selective accumulation of the enzyme in the tumor. When the discrimination between tumor and normal tissue enzyme levels is sufficient, a prodrug is given i.v., which is converted to an active cytotoxic drug by the enzyme within the tumor. Selectivity is achieved by the tumor specificity of the antibody and by delaying prodrug administration until there is a large differential between tumor and normal tissue enzyme levels. Drug resistance can be overcome by generating high levels of an alkylating agent in the tumor, and this is achieved through the capacity of each enzyme molecule to convert many molecules of prodrug into drug. ADEPT has shown antitumor activity in animal tumor models of human choriocarcinoma and colonic and breast carcinoma (2–4).

A convincing demonstration that such a complex system can be developed for clinical use requires evidence that each of the components of ADEPT functions by the mechanisms proposed. This can be provided by measuring antibody-enzyme conjugate concentration, enzyme activity, and prodrug and drug levels in tumor and normal tissues. We describe a clinical trial in which these parameters were measured along with conventional measurements of toxicity, efficacy, and immunogenicity.

## Materials and Methods

**Materials.** Affinity-purified mouse monoclonal A5B7 IgG1 antibody (5) to CEA (Celltech PLC, Slough, Berks, United Kingdom) was digested to F(ab′)$_2$ with cysteine-activated bromelain (6). Immunoreactivity was assessed by indirect ELISA against CEA. CPG2, a folate-depleting enzyme of bacterial origin, was produced by the Division of Biotechnology, Public Health Laboratory Service (Porton Down, United Kingdom; Ref. 7). CPG2 was covalently linked to the F(ab′)$_2$ fragment of A5B7 by a stable thio-ether bond (8, 9) to make the antibody

Received 6/23/99; revised 11/16/99; accepted 11/24/99.
The costs of publication of this article were defrayed in part by the payment of page charges. This article must therefore be hereby marked *advertisement* in accordance with 18 U.S.C. Section 1734 solely to indicate this fact.
[1] Supported by the Cancer Research Campaign, The Ronald Raven Chair in Clinical Oncology Trust, and the Royal Free Hampstead NHS Trust. Zeneca PLC (Macclesfield, Cheshire, United Kingdom) supplied a grant funding technical and nursing support during this trial.
[2] To whom requests for reprints should be addressed, at Department of Oncology, Royal Free and University College Medical School, University College London, Royal Free Campus, Rowland Hill Street, London NW3 2PF, United Kingdom. Phone: 44-171-794-0500, ext. 5488; Fax: 44-171-794-3341; E-mail: rjhb@rfhsm.ac.uk.

[3] The abbreviations used are: ADEPT, antibody-directed enzyme prodrug therapy; CEA, carcinoembryonic antigen; CPG2, carboxypeptidase G2; A5CP, A5B7 F(ab′)$_2$ antibody to CEA conjugated to CPG2; CMDA, benzoic acid mustard-glutamate prodrug; HAMA, human antimouse antibody; SPECT, single photon emission computerized tomographic; HPLC, high-pressure liquid chromatography; CTC, Common Toxicity Criteria; CT, computerized tomogram.

Downloaded from http://aacrjournals.org/clincancerres/article-pdf/6/3/765/2074869/df0300000765.pdf by guest on 31 March 2023

Case 1:23-cv-00328-JLH-SRF Document 125 Filed 02/20/24 Page 67 of 73 PageID #: 4374



*Table 1* Treatment schedule

| | |
|---|---|
| Day 0 | 10,000 enzyme units $m^{-2}$ (125 mg $m^{-2}$) of A5B7 F(ab′)$_2$ antibody-CPG2 conjugate in 500 ml of 0.9% saline over 2 h, 10 mg of conjugate labeled with 370 MBq of $^{131}$I were given as an i.v. bolus at the end of conjugate infusion |
| Day +1 | Infusion of SB43-gal antibody to CPG2, 7.5 mg $m^{-2}$ in 500 ml of 0.9% saline over 6 h, 15 mg $m^{-2}$ in 500 ml of 0.9% saline over 18 h, continued to day +4 at 8 mg $m^{-2}$ in 1 liter of 0.9% saline over 24 h |
| Day +2 | CMDA prodrug 200 mg $m^{-2}$ infused i.v. over 2 min in fast running 1.26% $NaHCO_3$ (given if CPG2 enzyme levels measured in blood were <0.2 enzyme units $ml^{-1}$) |
| Day +3 and +4 | Repeat day +2 |

*Table 2* Patient demography and pretreatment status

| Patient | Sex | Age (yr) | Performance status | Primary tumor | Prior surgery | Previous treatment | Assessable disease | Serum CEA |
|---|---|---|---|---|---|---|---|---|
| 1 | M | 38 | 0 | Colon | Hemicolectomy<br>Ileostomy | Ctx: 5FU/fa[a] | Stoma site<br>Liver<br>Inguinal node | 20 |
| 2 | M | 42 | 0 | Colon | Hemicolectomy<br>Hemi-hepatectomy | Ctx: 5FU/fa | Liver<br>(CT portography) | 10 |
| 3 | F | 63 | 0 | Colon | Hemicolectomy | XRT: liver<br>Ctx: 5FU/fa | Liver | 581 |
| 4 | M | 57 | 0 | Rectum | Anterior resection | Ctx: 5FU/fa, MMC | Lung | <3 |
| 5 | M | 31 | 0 | Colon | Sigmoid colectomy | XRT: pelvis<br>Ctx: 5FU/fa, 5FU/CDDP<br>IFN-a | Omental mass<br>Malignant ascites | <3 |
| 6 | F | 46 | 0 | Appendix | Appendectomy<br>Hemicolectomy | Ctx: 5FU/fa, 5FU/CDDP | Liver<br>Ovary | <3 |
| 7 | F | 42 | 1 | Sigmoid colon | Sigmoid colectomy<br>Small bowel resection<br>Hysterectomy<br>Ureteric stent | Ctx: 5FU/fa | Para-aortic nodes | 19 |
| 8 | F | 46 | 1 | Colon | Hemicolectomy<br>Oopherectomy | Ctx: 5FU/fa, 5FU/CDDP | Para-aortic nodes<br>Lung<br>Pelvic mass | <3 |
| 9 | M | 47 | 0 | Colon | Low anterior resection | Ctx: 5FU/fa | Lung<br>Liver | 155 |
| 10 | M | 75 | 1 | Rectum | Anterior resection | Ctx: 5FU/fa, oral 5FU/fa | Liver | 419 |

[a] Ctx, chemotherapy; XRT, radiotherapy, 5FU, 5fluorouracil; fa, folinic acid; MMC, mitomycin C; CDDP, cisplatin.
[b] Reference ranges, CEA < 10 μg $l^{-1}$.

enzyme conjugate A5CP. Ten mg of the antibody-enzyme conjugate were radiolabeled with 10 mCi of $^{131}$I by the *N*-bromosuccinimide/L-tyrosine technique (10).

SB43 is an IgG1 mouse monoclonal antibody against CPG2 (11). Purified antibody samples were galactosylated (SB43-gal) according to a modification of the method described by Mattes (12, 13). CMDA, a synthetic benzoic acid mustard prodrug, undergoes cleavage of its terminal glutamic acid residue by CPG2 to generate the active alkylating agent 4-[(2 chloroethyl)[2(mesyloxy)ethyl]-amino] benzoic acid (14). Quality and safety of the product were determined using the Cancer Research Campaign Operation Manual (15).

Freeze-dried CMDA was reconstituted in 1.5 ml of DMSO, a solution that is stable in B-D syringes for >12 h. The CMDA/DMSO solution was injected in free running 1.26% sodium bicarbonate. The treatment schedule is given in Table 1.

**Methods.** The catalytic activity of native and conjugated CPG2 was measured prospectively during the trial by a spectrophotometric methotrexate reduction assay (16, 17). Indirect assessment of A5CP concentrations were made by gamma counting of plasma samples (18).

HAMA and anti-CPG2 antibody (HACPG2A) response were measured by ELISA (19).

Patients had torso SPECT gamma camera imaging performed at intervals of up to 72 h after radiolabeled conjugate injection on an IGE Gemini 700 camera. Enzyme in tumor and normal tissue was estimated by measuring radioactivity as a percentage of injected radioactivity. SPECT images were reconstructed using General Electric filtered back projection software and corrected for decay, attenuation, and Compton scatter. Estimates of radioactivity per unit mass were then made using region of interest analysis as described previously (18).

Prodrug and active drug concentrations in plasma were determined by HPLC, and their presence was confirmed by liquid chromatography mass spectroscopy (20, 21) and CPG2 in plasma and tumor biopsies by HPLC (21, 22). Fractional clearance estimates were made assuming an exponential clearance and a single-compartment model. An exponential curve fit using the least sum of squares method was used. Fractional half-life of clearance was calculated using the equation $t_{1/2} = \ln 2/K$ where $K$ is slope of ln plasma concentration *versus* time. These results are descriptive only as the concentration of the drug at the time

Downloaded from http://aacrjournals.org/clincancerres/article-pdf/6/3/765/2074869/df0300000765.pdf by guest on 31 March 2023

Case 1:23-cv-00328-JLH-SRF Document 125 Filed 02/20/24 Page 68 of 73 PageID #: 4375



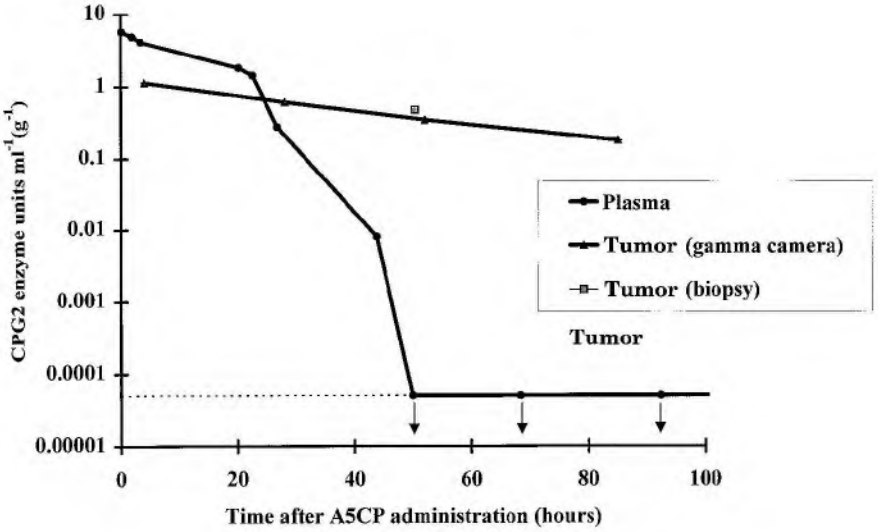


*Fig. 1* Enzyme levels in plasma and tumor after the infusion of antibody-enzyme conjugate. Plasma levels were measured by methotrexate reduction spectrophotometric assay (●) and HPLC (↓). The *arrow* indicates that the level was below the limits of detection of this assay (- - - -). Levels in tumor (▲) were estimated from SPECT gamma camera imaging. Each point is the median of 10 patients. The range includes 60% of data points. The enzyme level in tumor obtained from tumor biopsy and measured by HPLC (■) at 50.3 h is the median of five patients, and the range includes 60% of data points.

of administration ($C_0$) would theoretically be zero, and drug is being continually released from the prodrug by tumor localized antibody-enzyme conjugate. The pharmacokinetic details of the prodrug/drug system generated in this trial are reported in detail elsewhere (21). Area under the concentration *versus* time curve (AUC) to infinity was calculated by using the trapezoidal rule and by adding a tail by integrating the exponential curve-fit from the last measured time point to infinity.

Standard WHO criteria for response were used. Standard National Cancer Institute CTC (23) were used to evaluate toxicity. Survival times were calculated from the start of treatment. Duration of response was calculated from the onset of response to the date of disease progression.

**Patients.** The trial was performed with local ethical committee, Department of Health, United Kingdom, and Administration of Radioactive Substances Committee approval and according to Good Clinical Practice under the auspices of the Cancer Research Campaign Phase I/II Committee's Targeting Trials Group, by whose trials office the clinical data were monitored. All patients gave written informed consent. Eligibility criteria were unresectable or metastatic, histologically proven colorectal carcinoma; no antitumor treatment in the previous 4 weeks; measurable disease by plain X-ray, CT, or ultrasound scan; age >20 years; life expectancy >4 months; Eastern Cooperative Oncology Group performance status of 0–2; and normal hematological, renal, and cardiac indices unless abnormal due to tumor. Pretreatment serum CEA levels were required to be raised but <1000 μg l$^{-1}$; if they were not raised, then CEA had to be demonstrated immunohistochemically on tumor biopsy (24).

All patients had negative HAMA titers and negative reactions to intradermally administered A5CP and SB43-gal. All patients had previously been treated with 5-fluorouracil-based chemotherapy regimens and had either relapsed or shown no response. All patients had a triple lumen Hickman catheter inserted under direct radiographic screening into a subclavian vein. Cyclosporin A was given starting 2 days before A5CP administration, initially as a continuous i.v. infusion at 5 mg kg$^{-1}$ day for 7 days and then p.o. at 15 mg kg$^{-1}$/day in divided doses for 7 additional days. Dose adjustments were made to keep blood levels in the range 150–350 Ng ml$^{-1}$. Ondansetron and s.c. cyclizine were used as required. All patients were given a thyroid blockade against $^{131}$I using potassium iodide.

## Results

**Study Population.** Ten patients (six male and four female) with a median age of 46 years were enrolled into the study. All received one course of ADEPT, with two patients who had a negative HAMA and HACPG2A after cycle 1 receiving a second treatment. The pretreatment status of the patients is summarized in Table 2. Concentrations of the components of ADEPT were measured in tumor and normal tissues to determine whether conditions for effective therapy were met. The results were related to toxicity and of the components of ADEPT were measured in tumor and normal tissues to determine efficacy assessments.

**Antibody and Enzyme in Plasma.** A5CP cleared from the plasma as shown in Fig. 1. Indirect measurements of enzyme activity in plasma by HPLC and spectrophotometric assay correlated with the estimates of enzyme made from measurements of radiolabeled A5CP until clearing antibody was given. Thereafter, active enzyme measurements gave lower values, consistent with enzyme inactivation by SB43-gal in addition to clearance of complexed A5CP. The concentration of enzyme was less than the limits of detection ($5 \times 10^{-5}$ units of enzyme ml$^{-1}$ of plasma) 48 h after A5CP administration.

**Enzyme Levels in Tumor and Normal Tissues.** Quantitative SPECT gamma camera imaging showed $^{131}$I-labeled A5CP localization in the tumor (Fig. 2, *a* and *b*), reaching median peak levels of 6.8% of the injected radioactivity kg$^{-1}$ 4 h after administration. Initially, blood and other normal tissue levels of radioactivity exceeded those in the tumor, but this trend was reversed after SB43-gal administration (Fig. 3).

Downloaded from http://aacrjournals.org/clincancerres/article-pdf/6/3/765/2074869/df0300007 65.pdf by guest on 31 March 2023

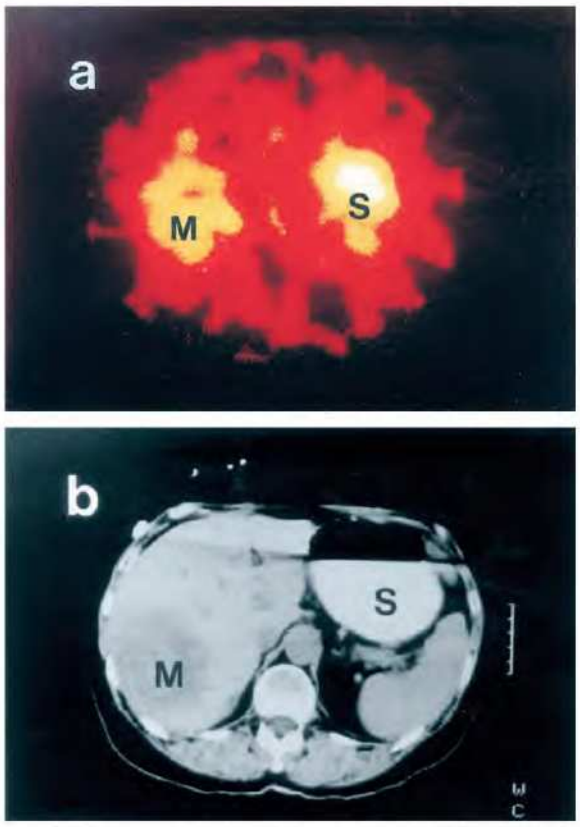


*Fig. 2* A5CP localization in liver metastasis. *a*, SPECT image in patient three 52 h after A5CP administration, showing the localization of the conjugate within a liver metastasis (*M*). Free $^{131}I$ is also seen in the stomach (*S*). *b*, corresponding CT scan through the liver showing the large posterolateral metastasis (*M*). *S*, stomach.

Enzyme activity was measured indirectly in tumor biopsies taken immediately before the start of prodrug administration from five patients (two liver metastases, one peritoneal metastasis, and one ovarian metastasis biopsied under ultrasound control and one metastasis of a stomal recurrence). Median enzyme concentration was 0.47 (range, 0.32–0.62) enzyme units $g^{-1}$, which correlated well with the concentration of 0.34 (range, 0.19–0.63) calculated from the amount of radioactivity measured by gamma camera imaging (Fig. 1). This showed that the enzyme in the tumor was inaccessible to inactivation by SB43-gal and that gamma camera estimates of enzyme concentration in tumor were valid.

Normal liver was obtained in biopsies from two patients, and no enzyme activity was detectable in them by HPLC. However, there was retention of some radioactivity, suggesting that enzyme activity was lost in the residual radiolabeled material.

**Selectivity.** Tumor:plasma ratios of enzyme were >10,000:1 (based on undetectable levels in the blood) at the time when prodrug administration was started. The validation of gamma camera estimates of enzyme concentration given by the biopsy studies supports the view that effective enzyme levels persist in the tumor for at least up to 85 h. Tumor:liver ratios in the two patients biopsied also exceeded 10,000:1 (based on concentrations below the limits of detection in normal liver).

**Prodrug and Drug Levels in Plasma.** Prodrug cleared from plasma with a biological half-life of 16 min (range, 5–27 min; Fig. 4*a*). Drug was detected in all cases within 3 min of the end of prodrug administration; the half-life recorded for drug was longer than for the prodrug at 46 min (range, 7–85 min; Fig. 4*b*). There was variation in the concentrations of prodrug and drug between patients and between days in the same patient. Calculated area under the curve to infinity correlated linearly for prodrug and drug for a given administration and patient. This showed that the prodrug was activated by the enzyme, and the available data on enzyme distribution suggest that this was principally occurring in the tumor with diffusion of drug into the circulation.

**Toxicity.** Neutropenia and thrombocytopenia occurred with median times to nadir of 35 and 25 days, respectively. Four patients reached CTC grade 3 or 4 toxicity for both parameters and required platelet transfusion, whereas five patients had grade 1 or 2 toxicity. One patient had a febrile neutropenic episode requiring hospitalization and antibiotic therapy. Nine patients had nausea or vomiting (CTC grade 3 or 4 in severity in four of these patients). This was attributed to the combination of DMSO and cyclosporin administered. Transient rises in urea and creatinine were seen in four patients (all grade 1 or 2 toxicity); again, these were probably attributable to cyclosporin A.

**Immune Response.** HAMA and human anti-CPG2 antibody were found in all patients after 2 weeks, preventing further therapy.

**Responses.** There was evidence of antitumor activity. One patient had a partial response lasting 4 months, six patients had stable disease after previous tumor progression with a median progression-free survival of 4 months (range, 2–16 months), and one of these patients had a decline in serum CA19/9 levels sustained for 4 months. Three patients had progressive disease. The tumor response in the patient with a partial response is shown in Fig. 5, *a–d*.

## Discussion

The conditions needed for effective ADEPT were achieved in patients, and tumor response was achieved after only one treatment. Tumor localization of the enzyme at a median of 0.5 units $g^{-1}$ (Fig. 1) was in the range that produced an antitumor effect in animal models (3). The very favorable tumor:plasma and tumor:liver ratios of enzyme recorded (>10,000:1) make it unlikely that there is a significant amount of enzyme remaining in normal tissues at the time of prodrug administration.

The levels of radioactivity in the tumor gave a reasonably accurate indication of the enzyme level in the tumor at the time of prodrug administration, as judged by comparison of enzyme measurements in biopsies and SPECT gamma camera data. Although there was only approximately 1.5% and 1% of injected radioactivity $kg^{-1}$ in the tumor after 52 and 85 h, respectively, this represented a satisfactory level of active enzyme for prodrug activation, as indicated above. Blood and other normal tissue levels of radioactivity remained close to those in the tumor until 85 h after administration. However, enzyme activity

Downloaded from http://aacrjournals.org/clincancerres/article-pdf/6/3/765/2074869/df0300000765.pdf by guest on 31 March 2023

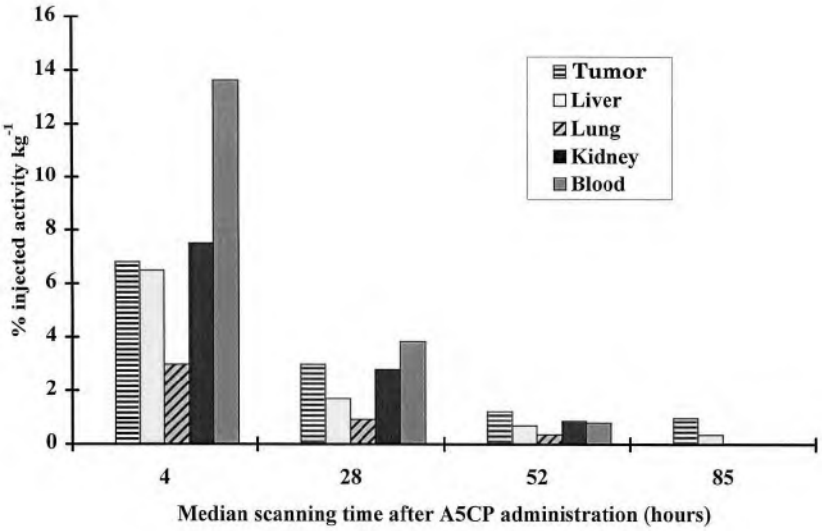


*Fig. 3* Distribution of radiolabeled A5CP in tumor and normal tissue over time as judged by SPECT imaging. Each point is the median of 10 patients. The range includes 60% of data points.

measurements in plasma and liver biopsies after the second antibody administration showed no measurable enzyme activity. This was consistent with inactivation of enzyme activity in normal tissues by the antienzyme antibody SB43-gal, whereas inactivation did not occur in the tumor. Thus, the levels of radioactivity in blood and normal tissues overestimated enzyme activity after the administration of SB43-gal.

The drug present in plasma was probably generated in the tumor, and it is interesting that the two patients with the highest plasma drug levels had large burdens of tumor. Treating smaller tumors may be advantageous because the potential for release of the drug into the circulation would be reduced in proportion to the targeted tumor volume, whereas the drug concentration in the tumor would be similar.

The characteristics of the CPG2 enzyme in prodrug activation are known (25) and indicate a $K_m$ for prodrug conversion of 3 μM. This optimal level of prodrug concentration was maintained for approximately 2 h in the plasma (Fig. 4*a*). Also the $IC_{50}$ of the drug is 200 μM (25), and this value was never exceeded in the blood in any of the study patients (Fig. 4*b*). Despite this, drug in the circulation appeared to cause myelosuppression. Given that no active enzyme was found in plasma by HPLC assay at any of the time points when prodrug was given, it is likely that the presence of drug in the circulation was the result of "leakback" from tumor. It is also probable that higher concentrations of drug were present in the tumor than were measured in the blood, and it is possible that a change in prodrug regimen (for instance, to an infusion over 3 or more days) would prevent plasma drug concentration from rising to a toxic level. The possibility that the prodrug itself caused myelosuppression was excluded in a previous study in which the prodrug was given alone (26).

The prodrug CMDA is converted to the cytotoxic parent drug 4-[(2-chloroethyl)[2-(mesyloxy)ethyl]amino]benzoic acid (14), which was found to be most effective *in vivo* in ADEPT experimental models, leading to complete regressions in transplanted human tumor xenografts that were resistant to all conventional cytotoxic agents (2). Relevant antibody-enzyme conjugates (2000 units/kg, i.v. injection) were administered to animals with transplanted choriocarcinoma xenografts, followed 72, 94, and 99 h later by CMDA (400 mg/kg, i.v. injection). Control groups of animals received saline alone, CMDA alone, or irrelevant antibody-enzyme conjugate followed by CMDA at the same doses and time points as the test groups. All control animals were dead by day 110, whereas 9 of 12 of the ADEPT test animals were still tumor free at day 300 ($P < 001$).

It is not known how the relatively small amount of drug leads to bone marrow suppression 25–35 days after injection. However, we have noticed that after CMDA incubation with cells in culture, the cells do not die immediately but appear to be primed for death and die later.[4]

We appreciated that the CMDA-derived drug might have a long half-life from the outset, but CMDA was a practical prodrug for synthesis and testing of the principles of ADEPT. The relatively long half-life of the drug found in plasma is consistent with it causing the dose-limiting myelosuppression. ADEPT with the same antibody and enzyme but with a drug with a shorter half-life has been shown to be an effective therapy for colorectal cancer in an animal model and is being developed for clinical use (27, 28).

This study shows how measurement of the parameters required for the function of ADEPT gives insight into its substantial ability for selective delivery of cancer therapy. The tumor responses demonstrate that generation of an alkylating agent at the tumor site can overcome the drug resistance usually seen with this class of drug in colorectal cancer (29). Although it was not possible to measure drug directly in the tumor because of the small size of the biopsies, the plasma drug levels and the absence of enzyme in normal tissues suggest that this was the result of generation of high concentrations of drug in the tumor.

[4] Unpublished observations.

Downloaded from http://aacrjournals.org/clincancerres/article-pdf/6/3/765/2074869/df0300007 65.pdf by guest on 31 March 2023

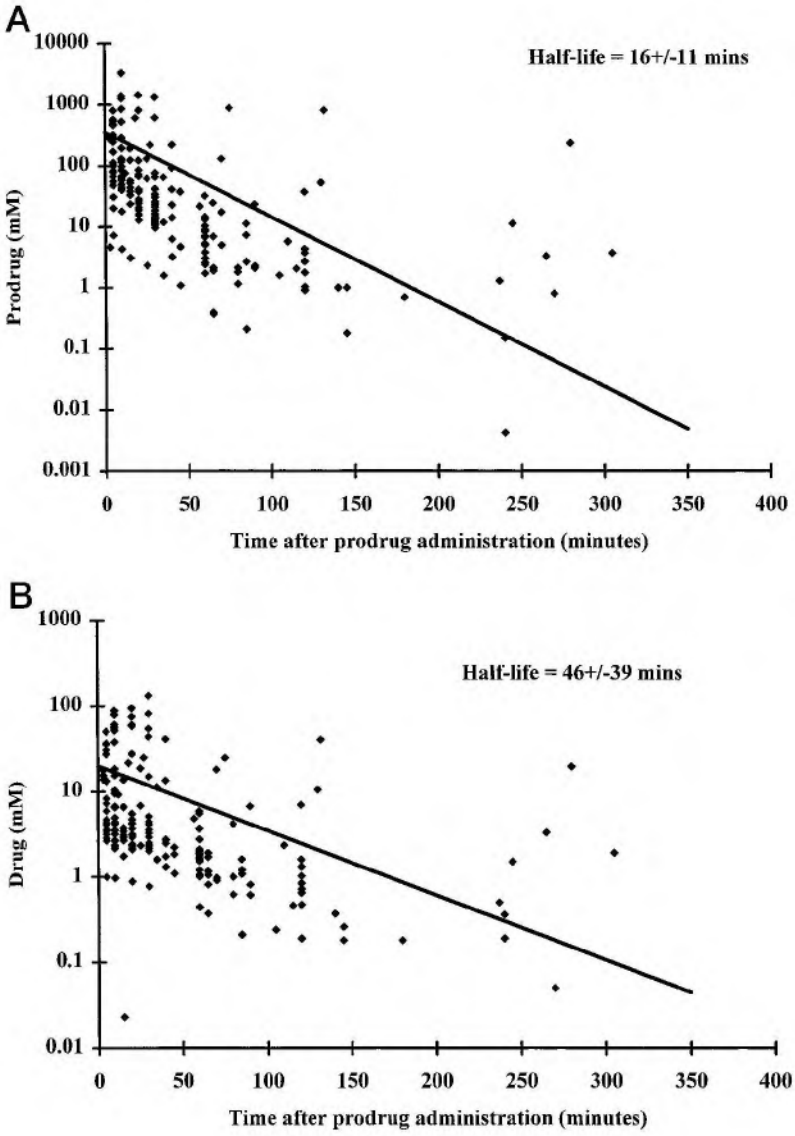


*Fig. 4* Prodrug and drug pharmacokinetics. Plasma concentration of the prodrug (CMDA; *a*) and drug (*b*) after bolus administration of CMDA. Each point indicates a separate determination. The *thick line* reflects a modeled "best-fit" exponential clearance, and the half-life was determined from this.

Conventional Phase I clinical trials in which tumor response and toxicity are studied in dose escalation studies are unlikely to be adequate for investigating such a complex system. For instance, a poor antitumor effect at the maximum tolerated dose of the prodrug could be caused by inadequate levels of enzyme in the tumor, excess enzyme in normal tissues, failure to continue administering prodrug while favorable tumor and normal tissue enzyme levels persist, an inappropriate prodrug regimen, or primary drug resistance. Little could be done about the latter, but knowledge of the first four components could lead to redesign of a clinical protocol to overcome the problems.

The immunogenicity of CPG2 is not surprising, considering its bacterial origin. It has the important advantage over most mammalian enzymes that it has no human equivalent that could activate the prodrug endogenously. Administration of cyclosporin A delays the production of a human antibody response to A5B7 antibody (30). With ADEPT, production of human antibodies directed against CPG2 and A5B7 antibody limits therapy to two or three doses, but this does not appear to prevent useful antitumor activity, as shown here and in a previous study (26). The proteins used in ADEPT studies were expected to be immunogenic in patients. In a previous clinical trial of ADEPT (26) with SB43gal and CMDA, 11 patients received antibody-enzyme conjugate without any immunosuppressive agent. All patients had detectable HAMA and anti-CPG2 antibodies in serum within 10 days after a single treatment with antibody-enzyme conjugate (19). Six patients received cyclosporin A 48 h before the ADEPT regimen (31). Two patients, who had very large hepatic metastases, received cyclosporin A p.o. and developed fatal hepato-renal failure after the first cycle of therapy. Subsequent patients receiving cyclosporin A by continuous i.v. infusion showed temporary increases in creatinine and urea

Downloaded from http://aacrjournals.org/clincancerres/article-pdf/6/3/765/2074869/df0300000765.pdf by guest on 31 March 2023

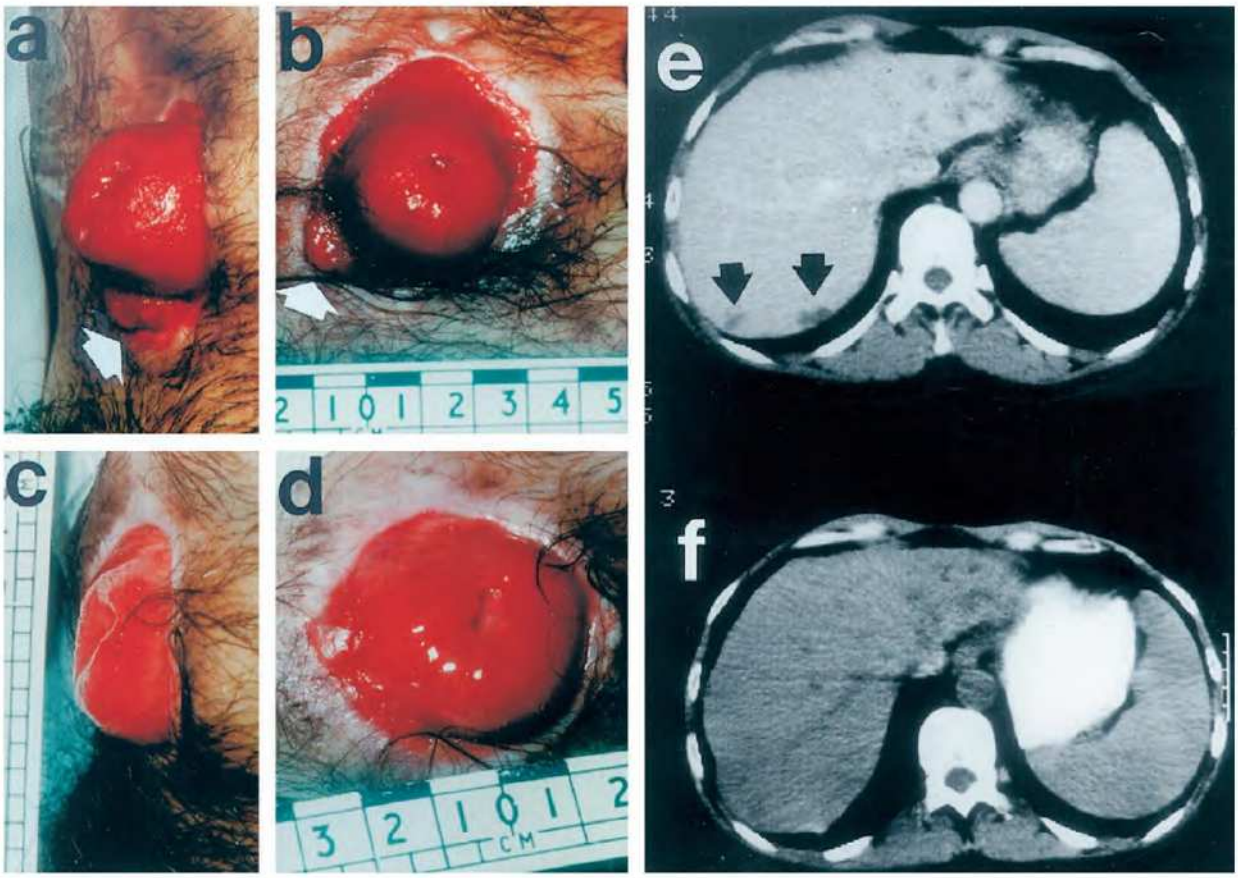


*Fig. 5* Response to treatment in patient 1. Stomal metastasis of rectal cancer (*a* and *b*) before and (*c* and *d*) 56 days after ADEPT therapy; a substantial reduction in the volume of tumor is seen. CT (*e*) showing hepatic metastases of rectal cancer (*arrows*) and resolution (*f*) 56 days after ADEPT.

levels. Two patients had antibody responses after a second cycle of therapy. Two patients had no detectable antibody responses until cyclosporin A was discontinued and were able to receive three cycles of ADEPT during a 21-day period.

Other immunosuppressive or tolerizing agents may also be considered for their potential to delay the antibody response (32, 33). Humanization of the antibody may reduce immunogenicity, and it is possible that less immunogenic enzymes can be identified.

The data presented here support the proposed mechanism of action of ADEPT and justify additional studies to develop the system for treatment for colorectal and other cancers.

## Acknowledgments

We thank C. Pagonis, L. Light, and the staff of the Drug Development Office, Cancer Research Campaign for assistance in protocol development, data monitoring, and data analysis.

## References

1. Bagshawe, K. D., Springer, C. J., Searle, F., Antoniw, P., Sharma, S. K., Melton, R. G., and Sherwood, R. F. A cytotoxic agent can be generated selectively at cancer sites. Br. J. Cancer, *58:* 700–703, 1988.

2. Springer, C. J., Bagshawe, K. D., Sharma, S. K., Searle, F., Boden, J. A., Antoniw, P., Burke, P. J., Rogers, G. T., Sherwood, R. F., and Melton, R. G. Ablation of human choriocarcinoma xenografts in nude mice by antibody-directed enzyme prodrug therapy with three novel compounds. Eur. J. Cancer, *27:* 1361–1366, 1991.

3. Antoniw, P., Springer, C. J., Bagshawe, K. D., Searle, F., Melton, R. G., Rogers, G. T., Burke, P. J., and Sherwood, R. F. Disposition of the prodrug 4-(bis(2-chloroethyl) amino) benzoyl-L-glutamic acid and its active parent drug in mice. Br. J. Cancer, *62:* 909–914, 1990.

4. Eccles, S. A., Court, W. J., Box, G. A., Dean, C. J., Melton, R. G., and Springer, C. J. Regression of established breast carcinoma xenografts with antibody-directed enzyme prodrug therapy against c-erbB2 p185. Cancer Res., *54:* 5171–5177, 1994.

5. Harwood, J., Britton, D. W., Southall, P. J., Boxer, G. M., Rawlins, G., and Rogers, G. T. Mapping epitope characteristics on carcinoembryonic antigen. Br. J. Cancer, *54:* 75–82, 1986.

6. Milenic, D. E., Estaban, J. N., and Colcher, D. Comparison of methods for the generation of immunoreactive fragments of a monoclonal antibody (B72.3) reactive with human carcinomas. J. Immunol. Methods, *120:* 71–83, 1989.

7. Sherwood, R. F., Melton, R. G., Alwan, S. M., and Hughes, P. Purification and properties of carboxypeptidase G2 from pseudomonas Sp strain R.S.16; use of a novel triazine dye affinity method. Eur. J. Biochem., *148:* 447–453, 1985.

Downloaded from http://aacrjournals.org/clincancerres/article-pdf/6/3/765/2074869/df0300007 65.pdf by guest on 31 March 2023

8. Duncan, R. J. S., Weston, P. D., and Wrigglesworth, R. A new reagent which may be used to introduce sulphudral groups into proteins and its use in the preparation of conjugates for immunoassay. Ann. Biochem., *132:* 68–73, 1983.

9. Melton, R. G., Boyle, J. M., Rogers, G. T., Burke, P., Bagshawe, K. D., and Sherwood, R. F. Optimisation of small-scale coupling of A5B7 monoclonal antibody to carboxypeptidase G2. J. Immunol. Methods, *158:* 49–56, 1993.

10. Adam, T. Radioiodination for therapy. Ann. Clin. Biochem., *26:* 244–245, 1989.

11. Sharma, S. K., Bagshawe, K. D., Burke, P. J., Boden, R. W., and Rogers, G. T. Inactivation and clearance of an anti-CEA carboxypeptidase G2 conjugate in blood after localisation in a xenograft model. Br. J. Cancer, *61:* 659–662, 1990.

12. Mattes, M. J. Biodistribution of antibodies after intraperitoneal or intravenous injection and effect of carbohydrate modification. J. Natl. Cancer Inst., *79:* 855–863, 1987.

13. Sharma, S. K., Bagshawe, K. D., Burke, P. J., Boden, J. A., Rogers, G. T., Springer, C. J., Melton, R. G., and Sherwood, R. F. Galactosylated antibodies and antibody-enzyme conjugates in antibody-directed enzyme prodrug therapy. Cancer (Phila.), *73:* 1114–1120, 1994.

14. Springer, C. J., Antoniw, P., Bagshawe, K. D., Searle, F., Bisset, G. M., and Jarman, M. Novel prodrugs which are activated to cytotoxic alkylating agents by carboxypeptidase G2. J. Med. Chem., *33:* 677–681, 1990.

15. Cancer Research Campaign Operation Manual for control of production, preclinical toxicology and Phase I trials of anti-tumor antibodies and drug antibody conjugates. Br. J. Cancer, *54:* 557–568, 1986.

16. Hughes, P., Lowe, C. R., and Sherwood, R. F. Metal ion-promoted binding of proteins to immobilized triazine dye affinity adsorbants. Biochim. Biophys. Acta, *700:* 90–100, 1982.

17. McCulloch, J. L., Chabner, B. A., and Bertino, J. R. Purification and properties of carboxypeptidase G1. J. Biol. Chem., *246:* 7207–7213, 1971.

18. Green, A. J., Dewhurst, S. E., Begent, R. H., Bagshawe, K. D., and Riggs, S. J. Accurate quantification of $^{131}$I distribution by gamma camera imaging. Eur. J. Nucl. Med., *16:* 361–365, 1990.

19. Sharma, S. K., Bagshawe, K. D., Melton, R. G., and Sherwood, R. F. Human immune response to monoclonal antibody-enzyme conjugates in ADEPT pilot clinical trial. Cell Biophys., *21:* 109–120, 1992.

20. Springer, C. J., Poon, G. K., Sharma, S. K., and Bagshawe, K. D. Identification of prodrug, active drug, and metabolites in an ADEPT clinical study. Cell Biophys., *22:* 9–26, 1993.

21. Martin, J., Stribbling, S. M., Poon, G. K., Begent, R. H. J., Napier, M. P., Sharma, S. K., and Springer, C. J. Antibody directed enzyme prodrug therapy (ADEPT): pharmacokinetics and plasma levels of prodrug and drug in a Phase I clinical trial. Cancer Chemother. Pharmacol., *40:* 189–201, 1997.

22. Stribbling, S. M., Martin, J., Pedley, R. B., Boden, J. A., Sharma, S. K., and Springer, C. J. Biodistribution of an antibody-enzyme conjugate for ADEPT in nude mice bearing a human colon adenocarcinoma xenograft. Cancer Chemother. Pharmacol., *40:* 277–284, 1997.

23. National Cancer Institute Common Toxicity Criteria. Bethesda, MD: National Cancer Institute, Division of Cancer Treatment, 1988.

24. Boxer, G. M., Abassi, A. M., Pedley, R. B., and Begent, R. H. J. Localisation of monoclonal antibodies reacting with different epitopes on carcinoembryonic antigen (CEA): implications for targeted therapy. Br. J. Cancer, *69:* 307–314, 1994.

25. Springer, C. J., Antoniw, P., Bagshawe, K. D., and Wilman, D. E. V. Comparison of half-lives and cytotoxicity of *N*-chloroethyl-4-amino and *N*-mesyloxyethylbenzoyl compounds, products of prodrugs in antibody-directed enzyme prodrug therapy (ADEPT). Anti-Cancer Drug Design, *6:* 467–479, 1991.

26. Bagshawe, K. D., Sharma, S. K., Springer, C. J., and Antoniw, P. Antibody directed enzyme prodrug therapy: a pilot scale clinical trial. Tumour Targeting, *1:* 17–30, 1995.

27. Springer, C. J., Dowell, R., Burke, P. J., Hadley, E., Davis, D. H., Blakey, D. C., Melton, R. G., and Niculescu-Duvaz, I. Optimisation of alkylating agent prodrugs derived from phenol and aniline mustards: a new clinical candidate prodrug (ZD2767) for antibody-directed prodrug therapy (ADEPT). J. Med. Chem., *38:* 5051–5065, 1995.

28. Blakey, D. C., Burke, P. J., Davies, D. H., Dowell, R. I., East, S. J., Eckersley, K. P., Fitton, J. E., McDaid, J., Melton, R. G., Niculescu-Duvaz, I. A., Pinder, P. E., Sharma, S. K., Wright, A. F., and Springer, C. J. ZD2767, an improved system for antibody-directed enzyme prodrug therapy that results in tumor regressions in colorectal tumour xenografts. Cancer Res., *56:* 3287–3292, 1996.

29. Korst, D. R., Johnson, F. D., Frenkel, E. P., and Challener, W. L. Preliminary evaluation of the effect of cyclophosphamide on the course of human neoplasms. Cancer Chemother. Rep., *7:* 1–12, 1960.

30. Ledermann, J. A., Begent, R. H. J., Massof, C., Kelly, A. M., Adam, T., and Bagshawe, K. D. A Phase I study of repeated therapy with radiolabelled antibody to carcinoembryonic antigen using intermittent or continuous administration of cyclosporin A to suppress the immune response. Int. J. Cancer, *47:* 659–664, 1991.

31. Bagshawe, K. D., and Sharma, S. K. Cyclosporine delays host immune response to antibody enzyme conjugate in ADEPT. Transplantation Proceedings, *28:* 3156–3158, .

32. Deierhoi, M. H., Kauffman, R. S., Hudson, S. L., Barber, W. H., Curtis, J. J., Julian, B. A., Gaston, R. S., Laskow, D. A., and Diethelm, A. G. Experience with mycophenolate mofetil (RS61443) in renal transplantation at a single center. Ann. Surg., *217:* 476–484, 1993.

33. Dhingra, K., Fritsche, H., Murray, J. L., LoBuglio, A. F., Khazaeli, M. B., Kelley, S., Tepper, M. A., Grasela, D. Buzdar, A., and Valero, O. Phase I clinical and pharmacological study of suppression of human antimouse antibody response to monoclonal antibody L6 by deoxyspergualin. Cancer Res., *55:* 3060–3067, 1995.

Downloaded from http://aacrjournals.org/clincancerres/article-pdf/6/3/765/2074869/df0300007 65.pdf by guest on 31 March 2023